

Functional Electrical Stimulation (FES) Leg Cycling Exercise in Paraplegia

—

A Pilot Study for the Definition and Assessment of Exercise Testing Protocols and Efficacy of Exercise

Chiara Ferrario

A thesis submitted for the degree of Doctor of Philosophy (PhD)

Department of Mechanical Engineering
Faculty of Engineering
University of Glasgow
February 2006

Copyright © C. Ferrario 2006

La scienza è una scoperta. Fai tutti i passi ben motivati, ben misurati, ma quel che scopri, scopri! Non è la conseguenza dei passi. I passi ti portano su quel davanzale naturale da cui vedi lo spettacolo della scoperta. La scoperta è uno spettacolo e l'autore di questo spettacolo è chi fa tutte le cose.

Don Luigi Giussani

Science is discovery. You make all the well founded steps, all the well measured steps, but what you discover, you discover! It's not a consequence of the steps. The steps bring you on that natural windowsill from which you can see the spectacle of discovery. Discovery is a spectacle and the author of this spectacle is the one who makes all things.

Father Luigi Giussani

Abstract

Spinal cord injury (SCI) is a medical condition that usually requires tremendous changes in a person's lifestyle. SCI people have severely reduced exercise capacity compared to able bodied (AB) people. Lower limb Functional Electrical Stimulation (FES) cycle ergometry is a well established means of exercise for people with SCI, and is associated with a range of physiological benefits. However, previous work has provided only limited means for characterising the cardiopulmonary fitness of SCI subjects performing FES-cycling. Moreover, considerable potential exists for optimization of stimulation parameters, such as muscle-group activation patterns.

A custom FES-cycling ergometer equipped with an electric motor and an integrated feedback system for accurate control of exercise workrate and cadence has been employed in this study. This experimental setup allowed the imposition of arbitrary workrate profiles with high precision and provided the potential for highly-sensitive exercise testing. One aim of the work described in this thesis was to propose and evaluate novel protocols for incremental exercise test (IET) and step exercise test (SET). Valid protocols would allow reliable estimation of the key markers of cardiopulmonary fitness in SCI subjects performing FES-cycling.

Measures which can be used to evaluate the effect on cycling performance of changes in stimulation parameters, and which might therefore be used to optimise them, were also investigated. Thus, a second aim of this work was to determine whether oxygen uptake and a new measure of stimulation cost (i.e. the total rate of stimulation charge applied to the stimulated muscle groups during cycling) are sensitive enough to allow discrimination between the efficacy of different activation patterns during constant-power cycling.

A discussion on the concept of metabolic efficiency in AB and SCI subjects is presented in this thesis. Efficiency of FES-cycling is much lower than that of voluntary cycling. Therefore, a third aim of this work was to define new efficiency measurements that are more appropriate for the SCI population.

Two volunteer subjects took part in this study and the data obtained from the tests they performed are presented as case studies. The main outcome shows feasibility of the two exercise testing protocols. Moreover, the first report of a

ventilatory threshold in SCI subjects during FES-cycling has been provided here. Oxygen uptake and stimulation cost measurements both allow discrimination between the efficacy of different muscle activation patterns. However, stimulation cost is more easily determined in real time, and responds more rapidly and with greatly improved signal-to-noise properties than oxygen uptake. These measures may find utility in the adjustment of stimulation patterns for achievements of optimal cycling performance. The new efficiency measures are expected to lead to better numerical properties. The limitations of this work have been identified and suggestions have been made for possible future work.

In summary, this work presents and validates new protocols for exercise testing in SCI subjects FES-cycling. Moreover, it introduces new stimulation and efficiency indices that help standardizing the assessment of SCI subjects fitness.

Acknowledgements

I would like to thank Ken Hunt for his help and support over the last few years. You are a great supervisor who kept me on the right path but also let me walk with my own legs. This work would not be as it is if I had not been helped by my “first” second supervisor Malcolm Granat and by my “second” second supervisor Bernie Conway: your support has been precious even if we have not met often over the course of the years. A special thank to Stan Grant for his advice on the “physiological side”, I would not have been able to get to grips with exercise physiology without your help. Thanks to Henrik Gollee too, who was always ready to give me help when I needed it.

Many thanks to Elaine McNamara who was always present to solve the issues that arose in the university bureaucratic labyrinth. I appreciate very much your help in the last months of my PhD, this thesis would not have been submitted without your help. Thanks to Nicola Coffield too, who sorted out all the conference stuff for us.

My thanks go to the people at the Queen Elizabeth National Spinal Injuries Unit at the Southern General Hospital. Sincere thanks go to Alan McLean, Matthew Fraser and David Allan who allowed us to use the Unit for our experiments and contributed to this work with helpful advice. A special thank goes to Jon Hasler who was always ready to answer all my questions.

Of course, all this would not have been possible without the help from the volunteers who participated in this study. Thank you for always being happy to work with me, for being patient when the technical stuff did not work and for laughing at all the problems that we had to face (especially at the beginning) and above all for being good friends, after all you had to endure...!

I would like to acknowledge the Synergy Scholarship for the financial support for this study.

Thanks to all those who are (or have been) part of the CRE: Barry who worked with me through all the tests, Sylvie who answered to all my questions (silly and not), Georg and Geraint my computer gurus, Calum my travel mate, Simon and

Emily who popped in the office every time with a smile for me, Manuel and Lorenzo my little Italy. Special thanks also to Ben, Bosun, Helen and Andrew. A very special thank goes to Lindsay, my office mate and great friend, who had to endure my moods, especially towards the end, and who has always been a great support!

Thanks to all my friends spread over the whole world. I want to thank especially Evelyn, Emma and Dan for their friendship and support throughout the last year, for always encouraging me through the hard times and sharing with me the happy ones. Ila, Al, James and Augu, we got together by chance and now we'll never let each other go: clamoroso! To Silvia whose support and friendship have been invaluable through the years I say thank you and to Marta who lived everything with me from far away. To Peppe who always had time to listen to me and to Betta and Trava who welcomed me in their home in a way I never experienced before, thank you! I want also to thank everybody at Turnbull Hall, especially Rosalind, Rafa, Louis, Teresa and Angela, Sr B and Fr J. Thank you to Samina, my flat mate, who managed to live with me for three years! Thanks to Lindsay, Robert, Eryn and Aimee my Scottish family. Thanks to the Boys in London, to Manu who always had a place for me when I needed it and to Raquel who kept telling me that I would have managed to do all this!

And last but not least... my family!

Thanks to Federico, my husband and best friend, for having always been there for me during the last nine years!?! Thanks for having an infinite patience and for showing me in all the little things that you love me so much. I would not have been able to do this without you.

Mamma e papà, Paola e Luigi: silenziosamente e con tanta pazienza mi avete accompagnata e sostenuta per questi tre anni, dandomi sempre più di quello che chiedevo. Grazie per avermi sopportata specialmente negli ultimi tre mesi, al culmine della mia tensione tra tesi, ricerca di un lavoro e preparazione della nuova casa.

Thesis Outline

Chapter 1: This chapter describes the anatomy and physiology of the intact spinal cord, neurones and muscles. Moreover, respiratory physiology and the principles of exercise testing are introduced and illustrated.

Chapter 2: In this chapter the principal causes of spinal cord injury (SCI) and the consequences that this pathology brings to the affected subjects are reported. Moreover, the concept of Functional Electrical Stimulation (FES) is introduced and its applications in paraplegia are described, together with the benefits that can be achieved by means of FES.

Chapter 3: This chapter includes the description of the experimental setup used for all the tests reported in this thesis. Moreover, novel protocols for incremental exercise test (IET) and step exercise test (SET) developed for use with paraplegic subjects are described here.

Chapter 4: This chapter reports the analysis of the IET and SET performed by the two SCI subjects who participated in this study. The key outcomes of the two tests are defined and analysed. Proof is given that the novel protocols deliver repeatable measures of metabolic and mechanical outcomes.

Chapter 5: This chapter reports results related to the detection of the presence of the ventilatory threshold (VT) in SCI subjects. The method used is described and the concept of VT in paraplegic subjects is discussed.

Chapter 6: In this chapter the optimisation of FES-cycling in terms of energy expenditure is discussed. The variations of oxygen uptake and of stimulation cost are analysed, depending on the stimulation pattern used.

Chapter 7: In this chapter the concept of traditionally computed efficiency in AB and SCI subjects is described and discussed. Moreover, a new, more appropriate definition of efficiency for SCI subjects is introduced and evaluated.

Chapter 8: This chapter reports the limitations that have been identified in analysing the results of the tests. Moreover, open questions that have arisen from this work are addressed.

Chapter 9: This chapter summarizes the main conclusions of this thesis.

Contributions

- In this thesis a new apparatus for exercise testing is used. This allowed the definition of novel protocols for incremental exercise test (IET) and step exercise test (SET), to be used with spinal cord injured (SCI) subjects. The protocols have been adapted from those used with able bodied (AB) subjects and tailored to the needs of SCI subjects.
- The application of the protocols has been successful and the estimation of the key outcomes has been proven repeatable. Thus, the feasibility of the protocols has been established.
- The presence of the ventilatory threshold (VT) has been detected in SCI subjects through IET. The meaning of VT in SCI subjects has been discussed and a new interpretation has been suggested.
- A new exercise cost measurement has been defined: the stimulation cost, i.e. the rate of charge delivered to the muscles during exercise. This index could be useful in determining the efficacy of exercise, since its kinetics are quicker than those for \dot{V}_{O_2} . Moreover, it does not need any special equipment to be measured, since the stimulation pulsewidth and the current amplitude are recorded in real time by the control system. Both oxygen uptake and stimulation cost have been shown to be affected by variations in stimulation parameters. This finding opens the possibility of studying optimized stimulation patterns based on \dot{V}_{O_2} or stimulation cost.
- New efficiency definitions have been introduced. These are more appropriate for SCI injured subjects, since they take into account also the negative power range, which is a significative percentage of the overall workrate range in this population.
- The limitation arisen from this study have been presented. Moreover, suggestions have been made for possible improvements.

Publications

1. K.J. Hunt, A.J. Cathcart, C. Ferrario, B. Stone, S. Grant, S.A. Ward, and M.H. Fraser. Workrate and cadence control for exercise testing in FES-cycling. *8th Annual International FES Society Conference*, July 2003, Brisbane, Australia.
2. K.J. Hunt, B. Stone, N. Negård, T. Schauer, M.H. Fraser, A.J. Cathcart, C. Ferrario, S. Grant, and S.A. Ward. Control strategies for integration of electric motor assist and functional electrical stimulation in paraplegic cycling: utility for exercise testing and mobile cycling. *IEEE Trans Neural Sys Rehab Eng*, 12(1): 89–101, 2004.
3. C. Ferrario, B. Stone, K.J. Hunt, A.N. McLean, and M.H. Fraser. Exercise testing during functional electrical stimulation cycling in paraplegia. *IEEE EMBS UKRI Postgraduate Conference on Biomedical Engineering and Medical Physics*, August 2004, Southampton, UK, 37–38.
4. C. Ferrario, B. Stone, K.J. Hunt, S.A. Ward, A.N. McLean, and M.H. Fraser. Oxygen cost of different stimulation patterns for FES cycling. *9th Annual International FES Society Conference*, September 2004, Bournemouth, UK, 171–173.
5. K.J. Hunt, C. Ferrario, S. Grant, B. Stone, A.N. McLean, M.H. Fraser, and D.B. Allan. Comparison of stimulation patterns for FES-cycling using measures of oxygen cost and stimulation cost. *Med Eng Phys*, in press.
6. C. Ferrario and K.J. Hunt and S. Grant and A.N. McLean and M.H. Fraser and D.B. Allan. Novel protocols for high sensitivity cardio-pulmonary exercise testing during Functional Electrical Stimulation cycle ergometry in spinal cord injured subjects. Submitted.

Contents

Abstract	i
Acknowledgements	iii
Thesis Outline	v
Contributions	vi
Publications	vii
List of Abbreviations	xv
1 Background	1
1.1 Summary	1
1.2 Spinal Cord and Neurones	1
1.2.1 Spinal Cord	1
1.2.2 The Neurone	3
1.3 Skeletal Muscle	4
1.3.1 Muscle Structure and Contraction	4
1.3.2 Muscle Fibres	6
1.3.3 Cellular Respiration	8
1.3.4 Substrate Utilisation	11
1.4 Respiratory Physiology	13
1.4.1 Anaerobic Threshold	14
1.4.2 Gas Exchange Kinetics	16
1.5 Exercise Testing	19
1.5.1 Incremental Exercise Test	19
1.5.2 Step Exercise Test	22
2 Spinal Cord Injury	25
2.1 Summary	25
2.2 Spinal Cord Injury	25
2.2.1 Causes	26
2.2.2 Classification	27

2.2.3	Related Problems	29
2.3	Functional Electrical Stimulation	32
2.3.1	Motor Unit Recruitment	35
2.4	Benefits of FES	36
2.4.1	Cardiovascular and Pulmonary System	36
2.4.2	Reduction in Atrophy of Skeletal Muscle	38
2.4.3	Other Benefits	40
2.5	Contraindications for FES	41
3	Exercise Testing Protocols	43
3.1	Summary	43
3.2	Introduction	43
3.3	Methods	45
3.3.1	Subjects	45
3.3.2	Apparatus	45
3.3.3	Stimulation Strategy	47
3.3.4	Metabolic Measurements	49
3.4	Protocols	50
3.4.1	Incremental Exercise Test	50
3.4.2	Step Exercise Test	51
3.5	Results	52
3.6	Discussion	53
3.7	Conclusions	55
4	Analysis of IET and SET Data	56
4.1	Summary	56
4.2	Key Outcomes	56
4.2.1	Incremental Exercise Test	56
4.2.2	Step Exercise Test	57
4.3	Editing of the Data	57
4.4	Results	58
4.4.1	Case Study S1	58
4.4.2	Case Study S2	63
4.5	Discussion	65
4.5.1	Case Study S1	65
4.5.2	Case Study S2	68
4.6	Conclusions	69

5	Ventilatory Threshold	71
5.1	Summary	71
5.2	Introduction	71
5.3	Methods	71
5.4	Results	72
5.4.1	Case Study S1	72
5.4.2	Case Study S2	76
5.5	Discussion	78
5.5.1	Case Study S1	78
5.5.2	Case Study S2	79
5.5.3	Concept of Ventilatory Threshold in SCI Subjects	80
5.6	Conclusions	81
6	Study for Angle-Range Variation	83
6.1	Summary	83
6.2	Introduction	83
6.3	Methods	85
6.3.1	Subjects and Apparatus	85
6.3.2	Stimulation Parameters	85
6.3.3	Evaluation Protocol	86
6.3.4	Data Analysis and Outcome Measures	88
6.4	Results	89
6.4.1	Oxygen Uptake	89
6.4.2	Stimulation Cost	91
6.5	Discussion	95
6.6	Conclusions	97
7	Efficiency in SCI Subjects	99
7.1	Summary	99
7.2	Introduction	99
7.2.1	Traditional Definition of Efficiency	99
7.2.2	Efficiency Baselines	101
7.2.3	Parameters That Influence Efficiency	103
7.2.4	Efficiency in FES-Cycling	106
7.3	Methods	107
7.3.1	A New Efficiency Measurement	107
7.3.2	Experimental Setup	109

CONTENTS

7.4	Results	109
7.5	Discussion	110
7.6	Conclusions	112
8	Future Work	113
8.1	Summary	113
8.2	Identification of Open Investigation Areas	113
8.3	Conclusions	115
9	Conclusions	116

List of Tables

1.1	Characteristics of muscle fibre types.	7
2.1	Principal causes of traumatic spinal cord injury.	26
2.2	ASIA impairment scale.	28
2.3	Key muscles for ASIA motor neurological level classification.	29
2.4	Classification of muscle grades.	29
3.1	Details for subjects S1 and S2.	45
3.2	Current intensity.	48
3.3	Static and dynamic muscle stimulation angles.	49
4.1	IETs outcomes for subject S1.	60
4.2	\dot{V}_{O_2} values for the SETs in subject S1.	62
4.3	R values for the SETs in subject S1.	63
4.4	Time constant values for the SETs in subject S1.	63
4.5	IETs outcomes for subject S2.	65
5.1	VT values for subject S1.	76
6.1	Stimulation patterns.	86
6.2	\dot{V}_{O_2} values for the TPTs.	90
6.3	Mean and standard deviation values for \dot{V}_{O_2} for the TPTs and the OPTs.	91
6.4	Total charge rate values for the TPTs.	92
6.5	Pulsewidth values for the TPTs.	94
7.1	Efficiency values from the literature.	101
7.2	Efficiency values for the TPTs.	110
7.3	Efficiency values for the OPTs.	110

List of Figures

1.1	Transverse section of the spinal cord.	2
1.2	Spinal cord.	3
1.3	A schematic of a neurone.	4
1.4	Schematic of a myofibril.	5
1.5	Gas transport mechanism.	8
1.6	Diagram of gas exchange during exercise.	10
1.7	Relationship between substrate utilisation and R.	12
1.8	Simplified diagram of the human respiratory system.	13
1.9	Spirogram.	14
1.10	Graph showing the V-slope method.	16
1.11	Ventilatory gas variables' response to the onset of a step increment in power output.	17
1.12	Schematic of an incremental exercise test.	20
1.13	Ventilatory compensation for O ₂ and CO ₂	21
1.14	Schematic of a step exercise test.	23
2.1	Schematic of Functional Electrical Stimulation.	33
3.1	Motorized and instrumented recumbent tricycle for exercise testing during FES-cycling.	46
3.2	Integrated closed-loop control scheme.	46
3.3	Diagram of the stimulation patterns.	48
3.4	Portable component of the Metamax gas analyser.	49
3.5	Diagram of the protocol for the incremental exercise test.	50
3.6	Diagram of the protocol for the step exercise test.	52
3.7	Results from an incremental exercise test.	53
3.8	Results from a step exercise test.	53
4.1	The three stages of the data editing process.	58

4.2	Results for the incremental exercise tests (subject S1).	59
4.3	\dot{V}_{O_2} /power output relationship during the incremental phase of the tests (subject S1).	60
4.4	Results for the step exercise tests (subject S1).	61
4.5	Results for the incremental exercise tests (subject S2).	64
4.6	\dot{V}_{O_2} /power output relationship during the incremental phase of the tests (subject S2).	65
5.1	Ventilatory threshold detection in IET1 (subject S1).	73
5.2	Ventilatory threshold detection in IET2 (subject S1).	74
5.3	Ventilatory threshold detection in IET3 (subject S1).	75
5.4	Ventilatory threshold detection in IET1 (subject S2).	77
5.5	Graphs used for the detection of the ventilatory threshold for IET2 (subject S2).	78
6.1	Diagram of the stimulation patterns.	86
6.2	Schematic diagram of the Two Pattern Test protocol.	87
6.3	Schematic diagram of the One Pattern Test protocol.	88
6.4	Time-course for the oxygen uptake during the four TPTs.	89
6.5	Bar chart showing mean \dot{V}_{O_2} (+ sd) for both patterns before and after removal of resting baseline.	90
6.6	Time-course for the oxygen uptake during the two OPTs.	91
6.7	Time-course for the rate of total charge delivered to the muscles during the four TPTs.	92
6.8	Time-course for the pulsewidth during the four TPTs.	93
6.9	Time-course for the rate of total charge delivered to the muscles during the two OPTs.	94
6.10	Time-course for the pulsewidth during the two OPTs.	95
7.1	Graphical representation of the traditional measures of efficiency. . .	100
7.2	Graphical representation of the slopes proportional to the inverse of gross efficiency at two different power output levels.	102
7.3	Graphical representation of the extended measures of efficiency. . . .	108

List of Abbreviations

AB = Able Bodied

ADP = Adenosine Diphosphate

AT = Anaerobic Threshold

ATP = Adenosine Triphosphate

BMD = Bone Mineral Density

fb = breathing frequency

FES = Functional Electrical Stimulation

$F_I\text{CO}_2$ = Fraction of Inspired Carbon Dioxide

$F_I\text{O}_2$ = Fraction of Inspired Oxygen

HR = Heart Rate

IET = Incremental Exercise Test

LAT = Lactic Acid Threshold

LT = Lactate Threshold

MRT = Mean Response Time

OPT = One Pattern Test

$\sim\text{P}$ = High Energy Phosphate Compound

P_{max} = Maximum Power Output

P_{peak} = Peak Power Output

PC = Phosphocreatine

$P_{\text{ET}}\text{CO}_2$ = End Tidal Carbon Dioxide Pressure

$P_{\text{ET}}\text{O}_2$ = End Tidal Oxygen Pressure

PO = Power Output

\dot{Q} = Cardiac Output

\dot{Q}_{CO_2} = Carbon Dioxide Production at the muscle level

\dot{Q}_{O_2} = Oxygen Consumption at the muscle level

$R = \dot{V}_{\text{CO}_2}/\dot{V}_{\text{O}_2}$, Respiratory Exchange Ratio

RCP = Respiratory Compensation Point

$RQ = \dot{Q}_{\text{CO}_2}/\dot{Q}_{\text{O}_2}$, Respiratory Quotient

RV = Residual Volume

SCI = Spinal Cord Injury

SET = Step Exercise Test

SV = Stroke Volume

TE = expiration time

TI = inspiration time

TLC = Total Lung Capacity

TPT = Two Pattern Test

VC = Vital Capacity

\dot{V}_E = Minute Ventilation

\dot{V}_E/\dot{V}_{CO_2} = Ventilatory Equivalent for \dot{V}_{CO_2}

\dot{V}_E/\dot{V}_{O_2} = Ventilatory Equivalent for O_2

\dot{V}_{CO_2} = Carbon Dioxide Output at the lungs

\dot{V}_{O_2} = Oxygen Uptake at the lungs

$\dot{V}_{O_{2max}}$ = Maximum Oxygen Uptake

$\dot{V}_{O_{2peak}}$ = Peak Oxygen Uptake

VT = Ventilatory Threshold

V_T = Tidal Volume

ϵ_g = Gross Efficiency

ϵ_n = Net Efficiency

ϵ_w = Work Efficiency

$\Delta\epsilon$ = Delta Efficiency

Chapter 1

Background

1.1 Summary

This chapter provides an overview of the anatomical characteristics of the intact spinal cord, neurones and skeletal muscles. The process of cellular respiration is described in detail, with aerobic and anaerobic ATP production pathways and substrate utilization. The description of the physiology of respiration follows, with a particular emphasis on the concept of ventilatory threshold (VT) and gas exchange kinetics. Then the principles of exercise testing in able bodied (AB) subjects are illustrated.

1.2 Spinal Cord and Neurones

The nervous system consists of two main interconnected parts: the central nervous system (CNS) and the peripheral nervous system (PNS). The CNS includes the brain and the spinal cord and the PNS consists of all the nerve cells outside the CNS. For the purpose of this work, the focus is on the spinal cord in the CNS and on the motoneurones in the PNS.

1.2.1 Spinal Cord

The spinal cord is the most caudal part of the central nervous system. It receives information from the periphery of the body, i.e. muscles, joints and skin. It also plays a crucial role in delivering and issuing commands to initiate movements [103].

The spinal cord is a cylinder of nervous tissue descending from the brain dorsally within the spinal column. A transverse section of the spinal cord is shown in

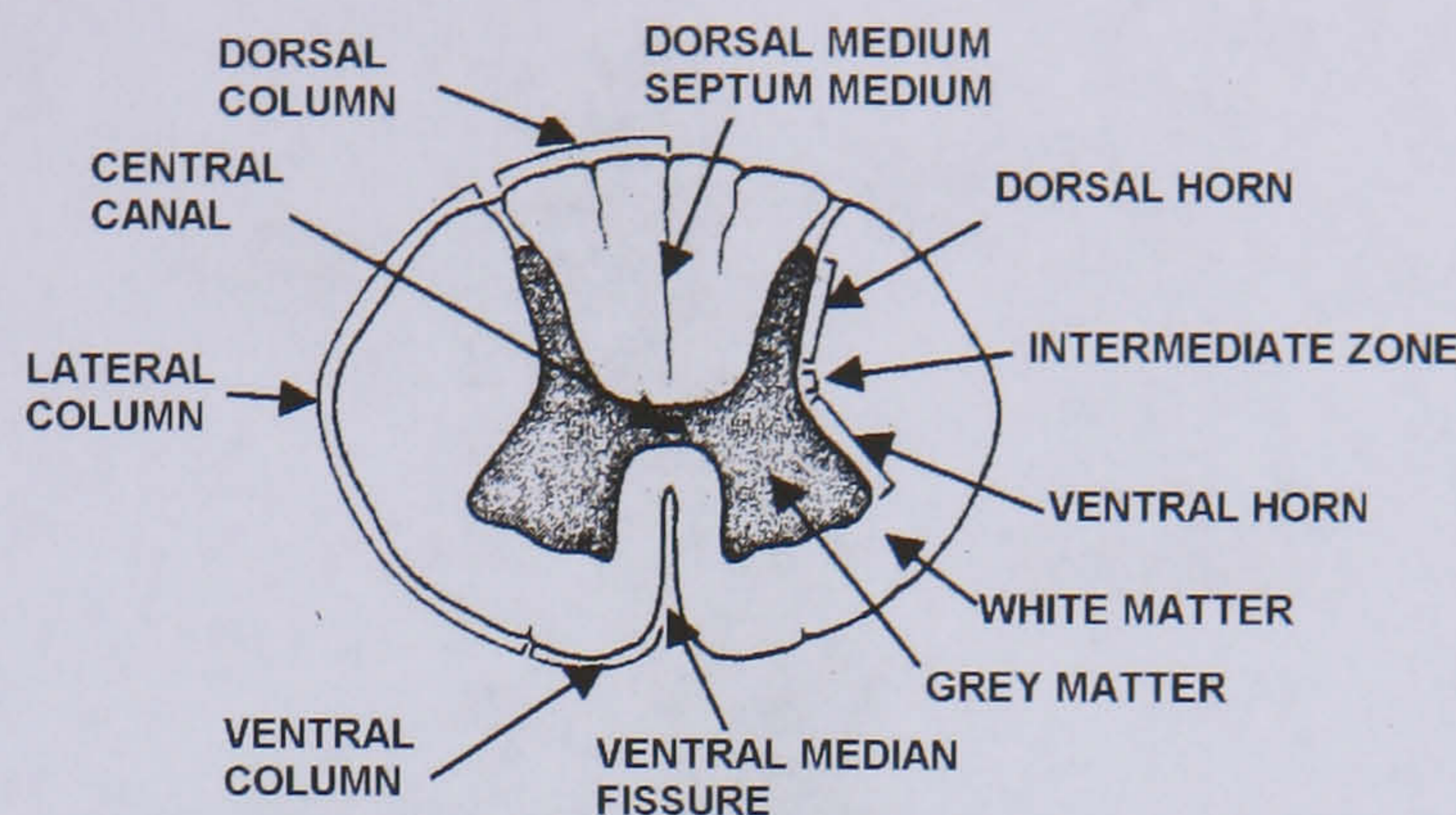


Figure 1.1: Transverse section of the spinal cord. Adapted from [103].

figure 1.1. In the butterfly-shaped centre is the *grey matter*; this is where the cell bodies of the spinal neurones are located, these cells are called *upper motoneurones*. The *lower motoneurones* stem from the horns of the grey matter and exit the vertebral column to reach the muscles [64]. The surrounding area is the *white matter* and it is composed of afferent and efferent axons. Afferent pathways carry the information from the periphery to the CNS. Efferent pathways carry commands out of the CNS to the peripheral nervous system [103]. The spinal cord is contained in the vertebral column, that is formed of bony rings called *vertebrae*. The vertebral column is divided into cervical, thoracic, lumbar, sacral and coccygeal regions. Figure 1.2 illustrates the structure of the spinal cord, the vertebral column and the position of the nerves. The nerves stem from the spinal cord in pairs through the spaces existing between the vertebrae [114]. There are 8 pairs of *cervical* nerves, twelve *thoracic* nerves, five *lumbar* nerves, five *sacral* nerves and one *coccygeal* nerve. The names of the spinal nerves are derived from the region of the vertebral column they come out from. Each nerve takes its name from the vertebra directly following (in the case of cervical nerves) or preceding it (for the others). The eighth cervical nerve is an exception, as it exits the vertebral column between the 7th cervical and the first thoracic vertebra. The vertebral column is longer than the spinal cord, therefore the origin of the nerves does not correspond to the vertebra the nerves exit from. Actually, the spinal cord reaches only the level of the first lumbar vertebra. The rest of the spinal column contains the roots of the lower nerves. These are much elongated and are known as the *cauda equina* [114].

The spinal cord links the brain and the body. One of its functions is to send orders from the brain to the peripheral body and to convey information from the body to the brain. Another important function is the coordination of the reflexes without sending information to the brain. These activities are implemented by

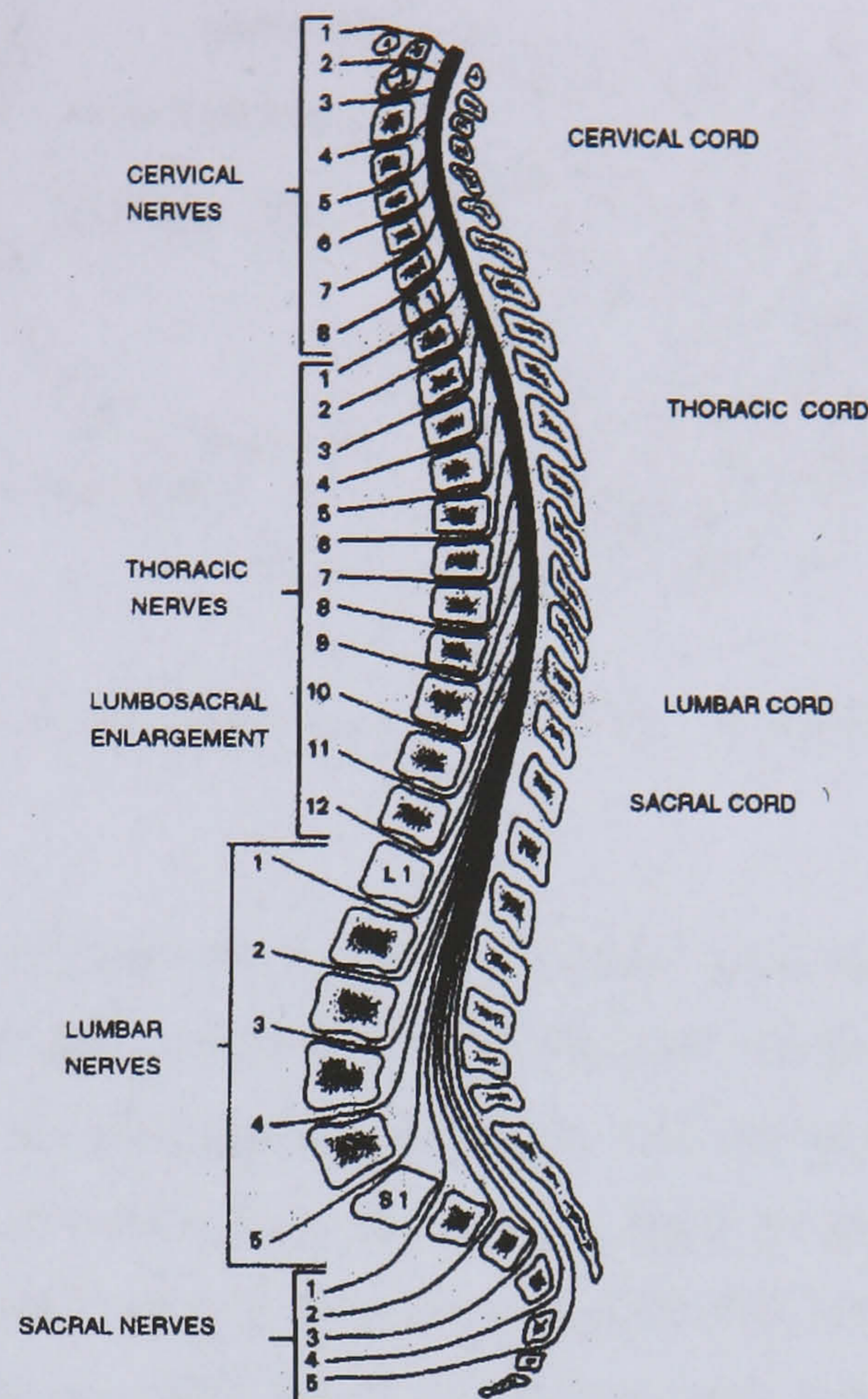


Figure 1.2: Spinal cord. Adapted from [103].

means of chemically mediated electrical signals.

1.2.2 The Neurone

The *neurone* is the functional unit of the nervous system [104]. It consists of three main parts: the body of the cell, the dendrites and the axon [114]. Figure 1.3 is a schematic representation of the anatomy of a neurone. The nucleus of the cell is located in the cell body and is the centre of operations for the neurone. The dendrites emerge from the cell body itself and have the function of receiving electrical impulses and conducting them towards the cell body. The axon is the only extension dedicated to transmitting the signal outside the cell, and it branches off towards its end to join various cells. The connection between two different cells through the dendrites or the axonal branches is called a *synapse*.

Neurones are considered excitable cells because of their capacity to receive and transmit electrical signals. All human cells present a membrane potential due to the

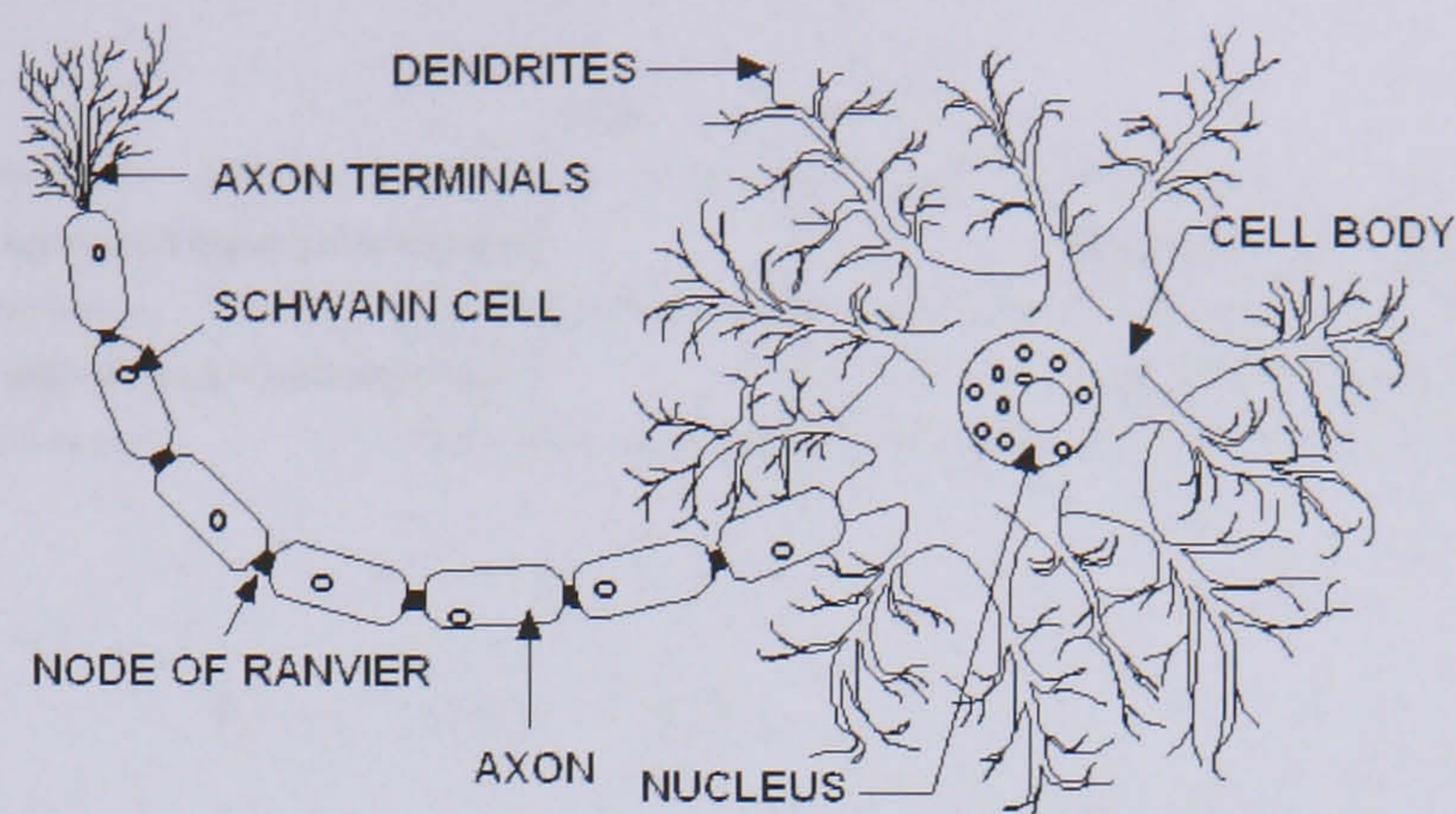


Figure 1.3: A schematic of a neurone. Adapted from [135]

different concentration of ions in the intracellular and extracellular fluids. There are two basic nervous states, unexcited and excited, each of them characterised by a membrane potential. In the unexcited state, the movement of ions into and out of the cell is controlled in order to maintain a negative membrane potential. Thus, the cell has a well defined, stable potential called the *resting potential*. This is a property of all cells. Some cells such as nerves and muscles can be excited. In addition, a nerve which is stimulated to carry a signal can rapidly become excited. This excitation is manifested in the movement of ions across the cell membrane, consequently changing the total charge within the cell itself. This signal, that can be propagated along great distances without losing its strength, is called an *action potential*.

1.3 Skeletal Muscle

1.3.1 Muscle Structure and Contraction

The muscle bulk is surrounded by three layers of connective tissue: the *epimysium* surrounding the entire muscle, the *perimysium* surrounding bundles of muscle fibres called *fascicles*, and the *endomysium* covering individual fibres. Each muscle fibre consists of numerous *myofibrils*, which in turn are composed of individual units called *sarcomeres*. Sarcomeres are the basic unit of contraction.

Myofibrils are made up of two major proteins: actin, forming thin filaments, and myosin, forming thick filaments. Two other proteins that are necessary for the contraction process are associated with the actin molecule: *troponin* and *tropomyosin*. Figure 1.4 shows the structure of a myofibril. The *Z line* defines the junction between two sarcomeres. Myosin filaments are located in the *H zone* and actin filaments in

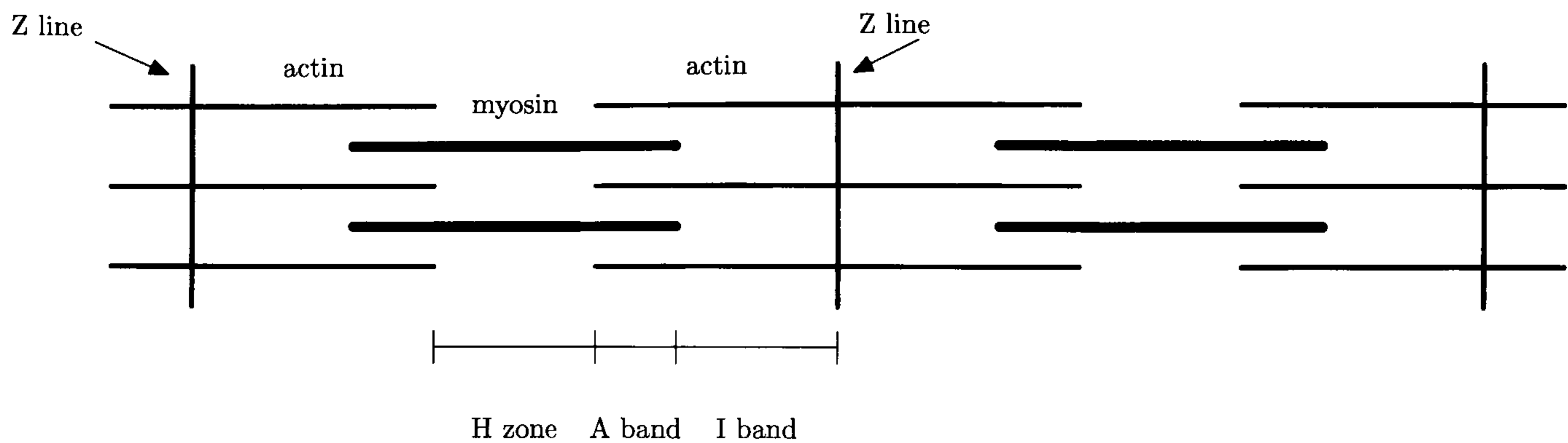


Figure 1.4: Schematic of a myofibril.

the *I band*. Actin and myosin filaments overlap in the *A band*, situated between the H zone and the I band. The cell membrane is called the *sarcolemma*. The *sarcoplasm* is the fluid contained inside the cell and it flows through a network of membranous channels called the *sarcoplasmic reticulum*, surrounding each myofibril. These channels store calcium, which plays an important role in muscle contraction. *Transverse tubules* (or T-tubules) extend inward from the sarcolemma penetrating the fibre. They pass between enlarged portions of the sarcoplasmic reticulum called the *terminal cisternae*. Both of these channels play an important part in muscle contraction.

Muscle contraction is a complex process involving a number of cellular proteins and energy production systems. The action potential causes the nerve cell to fire, inducing a reaction that releases a neurotransmitter (acetylcholine) at the level of the synapse. Thus, the process of muscular contraction begins when a nerve impulse arrives at the neuromuscular junction. The *neuromuscular junction* is the connection between the neural axon and the muscle fibre. It is at this level that the signal is transferred from one cell to another through the action of acetylcholine, and this causes the depolarization of the muscle cell. The motoneurone passes the signal to the muscle cell and it can supply different muscle fibres. Generally, the slower the electric conduction in a motoneurone is, the fewer fibres it innervates and vice versa. Usually, the fibres innervated by a single motoneurone are not adjacent, but are scattered in the muscle. The motoneurone and the fibres it innervates form a *motor unit*. When a motoneurone fires, all the fibres belonging to the corresponding motor unit are activated synchronously [69]. Each motor unit is composed by a varying number of muscle fibres. These range from 10 to several thousand fibres, and in a single muscle different sizes of motor units can be found. In general, in muscles used for precisely controlled movements, the size of the motor units is small and so is the number of fibres innervated by a single motoneurone. The diameter of

the axon determines its conduction velocity. The larger the diameter the higher the conduction velocity.

Muscular contraction is explained by the *sliding filament* model. The contraction of the muscle decreases the distance between couples of Z lines. This happens through the sliding of actin and myosin filaments across each other. For this purpose, the myosin molecule contains heads which can bind to actin. The action potential that arrives from the motoneurone propagates along the T-tubules. This stimulates the sarcoplasmic reticulum to release Ca^{2+} . The Ca^{2+} binds troponin, which in turn causes a positional change in tropomyosin uncovering the active sites of actin. The actin is thus free to bind with myosin. This process results in the release of the energy stored within the myosin molecule, thus causing the shortening of the muscle. The addition of fresh adenosine-triphosphate (ATP) breaks the strong binding state of the cross-bridge, resulting in a weak binding state. The ATPase enzyme hydrolyses the ATP providing energy for attachment to another active site on the actin molecule. The cycle is possible as long as free Ca^{2+} and ATP are available. The required ATP is in part stored in the muscle cells and in part produced in real time during exercise through metabolic pathways (see section 1.3.3).

When the nerve impulse ceases, the contraction is stopped. Ca^{2+} is actively removed from the sarcoplasm and pumped back into the sarcoplasmic membrane [104].

1.3.2 Muscle Fibres

Speed of contraction, level of peak force and rate of fatigue are typical characteristics used to classify muscle fibres. A muscle fibre is also characterised by its oxidative capacity and its ATPase isoform. The oxidative capacity of a muscle fibre depends on the number of mitochondria, as they produce ATP aerobically, on the number of capillaries surrounding it, as they provide the oxygen supply, and on the amount of myoglobin that binds and works as a shuttle for O_2 between the cell and the mitochondria. The overall behaviour of a muscle is determined by the different types of fibre that constitute it. There are essentially two types of fibres that are classified by their physiological and metabolic properties: Type I and Type II fibres. Table 1.1 shows the principal characteristics of the muscle fibre types. The most common criterion for classification is the time needed to reach the peak tension in response to stimulation [127]. Type I fibres are called *slow-twitch* fibres because of the relatively long time needed to develop peak tension. Moreover, they are

	Slow Oxidative (Type I)	Fast Oxidative (Type IIa)	Fast Glycolytic (Type IIb)
Contraction	Slow twitch	Fast twitch	Fast twitch
Fibre size	Small	Intermediate	Large
Color	Red	Red	White
Myoglobin Concentration	High	High	Low
Mitochondrial Content	High	High	Low

Table 1.1: Characteristics of muscle fibre types [125].

also characterised by a high resistance to fatigue due to the high levels of oxidative enzymes, concentration of mitochondria and capillaries. Thus, they are efficient at hydrolyzing ATP. They have a high capacity for aerobic metabolism, due to the high level of blood flow. Moreover, they develop a lower specific tension and show a slow velocity of contraction. Their efficiency is higher than for Type II fibres. Type II fibres differ from Type I because they have higher glycolytic activity. They are called *fast-twitch* fibres because their contraction time is faster. This fibre type can further be divided into two classes: IIa and IIb. Type IIb fibres possess a large anaerobic capacity and the specific tension they can develop is higher than for Type I fibres. They are less resistant to fatigue. Due to the high level of activity of ATPase, they have the fastest velocity of contraction. They are also the least efficient, because they use high amounts of energy. Type IIa fibres are highly adaptable, thus they can increase their oxidative capacity with training. Some muscles are composed mainly of slow or fast twitch fibres. However, most of the muscle groups contain the same amount of both fibre types. The large motor units are usually made of type IIb fibres [69]. Transformations between fibre type I and II is not likely to occur with training, but it can happen between fibre type IIa and IIb. A shift toward a higher percentage of type II fibres in the muscle has been seen in long term inactivity and chronic diseases [83, 125]. In general, it has been determined that the nerve that supplies the muscle determines the properties of the muscle fibres [111].

In physically healthy subjects the recruitment of muscle fibres for a voluntary contraction depends on the size of the motor units: the smaller units are recruited first and then the larger, where large means the actual number of muscle fibres and their diameter [73]. Therefore, in general type I fibres are recruited at the onset of exercise. As exercise progresses the first fibres fatigue and have to be replaced by those fibres that have not been recruited yet, that is fibre type II [39].

1.3.3 Cellular Respiration

The molecular interactions that cause the contractions in muscles require energy, which is provided by various interacting physiological mechanisms [127]. The cardiovascular and respiratory systems are activated in response to the higher demand for energy during exercise. The adequateness of the response is an index of cardiopulmonary fitness and health. Figure 1.5 is a diagram of the coupling of external to cellular respiration. O_2 is inspired through the lungs and diffused in the blood flow. The blood then carries the oxygen to the muscles. When the need for oxygen increases, it is extracted in greater quantities from the blood, selected peripheral blood vessels dilate and cardiac output (\dot{Q}) increases. Moreover, pulmonary blood flow and ventilation are increased. Consequently the production of carbon dioxide increases, the amount of CO_2 introduced in the blood also increases and the excess CO_2 is eliminated through the lungs.

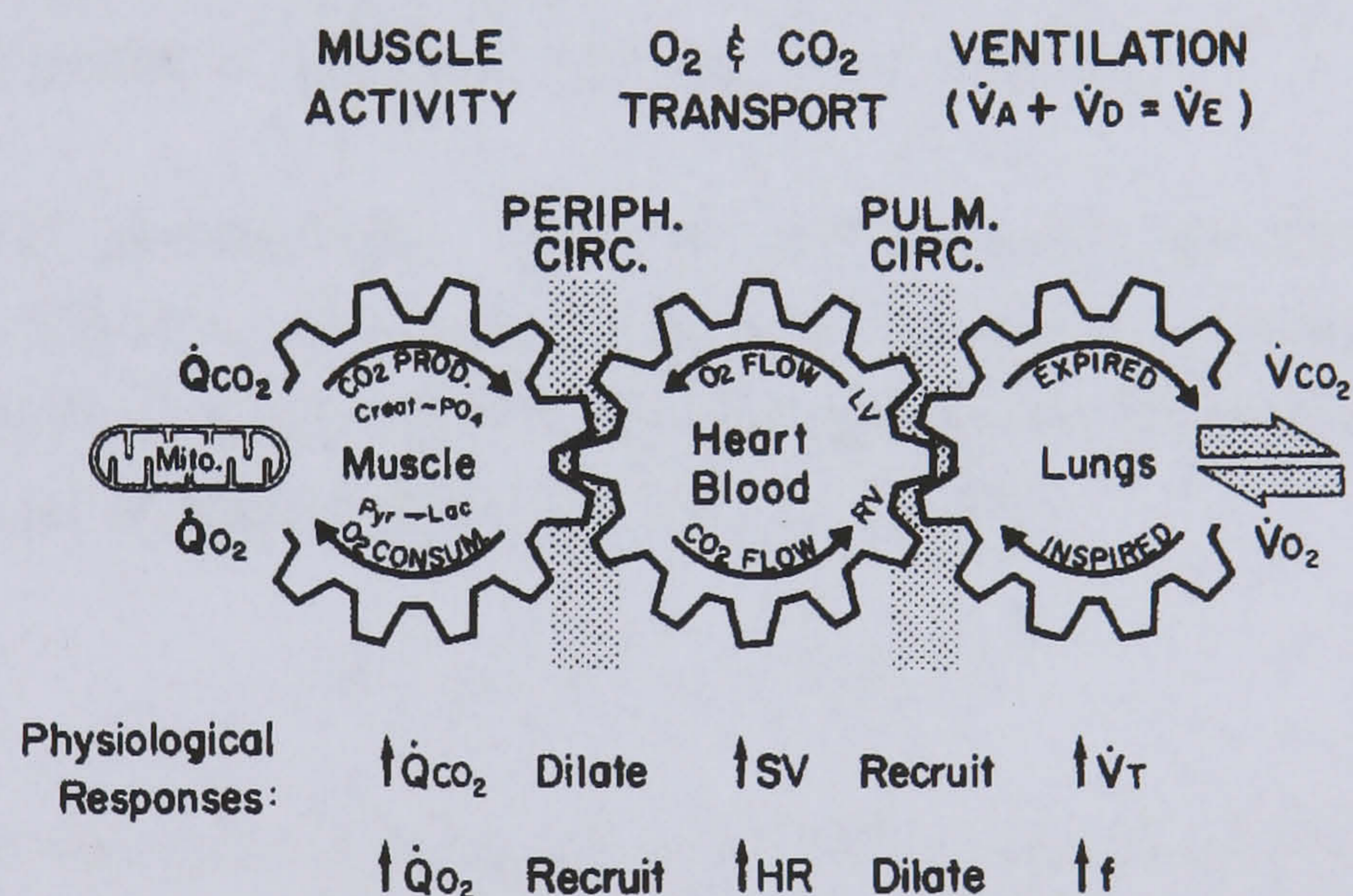


Figure 1.5: Gas transport mechanism showing the interaction between cellular and pulmonary respiration, adapted from [125].

Energy is obtained through a chain of chemical reactions leading to hydrolysis of the terminal phosphate bond of adenosine triphosphate into adenosine diphosphate (ADP). ATP is then reformed by linking ADP with an inorganic phosphate and this requires a high amount of energy. Each time an ATP molecule breaks down through the enzyme ATPase, the energy released is used for myosin cross-bridge linkage to, and subsequent release from, actin. The macroscopic output is the shortening or the increasing tension of the muscle. The amount of ATP stored in the cells is

limited, thus it is necessary to replenish the supplies. Three metabolic pathways exist to satisfy this requirement: a) formation of ATP from phosphocreatine (PC) hydrolysis, b) degradation of glucose or glycogen (glycolysis) into lactic acid, c) aerobic oxidation of glycogen or fatty acids. The first two pathways do not involve the use of O_2 , thus they are called *anaerobic pathways*, while the third one is called the *aerobic pathway* because it involves O_2 utilisation.

Aerobic ATP production Aerobic ATP production occurs in the mitochondria where there are two pathways which interact: the Krebs cycle and the electron transport chain. The details of these procedures are beyond the scope of this work; for more detail see [125]. In the Krebs cycle, fats, carbohydrates and proteins are oxidized using hydrogen carriers (NAD and FAD). This reaction results in CO_2 production, released in the blood, and the transfer of hydrogen to the electron transport chain. In the electron transport chain the electron possessed by the hydrogen is used to obtain the energy needed for combining ADP and P to form ATP. At the end of the chain the hydrogen is combined with O_2 to form water.

Anaerobic ATP production When the mitochondria are unable to reoxidize $NADH + H^+$ to NAD^+ at the required rate, the anaerobic pathway is activated.

Producing ATP by means of PC is simple and quick. PC donates a phosphate group and its bond energy to ADP and ATP is formed:



The drawback of this process is that only a limited amount of PC is stored in the cell and its reformation occurs only during recovery. Thus, this pathway is mainly used for short-term and high-intensity tasks and at the onset of exercise.

Pyruvic acid can also accept hydrogen ions, and lactic acid is formed. Glycolysis is the name of the pathway that breaks down glucose or glycogen to form pyruvic acid. All these reactions happen without the involvement of O_2 . The main aim of this procedure is to utilize the bond energy of glucose to join ADP with P. The lactic acid that is formed through this pathway induces disturbances in the acid-base balance in both the cell and the blood.

Figure 1.6 shows gas exchange during aerobic (A) and aerobic plus anaerobic (B) exercise. During aerobic exercise the oxygen is inspired through the lungs and is brought to the muscles, where it is used to produce energy. The exhaust product is CO_2 and is carried by the blood to the lungs, where it is released into the atmosphere.

Diagram B shows the energy being produced by the aerobic and anaerobic pathways together. The products of the anaerobic reaction are energy and lactic acid. The lactic acid is completely dissociated in the muscle cell, therefore it is necessary that the H^+ is buffered. HCO_3^- is the primary buffer. The bicarbonate is drawn into the cell from the blood by the difference in concentration. The products of the reaction between lactic acid and bicarbonate are $H_2O + CO_2 + K^+La^-$. Lactate subsequently passes from the cell to the blood because of the pH gradient across the sarcolemmal membrane. CO_2 is carried to the lungs and there released into the atmosphere.

It is important to underline that the onset of anaerobic ATP production does not imply that aerobic formation stops. The two pathways proceed together, with the anaerobic pathway slowly taking over as work rate increases.

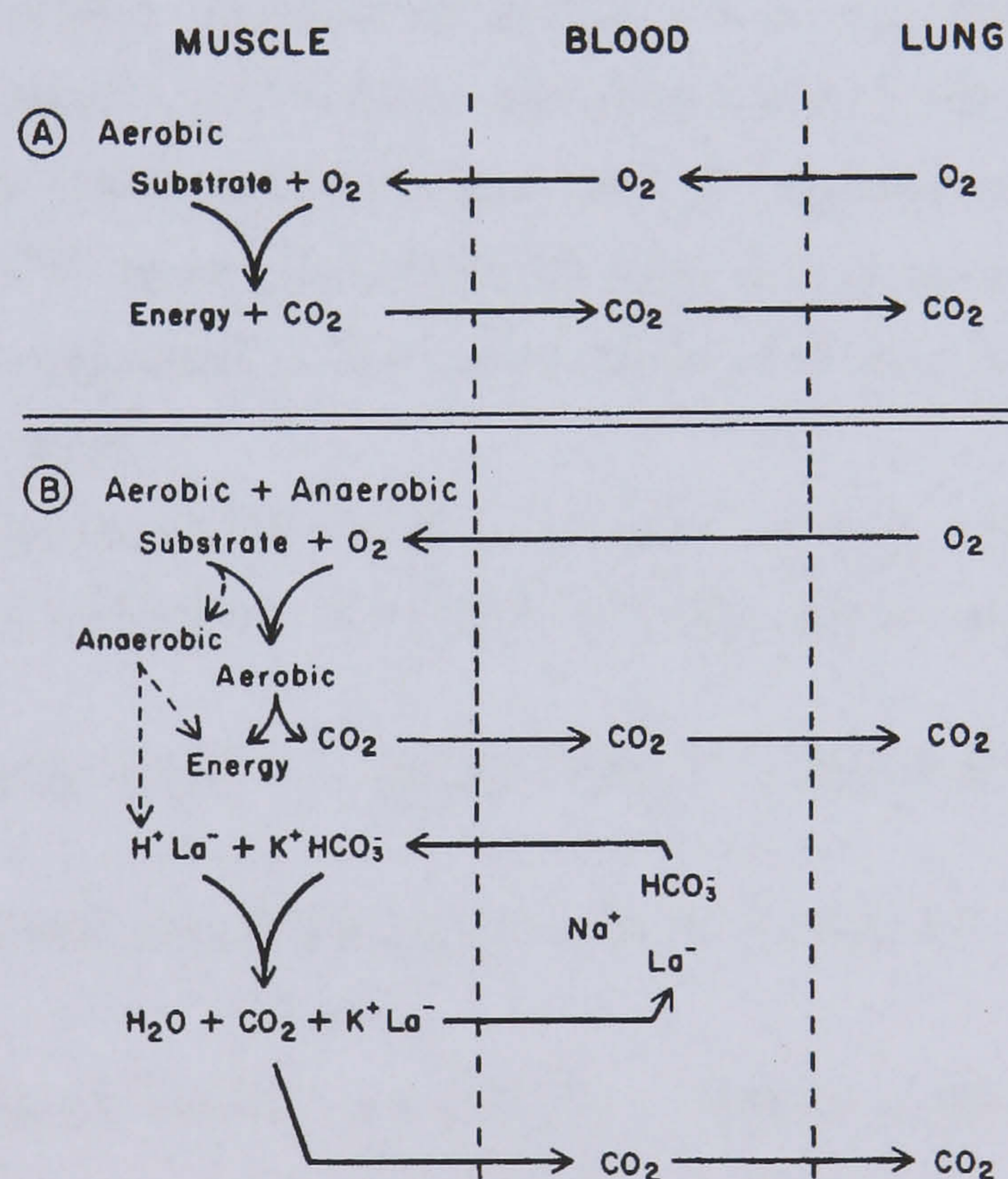
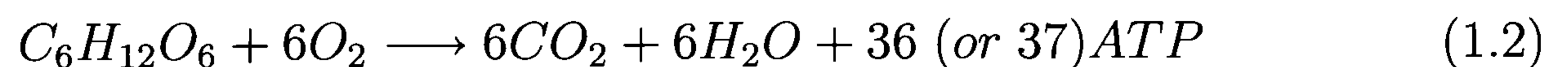


Figure 1.6: Diagram of gas exchange during exercise. In the aerobic pathway (A) inspired oxygen is used to produce energy and CO_2 is the other product of the reaction. When the anaerobic pathway is used (B), lactic acid is produced, therefore its amount inside the cell increases significantly. The lactic acid is buffered by bicarbonate. Thus, the chemical concentration gradient causes lactate to be extracted from the cell and bicarbonate to be imported into the cell. Adapted from [125].

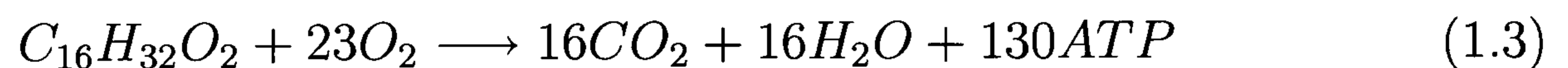
1.3.4 Substrate Utilisation

Ingested food is stored in the body in the form of carbohydrates, lipids and proteins. The energy contained in the food cannot be used directly, but it has to be stored in the terminal phosphate bond of ATP. The substrates need to be oxidized to produce the energy that is used to create the bond. When ATP is reduced to ADP the phosphate bond produces high levels of energy, thus it is called a *high energy* phosphate bond ($\sim P$). The different types of substrate require a different amount of O_2 for oxidation and produce different quantities of CO_2 in the process at the cell level. Therefore, the value of the respiratory quotient (RQ), defined as the ratio of CO_2 production to O_2 consumption at the muscle level) is linked to the type of substrate utilized. The respiratory exchange ratio (R, defined as the ratio of CO_2 output to O_2 uptake at the lungs level) at the level of the lungs reflects exactly the RQ only if the subject exercises in steady state. In this case, by monitoring steady-state oxygen uptake and carbon dioxide output at the level of the mouth it is possible to estimate which substrate and what percentage of it contributes to the energy metabolism. The amount of proteins used in the process is negligible, thus proteins will not be considered in the calculations and only fats and carbohydrates will be taken into account.

When only carbohydrates are used to produce energy, the RQ is equal to 1.0. Moreover, they have a $(\sim P):O_2 = 6.0$ (or 6.18 if glycogen is used instead of glucose):



If only lipids are oxidized, the RQ is equal to 0.71. Moreover, they have a $\sim P:O_2 = 5.65$:



There are also intermediate levels where fats and carbohydrates are used in different percentages. Figure 1.7 shows the relationship between substrate utilisation and R. It is a linear relationship where R increases with the percentage of carbohydrates used. R equal to 0.85 implies an equal utilisation of both substrates. In general, fats are more efficient considering the storage economy, but for O_2 utilisation carbohydrates are more efficient. It is generally agreed that in healthy subjects R during moderate exercise is approximately 0.95 [125].

If the exercise is low-intensity, fats are the main substrate utilized, but if the exercise is high-intensity carbohydrates are the main fuel used. When the intensity

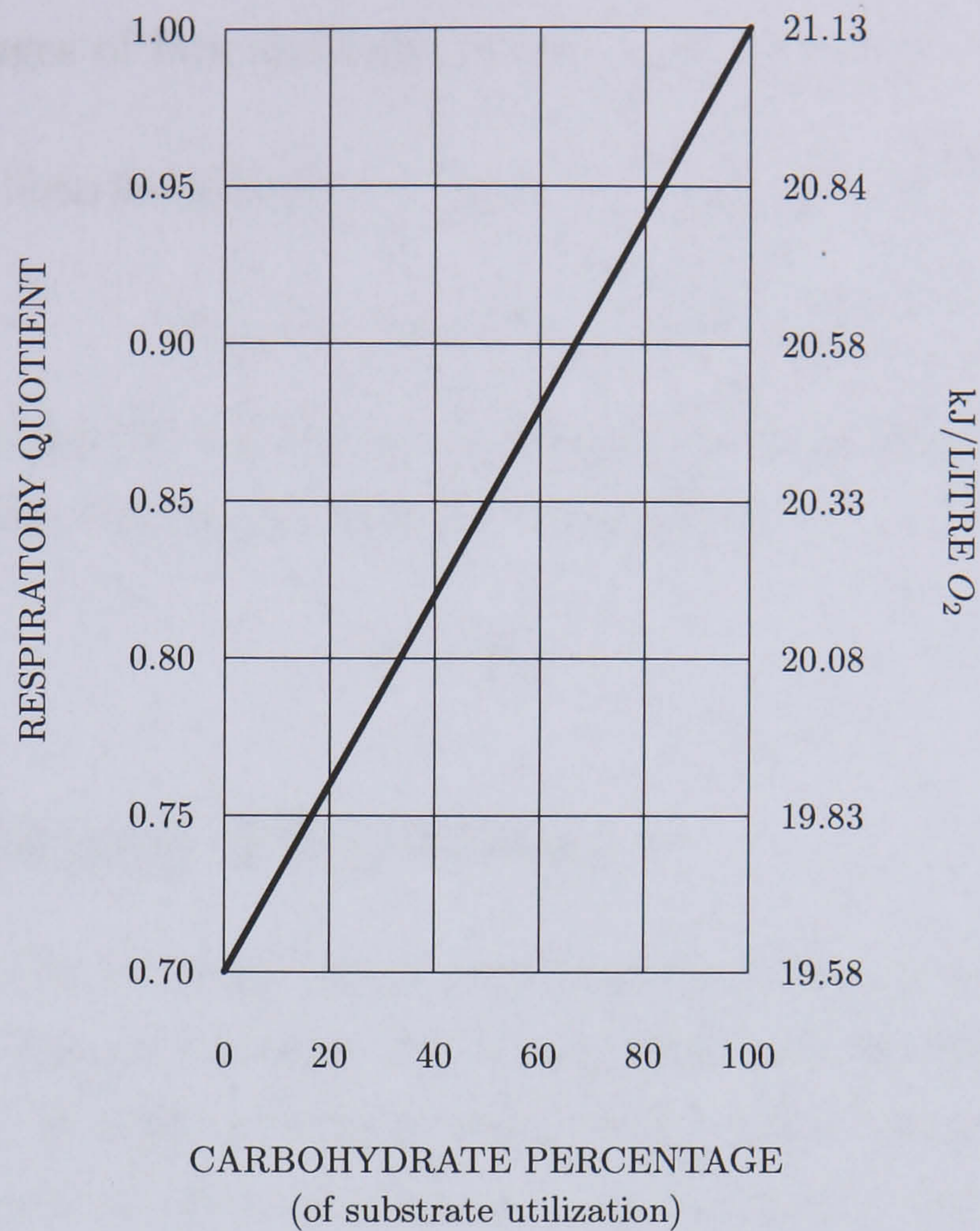


Figure 1.7: Graph showing the percentage of substrate used estimated from gas exchange measurements. The right ordinate shows the amount of energy obtained for each litre of O₂ depending on the substrate utilisation. Adapted from [125].

increases more fast fibres, that can metabolize carbohydrates better than fats, are recruited. When performing prolonged low-intensity exercise there is a shift from carbohydrate to fat utilisation, thus R decreases. The kind of substrate that is utilized is affected by the physical fitness of the subject. The fitter the subject, the lower R is, as fats are the main substrate used. Therefore, glycogen is preserved and the subject has the possibility of doing more work, as exercise has to stop once glycogen is completely used. This is the point of exhaustion.

To calculate the overall energy expenditure during exercise it is necessary to convert O₂ utilisation into energy. When only fats are used the energy liberated in the process is 19.58 kJ/l_{O₂}, while when carbohydrates are used the energy released is 21.13 kJ/l_{O₂}[125]. Thus, the energy produced with each litre of oxygen (E), measured in kJ/l, can be calculated with the following equation (1.4):

$$E = (19.58 * \%fat + 21.13 * \%carbohydrate)/100 \quad (1.4)$$

where the percentages of fats and carbohydrates can be calculated knowing R :

$$\%carbohydrate = 100 * (R - 0.7)/(1.0 - 0.70) \quad (1.5)$$

$$\%fat = 100 - \%carbohydrate \quad (1.6)$$

To obtain the workrate (W), measured in kJ/s, the energy expenditure is multiplied by the oxygen uptake during the interval of interest:

$$W = \dot{V}_{O_2} * E \quad (1.7)$$

1.4 Respiratory Physiology

Pulmonary respiration is comprised of ventilation and gas exchange. Ventilation is the act of moving the air between the atmosphere and the lungs. Gas exchange occurs in the lungs. It replaces oxygen and removes carbon dioxide from the blood. This happens through diffusion of the gases. As the oxygen tension is higher in the lungs than in the blood, O_2 diffuses into the blood. The opposite is true for CO_2 , it diffuses in the lungs. The area through which the gases diffuse is large, therefore the exchange happens quickly [104].

The respiratory system is divided into a *conducting zone* and a *respiratory zone*. The conducting zone comprises trachea, bronchial tree and bronchioles. The respiratory zone is constituted mainly by the alveoli, where the actual gas exchange takes place. Figure 1.8 shows the anatomy of the respiratory system.

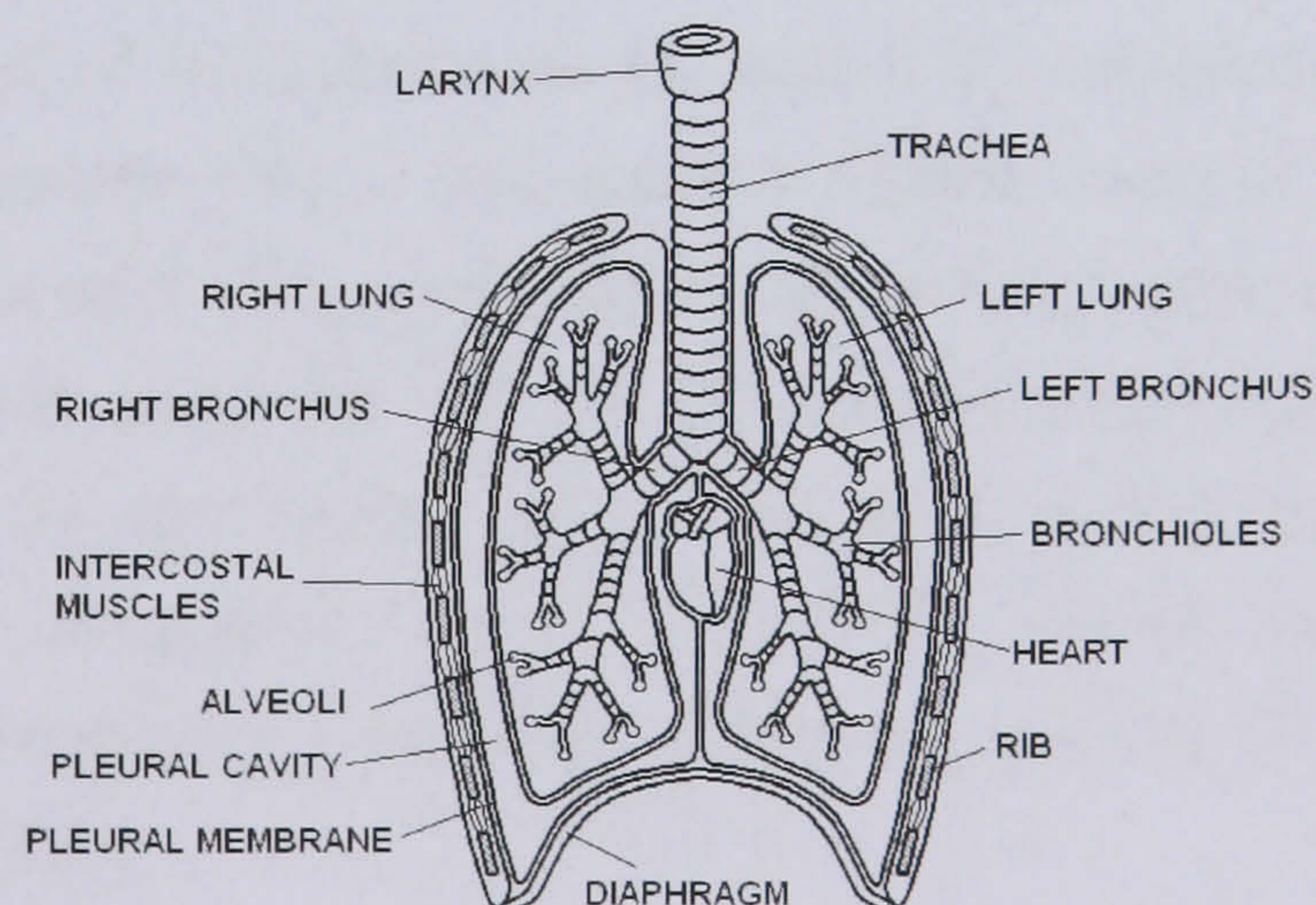


Figure 1.8: Simplified diagram of the human respiratory system. Adapted from [134].

The capacities and pulmonary volumes of the respiratory system of an individual can be measured with a spirometer. Figure 1.9 shows a spirogram. The *tidal volume* (V_T) is the amount of gas moved during each breath. The maximum quantity of air that can be exhaled after a maximum inspiration is called *vital capacity* (VC). The *residual volume* (RV) is what remains in the lungs after a maximal expiration. The *total lung capacity* (TLC) is the amount of gas that can be inspired with a maximal inspiration. The TLC is calculated as $VC + RV$. *Inspiratory reserve volume* and *expiratory reserve volume* are the volumes of gas that are added to the V_T during maximal inspiration and expiration to give the vital capacity [104].

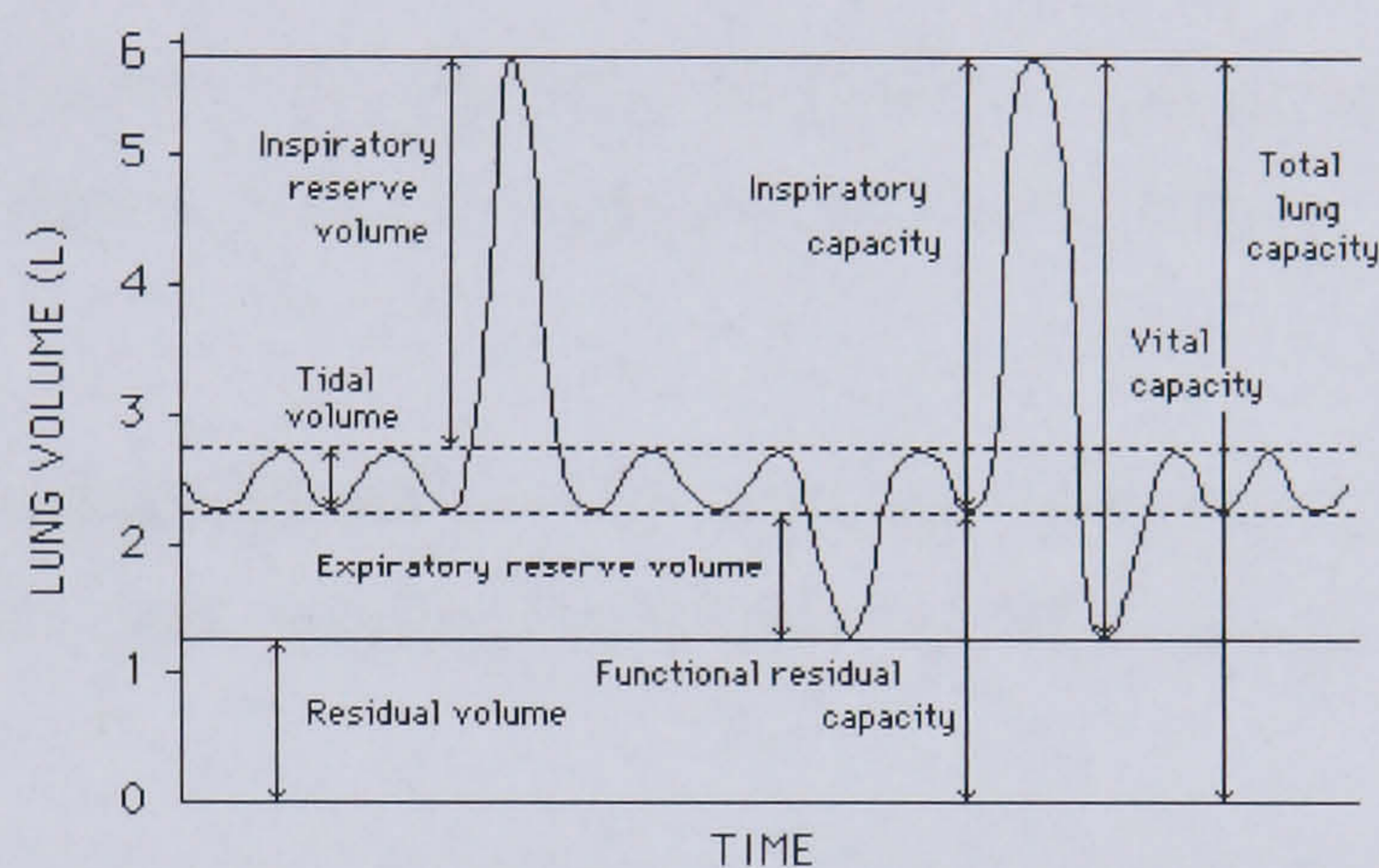


Figure 1.9: Spirogram. Adapted from [23].

The gas exchange concentrations, namely $[O_2]$ and $[CO_2]$, can be measured with a gas analyser. The primary variables that can be calculated from the flow data are breath frequency, V_T and \dot{V}_E . \dot{V}_E is the *minute ventilation*, the quantity of gas inhaled or exhaled in one minute. Moreover, with the information obtained by the measurement of instantaneous O_2 and CO_2 concentrations, it is possible to calculate oxygen uptake (\dot{V}_{O_2}) and carbon dioxide output (\dot{V}_{CO_2}) as the sum of the O_2 consumption and CO_2 production over a fixed period of time, typically one minute. *End tidal pressures* for O_2 and CO_2 ($P_{ET}O_2$ and $P_{ET}CO_2$) are measured in the respired air at the end of exhalation. $P_{ET}CO_2$ is the highest value and $P_{ET}O_2$ is the lowest value measured during exhalation. Other useful variables that are calculated are the *ventilatory equivalents* for CO_2 and O_2 ($\dot{V}_E / \dot{V}_{CO_2}$ and $\dot{V}_E / \dot{V}_{O_2}$) (see section 1.4.1) [125].

1.4.1 Anaerobic Threshold

There is one mechanism which underlies the phenomenon of the anaerobic threshold (AT), i.e. the buffering of lactic acid by means of bicarbonate, but the threshold

itself can be identified with various methods. Therefore, it is necessary to give some definitions of the various thresholds that can be used, taken from [118] and [127]:

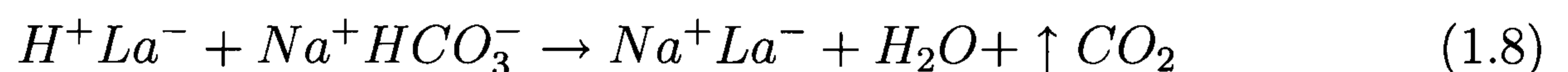
Anaerobic Threshold: “the intensity of exercise above which \dot{V}_{O_2} at the level of the lungs cannot account for all the energy required to exercise. This is the exercise intensity above which the anaerobic pathway associated with lactate accumulation starts to contribute to the energy production”;

Lactate Threshold (LT or θ_L): “the exercise intensity that refers to a substantial increase in lactate concentration in the blood”;

Ventilatory Threshold: “the exercise intensity at which the link between the increase in ventilation and the increase in power output (PO) becomes disproportionate”;

Lactic Acid Threshold (LAT): “the exercise intensity above which a net increase in lactic acid production causes a decrease in the arterial standard HCO_3^- ”.

The AT has been used as an index of fitness in healthy people, athletes and cardiorespiratory diseased patients [10]. The most accurate method of measuring the AT is to measure arterial lactate, but the gas exchange method can be a useful alternative, in terms of cost and simplification of the procedure. When using the gas exchange method, the correct term to be used is Ventilatory Threshold. The development of breath-by-breath gas exchange methods to identify the VT is based on the knowledge that CO_2 is a product of the bicarbonate buffering of the lactic acid [124]:



When exercising at a level below the VT, all the CO_2 produced is due to the oxygen consumption and the substrate utilized. When the intensity of work is increased above the VT, anaerobic mechanisms for energy production start to take over and gradually supplement the aerobic mechanism. The lactic acid is buffered by HCO_3^- and this generates additional CO_2 that is readily seen in the exhaled air [124].

There are two gas exchange responses that are altered as a consequence of the onset of lactic acidosis: the \dot{V}_{CO_2} - \dot{V}_{O_2} relationship and the ventilatory equivalents. The first response is analysed through the *V-slope method* (see figure 1.10). This analysis is carried out on data sets obtained with an incremental exercise test (see section 1.5.1). It compares the amount of CO_2 production with the amount of

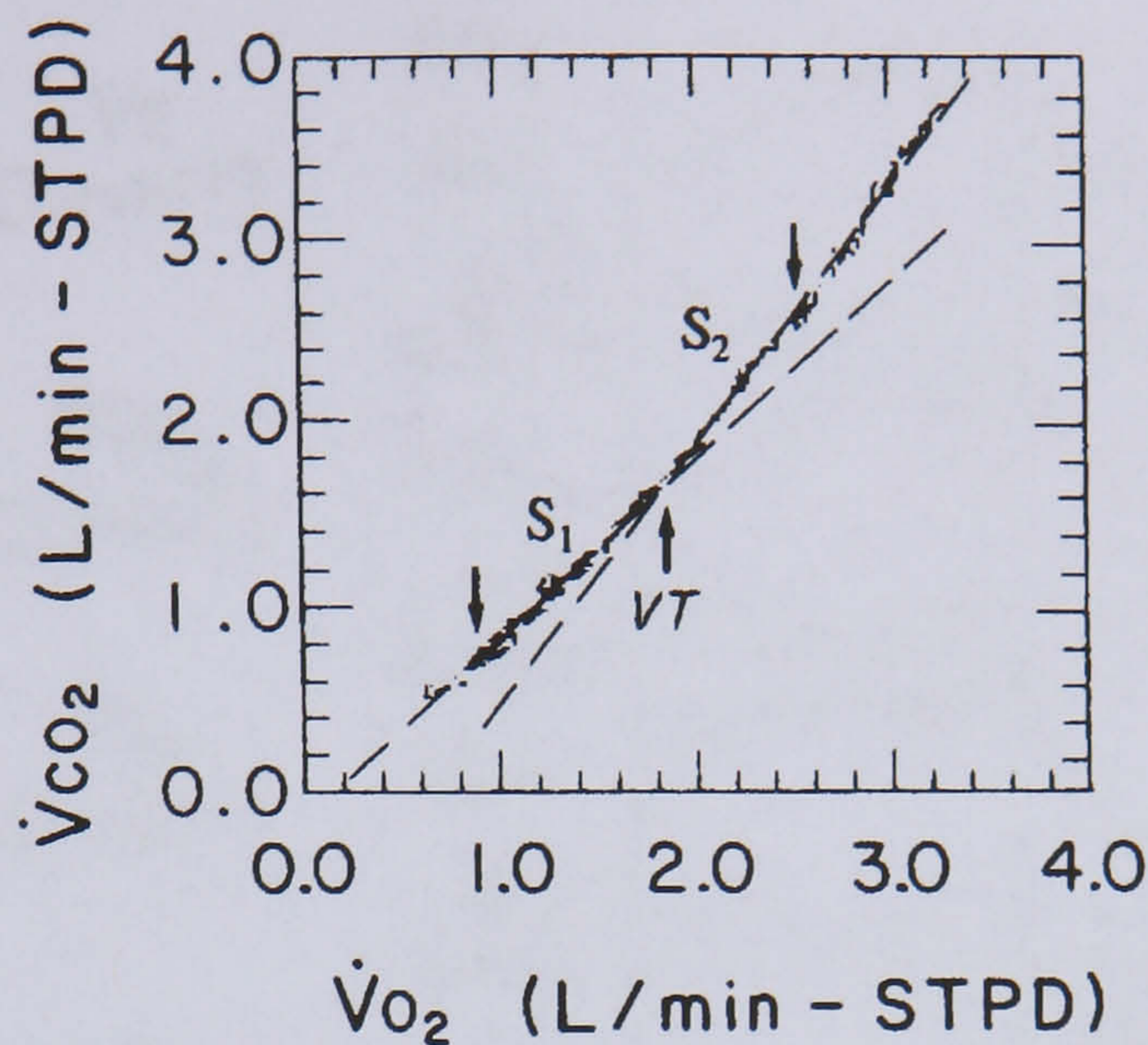


Figure 1.10: \dot{V}_{CO_2} plotted against \dot{V}_{O_2} . VT is the point where there is a deflection from linearity in the graph. S_1 indicates the region in which the subject is exercising aerobically. S_2 indicates the region in which the anaerobic pathways start to take over. Adapted from [125].

O_2 uptake. \dot{V}_{CO_2} is plotted against \dot{V}_{O_2} and the resulting graph is V-shaped, as can be seen in figure 1.10. In the figure, the arrow pointing upwards indicates the transition from pure aerobic metabolism to aerobic plus anaerobic metabolism. The slope before the VT (S_1) is usually between 0.85 and 1.00. Above VT the slope is steeper (S_2) and generally it is greater than 1.15. The VT is slightly higher than the LT. This is because at first H^+ can be removed without changes in pH, then the buffering occurs. Thus, there is a delay before the changes can be seen in the gas exchange measurements. The second mechanism is analysed with the *ventilatory equivalent method*. When the VT is exceeded \dot{V}_E increases in response to the increase in \dot{V}_{CO_2} . Therefore, the increase in \dot{V}_E maintains $P_{\text{ET}}\text{CO}_2$ constant. The elimination of excess CO_2 is very precise and this is reflected in the increase in $P_{\text{ET}}\text{O}_2$. Thus, studying both $P_{\text{ET}}\text{CO}_2$ and $P_{\text{ET}}\text{O}_2$ at the same time it is possible to detect the VT, when $P_{\text{ET}}\text{O}_2$ starts to increase while $P_{\text{ET}}\text{CO}_2$ remains constant. Moreover, \dot{V}_{O_2} increases linearly throughout the incremental phase of the test. Thus, $\dot{V}_E/\dot{V}_{\text{O}_2}$ increases and $\dot{V}_E/\dot{V}_{\text{CO}_2}$ remains constant or decreases at the VT.

1.4.2 Gas Exchange Kinetics

Following a step increment in power output, the response of \dot{V}_E , \dot{V}_{O_2} and \dot{V}_{CO_2} show a characteristic time-course, that can be seen in figure 1.11. This response, for able

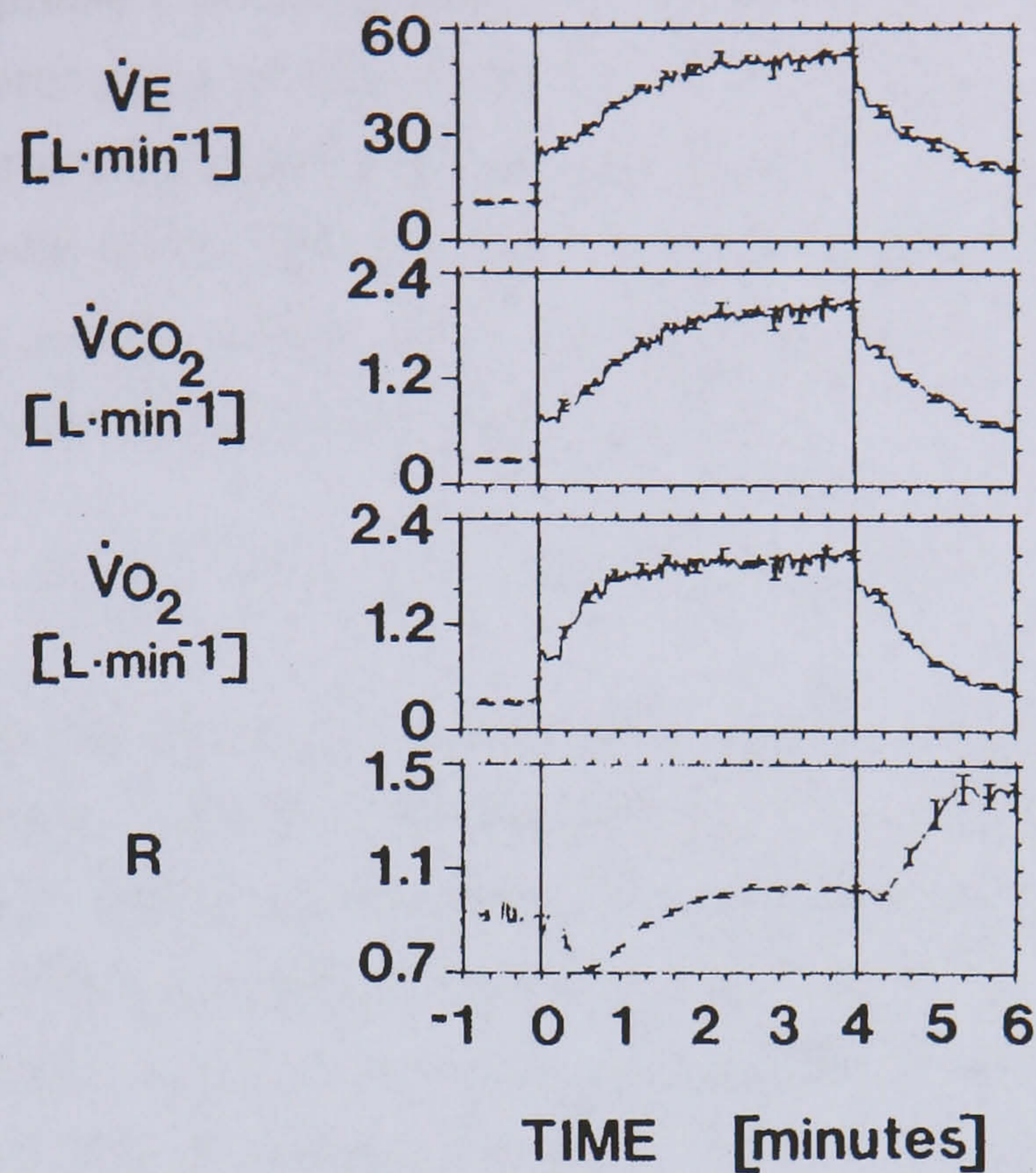


Figure 1.11: Ventilatory gas variables' response to the onset of a step increment in power output. The data are averaged over 6 repetitions and the vertical bars are the standard errors. Adapted from [125].

bodied subjects, can be divided in three phases [125]:

Phase I: it lasts about 15 s and shows the immediate response to exercise, as it takes into account the abrupt increase in pulmonary blood flow due to the increase in heart rate (HR) and stroke volume (SV). Typically, it is referred to as the *cardiodynamic phase* [8]. In this phase the blood that reaches the lungs still has the same gas composition as at rest: R does not change.

Phase II: \dot{V}_{O_2} , \dot{V}_{CO_2} and \dot{V}_E increase towards higher values. It is the *non-steady state* phase. It lasts for about 3 minutes for \dot{V}_{O_2} and is longer for \dot{V}_{CO_2} and \dot{V}_E , if the exercise level is below the ventilatory threshold. In this case a steady state is reached within this time. This is the period in which cellular respiration increases most. As \dot{V}_{O_2} increases more quickly than \dot{V}_{CO_2} , R decreases in the first minutes.

Phase III: it is the steady-state phase for \dot{V}_{O_2} and \dot{V}_E if the subject is exercising below the VT, otherwise they keep rising until the subject reaches fatigue. \dot{V}_{CO_2} kinetics are not affected by the workrate [17].

For oxygen uptake, phase I becomes less important with the increase in work rate, i.e. it is a smaller percentage of the whole \dot{V}_{O_2} step. When a subject is exercising in steady state, the gas exchange at the mouth reflects accurately the gas exchange occurring at the muscle level [129]. Phase II can be considered the transition stage necessary to reach a steady state. The \dot{V}_{O_2} time-course can be described with a monoexponential function if the work rate is below the VT:

$$\dot{V}_{O_2}(t) = \dot{V}_{O_2}(t_0) + \Delta\dot{V}_{O_2}(1 - e^{-(t-\delta)/\tau}) \quad (1.9)$$

where $\Delta\dot{V}_{O_2}$ is the magnitude of the steady-state increase in \dot{V}_{O_2} resulting from the step change in workrate, τ is the time constant and δ is a delay term. The gain is defined as $G = \Delta\dot{V}_{O_2} / \Delta WR$, where ΔWR is the increase in workrate [14]. This term is also called “cycling economy” [20] or “oxygen cost” [5, 125]. In leg cycling, typical values for the gain and the time constant are 9-10 ml·min⁻¹·W⁻¹ and 15-40 s, respectively [3, 14, 16, 131]. For work rates above the VT, the \dot{V}_{O_2} kinetics are better described by a combination of two exponential functions. The first component is a fast exponential function with a gain and time constant similar to those found in moderate exercise. The second component is a slow exponential function rising after a delay of some minutes [5, 8]. The gain of the slow component increases with work rate and it is approximately in the range 11-17 ml·min⁻¹·W⁻¹ [5, 8, 17]. Thus, the overall gain and τ become larger at exercise levels above the VT. During phase II, part of the oxygen utilized by the cells is taken from the blood stores. Thus, at first the oxygen uptake at the mouth level equals the oxygen consumed by the cells minus the decrease in O₂ concentration in the blood. The decrease in blood O₂ stores can be quantified and it is called the *oxygen deficit*. It is calculated as the difference between the oxygen uptake during exercise and the product of \dot{V}_{O_2} during steady state and the duration of exercise. The mean response time (MRT) is defined as the sum of τ and δ [2]. Once the exercise is stopped there is a delay before \dot{V}_{O_2} returns to the resting values. The surplus of \dot{V}_{O_2} in the recovery phase is called the *oxygen debt* and is calculated as the difference between the actual oxygen uptake and the resting values of \dot{V}_{O_2} over the recovery period. Typically, if exercise is below the VT, \dot{V}_{O_2} returns to resting levels in 5 minutes. Alternatively, if exercise is above the VT, it could take up to one hour or more to return to resting values [125].

Below the VT, for carbon dioxide output, the kinetics are slower. This can be explained by the fact that at the beginning of exercise phosphocreatine is hydrolyzed.

This causes an alkalinizing reaction, thus the CO_2 derived by the aerobic metabolism is converted to HCO_3^- and does not have to be expelled through the lungs. \dot{V}_{CO_2} kinetics are constant through the range of power output sustainable by the subject. \dot{V}_{CO_2} reaches a steady state in approximately 4 minutes [125]. Moreover, it seems that a single exponential function can describe well the response even at severe work rates [17].

At the beginning of phase II, R decreases because the different solubility in tissues of O_2 and CO_2 causes \dot{V}_{O_2} to increase faster than \dot{V}_{CO_2} . Then R increases to a value that is typically above the resting value. R keeps rising until lactate stops increasing.

\dot{V}_E kinetics are slower than \dot{V}_{CO_2} kinetics at moderate workrates. At heavy workrates a slow component can be seen, similar to \dot{V}_{O_2} . The adding of the second component causes a further slowing of the overall ventilatory response [17].

1.5 Exercise Testing

The performance of a subject during exercise depends on the response of the cardiovascular and the ventilatory system to the increase in energy demand from the muscles. The normal behaviour of the physiological mechanisms that link cellular respiration to gas exchange at the level of the mouth during exercise is quite predictable. Thus, it is useful to study it to verify the normality or the abnormality of the response to exercise [125].

1.5.1 Incremental Exercise Test

An incremental exercise test (IET) consists of ramping or regularly incrementing by a fixed amount the workrate, until the subject reaches exhaustion. This kind of test is used to test the capacity for exercise in terms of the maximum power output that can be achieved. It is also used to assess the stress involved in terms of maximum ventilatory capacity, i.e. the maximum oxygen uptake that can be achieved by a subject ($\dot{V}_{\text{O}_{2\text{max}}}$). An outline of an incremental test is shown in figure 1.12. The test starts with a period of rest. After an initial period of very low level or “unloaded” cycling (i.e. 0 W level) the power output is increased continuously [128] or each minute in steps of pre-defined amplitude [9, 10, 126]. The subject is encouraged by the experimenter to exercise as long as possible and the test is stopped only when the subject reaches exhaustion. A period of recovery in which the subject cycles

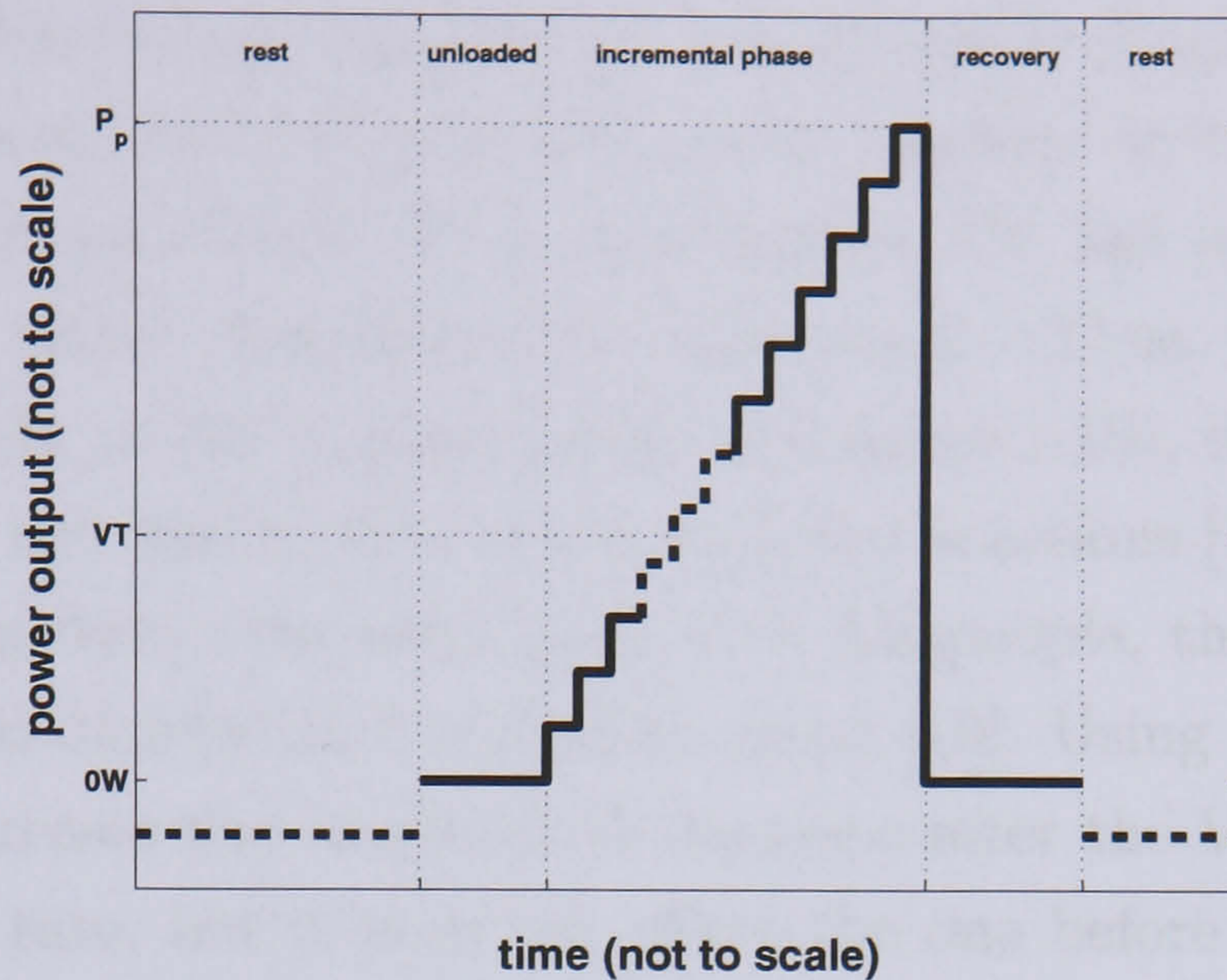


Figure 1.12: Schematic of an incremental exercise test. The dotted line in the incremental phase indicates an approximative range in which the VT can be found.

at an unloaded power output is advisable, to avoid a sudden fall in blood pressure [109, 125].

The outcome measures for this test are: peak oxygen uptake ($\dot{V}_{O_{2peak}}$), peak exercise workrate (P_{peak}), the time constant of oxygen uptake dynamics (τ), the oxygen uptake-work rate relationship ($\Delta\dot{V}_{O_2}/\Delta WR$) and an estimate of the oxygen uptake and workrate at the ventilatory anaerobic threshold. The respiratory system can approximately be considered a linear system [33], as shown in equation (1.9). Under this assumption, the time constant of the response is the same when either a step (in a step test, see section 1.5.2) or a ramp (in an incremental test) are the inputs.

If the increment rate in power output is slow, $\dot{V}_{O_{2max}}$ is likely to be underestimated. One of the reasons for the underestimation is the progressive lack of motivation in long tests. Moreover, it is more difficult to detect the VT. This happens because the increase in \dot{V}_{CO_2} depends on the rate of dissociation of the concentration of HCO_3^- and thus on the rate of increase of the concentration of lactate, not on the concentration itself. Thus, if the increments in work rate are small, the lactate increase could be too small to be detected by the increase in CO_2 [127].

Vallier *et al.* [123] suggest to avoid pauses prior to exercise and to eliminate recovery time within the protocol for IET in order to maximize the sensitivity of the detection of the VT.

Tests that increase power output too quickly also increase the risk of underestimating $\dot{V}_{O_{2max}}$. The forces required to overcome large steps in power output due

to the quick change are high, therefore the subject might fatigue earlier. Moreover, a rapid test induces a nonlinearity in the initial response of \dot{V}_{CO_2} , as \dot{V}_{CO_2} at first flows into the body gas stores. As a consequence, the fall in R is deeper at the beginning of rapid rather than slow incremental tests. Thus, when \dot{V}_{CO_2} starts to increase more rapidly in the V-slope graph (see figure 1.10), it is because it is less stored in the body and not because of the buffering reactions [127]. Therefore, usually when analyzing data from tests done with AB people, the first minute of the incremental phase is omitted in the V-slope graph [10]. Using the V-slope method, a fast workrate increases the steepness of the slope after the VT because lactate is formed at a faster rate, but it does not affect the one before the VT. When it is difficult to detect the change in slope, a 45° line can be plotted on the graph; the point in which the line is tangent to the curve is the VT.

When the power output increases rapidly, the compensatory hyperventilation for CO_2 is attenuated. Thus, just above VT, \dot{V}_E and \dot{V}_{CO_2} increase at the same rate, while \dot{V}_E/\dot{V}_{O_2} increases. This region has been called *isocapnic buffering*. Figure 1.13 shows the ventilatory compensation for O_2 and CO_2 during an incremental test. \dot{V}_E/\dot{V}_{CO_2} starts to increase only about midway between VT and $\dot{V}_{O_{2max}}$. This point is called Respiratory Compensation Point (RCP) and it is dependent on the increment rate [109].

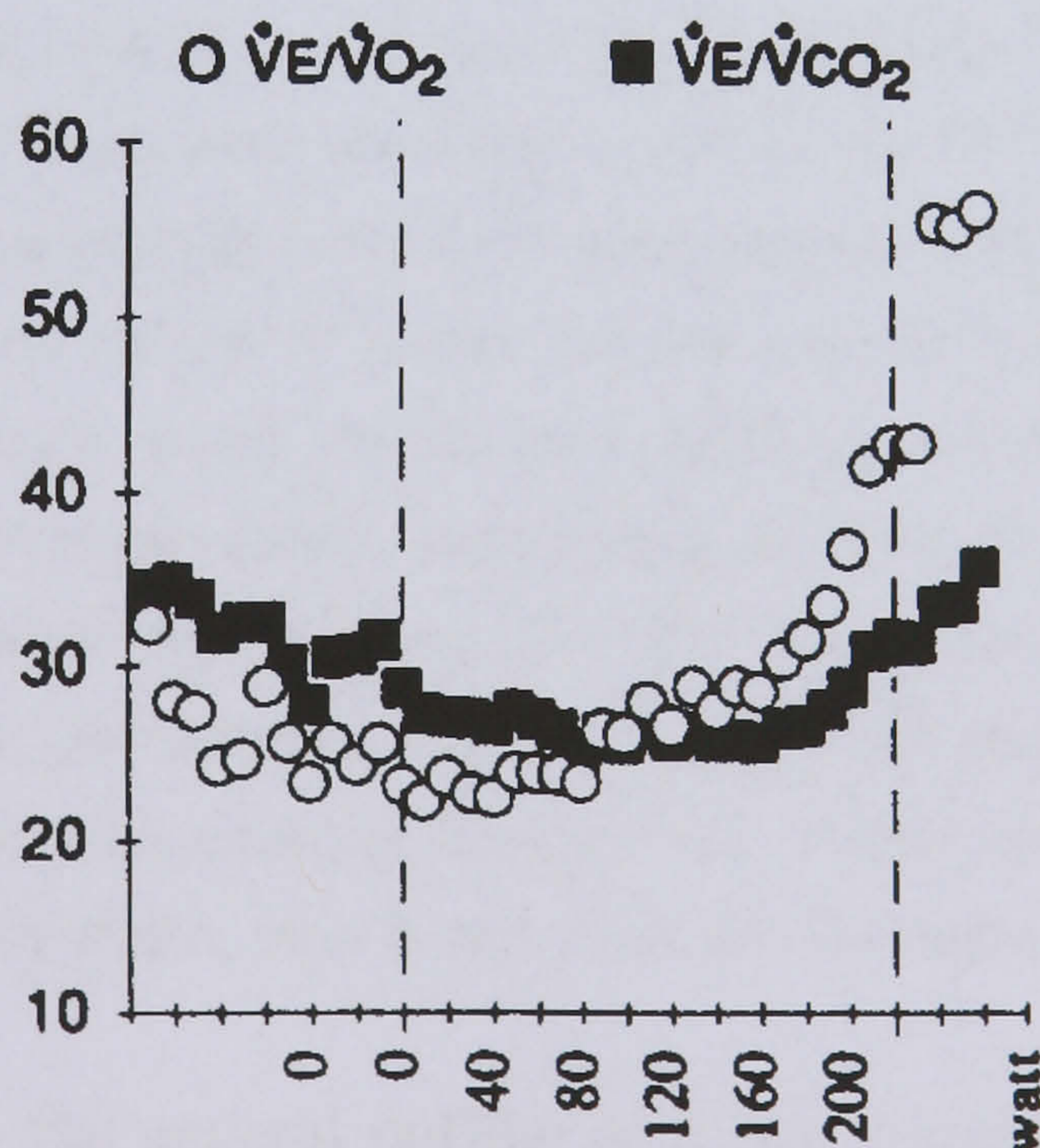


Figure 1.13: Ventilatory compensation for O_2 and CO_2 during an incremental test with an AB subject. Adapted from [125].

Reducing the number of steps in an incremental test causes an increase in the amplitude of the steps in power output. Using the gas exchange measurements it is still possible to detect the VT, but interpretative caution is needed. The increase in blood lactate begins at the muscle level, and there is a delay before the effect can be seen at the mouth level. During this time, the workrate is constantly changing. Thus, the effect cannot be seen during the transit time. Therefore, with a work rate changing too rapidly, the power output at the VT is overestimated. Thus, the more appropriate method to measure the VT is in terms of \dot{V}_{O_2} [128]. A test duration of 10-12 minutes is a good compromise between slow and fast testing. Changing the rapidity of the power output increments does not modify VT and $\dot{V}_{O_{2max}}$, but it causes them to occur at higher power output levels [127].

The slope of \dot{V}_{O_2} plotted against time depends on the size of the increments. It becomes steeper if the increments in power output are slow and it becomes less steep if the increments are too rapid [127].

1.5.2 Step Exercise Test

During a step exercise test (SET), the subject exercises at a constant power output, in order to allow the cardiorespiratory responses to stabilize over time if exercise is below the VT. The SET provides information on the magnitude and velocity of response of the cardiorespiratory system, i.e. the gas exchange kinetics, given the state of training. The endurance of the subject can also be detected. In the past, series of Step Exercise Tests were used also to detect the VT and to determine $\dot{V}_{O_{2max}}$. The advantage of using multiple constant load tests at different power output levels lies in the fact that the choice of power output can be based on the results of the previous tests. Moreover, when breath by breath gas analysers were not available, this kind of test did not need rapidly-responding devices. In addition, when \dot{V}_{O_2} does not increase with workrate it is an indicator that $\dot{V}_{O_{2max}}$ has been reached. However, the length of the whole procedure is exhausting for both experimenters and subjects, especially for patients with exercise limitations. Moreover, even if these tests are considered to be steady-state, this is not true for the tests at a workrate above the VT [125].

Figure 1.14 shows the general outline of a step exercise test. It begins with a period of rest. In most studies an interval of cycling at an “unloaded” level (i.e. 0 W) [17, 27, 74] or at a fixed baseline, which is generally the lower power output available on the ergometer [5, 133], follows. Whipp and Wasserman [130] chose to

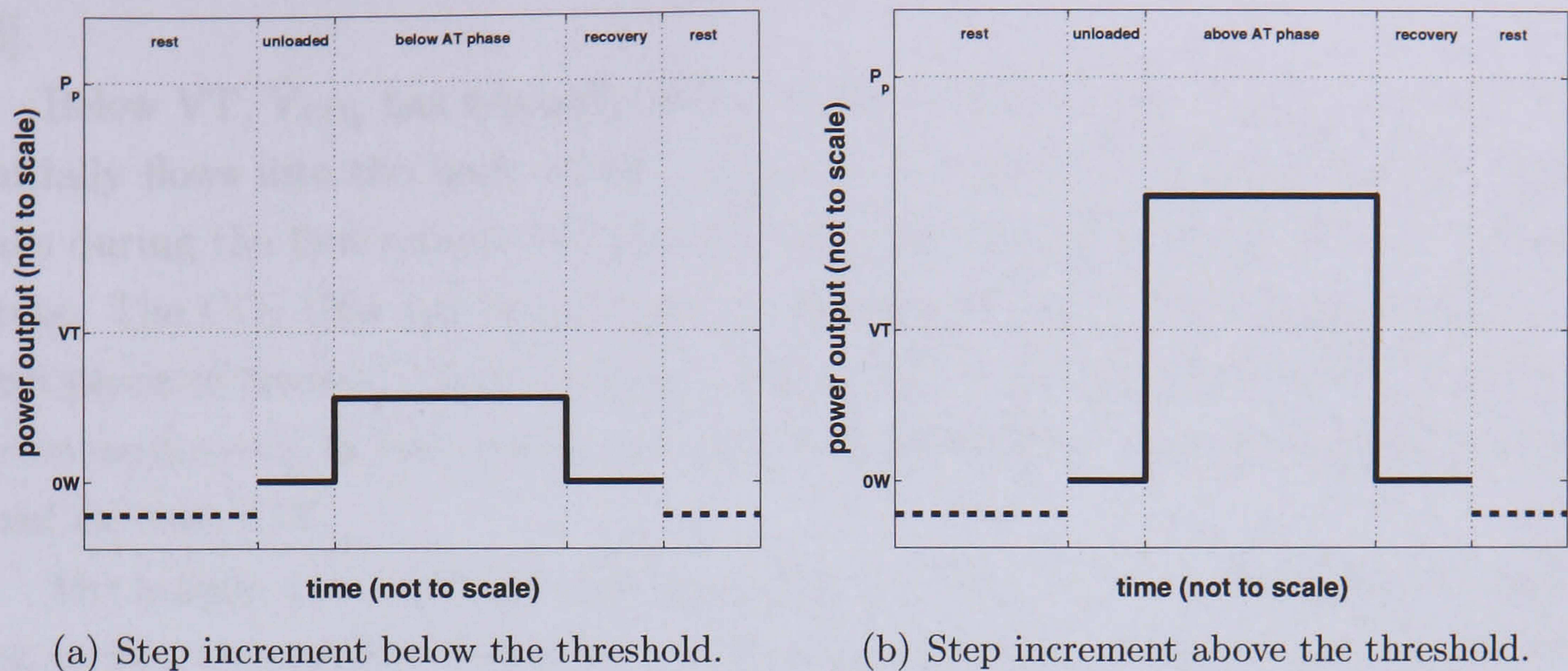


Figure 1.14: Schematic of a step exercise test.

pass directly from rest to work. A step increment in power output follows, and its amplitude depends on the aim of the study.

The highest work rate at which \dot{V}_{O_2} can reach a steady state is called the *critical power*. This lies approximately halfway between VT and $\dot{V}_{O_{2max}}$. For higher power outputs exhaustion is reached just after $\dot{V}_{O_{2max}}$ [127]. A *moderate* workrate is any level of power output up to the VT (see figure 1.14(a)). A workrate between the VT and the critical power is considered *heavy*. Workrates above the critical power, that lead the subject to exercise at the $\dot{V}_{O_{2max}}$, are termed *severe* [127].

The outcome measures for this test are: the time constant of oxygen uptake dynamics (τ , see equation (1.9)), the steady-state oxygen uptake and the efficiency of exercise. Efficiency is defined as the ratio of work accomplished to energy expended (see chapter 7).

When a subject is exercising in steady state below the VT, the gas exchange at the mouth reflects accurately the gas exchange occurring at the muscle level [129]. A steady-state response can be obtained when the subject performs a constant load test of moderate intensity. All the gas exchange variables need some time to reach a steady state. This time delay is different for each of the variables and it depends on the fitness level of the subject [109].

\dot{V}_{O_2} at the lungs increases monoexponentially at the beginning of constant load exercise, without appreciable difference in τ in a given subject if the workrate is below the VT. Fitter subjects tend to have smaller time constants. Thus, the steady state is reached more quickly and the O_2 deficit is smaller. In general, the kinetics of \dot{V}_{O_2} , if measured with a single exponential, become slower if work rate increases

[5].

Below VT, \dot{V}_{CO_2} has typically slower kinetics with respect to \dot{V}_{O_2} , because CO₂ initially flows into the body stores. This is reflected in the behaviour of R, which falls during the first minutes of exercise and then rises again to reach a new steady state. The CO₂ that has been stored is released at the end of exercise, during the first phase of recovery (R overshoots). R generally increases with workrate, but at a given workrate it is lower in fitter subjects. It decreases during prolonged constant load exercise [127].

The oxygen cost of work is approximately $10 \text{ ml}\cdot\text{min}^{-1}\cdot\text{W}^{-1}$ in AB subjects doing leg cycling at moderate intensity. For heavier exercise intensities the oxygen cost is greater, generally in the range $12\text{-}17 \text{ ml}\cdot\text{min}^{-1}\cdot\text{W}^{-1}$, when it is still possible to reach a steady state [5, 8, 17].

Chapter 2

Spinal Cord Injury

2.1 Summary

This chapter provides information on spinal cord lesions. It gives an overview of the causes of spinal cord injury (SCI), the classification used and the related health problems that arise with this pathology.

The concept of Functional Electrical Stimulation (FES) is introduced and its applications on paralysed subjects discussed. A particular focus is placed on muscle fibre type recruitment during FES exercise, since it is important in explaining the achievements of this kind of exercise. The literature reports two main hypotheses: the inverse recruitment pattern theory and the non-selective recruitment pattern.

The main benefits that can be achieved by means of FES are reported. The possibility of training the cardiovascular and pulmonary systems relatively quickly and with better results than with traditional physiotherapy methods, and the reduction in atrophy of skeletal muscles are discussed in detail.

2.2 Spinal Cord Injury

Spinal cord injury is a medical condition that usually requires tremendous changes in a person's lifestyle. The onset of a spinal injury introduces many physical impairments that change people's capacity to carry out activities of daily living. These drastic changes in lifestyle occur in seconds [86]. A spinal lesion totally or partially destroys the flow of sensory and motor information from the brain to the periphery of the body and vice versa. Not only do injured people lose the capacity to walk, but changes that are more important occur also in the sensory and autonomic sys-

tems [71]. The principal factors that control SCI people's lives are impairment of bowel, bladder and sexual function, and in some cases also limitations in hand use. Moreover, there are psychosocial consequences that have a deep impact on people's perception of themselves [121].

Prior to World War II the main causes of death in SCI people were infections of the lungs and urogenital system and septicemia from infection of pressure sores. Now the main cause of death is cardiovascular disease, which occurs earlier in SCI people than in AB people [86, 132]. Other complications are deep venous thrombosis, pulmonary embolism and autonomic dysreflexia [100]; all these conditions can be life-threatening. Moreover, most spinal cord injured patients are young and, with the advances in medical care and rehabilitation, they can achieve a life expectancy not too different from that of able bodied persons [47].

2.2.1 Causes

Spinal cord injuries can be traumatic, following sports or car accidents, or due to nontraumatic disorders, such as lateral or multiple sclerosis and tumours. The main causes of traumatic spinal cord injury in the United Kingdom are reported in table 2.1. Falls are the most common cause, accounting for approximately 45.5% of injuries. Road traffic accidents follow, accounting for another 39.2% of injuries. Sports accidents do not have a high incidence. Only 7.8% of the SCI are due to sports, but most of them are caused by diving and horse riding [58]. Only rarely is the spinal cord completely severed. It is usually contused or mechanically deformed, but it remains anatomically intact [64]. The principal cause of spinal damage is the mechanical compression of the spinal cord caused by the displacement of one or more fractured vertebrae or the intrusion of a disc in the spinal cord [70]. This displacement can be momentary, but the spinal cord is immediately damaged

Causes of SCI	percentage
Falls	45.5%
Road traffic accidents	39.2%
Sport	7.8%
Sharp trauma/assault	2.4%
Other (knocked over, collision, lifting, trauma (not specified),...)	5%

Table 2.1: Principal causes of traumatic spinal cord injury in the United Kingdom [58].

because at the moment of the impact the nervous tissue and its blood supply are destroyed [51]. In addition to compression, there can be some degree of rotation, distraction or distortion depending on the type of injury [71]. Thus, the classification of vertebral injuries includes flexion, deflection, vertical compression, rotation and injuries with combined factors [70].

2.2.2 Classification

A spinal cord injury can affect sensory and motor functions of all the limbs or only of the lower limbs. The first case is called *tetraplegia* and it is defined in the International Standards for SCI classification [82] as the “impairment or loss of motor and/or sensory function in the cervical segments of the spinal cord due to damage of neural elements within the spinal canal. Tetraplegia results in impairment of function in the arms as well as in the trunk, legs and pelvic organs. It does not include brachial plexus lesions or injury to peripheral nerves outside the neural canal”. The second case is called *paraplegia* and it is defined again in the International Standards for SCI classification [82] as the “impairment or loss of motor and/or sensory function in the thoracic, lumbar or sacral (but not cervical) segments of the spinal cord, secondary to damage of neural elements within the spinal canal. With paraplegia, arm functioning is spared, but, depending on the level of injury, the trunk, legs and pelvic organs may be involved. The term is used in referring to cauda equina and conus medullaris injuries, but not to lumbosacral plexus lesions or injury to peripheral nerves outside the neural canal”. Quadriparesis and paraparesis refer to an incomplete injury at the cervical level of the spinal cord and at the thoracic, lumbar or sacral level, respectively [103]. Paraplegia and tetraplegia occur approximately in the same percentage [100].

A spinal cord injury to a given segment is identified by a spinal cord region, a corresponding nerve and the degree of completeness [64]. An injury can be neurologically *complete*, *incomplete* or *discomplete* according to the amount of functionality retained below the level of injury. Immediately after the sectioning of the cord has occurred, all the reflexes below the level of the section are lost. This state of *spinal shock* can remain present for several weeks and is due to the blood hypoperfusion that slows the propagation of electrical signals along the axons of the nerves [84]. With a complete transection the sensory and motor functions below the level of the injury are lost. In the case of a partial, or incomplete, transection of the spinal cord, some tracts may be spared. Usually, if the cause of the lesion is a tumour, some

tracts may be affected only partially. A motor and sensory complete lesion in which the passage of some electrophysiological signals is retained is called discomplete [103].

The severity of injury is classified using the American Spinal Injury Association (ASIA) impairment scale (see table 2.2).

Grade	Description
A	Complete; no sensory or motor function preserved in the sacral segments S4-S5
B	Incomplete; sensory but no motor function preserved below the neurological level and extending through the sacral segment S4-S5
C	Incomplete; motor function preserved below the neurological level; most key muscles have a grade <3
D	Incomplete; motor function preserved below the neurological level; most key muscles have a grade >3
E	Normal motor and sensory function

Table 2.2: ASIA impairment scale [84].

Grade A corresponds to a complete injury. Grades B, C and D indicate different levels of incomplete injury. Grade E indicates normal functionality.

The level of injury can be identified in different ways. The *neurological level* identifies the most caudal segment of the spinal cord that retains normal motor and sensory functions. The *sensory level* and the *motor level* are used to identify the most caudal segment of the spinal cord that retain normal sensory and motor function, respectively. The *skeletal level* refers to the greatest vertebral damage found [103].

A list of the key muscles used in the classification of the motor level of the spinal cord injury is reported in table 2.3. Table 2.4 shows the classification of muscle grades. The grades range from 0, total paralysis, to 5, complete control of the muscle.

It is necessary to make a distinction between upper and lower motoneurone injuries. An upper motoneurone injury results in spastic paralysis and exaggerated reflexes below the injury. A lower motoneurone injury causes the loss of sensorimotor reflexes, thus resulting in a flaccid paralysis [64]. Therefore, the muscles innervated by the nerves exiting from the vertebral column at the segmental level of the injury suffer from a flaccid paralysis. On the contrary, below the level of the lesion the reflex arcs are still intact, thus the paralysis is of a spastic type [51]. The correct

Motor level	Key muscle function
C5	Elbow flexion
C6	Wrist extension
C7	Elbow extension
C8	Finger flexion
T1	Finger abduction
L2	Hip flexion
L3	Knee extension
L4	Ankle dorsiflexion
L5	Long toe extension
S1	Ankle plantarflexion

Table 2.3: Key muscles for ASIA motor neurological level classification [84].

Grade	Description
0	total paralysis
1	palpable or visible contraction
2	active movement, gravity eliminated
3	active movement, against gravity
4	active movement, against some resistance
5	active movement, against full resistance
NT	not testable

Table 2.4: Classification of muscle grades [84].

functioning of the synapses is fundamental for the normal maintenance of the nerve. A neurone may degenerate, shrink or atrophy if the synaptic terminal is missing. Therefore, the neurones connected to those that are damaged may also be affected [103].

2.2.3 Related Problems

After a spinal cord injury, the connection between the brain and the alpha motor neurones which are connected to the muscles in the limbs is interrupted, but the motor neurones themselves can still be intact. One or two years after the injury the damaged spinal cord area reaches a steady state condition, that will not change for the rest of the patient's life. However, other parts of the body continue to decondition [94]. Circulation is reduced and the risk of cardiovascular diseases increases, as the stress on the heart is lower than in AB people. Moreover, paralysed muscles

become atrophic, bone begins to demineralize and to be resorbed and pressure sores are likely to develop.

SCI people generally lead very sedentary lives and therefore are more susceptible to cardiopulmonary and muscular deconditioning than AB people. For example, in paraplegic people with a motor-complete lesion the muscle mass available for voluntary exercise is limited to the upper limbs. Therefore, it is harder to challenge the cardiorespiratory system, as the number and the size of the muscles involved in the exercise is small. It has been shown that even in AB people arm exercise is less effective than leg exercise in improving fitness [29]. For equal submaximal workloads, the physiological cost is higher for arms than for legs. However, at maximal effort leg exercise elicits greater physiological responses [100].

Paralysed muscles cannot contribute to venous return during exercise, thus causing blood pooling and reducing systemic filling pressure [100]. Therefore, in SCI people the peripheral system can be fatigued before the cardiovascular system has reached its limit [132]. In general, persons with paraplegia develop “circulatory hypokinesia”, which means that they have lower cardiac output (\dot{Q}) for any oxygen uptake than AB people and an inability to distribute the blood in the vascular system properly [63]. This can be due in part to the fact that while in AB people during exercise the blood is summoned from the inactive tissues to be sent where it is needed, in SCI people the sympathetic nervous system is partially or completely impaired. Thus, the cardiac response is reduced, as the absence of sympathetic control impairs vasoconstriction of the lower limbs [63].

The physiological responses of the body to the requirements of exercise in AB people are higher heart rate (HR), \dot{V}_{O_2} and stroke volume (SV). These responses cause an increment in \dot{Q} to match the need of oxygen in the skeletal muscles. Persons with SCI show significantly higher HR and lower SV and \dot{Q} during voluntary submaximal arm-cranking. The level of SV is lower because of the diminished venous return from the paralysed limbs. Moreover, the sympathetic reflexes are important in controlling the body temperature [71]. Thus, the sweating response to exercise is inadequate, since these reflexes are affected by spinal cord injury [24]. This leads to an early onset of fatigue.

Many studies have shown that $\dot{V}_{O_{2peak}}$, HR and power output (PO) are much lower in the SCI population than in AB people [44, 45, 108]. Barstow *et al.* [6] reported that oxygen uptake kinetics in SCI subjects are slower than in AB subjects. They also reported a threefold increase above rest of the metabolic rate in SCI subjects during unloaded cycling, compared to a doubling in AB. They suggested

that the slower pulmonary gas exchange and ventilation kinetics in SCI subjects could be due to the reduced aerobic capacity. Raymond *et al.* [108] compared FES cycling in paraplegics with voluntary cycling in AB subjects. The outcome was that when the SCI and AB groups cycled at a similar steady-state oxygen uptake, the power output was 4.5 times lower for SCI subjects.

Paralysed muscles become atrophic and can develop less force than healthy muscles. Muscle atrophy can be due to *disuse* or *denervation* and it consists of a reduction in the size and/or the number of fibres present in a muscle. Denervation atrophy occurs when the nerves that supply the skeletal muscles are severed, while disuse atrophy is caused by loss of muscle activation due to an injury to the spinal cord segments. The second kind of atrophy is more pronounced in muscles that normally would bear weight than in the others, because it is the change in the load sustained by the muscles themselves that causes atrophy. It is possible to see a similar pattern of atrophy in other conditions in which the weight borne by the muscles changes, such as space flight, limb immobilization, etc. [103].

The presence of spasticity in paralysed muscles causes a shift in distribution from type I fibres to type IIb fibres [132]. Spasms are triggered by peripheral inputs, such as touching the skin or moving the limb passively for example. The change in fibre type distribution starts to take place 4 to 6 weeks post injury and in approximately 5 months 62% of the fibres have undergone the transformation [15]. This finding is confirmed by Round *et al.* [111] who found that the subject with the most recent injury had the higher percentage of type I fibres. They maintain that it is necessary a continuous activity in order to preserve the expression of the slow-twitch fibre characteristics. A study from Cramer *et al.* [21] showed a small cross-sectional area in paralysed muscle fibres and a predominance of type IIb fibres. Grimby *et al.* [50] found that in paraplegic people the muscle fibre type composition is normal in the arms, while mainly type II muscle fibres are present in the paralyzed limbs. Moreover, in their study most type II fibres were type IIb. Thus, they concluded that a spinal cord lesion causes a change in the influence of neurones on the muscle fibres.

Bone demineralisation occurs principally during the first year after injury and it continues at a slower rate subsequently [64]. It is caused by bone resorption occurring at a higher rate than bone growth in the paralysed limbs [132]. Thus, SCI subjects can more easily fracture their bones, even during daily life activities, such as transferring.

Prolonged pressure applied on the same area of skin and inadequate circulation

can create decubitus ulcers [43]. Generally, bony prominences are the parts of the body where pressure sores occur [67].

Traditionally, SCI people undergo medical and surgical stabilization in the acute phase of injury. Subsequently, acute and long-term rehabilitation takes place, not necessarily in units equipped with spinal cord injury specialists and resources. After the acute rehabilitation period the patient is expected to start again to live in the community. However, physicians outwith the spinal units of the hospitals are often not familiar with spinal cord patient issues. Recently, new options for SCI people have been proposed, thanks to innovations in technology and science. Such options are surgical rehabilitation of upper extremities through tendon transfer and Functional Electrical Stimulation (FES, see section 2.3) for restoration and improvement of functionality and strength in paralysed muscles [112].

2.3 Functional Electrical Stimulation

An effective method for reconditioning the body is by dynamic exercise, because this produces a remarkable cardiovascular and respiratory stress along with stressing bones, joints and muscles [96]. The concept of FES is based on the fact that muscles with an intact reflex arc, i.e. with intact lower motoneurons, are electrically excitable. Therefore, denervated muscles cannot be stimulated with commercially available stimulators [65]. In other words, only people who have an upper motoneurone damage and whose motor units are intact can successfully use FES outside the research environment [43].

Traditionally, to obviate the health problems listed in section 2.2.3 voluntary arm cranking exercise was used. However, the muscle mass used with this kind of exercise is very limited. Moreover, it does not help to solve the problem of venous pooling and muscle atrophy in the lower limbs.

FES is the application of a controlled electrical stimulus to the intact peripheral nervous system in order to provide muscular contraction and to produce a functionally useful movement. Figure 2.1 shows schematically the delivery of an electrical stimulus to the nerve through surface electrodes. Electric current flows from one electrode (the anode) to the second electrode (the cathode) mounted on the skin and stimulates the nerve bundle lying underneath. The capacity of the nerve to be stimulated depends on the properties of the nerve itself (membrane permeability, diameter of the axon, relative position of electrode and nerve) and on the parameters of the electrical impulse [65].

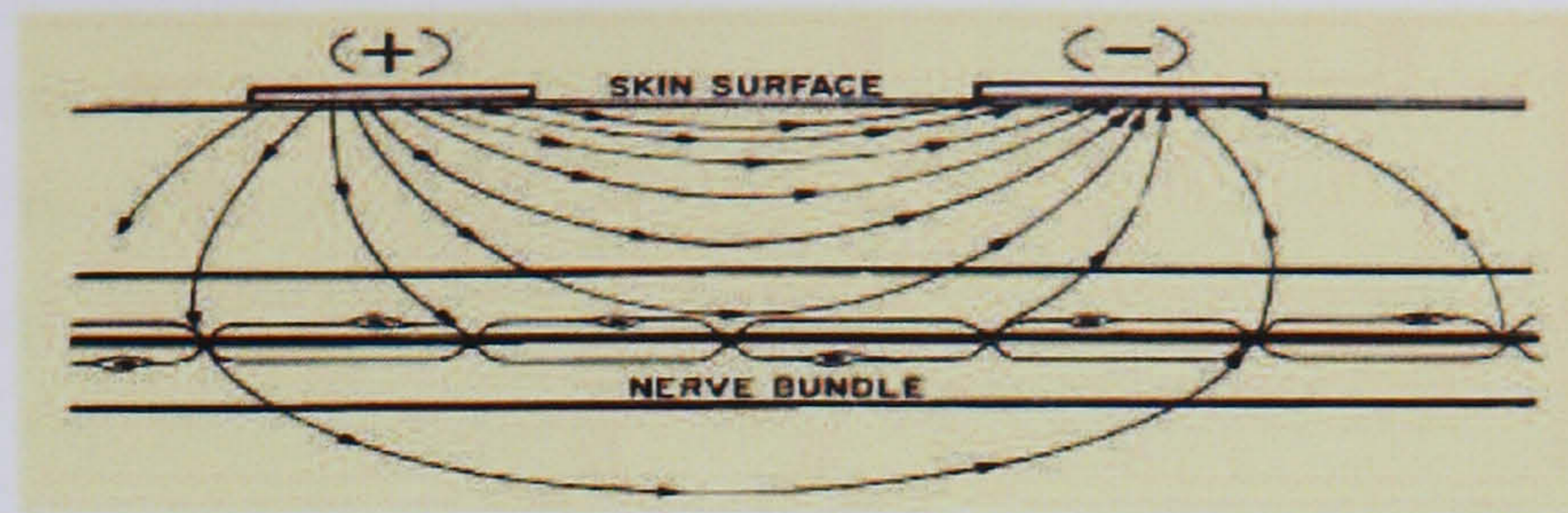


Figure 2.1: Schematic of Functional Electrical Stimulation. Adapted from [12].

Electrical stimulation is an “all-or-none” event. If the charge flowing through the electrodes is below the nerve threshold, nothing happens. When stimulation is increased above the threshold, an action potential is generated. The contraction subsequently taking place in the stimulated muscle is in no way different from a natural one. Generally one electrode stimulates various nerve fibres, and the number of activated fibres depends on the intensity of stimulation [65]. The intensity of stimulation is determined by the pulsewidth level, the frequency and the current amplitude up to a saturation level. The instantaneous charge delivered is given by the product of current amplitude and pulsewidth. Therefore, different combinations of pulsewidth level and current amplitude can produce the same response in the muscles. The force output depends on the charge delivered to the muscles and it is also affected by the position of the electrodes and by the physical condition of the subject [113].

One pulse of stimulation generates a single muscle twitch. If a series of pulses is delivered to the muscle, a prolonged contraction can be obtained. Increasing the frequency of the pulses increases the smoothness of the contraction and the force developed by the muscle, up to a limit. The drawback of increasing the frequency is the onset of fatigue. Fatigue occurs in all muscle contractions, be it volitional, caused by reflexes or stimulated. When muscles are activated by means of FES, fatigue occurs earlier at higher frequencies. Fatigue can be retarded by varying the duty cycle of the stimulation, i.e. the ratio of time during which the muscle is stimulated versus the time during which the muscle rests [65].

Three types of electrodes are typically used for FES, and each of them presents advantages and disadvantages.

Surface electrodes: this kind of electrode is the most widely used. The main advantage of surface electrodes is that they can easily be applied and removed without the need of surgery. A disadvantage is the poor selectivity in the

discrete stimulation of muscles. Moreover, it is not easy to stimulate deep muscles, and the presence of wires to connect the electrodes to the PC or the stimulator is cumbersome. The time needed for donning and doffing the apparatus is long, and this can be time-consuming if done daily. Sometimes surface electrodes can provoke allergic reactions on the skin [54, 65]. Another main disadvantage is that it is difficult to position the electrodes in exactly the same way day to day. To solve this problem a tight fitting garment with incorporated electrodes has been created, thus the position of the electrodes is guaranteed to remain the same through all the sessions and the donning/doffing time is reduced [132]. Surface electrodes stimulate sensory nerves too, thus it is possible that if the subject has intact or partial sensation the stimulation becomes uncomfortable. Moreover, stimulation of the sensory nerve can cause spasticity or reflex responses. There is also the possibility of skin burns if the stimulation is not well controlled [65].

Percutaneous electrodes: these electrodes are implanted via a hypodermic needle and they are intramuscular. The main disadvantages of these electrodes are that they are liable to breakage, thus they need to be replaced periodically (their failure rate is 4% per month after 6 months) and the insertion site has to be maintained clean as they have problems of infection [65]. The selectivity is better with respect to surface electrodes and they can easily be removed and replaced in case of breakage, the current needed to stimulate the muscles is lower with respect to surface electrodes and they can reach deeper muscles [54, 65].

Implanted electrodes: these electrodes are suited for long term application. Once in situ their recruitment characteristics are likely to remain the same, and they do not require donning and doffing time. One of the disadvantages is that a surgical procedure is required for the implantation. Only recently a new kind of implanted electrode has been developed that does not require major surgery to be positioned (BION microstimulators, Alfred Mann Foundation, Valencia, CA, USA). Being completely implanted, possible infections may not remain confined but they could spread throughout the body [54].

Electrical stimulation can be applied to the paralysed limbs in order to obtain a functional movement, hence the name “Functional”. Exercise by means of FES can be performed in different ways. The most investigated kinds of exercise are knee extension, standing, cycling and walking. Typically, muscle strengthening is

suggested before starting any kind of FES exercise. This can be done through an FES-knee extension training program. The quadriceps are stimulated intermittently while the subject is sitting or lying. Once the subject is able to perform a predefined number of extensions, weight is added to the ankle until the muscles are sufficiently strong to start the training program for standing, cycling or walking. FES can be considered as a therapeutic technique since it can promote higher levels of health with respect to traditional exercise in SCI and it has a rehabilitation potential higher than that accomplished with voluntary arm cranking [43].

The work related in this thesis is focused on FES-Leg Cycle Ergometry (FES-LCE) exercise. FES can be applied to the lower limb muscles according to a specific pattern in order to obtain a cyclic motion.

2.3.1 Motor Unit Recruitment

It is generally agreed that during voluntary muscle contractions the nerve fibres are recruited in size order, i.e. from the smallest to the largest [39, 73] (see also section 1.3.2). The debate is still open regarding what happens when FES is used to obtain contractions.

Some authors maintain that the recruitment order is inverted with respect to voluntary exercise. Trimble and Enoka [122] say that the recruitment order depends on the axon diameter and also on the distance between the axon and the electrodes. They found that the time needed to reach the peak force increased with the intensity of the stimulus. They suggested that this is a sign that slower motor units were progressively recruited. Thus, they concluded that the activation of motor axons through surface FES takes place with a recruitment order opposite to that seen in voluntary contractions. They also suggested that this finding could be useful in rehabilitation, as with FES it is possible to recruit muscle fibres that can be trained only at high intensities in voluntary exercise. Hamada *et al.* [52] found that during FES the large motor units progressively stop contributing to the muscle contraction. They maintain that with FES the first fibres to be recruited are type II fibres, because of their large axonal diameter. They justify this affirmation by evidencing the significant increase in blood lactate and R after FES exercise, which they say is caused by the utilization of fatigable glycolytic fibres. Fang and Mortimer [30] argue that the poor force gradation and muscle fatigue seen in FES exercise is due to the reverse recruitment order of muscle fibres. Feiereisen *et al.* [31] report that the axon's impedance, the size of its branches and its orientation in the current

field control the reverse activation of the muscle fibres. They also maintain that the fact that in only 38% of their trials reverse activation occurred was due to the deeper localization of the larger axons in the muscles. This is why they were not recruited first in most cases.

Other authors refute the previous hypothesis. Thomas *et al.* [120] found that with FES the weaker motor units were activated first and the stronger ones were activated subsequently. This is what happens also in voluntary contractions: the weak and fatigue-resistant fibres are activated first, then the fast-conducting, stronger fibres are recruited. Knaflitz *et al.* [73] maintain that the reverse recruitment occurs when the nerve is stimulated directly. On the contrary, with surface stimulation, muscle fibre recruitment depends on the size of the motoneurons and their branches, on the location and orientation with respect to the current field of the branches, and on the position of the electrodes. In their study, 23 out of 32 experiments showed a similar recruitment pattern as in voluntary contractions. Gregory and Bickel [49] say that during voluntary contractions additional units are recruited when necessary and that the firing rate can be modulated to retard fatigue. With FES this is not possible. The fibres are recruited together and the force that the subject can develop drops when the fibres fatigue. They maintain that if the inverse recruitment pattern took place, fatigue would decrease with the increase in stimulation intensity. Indeed, if this was the case, the slow, less fatigable fibres would be recruited at higher intensities. However, this does not happen. Moreover, they argue that increasing the stimulation intensity would provoke a decrease in the rate of rise of the torque developed, as more slow fibres are recruited. This does not occur and the rise time is similar at different intensities. Thus, they conclude that at low or high force levels the selection of the fibres is non-selective. In addition, the recruitment pattern is spatially fixed and temporally synchronous, and there is no particular sequencing connected to fibre types.

2.4 Benefits of FES

2.4.1 Cardiovascular and Pulmonary System

FES-LCE can induce high levels of aerobic and cardiac responses. Moreover, it can also elicit positive central and haemodynamic responses [44, 101, 105]. Because of the non-physiological activation of the muscles, the histochemical changes in the paralysed muscles and the inappropriate joint biomechanics, FES exercise is

intrinsically highly inefficient [45]. However, when the purpose of FES exercise is to improve the subject's fitness, the inefficiency can be considered an advantage. Indeed, it is possible to elicit high cardiopulmonary responses with low mechanical stresses to the limbs [45].

In general, after several weeks of training, SCI subjects can exercise at power outputs that elicit \dot{V}_{O_2} levels similar to those found in AB people when walking [43]. Davis [24] maintains that SCI subjects who exercise regularly have higher $\dot{V}_{O_{2peak}}$ and exercise capacity with respect to those who do not exercise.

Barstow *et al.* [3] found that in constant load exercise R was reduced after training, thus showing that the aerobic capacity of the subjects increased. Moreover, the kinetics of \dot{V}_{O_2} , \dot{V}_{CO_2} and \dot{V}_E were significantly faster after training and the intersubject variability of kinetics decreased [2]. This finding implies that the subjects' fitness was improved. Faghri *et al.* [29] reported that resting blood pressure decreased with training, thus showing a similar behaviour as in AB subjects. Their study also showed an increase in SV and \dot{Q} following training, thus suggesting an improvement in cardiovascular fitness. They argue that this outcome could be helpful in increasing the performance of daily activities and in reducing the risk of cardiopulmonary complications. The increase in SV and \dot{Q} has also been found by Glaser [43].

Glaser *et al.* [44] found that at the same power output SCI subjects had significantly higher \dot{V}_{O_2} than AB subjects, while the maximum power output that they could sustain was lower. They explained this as the result of the non-physiological activation of the muscles and their deteriorated condition. Therefore, they suggested that there is much scope for improving SCI people's cardiorespiratory system by means of FES exercise, because of the relatively high metabolic rate it elicits. In a review paper about the benefits of FES exercise, Janssen *et al.* [67] said that this type of exercise elicits high levels of aerobic metabolic and cardiopulmonary responses.

Barstow *et al.* [7] compared voluntary arm exercise and FES leg cycling in SCI subjects. They found that $\dot{V}_{O_{2peak}}$ was similar for both exercise modalities, but peak heart rate and power output were significantly lower during leg exercise. In constant load tests during arm exercise heart rate was higher and gas exchange kinetics quicker than during leg exercise. They concluded that gas exchange responses during arm cranking were in the normal range for paraplegics doing voluntary exercise, thus the changes that occur during FES cycling depend on the lower limb exercise only. Figoni *et al.* [35] found that within a group of tetraplegic subjects HR was lower

during FES cycling than during voluntary arm cranking, while $\dot{V}_{O_{2peak}}$ was equal. In contrast, cardiac output, stroke volume and arterial blood pressure were higher during FES-cycling.

Davis *et al.* [25] studied hybrid exercise (i.e. voluntary arm-cranking and FES-LCE exercise) in paraplegic subjects. They reported that steady state HR and \dot{V}_{O_2} did not change significantly. However, \dot{Q} and SV increased. Thus, they also suggested that FES can help in reducing oedema and orthostatic hypotension as well as coagulation risks. Moreover, they hypothesize that upper body exercise capacity can be improved through the increase in SV and \dot{Q} , as more blood is available. Glaser [43] suggests that hybrid exercise can improve cardiopulmonary fitness better than arm-cranking or FES-LCE exercise alone. This belief is based on the larger muscle mass utilized during hybrid exercise. Moreover, venous return is enhanced and \dot{Q} consequently increases. It has also been shown that \dot{V}_{O_2} is higher in hybrid exercise: the \dot{V}_{O_2} elicited by this kind of exercise is about 2 l/min in non-athletic paraplegic subjects [43]. In the same study an interaction between arms and legs was pointed out. If the power output required of the arms is increased beyond a certain level, the exercise capacity of the legs decreases. The inverse is also true. Mutton *et al.* [89] confirm these findings. In a study involving 11 paraplegic volunteers undergoing FES-LCE and hybrid exercise, they found that \dot{V}_{O_2} significantly increased after the hybrid exercise. Moreover, the work rates reached with the hybrid exercise were higher than with FES-LCE alone.

2.4.2 Reduction in Atrophy of Skeletal Muscle

Untrained SCI subjects can achieve significant improvements in fitness following FES-LCE exercise [1, 2, 98, 105, 116].

Glaser *et al.* [43, 44] state that FES resistance training leads to improvements in muscle strength and endurance. In their study, the subjects were able to cycle only for a few minutes at a power output of 0 W at the beginning. After training the subjects were able to cycle consecutively for 30 min at a power output of up to 30 W. It is also reported that the relationship between power output and \dot{V}_{O_2} is linear. Glaser [43] suggests that the increase in PO and \dot{V}_{O_2} after training is due mainly to peripheral adaptations with some central adaptations. It is difficult to determine exactly the relative contributions of the two types of adaptation. In general, long-term training at high PO and \dot{V}_{O_2} levels leads to an enhancement in central adaptations, with an increment in the functional capacity of the cardiovascular system. Pollack

et al. [101] hypothesize that the increase in muscle endurance and the decrease in muscle shortening velocity found in their study is due to a disproportionate increase in slow-twitch fibres with FES training.

Ragnarsson *et al.* [105] report that after 4 weeks of knee extension training, their subjects increased the resistance from 25 N to 37 N. Rodgers *et al.* [110] confirm the usefulness of knee-extension training reporting an increase of 91% (from 58 N to 111 N) in the resistance after 12 to 18 weeks of training.

Sloan *et al.* [116] completed a study on a group of incomplete SCI subjects treated with FES-cycling training. Endurance and cycling load increased in all the subjects with increments of 11.7 min and of 30 N, respectively. Voluntary function in the legs was also partially recovered and the muscle gradings were increased.

Gerrits *et al.* [40] report an increase in resistance to fatigue in the quadriceps muscles of their subjects, following an FES-LCE training programme. Martin *et al.* [80] report that electrical stimulation contributes to increasing fatigue resistance. However, they did not find any hypertrophy of the muscles. This was explained with the lack of resistive load in their training protocol, as it is proven that muscle hypertrophy is obtained with chronic exposure to high resistive loads [80].

Six subjects took part in a study from Crameri *et al.* [21]. The result of 10 weeks of FES exercise, three times per week, was an increase in total power output developed. Moreover, the cross-sectional area of the muscle fibres significantly increased, the percentage of type IIb fibres decreased in favour of type I fibres and the density of capillaries was augmented. However, the increase in percentage of type I fibres was not significant. Janssen *et al.* [67] maintain that the shift in distribution in muscle fibre type contributes to the enhanced performance of SCI people after training with FES. They also argue that FES training induces an increase in the concentration of oxidative enzymes and mitochondria, an augmentation in capillary density and in arterial blood flow.

Several authors report an increase in thigh girth following FES training [1, 96, 99]. Arnold *et al.* [1] stimulated quadriceps, hamstrings and gluteal muscles of 12 SCI subjects to obtain FES-cycling. They found significant increases in thigh girth and also a slight but not significant increase in the girth of the calf muscles. They explained the non-significance of the change by saying that the calf muscles were not stimulated directly. Petrofsky *et al.* [96] report an improvement in endurance and muscle size after training, despite the short duration of their study, of only 30 days. Pacy *et al.* [91] showed that a training period of 10 weeks leads to an increase in the mid-thigh muscle area of 27%. Sloan *et al.* [116] reported that the

improvements in thigh girth, endurance and strength occurred regardless of the time elapsed between the injury and the start of their 3-month training period. Rodgers *et al.* [110] carried out a study on 12 subjects who trained up to three times per week for 36 sessions. They did not notice any dependence of the fitness on the number of session attended per week. They did not find significant change in thigh girth, which they explained through the possible reduction in oedema or subcutaneous fat as opposed to a lack of hypertrophy. They also reported an increase in maximum load resistance.

A possible advantage of FES is also an enhanced stretching of the musculature by inducing contractions in the antagonist muscles [67]. Rodgers *et al.* [110] found an improvement in the knee joint passive range of motion from 133 to 145 degrees. This improvement may help in performing activities of daily living, such as transferring, and reduce the incidence of joint contractures.

Improvements in spasticity due to FES have also been shown [1, 115], even if not everybody agrees on this point [115]. Arnold *et al.* [1] reported that their subjects noticed a reduced incidence in spasticity events, but an increase in the intensity of spasms. This could be due to the higher strength of the muscles after training. Sipski *et al.* [115] reported that some of their subjects felt a worsening in spasticity following FES-LCE exercise.

2.4.3 Other Benefits

FES activates a larger muscle mass, not otherwise available to paraplegic people, thus blood circulation is enhanced [43]. Sloan *et al.* [116] found that FES induced exercise improved lower limb circulation also in terms of temperature. It has been shown that contractions of the gluteal muscles induced by FES cause a change in seating pressure [67]. Petrofsky [92] found that during a two-year study with FES-cycling, the incidence of pressure sores in his subjects was reduced by 80%. Moreover, FES-induced contractions relieve ischial pressure [67].

Results on the effect of FES-LCE on bone mineral density (BMD) are controversial. Mohr *et al.* [87] report a significant increase in bone density in the proximal tibia following FES exercise three times per week. Their results also show that the frequency of training determines the amount of increase in bone density. During a follow up of six months with only one FES session per week, BMD in the proximal tibia decreased to pre-training levels. Chen *et al.* [18] report site-specific BMD changes following FES-LCE exercise. BMD increased significantly in the proximal

tibia and distal femur following training 5 times per week. However, BMD in the femoral neck showed a decreasing trend throughout the training. Moreover, once exercise was discontinued the effect faded. On the other hand, various studies reported no increase in bone density following FES-LCE exercise programmes [11, 91, 110]. BeDell *et al.* [11] found no change in bone density after training and argued that it was possible that the result indicated that osteoporosis was retarded. Rodgers *et al.* [110] found that bone resorption was slower in SCI people training with FES than expected. Thus, they concluded that FES-training could be more useful for recently injured subjects, so that muscle integrity and range of motion in the joints could be maintained and bone loss retarded. However, it is generally agreed that the reason for the lack of osteogenic response is the fact that the stresses involved have always been too low [78].

FES can also be useful in alleviating the problem of changes in articular bone and cartilage. It is proven that FES-knee extension training helps in reducing existing knee joint abnormalities due to SCI [67].

Moreover, improved capacity of dressing, transfers and general functional performance have been reported in incomplete subjects following FES training [67]. Psychological benefits have also been noticed [67]. In a study by Sipski *et al.* [115] 68% of the subjects said that their appearance was better after training and that they noticed an improvement in their self-image. They also found that the rate of incidence of depression was reduced and in general the subjects had a feeling of comprehensive well-being.

Ragnarsson *et al.* [105] recommend that the participants in an FES training programme have to be in good health and emotionally stable. Moreover, they have to be reliable and have realistic expectations regarding the outcome of the study. An important factor to be remembered is that the effects that FES training can have are quickly lost when training is discontinued. Janssen *et al.* [67] made a point of recommending the importance of making FES exercise a part of everyday life, if results are desired. It is important that FES-exercise be performed regularly and adequately.

2.5 Contraindications for FES

Wilder *et al.* [132] list a series of contraindications for FES that include implanted pacing devices, high or abnormal heart rate, heart disease, possible blood clots, some types of tumours, pregnancy, unhealed wounds, infection in the area of treatment,

denervated muscles, severe osteoporosis, limited range of motion, abnormal bone formation, severe muscle spasticity, autonomic dysreflexia, history of joint disarticulation and high fever.

Chapter 3

Incremental and Step Exercise Test Protocols for FES-cycling

3.1 Summary

This chapter introduces the experimental setup used throughout the tests and describes the development of novel protocols for exercise testing. The characteristics of the subjects participating in the study, the mechanical apparatus, the stimulation strategy and the metabolic measurements performed are described. The test apparatus allows accurate feedback control of cycling cadence and workrate. We propose new protocols for the determination of the key markers of cardiopulmonary status in the incremental exercise test (IET) and the step exercise test (SET). In the IET the new feature is the possibility of imposing arbitrarily small power output (PO) increments, thus obtaining a scaled protocol with respect to that used for able bodied subjects. In the SET it is now possible to impose power output changes that are a precise percentage of the peak power output (P_{peak}) or of the ventilatory threshold (VT). the content of this chapter is also available in a paper [33].

3.2 Introduction

Exercise tests with spinal cord injured subjects have often been performed on commercially available FES-cycle ergometers (e.g. ERGYS system, Therapeutic Technologies, Inc., Tampa, FL; StimMaster, Electrologic of America). Such ergometers typically have the limitation that the minimum increment possible in power output is 0.125 kp, equivalent to 6.1 W. Thus, incremental test protocols included steps of

6.1 W, starting from 0 W (unloaded cycling). Considering that the peak power output reached by SCI subjects is generally reported to be below 20 W [2, 48, 57, 108], the maximum number of steps achievable in an incremental test is usually no more than three. This is in contrast to what Wasserman *et al.* [125] suggest for an optimal IET for AB subjects, i.e. an increment every minute for 10-12 minutes (see also section 1.5.1). In previous studies increments in power output were imposed every 5 minutes. The average duration of the incremental tests was between 15 minutes [36, 57] and 20 minutes [56]. Moreover, rest bouts have sometimes been introduced between steps, thus breaking the continuity of the test [36, 56].

Previously, constant load tests have typically been performed in an “unloaded” condition (0 W). However, this is considered unsatisfactory, because the power needed to move the legs is relatively high for SCI subjects. Barstow *et al.* [6] quantified this power and found that it corresponded to approximately 12 W in their subjects. For AB subjects the peak value for power output is much higher than for SCI subjects. Therefore, the gap between rest and 0 W would account for a small percentage of their total capacity, i.e. small enough to be neglected. In Barstow’s study an SCI subject could reach a peak power output of about 14.5 W above unloaded. Thus, the “unloaded” cycling was a significant percentage of the total: 45%. It is likely that for untrained subjects, such as those at the beginning of the training, this level could be close to 100% or could even exceed their capability.

In subjects who are able to sustain at least 0 W, the next available level in previously used ergometers is 6.1 W. This represents a very large increment, since 6.1 W is generally a large proportion of the total workrate range in these subjects. Therefore, it is important to be able to use smaller steps for the increments in power output. It would be highly advantageous to be able to set the constant load power output to an arbitrary level within the “negative workrate range”, i.e. at an effective power of less than 0 W.

It is also possible that 0 W is a level above the ventilatory threshold, thus causing the apparent \dot{V}_{O_2} kinetics to be slower. This hypothesis could explain why in most of the previous studies the R values were above 1 during the constant load tests [6, 2, 57, 89]. 0 W could also be a level between the critical and the peak power for SCI individuals. This means that \dot{V}_{O_2} does not reach a steady state, but keeps increasing until it reaches the maximum level for the subject.

In all the previous studies the target cadence was 50 rpm, but it was allowed to vary within the range of 35-50 rpm and to drop down to 35 rpm before the test was stopped [2, 6, 29, 36, 56, 57]. The energy required to turn the legs of the subject,

i.e. to overcome inertia, can be considered a constant loss only if it does not change during exercise. However, if the cadence changes, this energy is bound to change too. Given the low value of \dot{V}_{O_2} during exercise, the energy required to overcome the inertia due to the weight of the legs is likely to be a considerable percentage of the overall metabolic expenditure. Therefore, it is important to be able to keep the cadence constant during the tests.

3.3 Methods

3.3.1 Subjects

Two subjects were recruited for this study. Both of them had just ended their participation in a bigger FES-assisted cycling study which lasted 2 years and included weekly FES-cycling sessions for up to an hour. The characteristics of the subjects are reported in table 3.1.

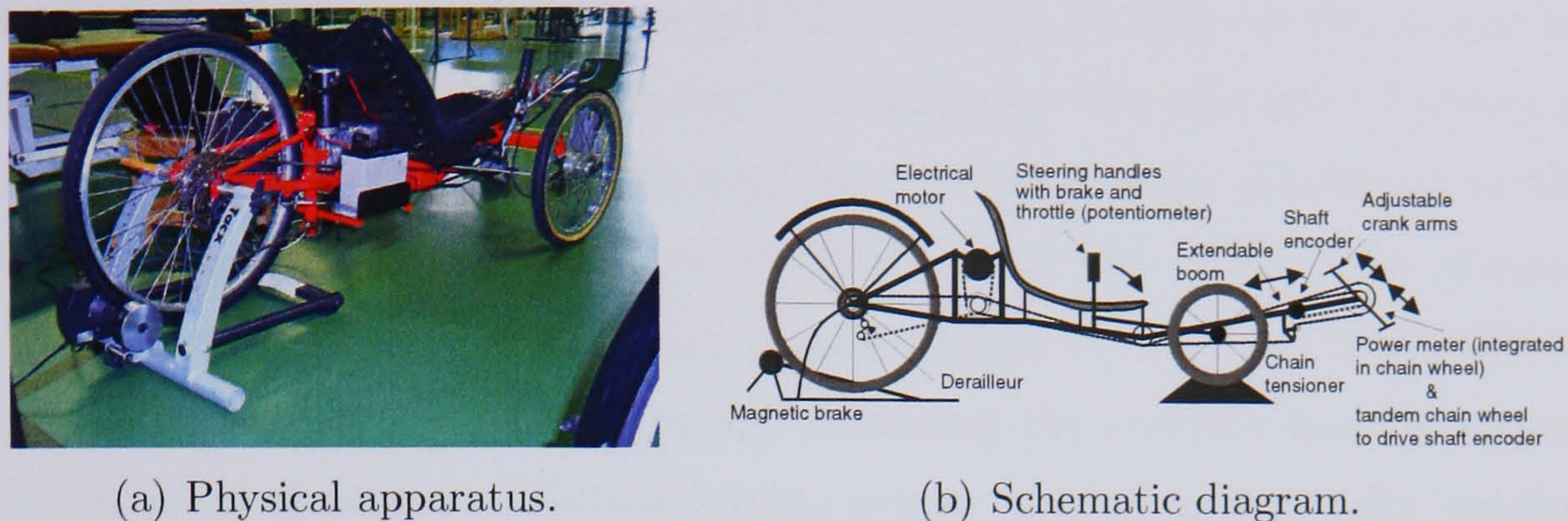
Subject	Gender	Lesion level	Age (years)	Time post injury (years)
S1	Male	T8/9	30	5
S2	Male	T10	59	5

Table 3.1: Details for the subjects who participated in the study.

The programme was approved by the Southern General Hospital ethics committee and the subjects provided written, informed consent prior to participation.

3.3.2 Apparatus

The FES apparatus used in this study is based upon a standard recumbent tricycle, which was adapted for use by SCI subjects (ICE Ltd, <http://www.ice.hpv.co.uk>) (see figure 3.1). An electric motor, positioned behind the seat, is connected to the rear drive wheel and is coupled with the cranks at the front of the tricycle. The tricycle is mounted on a cycle trainer (Tacx, Holland) that permits exercise indoors and allows different levels of resistance to be set. A shaft encoder is mounted on the crank in order to measure the angle, and the cadence is obtained by differentiation. The right crank contains a torque measurement sensor, so that the power output produced by the subject can be computed in real time. The signals obtained from the shaft encoder and the torque sensor are sent to a laptop computer and then processed



(a) Physical apparatus.

(b) Schematic diagram.

Figure 3.1: Motorized and instrumented recumbent tricycle for exercise testing during FES-cycling.

by the software. Thus, the laptop provides real-time feedback control of cycling cadence (by continuously altering the motor command signal) and of leg power (via automatic adjustment of stimulation intensity), according to the control structure shown in figure 3.2. The control software is implemented in Matlab/Simulink. The sampling frequency and the stimulator frequency are both 20 Hz.

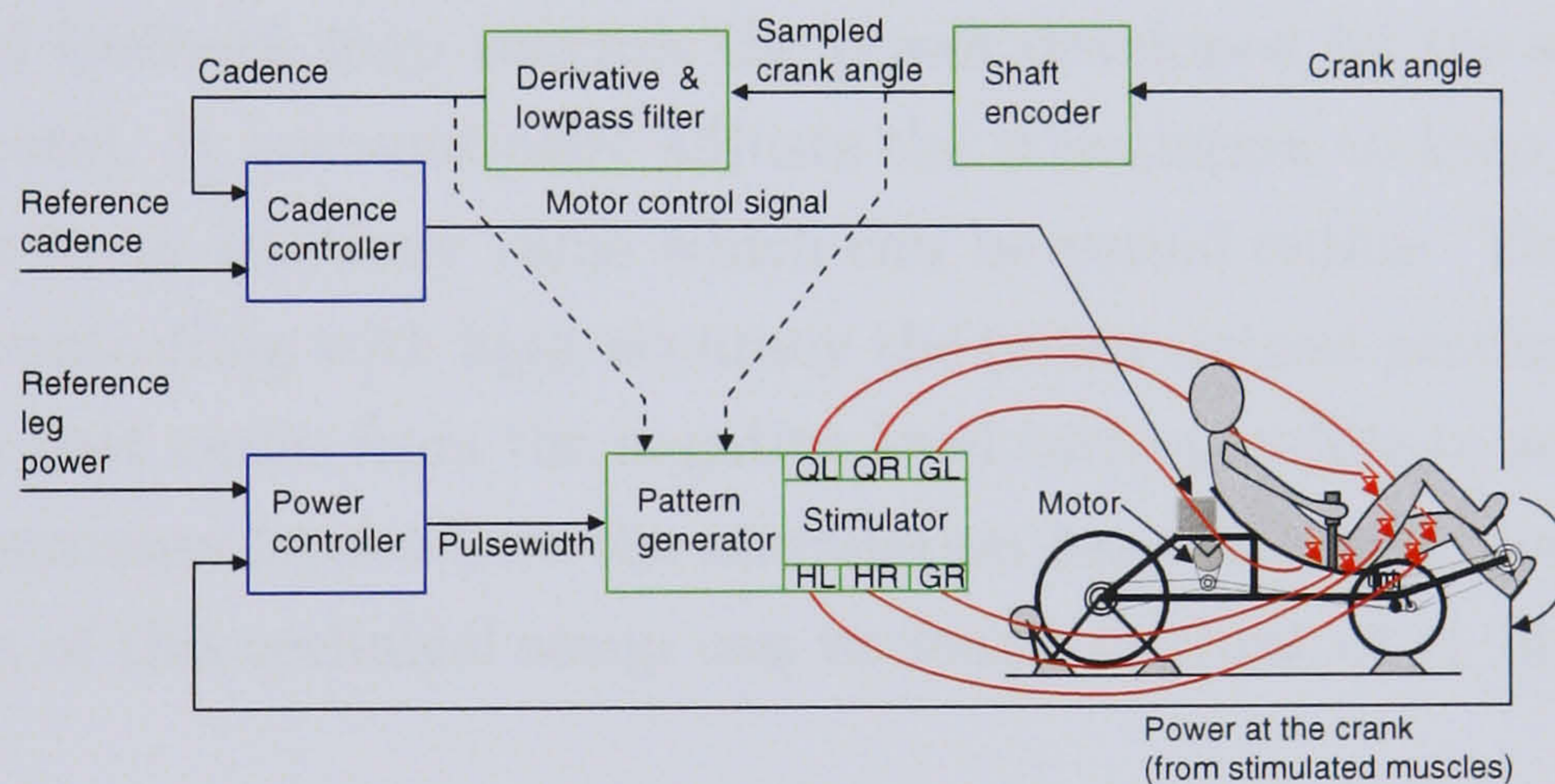


Figure 3.2: Integrated closed-loop control scheme. One loop automatically adjusts the motor input to keep the cycling cadence close to a setpoint value. The second loop automatically adjusts the stimulation pulsewidth to keep the leg power close to an arbitrary reference value. In the stimulator: QL - Quadriceps Left; QR - Quadriceps Right; GL - Gluteus Left; HL - Hamstring Left; HR - Hamstring Right; GR - Gluteus Right.

The whole control system is constituted by two independent feedback loops. The motor feedback loop is designed with the aim of keeping the cadence constant. Thus, the motor supplies the power output necessary to maintain the pedalling speed constant at a chosen rate regardless of the energy input from the legs. Therefore, without stimulation, the motor turns the legs and maintains the cadence at the

prescribed level: this is referred to as *passive cycling*. In this condition the leg power measured at the cranks is negative, corresponding to the amount of power supplied by the motor to turn the mass of the legs (in the test results presented in this work, the passive leg power is in the range of -5 W to -8 W). When the stimulation is gradually increased from zero, the leg power begins to increase from this negative value of power towards 0 W and beyond, assuming the subject has the capability to produce this level of power. The maximum power output is generally reached when the stimulation reaches its maximum (saturation) level. In this scenario, where the stimulation and leg power output are gradually increasing (as in the incremental exercise test), the motor feedback loop automatically reduces the motor output power to ensure that the cycling cadence stays at the prescribed level.

The leg power output range from the passive level up to 0 W is referred to as the *negative workrate range* in the present work. It has to be noted also that the 0 W level in this setup corresponds to the notion of unloaded cycling referred to in previous studies: in this condition, the stimulation is just sufficient to move the mass of the legs at the desired cadence.

The second feedback loop controls the power developed by the subject (i.e. the exercise workrate). It automatically adjusts the stimulation to keep the power output level close to an arbitrary value which can be varied online. Thus, there is the possibility of controlling with high accuracy the power output produced by the subject in a range that varies from the negative level corresponding to zero stimulation, up to some maximum level where the stimulation has reached its limit.

Full details of this technical setup can be found in Hunt *et al.* [61].

3.3.3 Stimulation Strategy

A multi channel current controlled stimulator (Stanmore Stimulator, UK [46]) was used to activate quadriceps, hamstrings and gluteal muscles, using round surface electrodes (PALS PLATINUM, Nidd Valley Medical Ltd). The frequency of stimulation was 20 Hz and the current amplitude could be fixed for the duration of the exercise at different levels depending on the muscle group and the subject. Table 3.2 shows the values of current amplitude that have been used with the two subjects. The stimulation pulsewidth could be varied in real time in a range from zero to a pre-defined saturation level and was the same for all the muscles. The saturation level could be changed depending on the subject. The maximum level was set to either 600 μ s or 700 μ s.

Subject	quadriceps	hamstring	gluteus
S1	110mA	80mA	80mA
S2	120mA	110mA	90mA

Table 3.2: Current intensity applied to the three muscle groups for the two subjects who participated in the study.

The angle measured at the crank was used to switch on and off the stimulation, according to a pre-specified pattern that was the same for all the subjects. The stimulation pattern is shown in figure 3.3. The arcs indicate the angle intervals during which the stimulation is on. The static stimulation pattern, figure 3.3(a), has been obtained under static conditions. When the subject is cycling it is necessary to compensate for the dynamic response of the muscle and the patterns have to be shifted forward by an angle that is proportional to the cadence. The modified pattern for a cadence of 50 rpm, i.e. that used in the tests, is shown in figure 3.3(b). The stimulation is switched on 45° in advance. The numerical values for the stimulation angles during each cycle are reported in table 3.3.

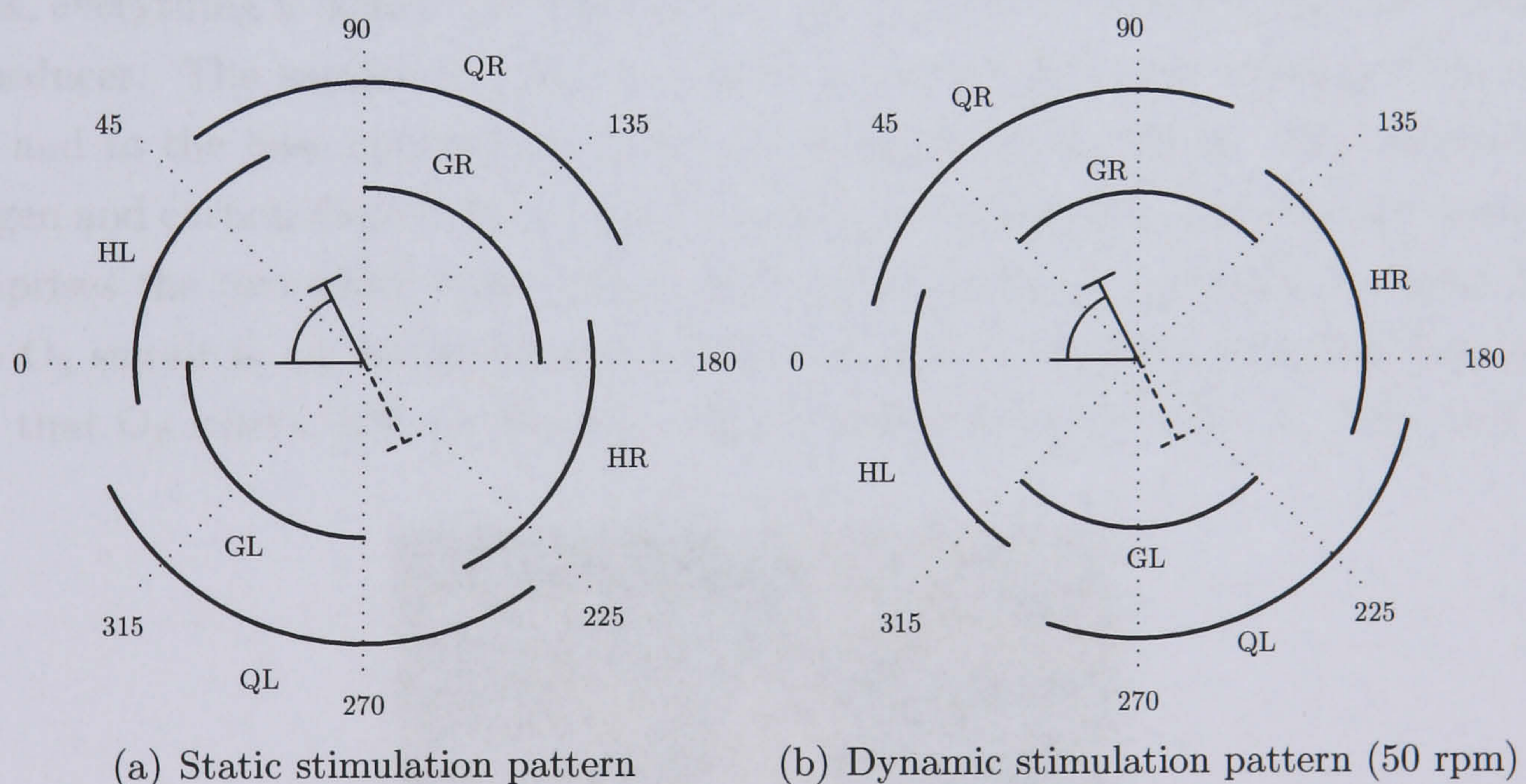


Figure 3.3: Diagram of the stimulation patterns. The arcs show when stimulation is on for each muscle group over the crank cycle: QL - Quadriceps Left; QR - Quadriceps Right; HL - Hamstring Left; HR - Hamstring Right; GL - Gluteus Left; GR - Gluteus Right. Zero position has the crank horizontal with the right foot close to the body.

Pattern	Quadriceps	Hamstring	Gluteus
Static	55°-155°	168°-245°	90°-180°
Dynamic (50 rpm)	10°-110°	123°-200°	45°-135°

Table 3.3: Static and dynamic stimulation angles for the right leg in the three groups of muscles.

3.3.4 Metabolic Measurements

During all the tests respiratory gas exchange variables were measured using a portable breath-by-breath system (MetaMax 3B, Cortex Biophysik GmbH, Germany). The subject breathed through a low dead-space mask. Respired O_2 and CO_2 concentrations were monitored in real time by discrete gas analysers. Respired volume and flow were monitored continuously through a turbine. \dot{V}_{O_2} , \dot{V}_{CO_2} , minute ventilation (\dot{V}_E) and R were derived in real time.

Figure 3.4 shows the portable component of the gas analyser. The breath-by-breath system includes a face mask, that comes in three different sizes. The mask is tightly fitted to the face of the subject through straps attached to a head cap. Thus, everything is sealed and the respired air is forced to pass through the volume transducer. The sample line for the gases is connected to the transducer on one end and to the base component of the gas analyser on the other. The sensors for oxygen and carbon dioxide are located on the base component. The base component comprises the two white boxes positioned on the subject's shoulders in figure 3.4. The O_2 sensor is an electrochemical oxygen analyser. Its function is based on the fact that O_2 reacts with a substrate and generates electrical current. The amount

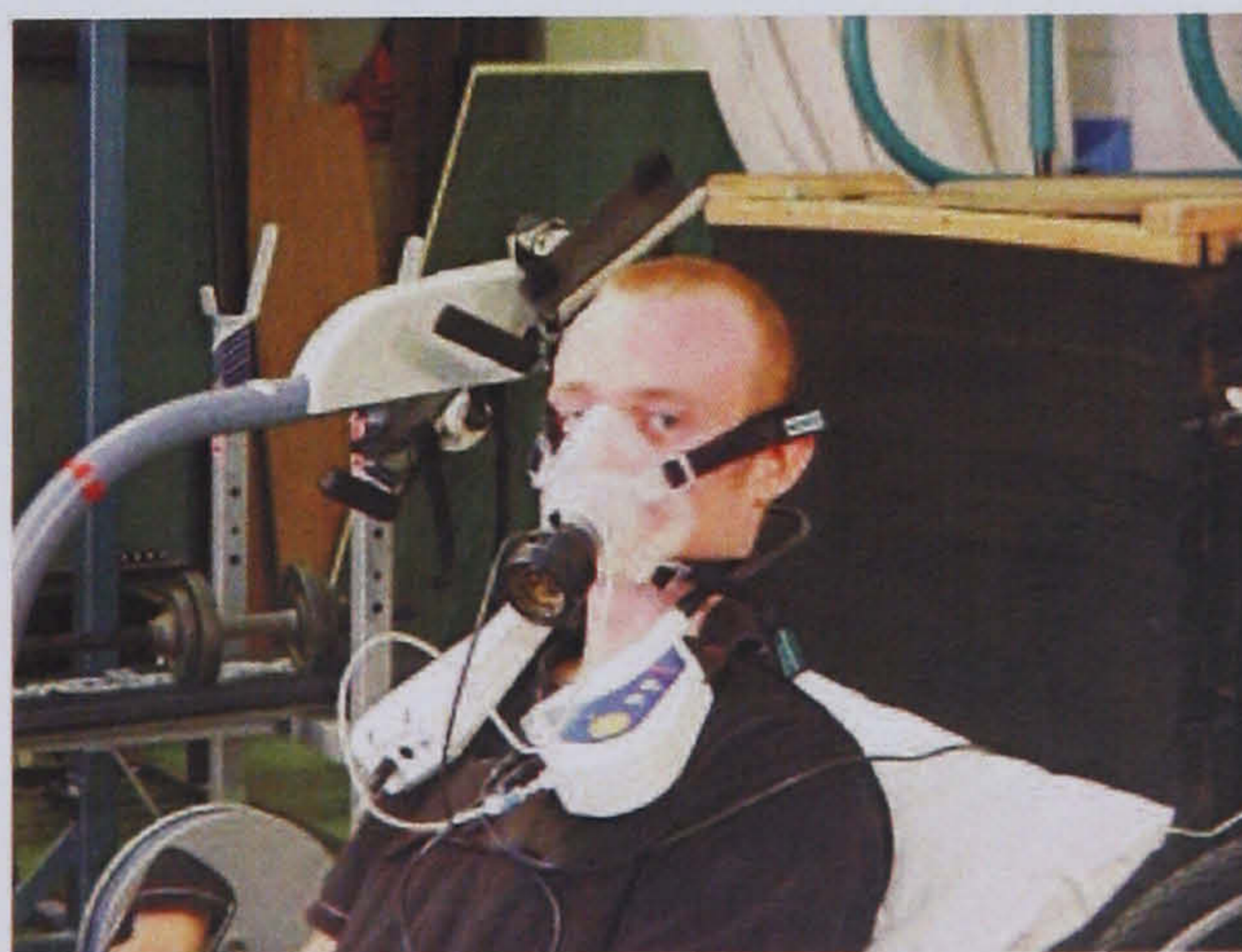


Figure 3.4: Portable component of the Metamax gas analyser.

of current that is created is proportional to the concentration of O_2 . The CO_2 analyser is an infrared cell. The gas is contained in the cell and infrared light is passed through it. The concentration of CO_2 is proportional to the absorption of the light. Thus, comparing the amount of light transmitted through the gas with a reference value, it is possible to establish the concentration of CO_2 [125].

3.4 Protocols

3.4.1 Incremental Exercise Test

Figure 3.5 shows the outline of the proposed protocol for the incremental exercise test. The times shown in the graph are approximate and depend on the progress of the test. This protocol includes an initial period of warm-up of 5 minutes, consisting in stimulated cycling at a low workrate. This is followed by a period of rest of

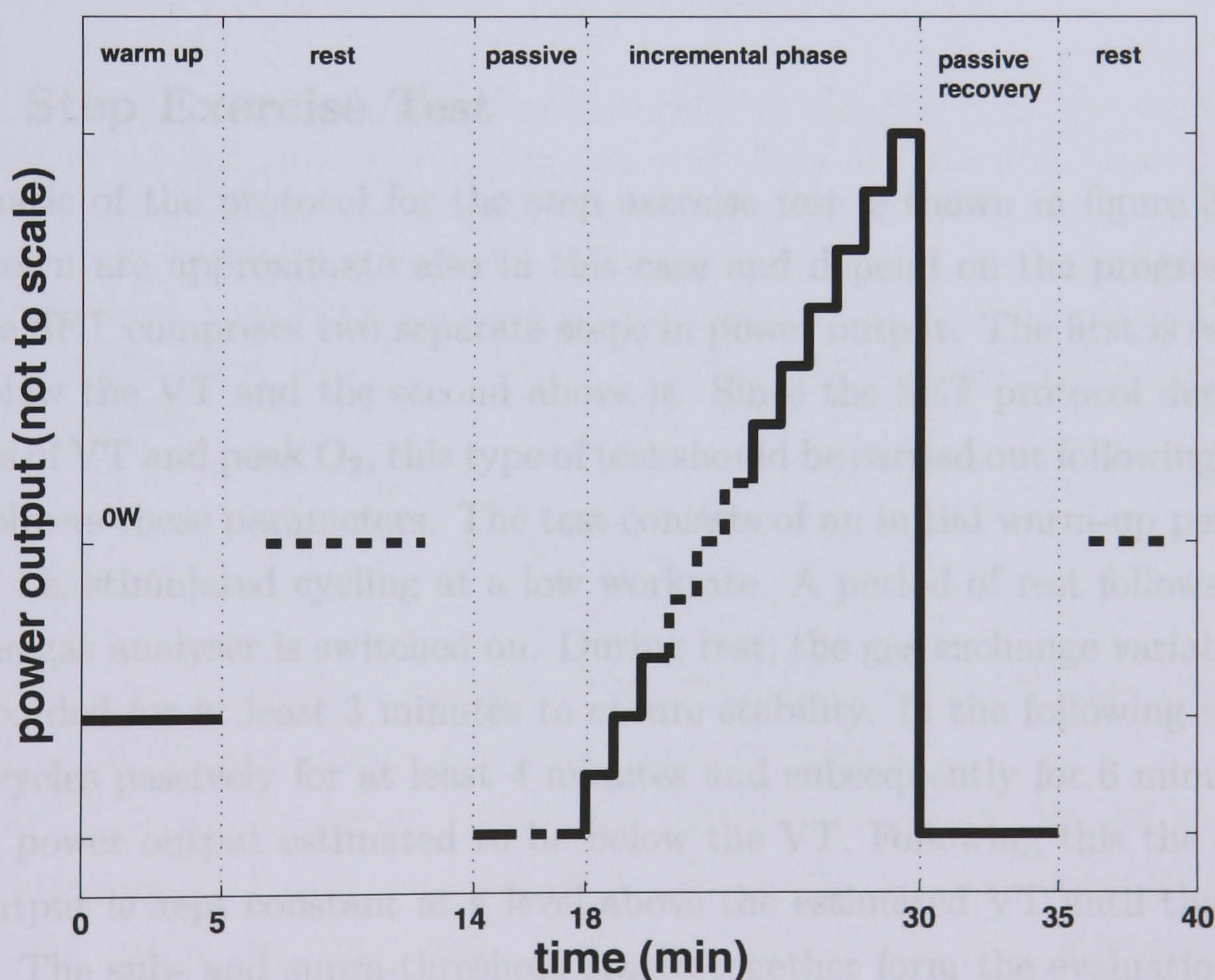


Figure 3.5: Diagram showing the proposed protocol for the incremental exercise test. The dotted line in the rest and passive intervals symbolizes the variable duration of these intervals, as it depends on stability of the gas exchange variables. In the incremental phase, the dotted line shows where the ventilatory threshold could possibly occur, either above or below the 0 W level, depending on the subject's fitness.

variable length. Gas exchange measurements start during rest. The test proceeds to the following phase only once the respiratory variables are stable, i.e. observation of the gas exchange variables on the laptop screen shows a plateau. Typically, the variables that are monitored are R , \dot{V}_{O_2} , \dot{V}_E or the fraction of end tidal O_2 ($F_{ET}O_2$). To ensure stability, the gas exchange variables have to be monitored for at least three minutes during rest. Thus, depending on the state of the subject, the length of the rest period can vary. In the next stage the subject cycles passively for at least 4 minutes (i.e. with no stimulation, the legs are turned by the motor at the desired cadence). Again the test proceeds to the following phase when the gas exchange variables are stable. Subsequently, in the incremental or evaluation phase, the power output is increased every minute in pre-defined fixed steps. The test is stopped when the power output required can no longer be sustained, i.e. the stimulation pulsewidth reaches the saturation level and consequently cannot be increased any further. A 5 minute period of passive cycling follows to allow the subject to cool down and then a period of rest of equal length follows.

3.4.2 Step Exercise Test

A schematic of the protocol for the step exercise test is shown in figure 3.6. The times shown are approximate also in this case and depend on the progress of the test. The SET comprises two separate steps in power output. The first is estimated to be below the VT and the second above it. Since the SET protocol depends on estimates of VT and peak O_2 , this type of test should be carried out following an IET, which delivers these parameters. The test consists of an initial warm-up period of 5 minutes, i.e. stimulated cycling at a low workrate. A period of rest follows, during which the gas analyser is switched on. During rest, the gas exchange variables have to be recorded for at least 3 minutes to ensure stability. In the following stage the subject cycles passively for at least 4 minutes and subsequently for 6 minutes at a constant power output estimated to be below the VT . Following this the required power output is kept constant at a level above the estimated VT until the subject fatigues. The sub- and supra-threshold stages together form the evaluation phase. A passive cycling recovery of 5 minutes follows and then 5 minutes of rest.

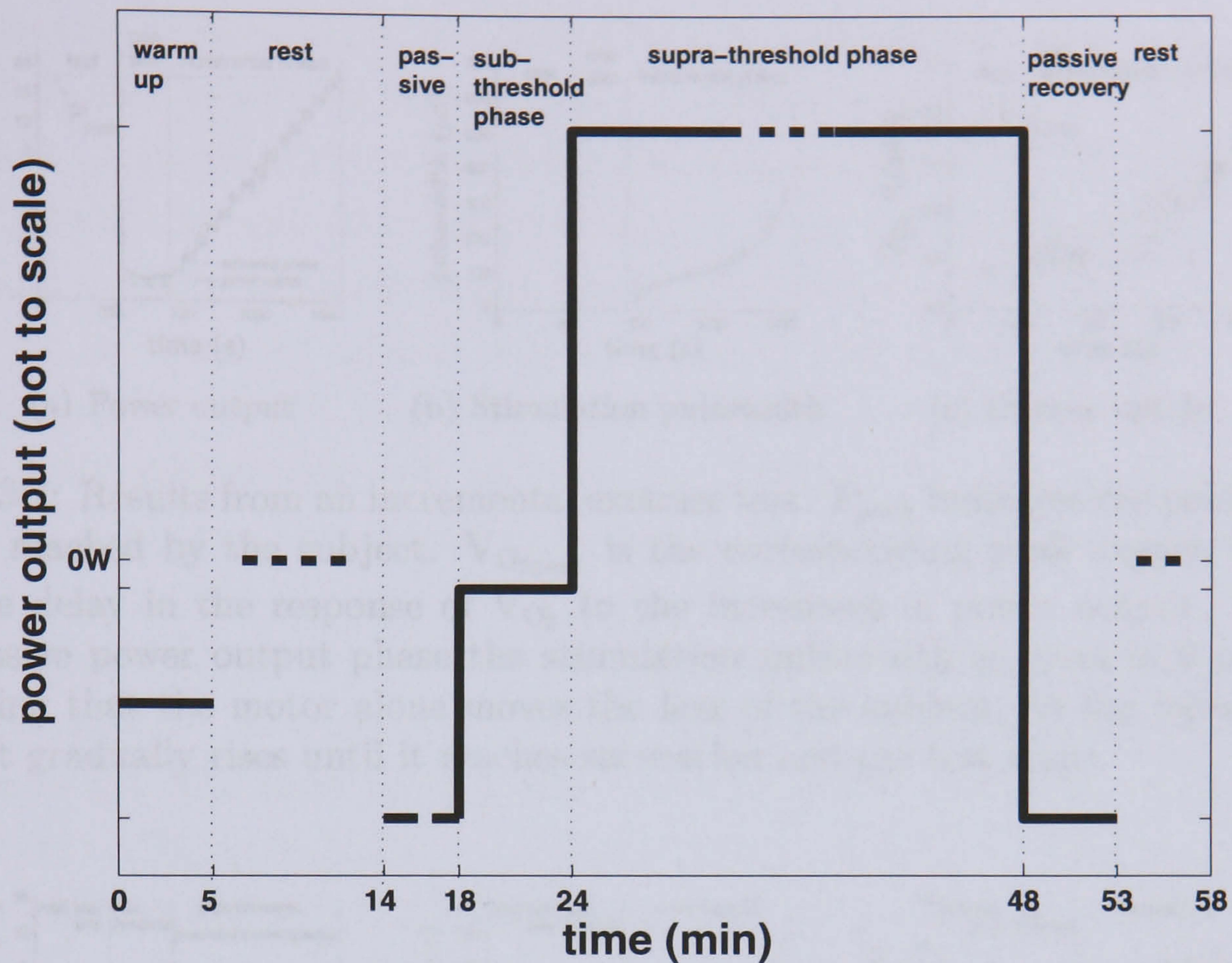


Figure 3.6: Diagram showing the proposed protocol for the step exercise test. The dotted line in the rest and passive intervals symbolizes the variable duration of these intervals, as it depends on stability of the gas exchange variables. The sub-threshold phase power output level is set below 0 W in this diagram, as an indication. The actual level varies depending on the subject's fitness and could be above 0 W. The dotted line in the supra-threshold phase shows that the duration of this phase cannot be defined a priori.

3.5 Results

To exemplify the protocols, the results from one IET and one SET are shown here. The analysis of the key outcomes is reported in chapter 4.

Figure 3.7 shows the power output, the stimulation pulsewidth and the oxygen uptake during one of the incremental tests. The power output follows the reference value closely during the whole test. The stimulation pulsewidth increases with the increase of the power requested from the subject, until it reaches saturation. The oxygen uptake increases linearly with power output to reach its peak value at the end of the incremental phase.

Figure 3.8 shows the power output, stimulation pulsewidth and oxygen uptake during a step test. The power output again follows the reference value closely. The stimulation pulsewidth is approximately constant during the sub-threshold phase

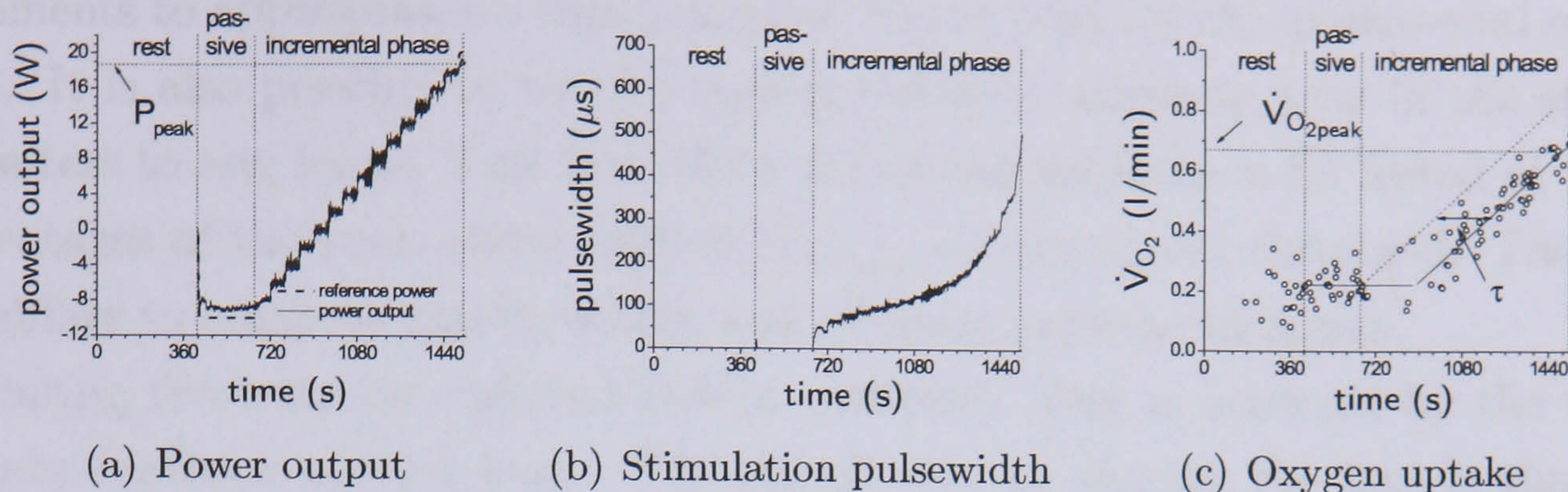


Figure 3.7: Results from an incremental exercise test. P_{peak} indicates the peak power output reached by the subject. $\dot{V}_{O_{2peak}}$ is the corresponding peak oxygen uptake. τ is the delay in the response of \dot{V}_{O_2} to the increment in power output. During the passive power output phase the stimulation pulsewidth is equal to 0 μs , thus indicating that the motor alone moves the legs of the subject. In the incremental phase it gradually rises until it reaches saturation and the test stops.

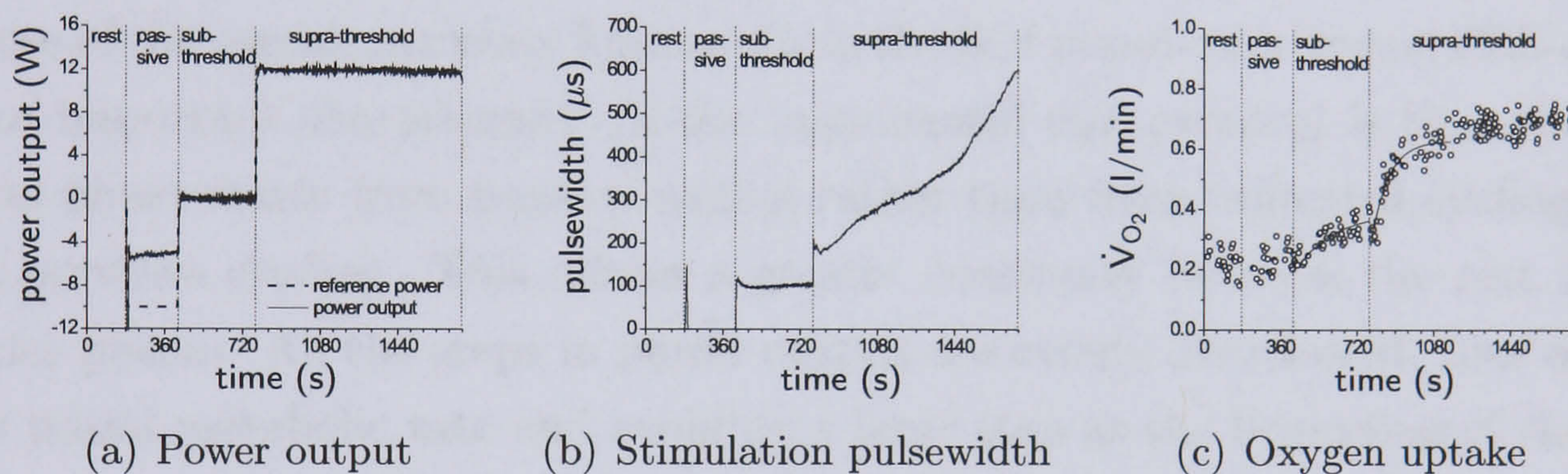


Figure 3.8: Results from a step exercise test. The stimulation pulsewidth is 0 μs during the passive phase, when the motor supplies the power output necessary to move the legs. During the subthreshold phase it increases to a constant level. Subsequently it rises until it reaches saturation in the supra-threshold phase. In the oxygen uptake graph, two curves have been fitted to the data to show the approximately monoexponential increase in \dot{V}_{O_2} in response to a step increment in power output.

and it increases until it reaches saturation during the supra-threshold phase. The oxygen uptake reaches a steady state in the sub-threshold phase and it gradually increases during the supra-threshold phase.

3.6 Discussion

The results show that it is possible to achieve accurate workrate control. The set-points can be arbitrarily changed in real-time. Thus, arbitrarily small workrate

increments to approximate a true ramp can be imposed (in the incremental exercise test). It is also possible to set the constant desired workrate level in the step exercise test to any value. This possibility allows the subjects to be tested at precise percentages of the peak power output, $\dot{V}_{O_{2peak}}$ or ventilatory threshold. Therefore, the ability to compare results within and between subjects increases.

During the tests the cadence is kept constant. This is achieved by the motor-cadence feedback control loop. The energy cost of moving the legs is thus kept constant throughout each test, and does not confound the gas exchange results. This is an advantage in calculating the outcomes, because the baseline does not vary.

The exercise workrate can be controlled smoothly throughout the workrate range, from the negative value measured during passive cycling (with zero stimulation), through to the maximum value possible (usually at the maximum preset level of stimulation). Thus, the total workrate range can be utilised. This is important because of the overall workrate limitations in the SCI population during FES-cycling.

An important characteristic of the incremental test protocol is that the incremental phase starts from passive cycling rather than from unloaded cycling (0 W) as in previous studies. This allows a greater continuity between the rest and the exercise phases. All the steps in power output are evenly distributed, thus allowing a low initial metabolic rate and avoiding a large step at the beginning of the incremental phase that could affect the results of the test. Indeed, it could be possible for the first step to be too big and thus to lead the subject directly into anaerobic exercise. In the test shown here the difference between passive and 0 W cycling is 8 W, which is almost a third of the whole range for the subject.

A great advantage of this new protocol is the possibility of personalizing the amplitude of the steps. Thus, the definition of the amplitude is an important issue. The aim is to perform a test in which the duration of the incremental phase is approximately 10-12 minutes. Moreover, a 1-minute increment in power output is recommended by Wasserman *et al.* [125] for the purpose of detecting the ventilatory threshold. Thus, the workrate increment is taken as one-twelfth of the estimated total workrate range. An incremental test to fatigue without gas exchange monitoring can be used to obtain an estimate of the total workrate range.

Relying on the findings of the IET, it is then possible to determine the power output levels desired for the step test. The amplitude of the first step in workrate (sub-threshold stage) is established either as the workrate that elicits 90% of the VT or as 25-35% of the peak workrate (relative to passive). The size of the second step

(supra-threshold stage) is defined as 70-80% of the difference between $\dot{V}_{O_{2peak}}$ and the VT or as 70-80% of the peak workrate (again relative to passive). The power output criterion is useful when it is not possible to determine the VT, as it is always possible to determine the peak power output.

3.7 Conclusions

The technical setup used in this study provided accurate control of exercise workrate and cadence throughout the tests. Thus, we were able to impose arbitrary workrate profiles with high precision.

This allowed the creation of optimized exercise testing protocols that are a scaled version of those used in AB subjects, in terms of power output. Thus, it is now possible to have a relatively high number of steps in the IET, or to impose a ramp in workrate. This improves the possibility of being able to detect the presence of the ventilatory threshold.

The new SET protocol allows precise definition of the sub- and supra-threshold power output levels. Thus, it is possible to compare more accurately the results obtained with different subjects.

Chapter 4

Analysis of Incremental and Step Exercise Test Data

4.1 Summary

This chapter reports the analysis of the key outcomes of the incremental and step exercise tests obtained from repeated tests in two SCI subjects.

The proposed incremental exercise test allows estimation of peak oxygen uptake, the time constant of the dynamic oxygen uptake response, the peak exercise workrate, the oxygen uptake-workrate relationship and VT.

The proposed step exercise test gives the time constants of oxygen uptake, carbon dioxide and minute ventilation response kinetics, for operating regimes which are designed to be either below or above the estimated ventilatory threshold. The SET also allows estimation of various measures of steady-state metabolic efficiency.

The testbed and protocols allow these variables to be measured with high sensitivity, thus giving good discrimination within and between subjects.

Part of the results reported in this chapter can be found in the paper [33].

4.2 Key Outcomes

4.2.1 Incremental Exercise Test

As previously stated (see section 1.5.1) the outcome measures for the incremental exercise test are: peak oxygen uptake ($\dot{V}_{O_{2\text{peak}}}$), peak exercise power output (P_{peak}), the time constant of oxygen uptake dynamics τ , the oxygen uptake-workrate relationship and an estimate of oxygen uptake and workrate at the ventilatory anaerobic

threshold. In the tests reported here we have calculated them as follows: the $\dot{V}_{O_{2peak}}$ has been computed by averaging \dot{V}_{O_2} data over the last 30 s of the incremental phase of the test. τ is the time lag between the \dot{V}_{O_2} regression line and the corresponding workrate ramp. The oxygen uptake-workrate relationship has been calculated as the slope of the linear fit of the \dot{V}_{O_2} vs PO plot in the incremental phase. The plot does not include the data points belonging to the initial part of the incremental phase, where the rise in \dot{V}_{O_2} is delayed. Results from the ventilatory threshold analysis are reported in chapter 5.

4.2.2 Step Exercise Test

The outcome measures for the step exercise test, listed in section 1.5.2, are: the time constants of oxygen uptake, carbon dioxide and minute ventilation dynamics, the steady-state oxygen uptake, and the efficiency of exercise. The phase II kinetics for the three gas exchange variables have been fitted with a monoexponential function, using the Levenberg-Marquardt algorithm for the optimization of the parameters. The equation used is:

$$\dot{V}_X(t) = \dot{V}_X(0) + \Delta\dot{V}_X(1 - e^{-t/\tau}), \quad t \geq 0 \quad (4.1)$$

where X is either O₂, CO₂ or E, $\dot{V}_X(0)$ is the previous stage steady-state value, $\Delta\dot{V}_X$ is the magnitude of the steady-state increase in \dot{V}_X resulting from the step change in workrate, and τ is the time constant. This equation describes Phase II of the \dot{V}_X kinetics for work rates below the VT. For work rates above the VT, the \dot{V}_{O_2} and \dot{V}_E kinetics are better described by a combination of two exponential functions, the first describing Phase II and the second being a slow component rising after some minutes [5, 17]. Thus, the first minutes of exercise at a power output level above the threshold can be described by a monoexponential function.

The details on efficiency calculations and results can be found in chapter 7.

4.3 Editing of the Data

The raw data obtained from the breath-by-breath system have to be edited before being analysed. The data editing, i.e. the removal of visually identified outliers, was done manually on the following variables: inspiration time (TI), expiration time (TE), breathing frequency (fb), minute ventilation (\dot{V}_E), pressure of end tidal O₂ (P_{ET}O₂), pressure of end tidal CO₂ (P_{ET}CO₂), tidal volume, fraction of inspired O₂

($F_{I}O_2$), fraction of inspired CO_2 ($F_{I}CO_2$), oxygen uptake, carbon dioxide production, and respiratory exchange ratio. Figure 4.1 shows the editing process. Figure 4.1(a) shows the raw data for the expiration time for one of the tests. The visually obvious outliers are removed manually and figure 4.1(b) is obtained. For each stage of the test a best fit curve is plotted, either using a linear fit or an exponential fit, depending on the data. 95% is the value chosen for the prediction bands. The data points lying outside these boundaries are subsequently removed. Figure 4.1(b) shows the data before removal of the data points lying outside the confidence lines. Figure 4.1(c) shows the final result of the editing.

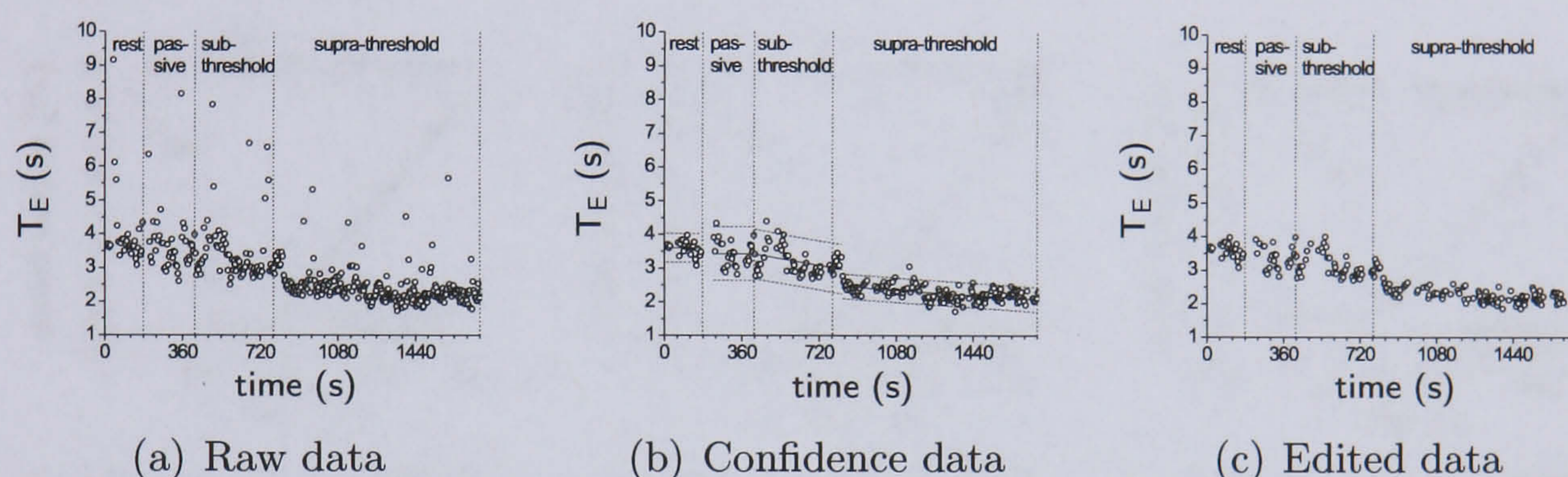


Figure 4.1: The three stages of the data editing process. Raw data show the data as they are provided by the gas analyser. Confidence data show the data after the manual removal of the outliers. The lines delimit the 95% confidence interval. Edited data show the final result, after the removal of the data points lying outside the confidence interval.

4.4 Results

4.4.1 Case Study S1

Incremental exercise test

The subject performed three incremental tests (IET1, IET2 and IET3) on different days separated by at least one week according to the IET protocol of figure 3.5. The time of day was the same for all the tests. The increment in power output during the incremental phase was 2 W/min. Power output, stimulation pulsewidth and the time course for \dot{V}_{O_2} during all the tests are shown in figure 4.2. The power output developed by the subject was well controlled during all the phases of the tests and it followed the reference power closely (indicated by the dashed line

in figures 4.2(a)–4.2(c)). In IET2 during the passive phase the subject had some spasms, which are reflected in the peaks in the power and stimulation pulsewidth plots (figures 4.2(b) and 4.2(e)). However, this did not affect the overall outcome. During the incremental phase, where an increasing amount of power is taken over by the subject's legs, the stimulation pulsewidth starts to rise. It first increases in steps together with the power, while in the second part it increases more steeply, until it reaches saturation (see figure 4.2(d)–4.2(f)). A linear regression line for \dot{V}_{O_2} has been plotted for the incremental phase to better illustrate the relationship between \dot{V}_{O_2} and time (figures 4.2(g)–4.2(i)). On the graphs we have indicated the

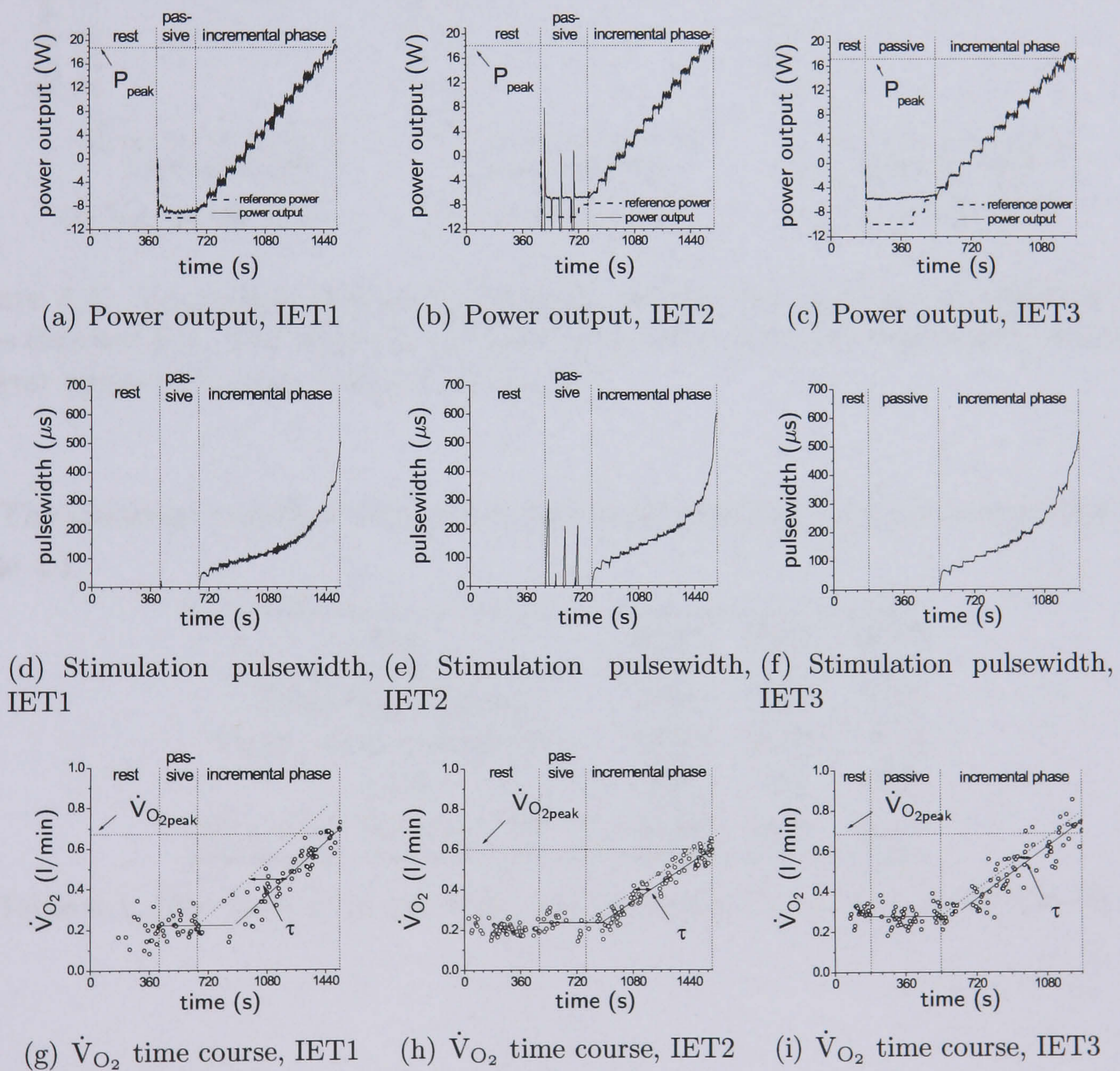


Figure 4.2: Incremental exercise tests (subject S1): power output, stimulation pulsewidth and oxygen uptake. P_{peak} indicates the peak power output reached by the subject. $\dot{V}_{O_{2peak}}$ is the corresponding peak oxygen uptake. τ is the time constant of the response of \dot{V}_{O_2} to the increase in power output.

outcome measures as follows: peak power (figure 4.2(a)–4.2(c)), peak \dot{V}_{O_2} and τ (figure 4.2(g)–4.2(i)).

Figure 4.3 shows \dot{V}_{O_2} as a function of power output. The values for \dot{V}_{O_2} have been obtained averaging \dot{V}_{O_2} over each minute of the incremental phase, excluding the initial delay in the rise of \dot{V}_{O_2} . For all the graphs in figure 4.3 a regression line has been fitted to better show the linear relation between \dot{V}_{O_2} and power output, the slope of these lines representing the relationship between oxygen uptake and workrate as indicated.

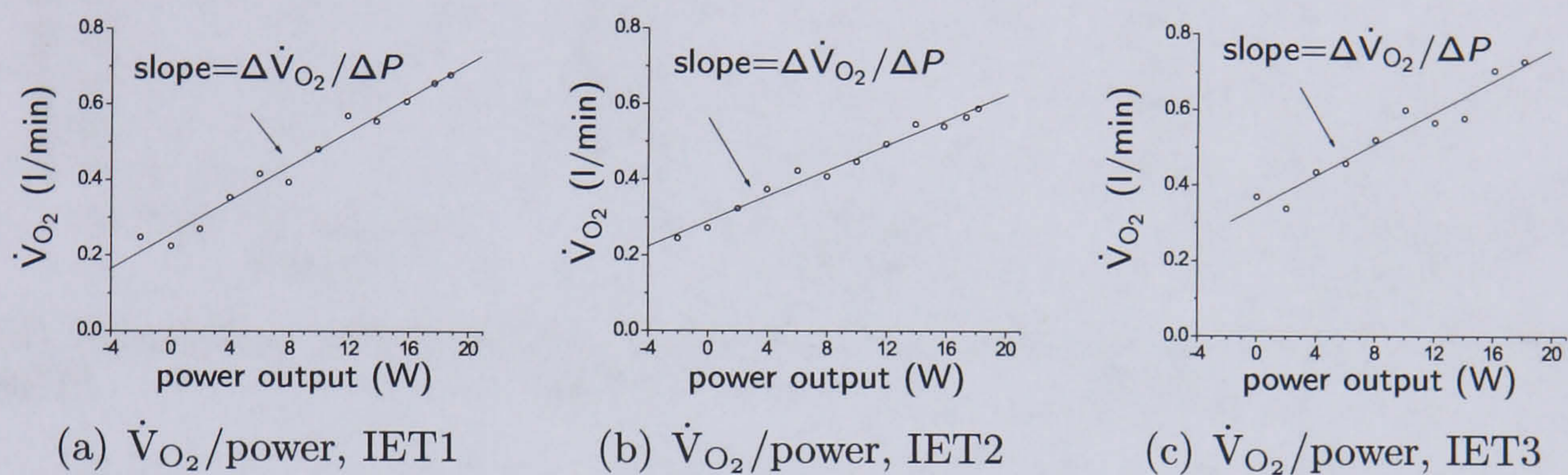


Figure 4.3: \dot{V}_{O_2} /power output relationship during the incremental phase of the tests (subject S1). The slope of each linear regression gives the relationship between oxygen uptake and power output, $\Delta\dot{V}_{O_2}/\Delta P$.

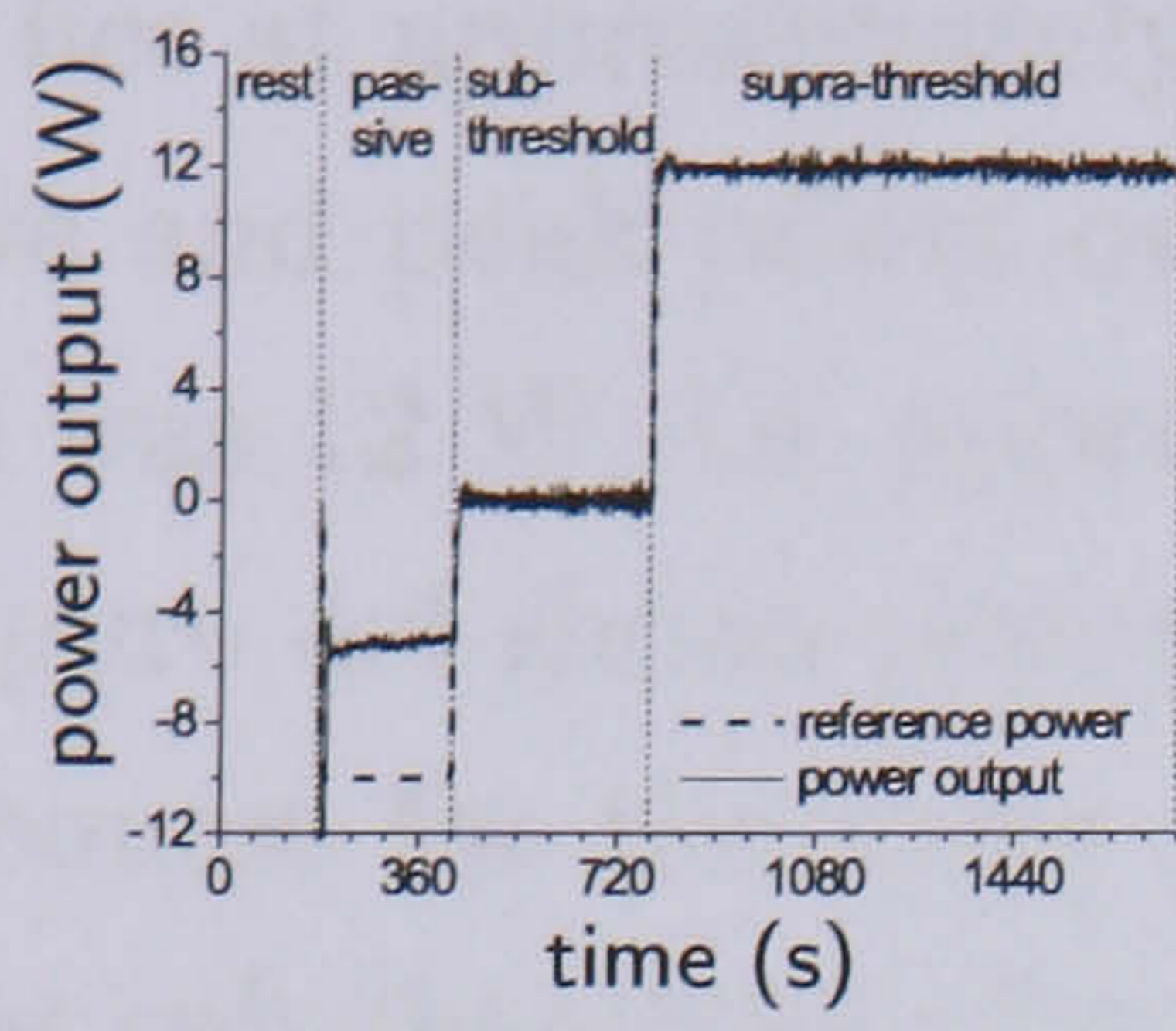
The outcome measures obtained from the incremental tests are summarized in table 4.1.

Test	IET1	IET2	IET3
Peak \dot{V}_{O_2} (l/min)	0.69	0.60	0.68
Peak power output (W)	18.77	18.09	17.22
τ (s)	225	100	68
$\Delta\dot{V}_{O_2}/\Delta P$ ($\text{ml}\cdot\text{min}^{-1}\cdot\text{W}^{-1}$)	22.63	16.76	21.00

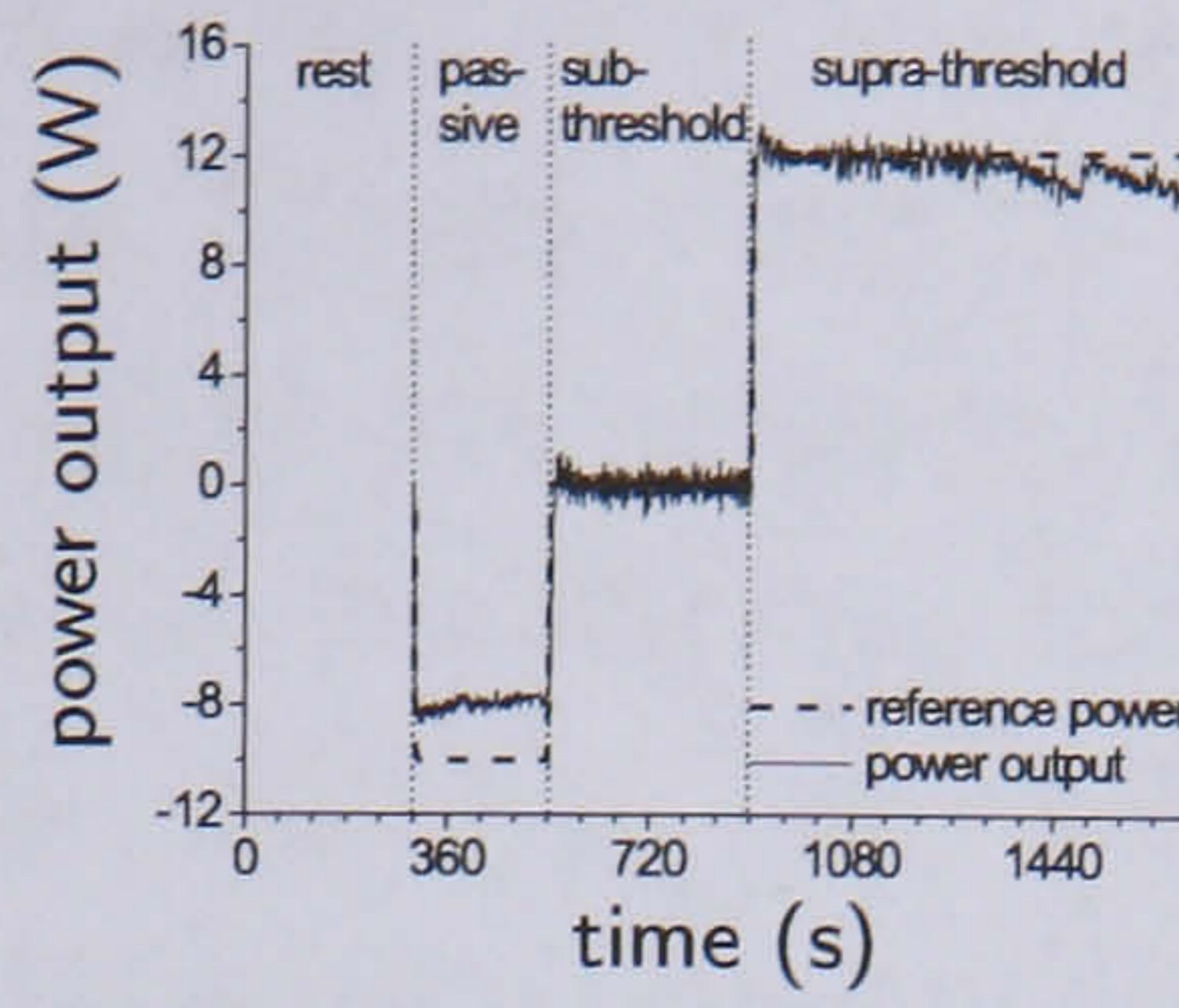
Table 4.1: Summary of incremental test outcomes for all tests in subject S1.

Step exercise test

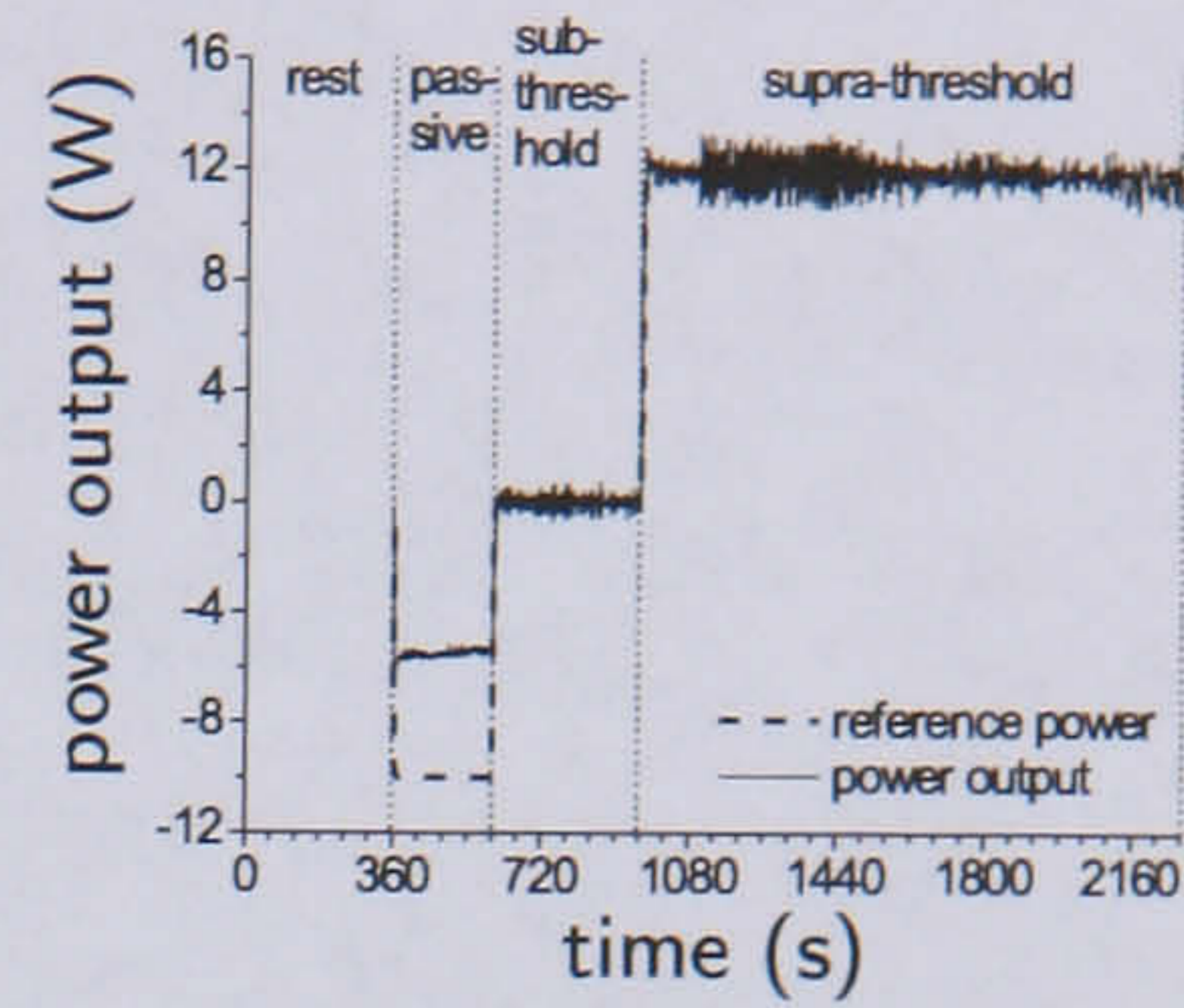
The subject completed three constant load tests (SET1, SET2 and SET3) on different days, separated by at least one week. The preceding IET showed that the VT occurred at a power output of 2-4 W (see chapter 5), therefore it was deemed reasonable to choose 0 W as the constant workrate for the sub-threshold stage. This



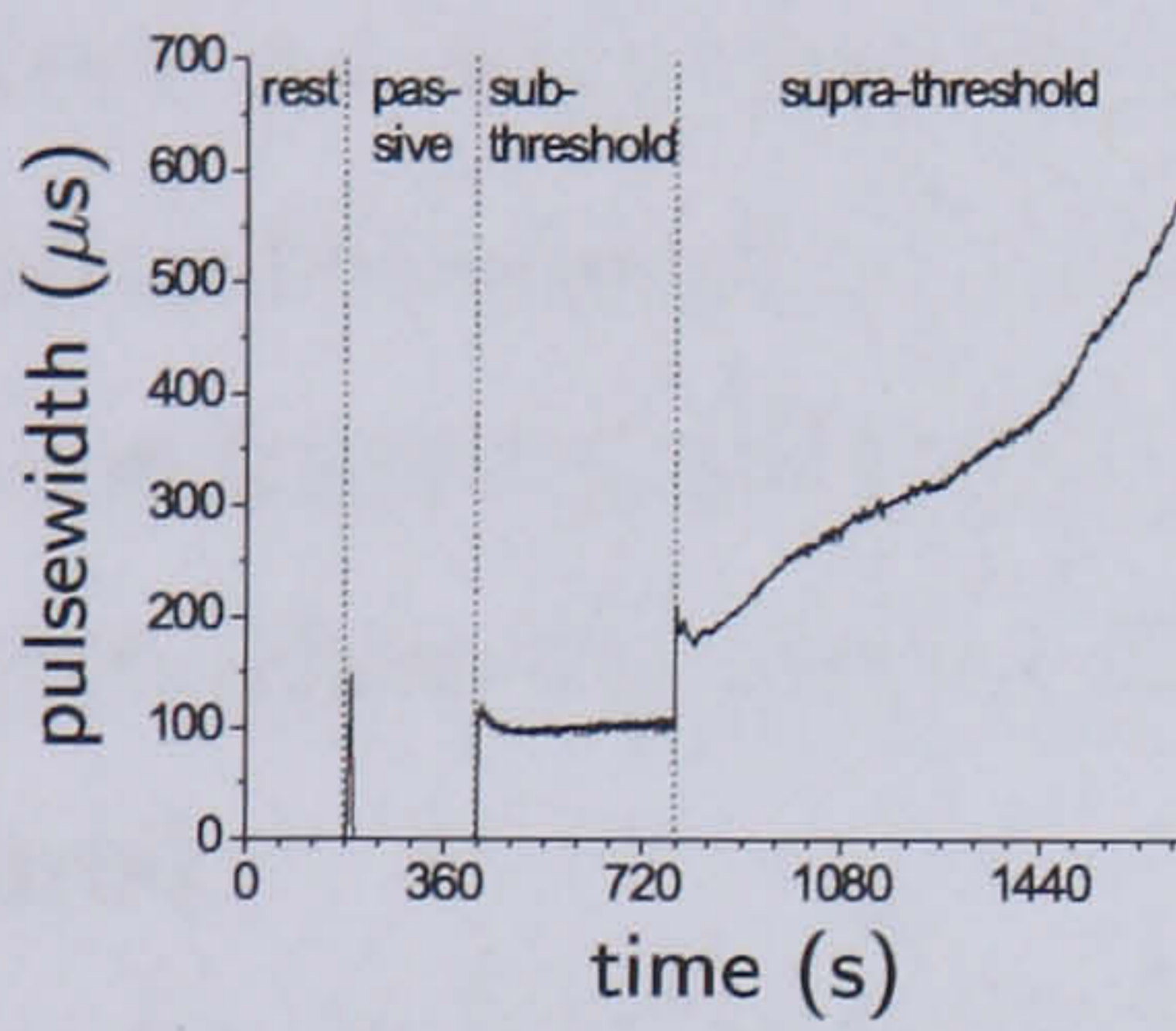
(a) Power output, SET1



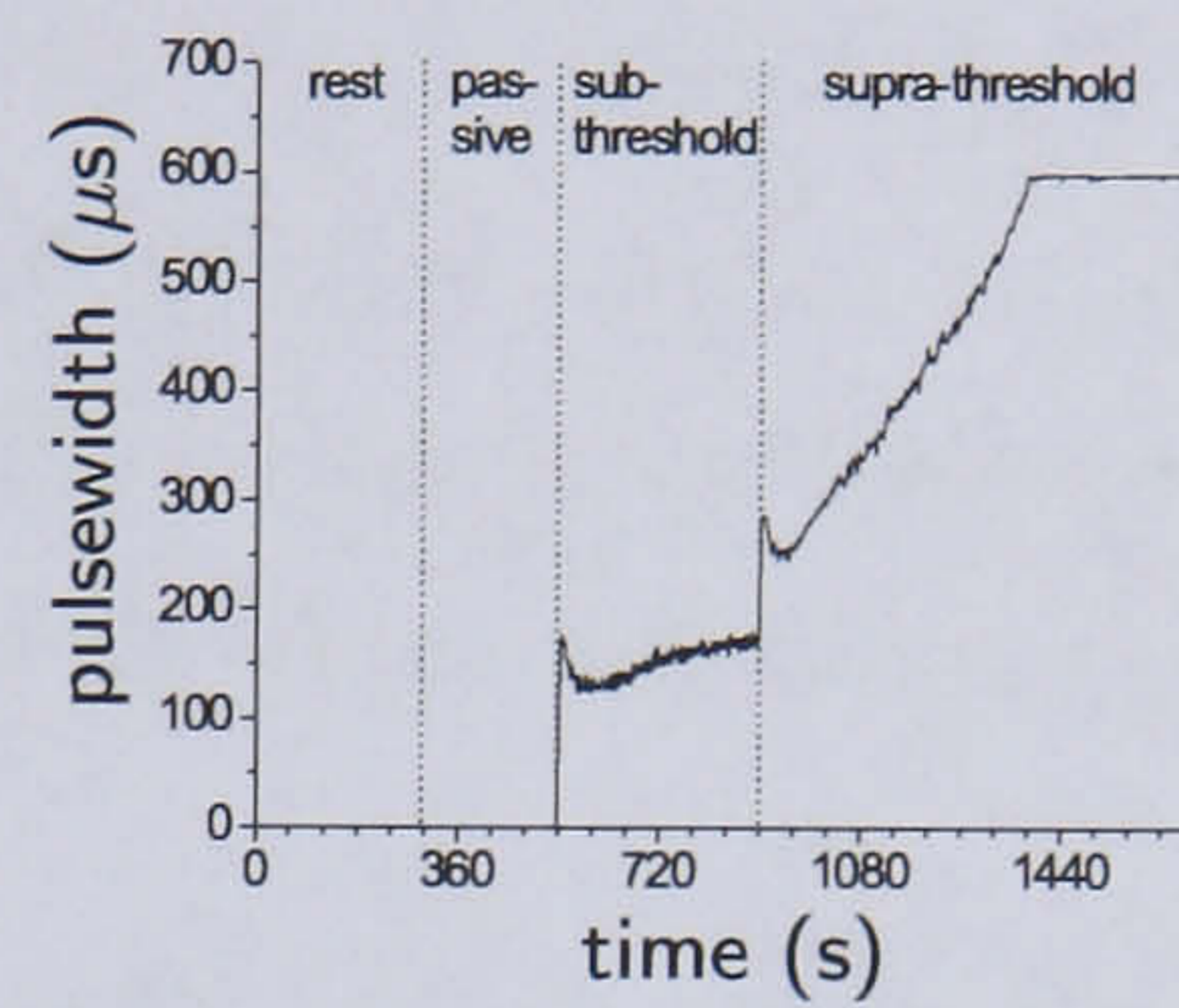
(b) Power output, SET2



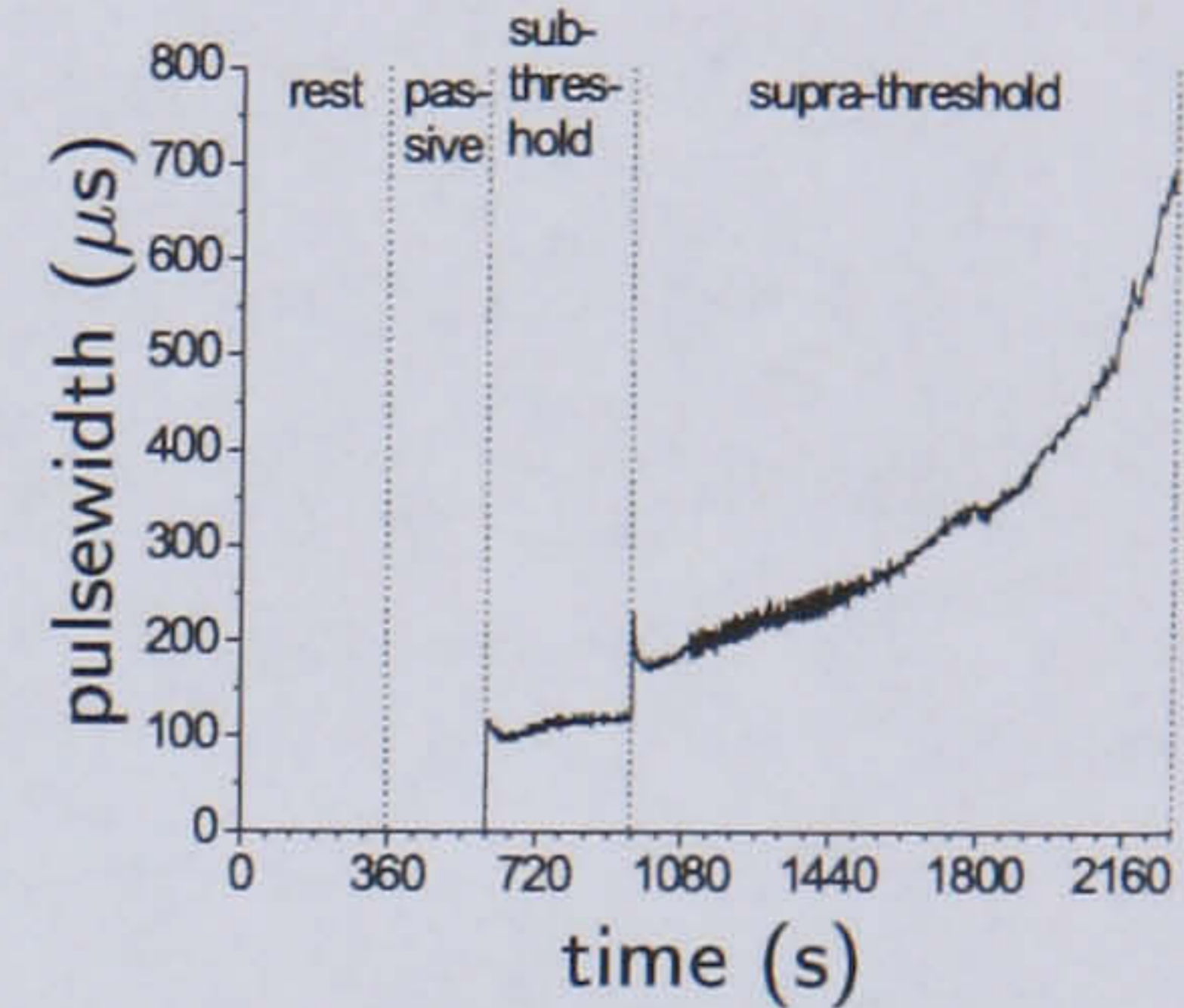
(c) Power output, SET3



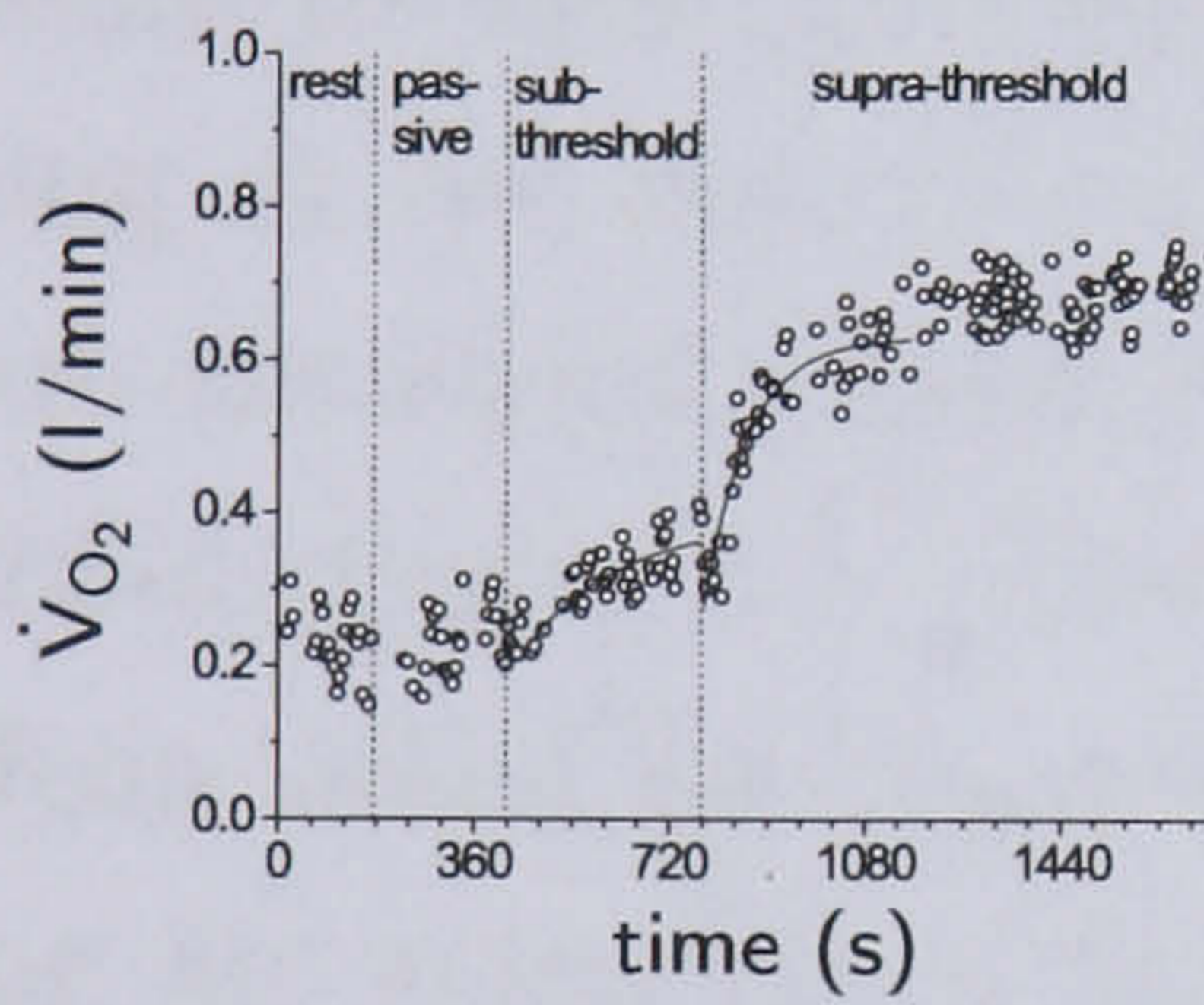
(d) Stimulation pulsewidth, SET1



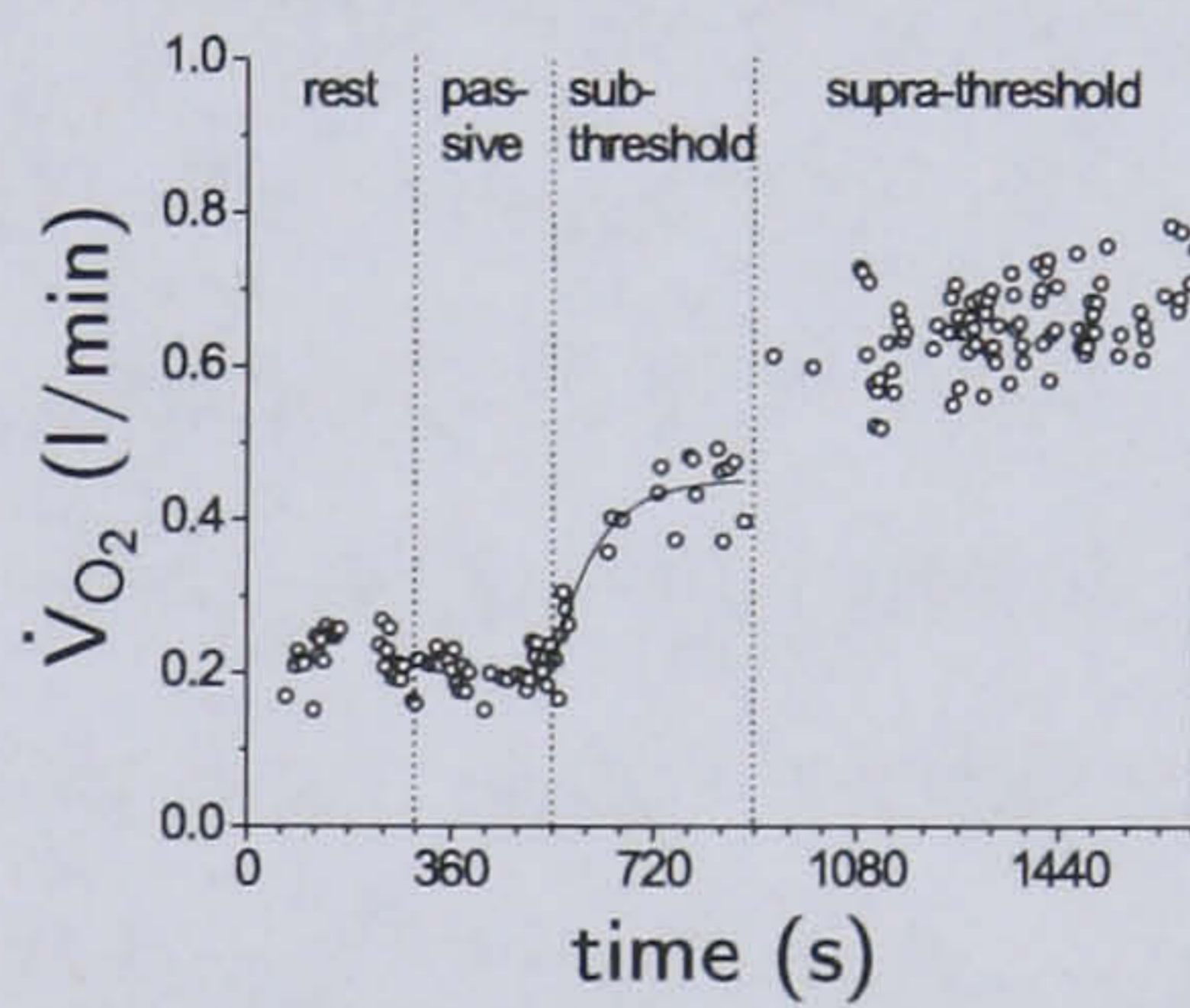
SET2



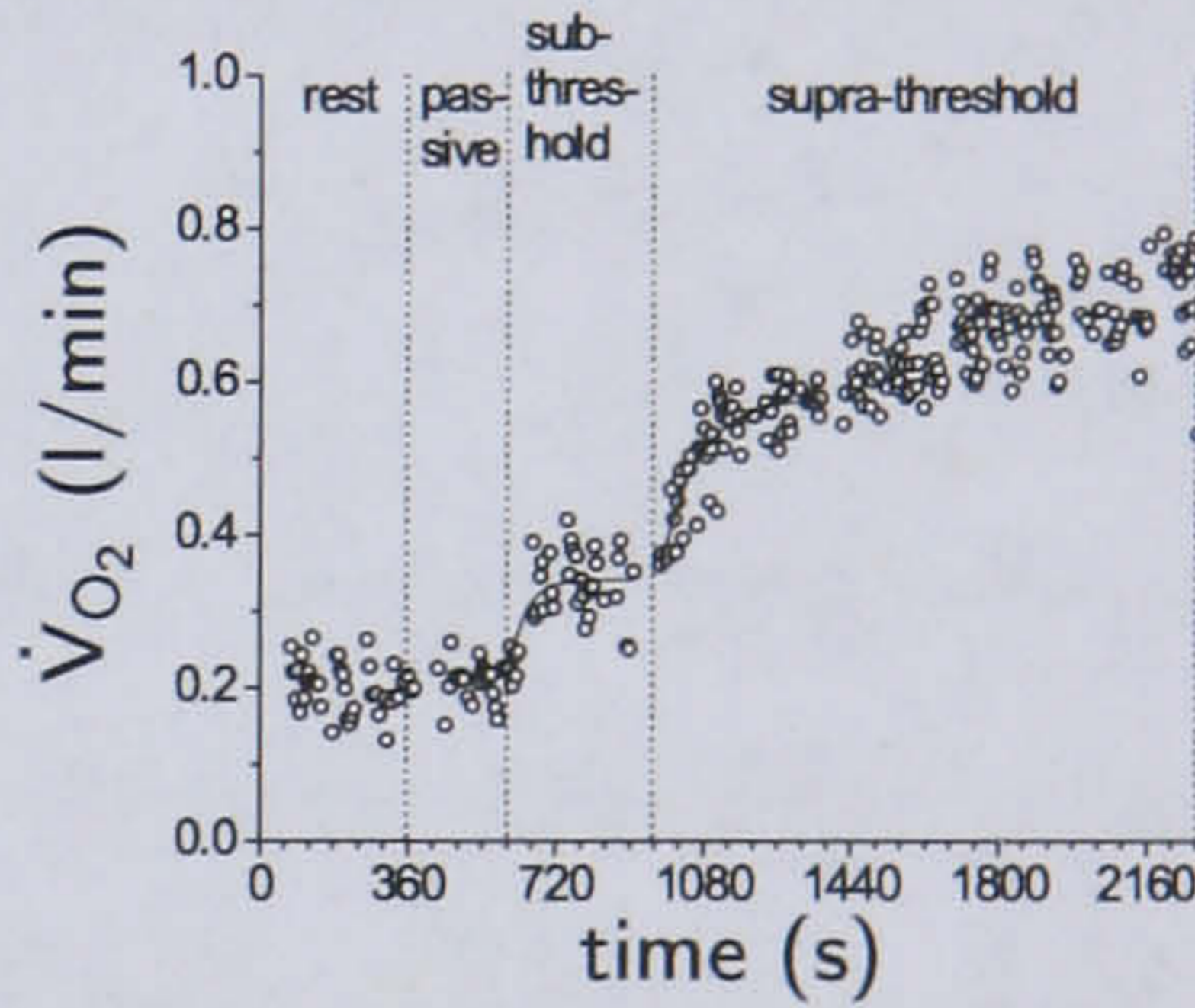
SET3



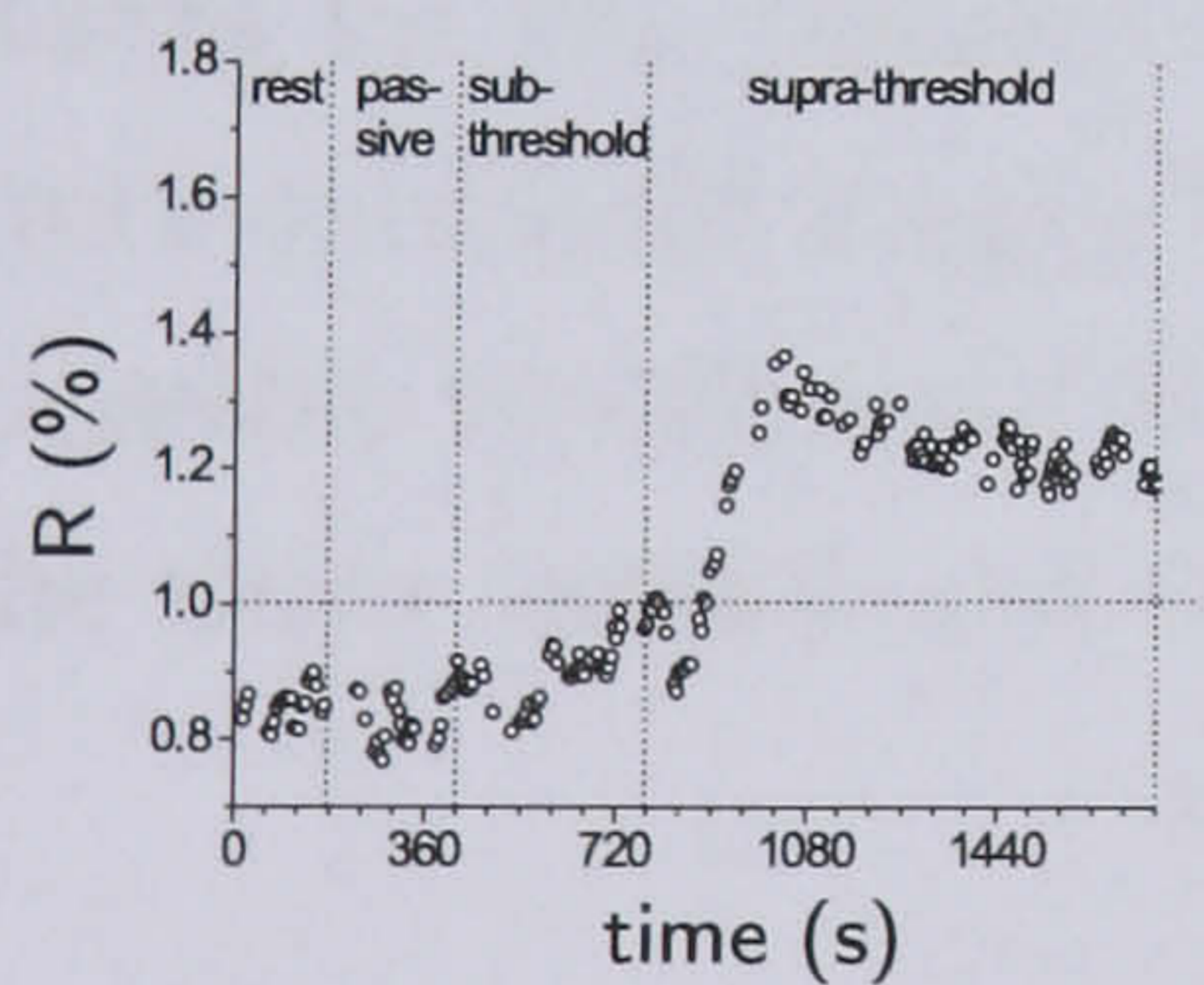
(g) Oxygen uptake, SET1.



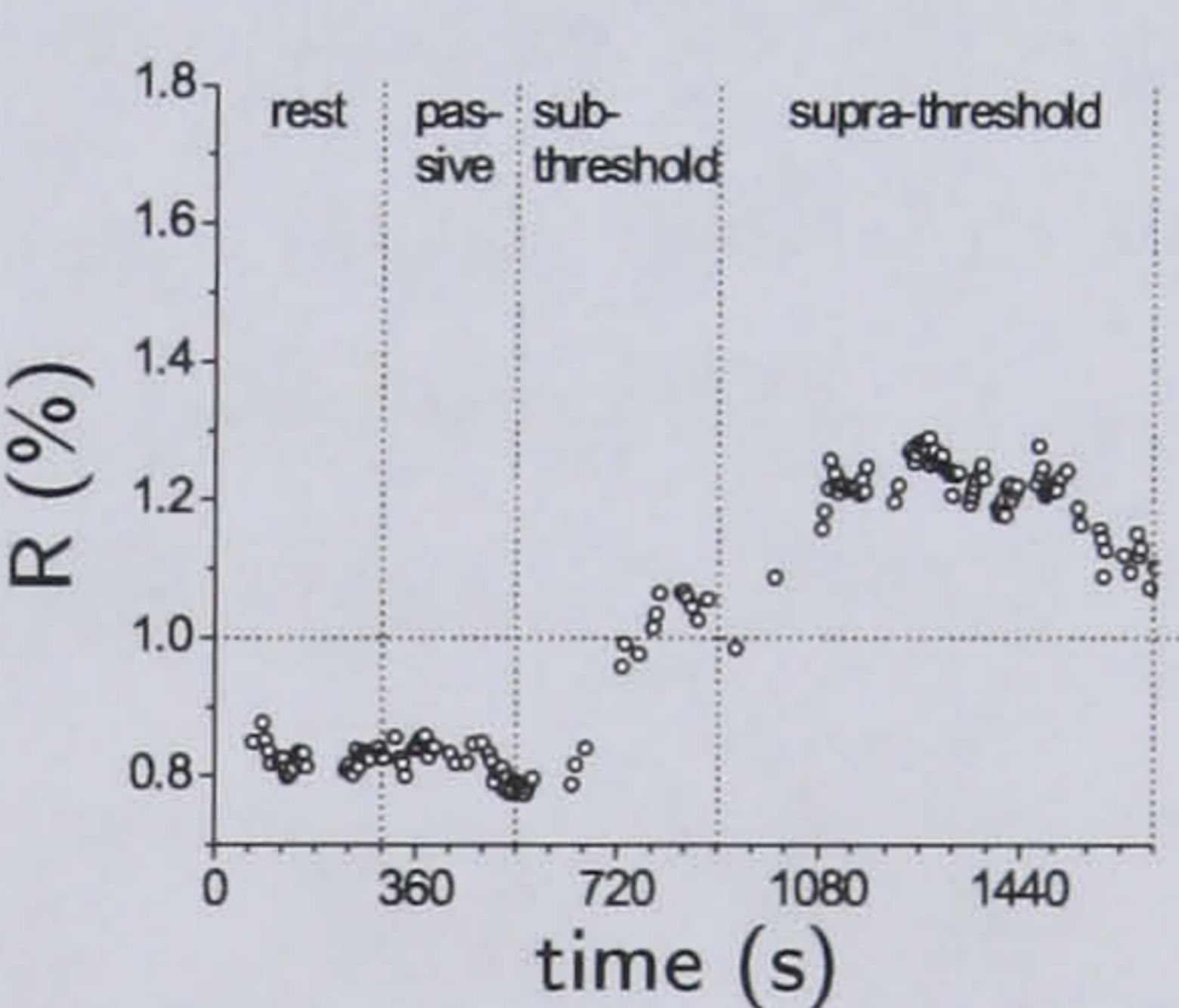
(h) Oxygen uptake, SET2.



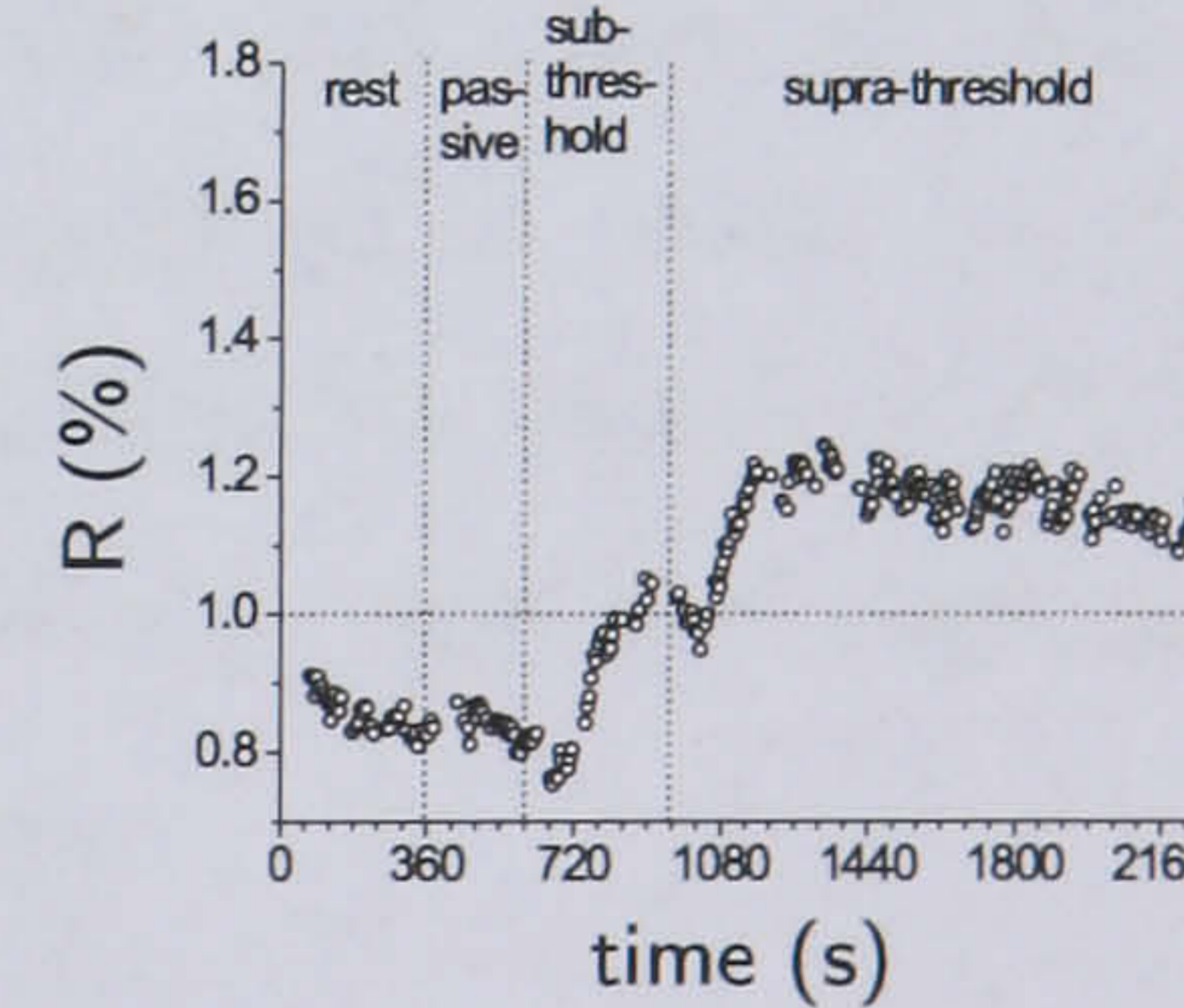
(i) Oxygen uptake, SET3.



(j) R, SET1.



(k) R, SET2.



(l) R, SET3.

Figure 4.4: Step exercise tests (subject S1): power output, stimulation pulsewidth, oxygen uptake and respiratory exchange ratio. In the oxygen uptake graph, the curves that have been fitted to the data show the approximately monoexponential increase in \dot{V}_{O_2} in response to a step increment in power output. In the respiratory exchange ratio graphs, the horizontal line depicts $R=1$, indicating when anaerobic metabolism starts to take over.

value lies at approximately 28% of the total workrate range, as determined from the passive and peak power outputs. The power output chosen for the supra-threshold phase was 12 W, i.e. approximately 76% of the peak power output.

Figure 4.4 shows power output, stimulation pulsewidth, \dot{V}_{O_2} time-course and R time-course for the three tests. The \dot{V}_{O_2} time-course was similar in all the tests for the sub-threshold phase, showing an exponential rise (see figures 4.4(g), 4.4(h) and 4.4(i)). During the supra-threshold phase in SET1 and SET3 it was possible to detect an exponential rise for \dot{V}_{O_2} , followed by a second slow component. In the supra-threshold phase of SET2 \dot{V}_{O_2} seems to rise in a step at first and then it increases linearly with time. The tests end when the stimulation pulsewidth reaches or approaches its limit, or when the supra-threshold workrate can no longer be sustained.

Figures 4.4(j), 4.4(k) and 4.4(l) show the R time-course during exercise for the three tests. At the change of phase from passive to sub-threshold and from sub-threshold to supra-threshold it shows the typical trend found in AB subjects, decreasing in the first minutes of the new stage and then increasing [127]. During the sub-threshold phases R is generally lower than or around 1. During the supra-threshold phases it is above 1, indicating the development of anaerobic exercise.

Mean values for \dot{V}_{O_2} and R at rest, and during passive, sub- and supra-threshold cycling are reported in table 4.2 and table 4.3, respectively. The \dot{V}_{O_2} values (table 4.2) give an indication of the mean oxygen cost during each stage. The time constants for the transition from passive to sub-threshold and from sub-threshold to supra-threshold stages for \dot{V}_{O_2} , \dot{V}_{CO_2} and \dot{V}_E are reported in table 4.4. It was not possible to calculate the time constant for \dot{V}_{CO_2} in the 0 W phase of SET1 and for the three variables in the 12W phase of SET2, as the rise was not exponential.

Test	SET1	SET2	SET3
Rest	0.23	0.21	0.19
Passive	0.25	0.21	0.21
0W	0.35	0.43	0.32
12W	0.71	0.72	0.73

Table 4.2: \dot{V}_{O_2} (l/min) values averaged over the last minute of each stage for the three constant load tests for subject S1.

Test	SET1	SET2	SET3
Rest	0.86	0.82	0.83
Passive	0.84	0.80	0.83
0W	0.97	1.05	1.02
12W	1.19	1.11	1.13

Table 4.3: R values averaged over the last minute of each stage for the three constant load tests for subject S1.

Test Phase	SET1 sub-threshold	SET2 (0W)	SET3	SET1 supra-threshold	SET2 (12W)	SET3
τ for \dot{V}_{O_2} (s)	186	74	38	80	-	90
τ for \dot{V}_{CO_2} (s)	-	163	103	176	-	135
τ for \dot{V}_E (s)	231	221	78	182	-	137

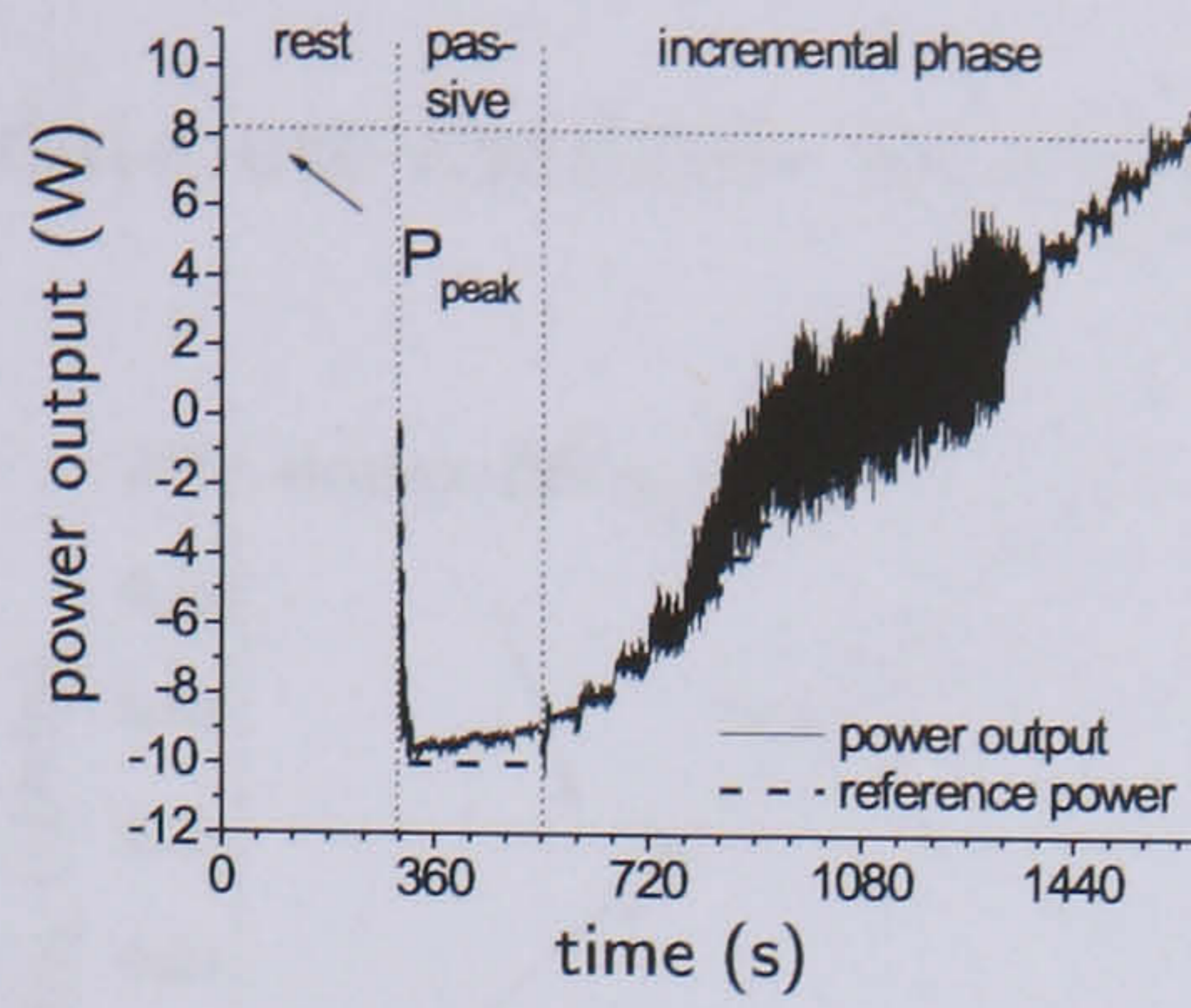
Table 4.4: Time constant values (s) for the sub-threshold and supra-threshold steps in the three constant load tests for subject S1.

4.4.2 Case Study S2

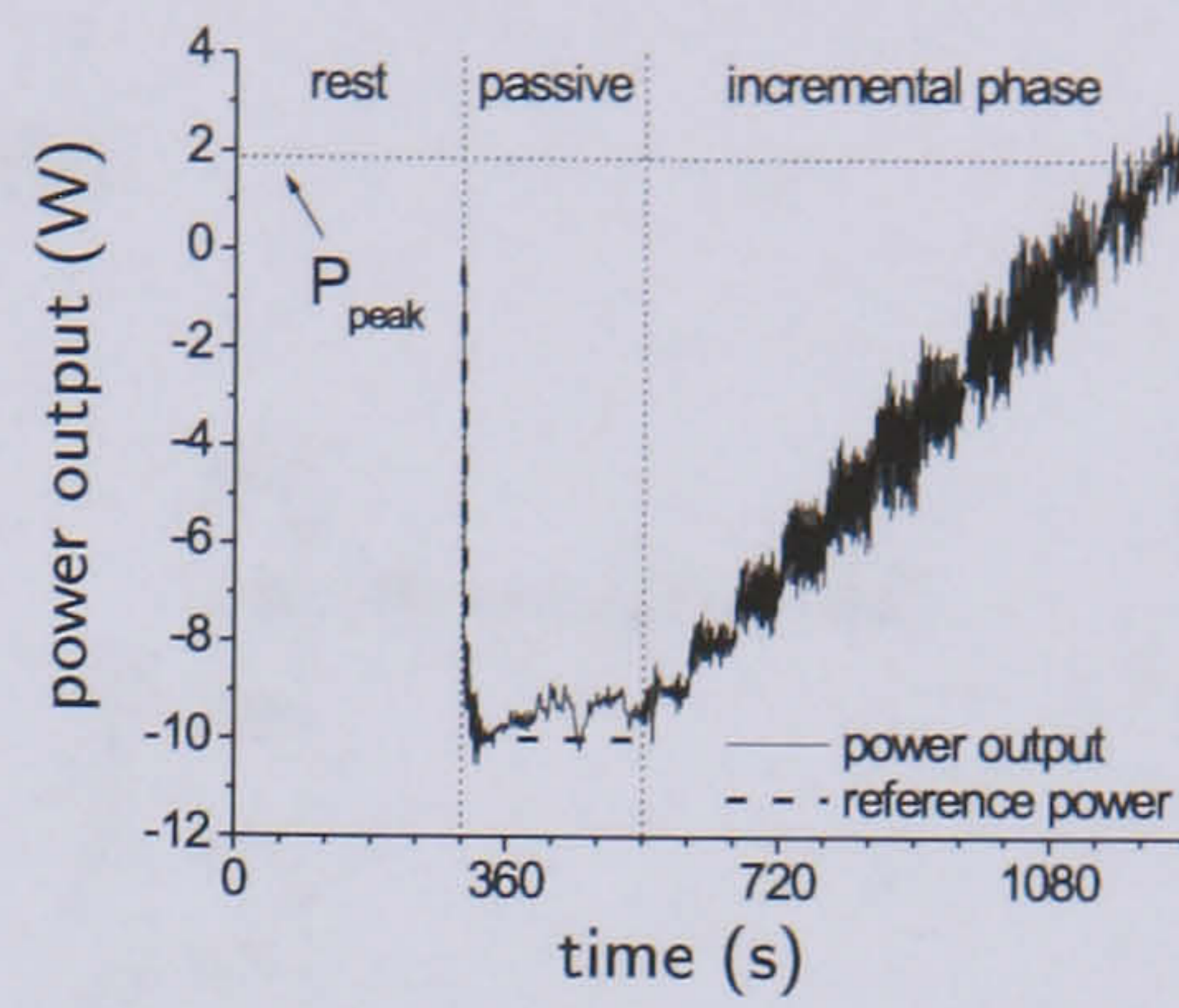
Incremental exercise test

Subject S2 performed two incremental exercise tests (IET1 and IET2), one week apart, at the same time of the day. The IETs were performed according to the protocol presented in chapter 3. The increment in power output during the incremental phase was 1 W/min. Figure 4.5 shows power output, stimulation pulsewidth and the time course for \dot{V}_{O_2} during the two tests. In the first test the control of the power output was not as precise as with subject S1. The actual power fluctuated widely around the reference value (figure 4.5(a)). The stimulation pulsewidth varied in the range of 0-300 μ s during the first 13 minutes of the incremental phase (figure 4.5(c)). The oxygen uptake time-course shifts from linearity in correspondence with the fluctuations in power output (figure 4.5(e)). In the second test the power output control is still not as accurate as for subject S1, but it is possible to see each step increment (figure 4.5(b)). The stimulation pulsewidth fluctuates, but the variation range is smaller than in the previous test, being approximately 100 μ s (figure 4.5(d)). The oxygen uptake time-course shows the typical linear trend of the IET in the incremental phase (figure 4.5(f)).

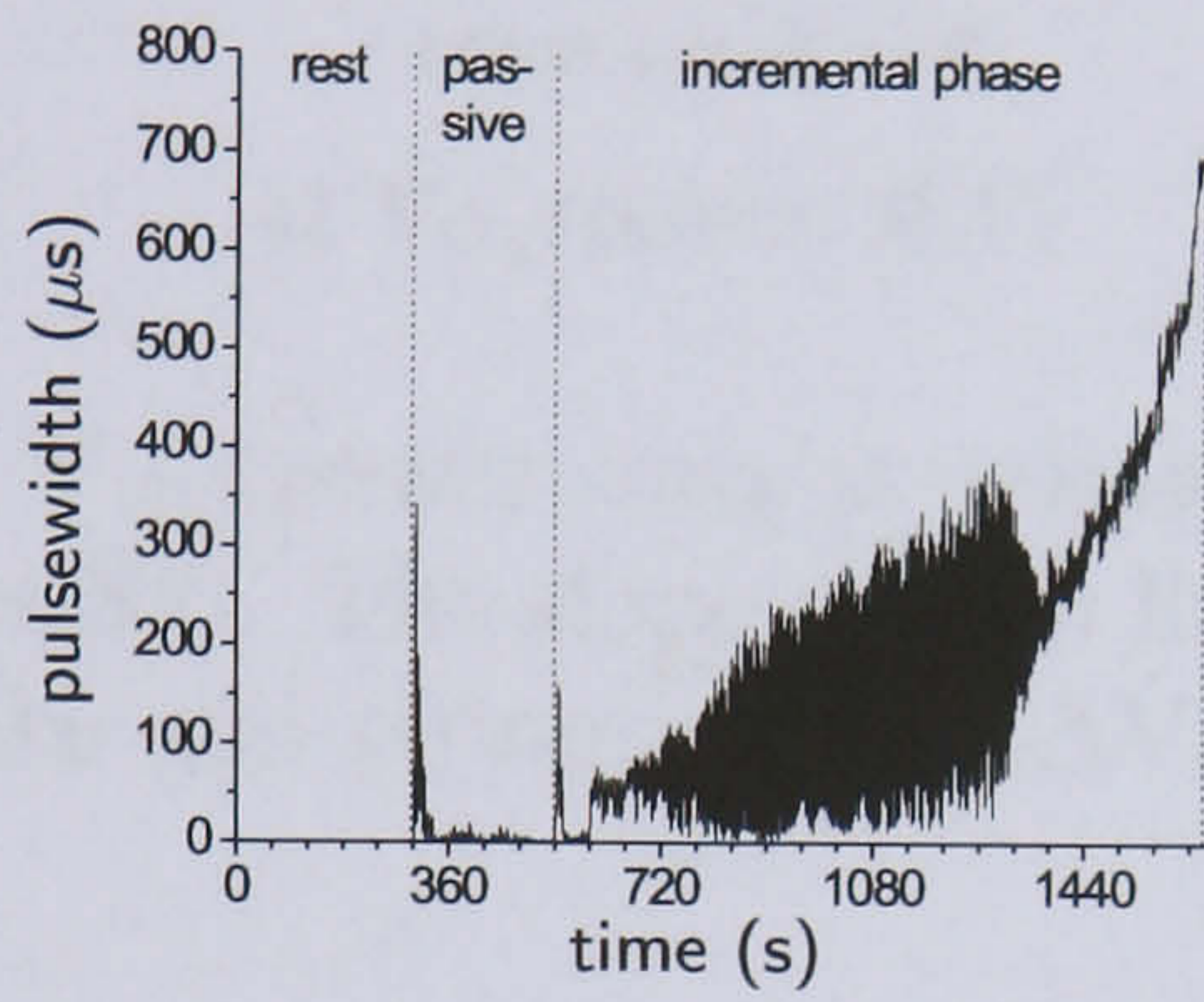
Figure 4.6 shows \dot{V}_{O_2} as a function of power output. A regression line has been



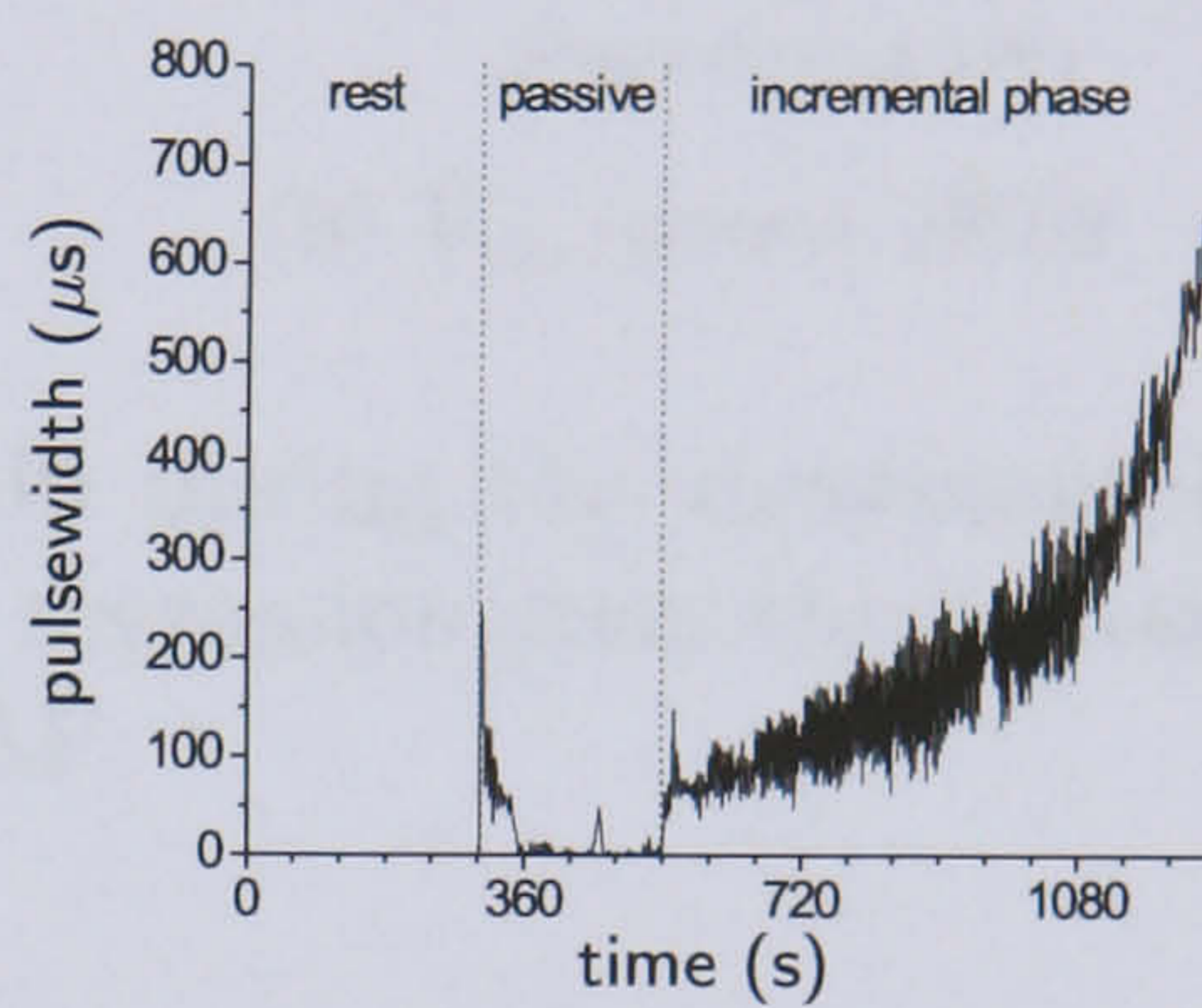
(a) Power output, IET1



(b) Power output, IET2



(c) Stimulation pulsewidth, IET1



(d) Stimulation pulsewidth, IET2

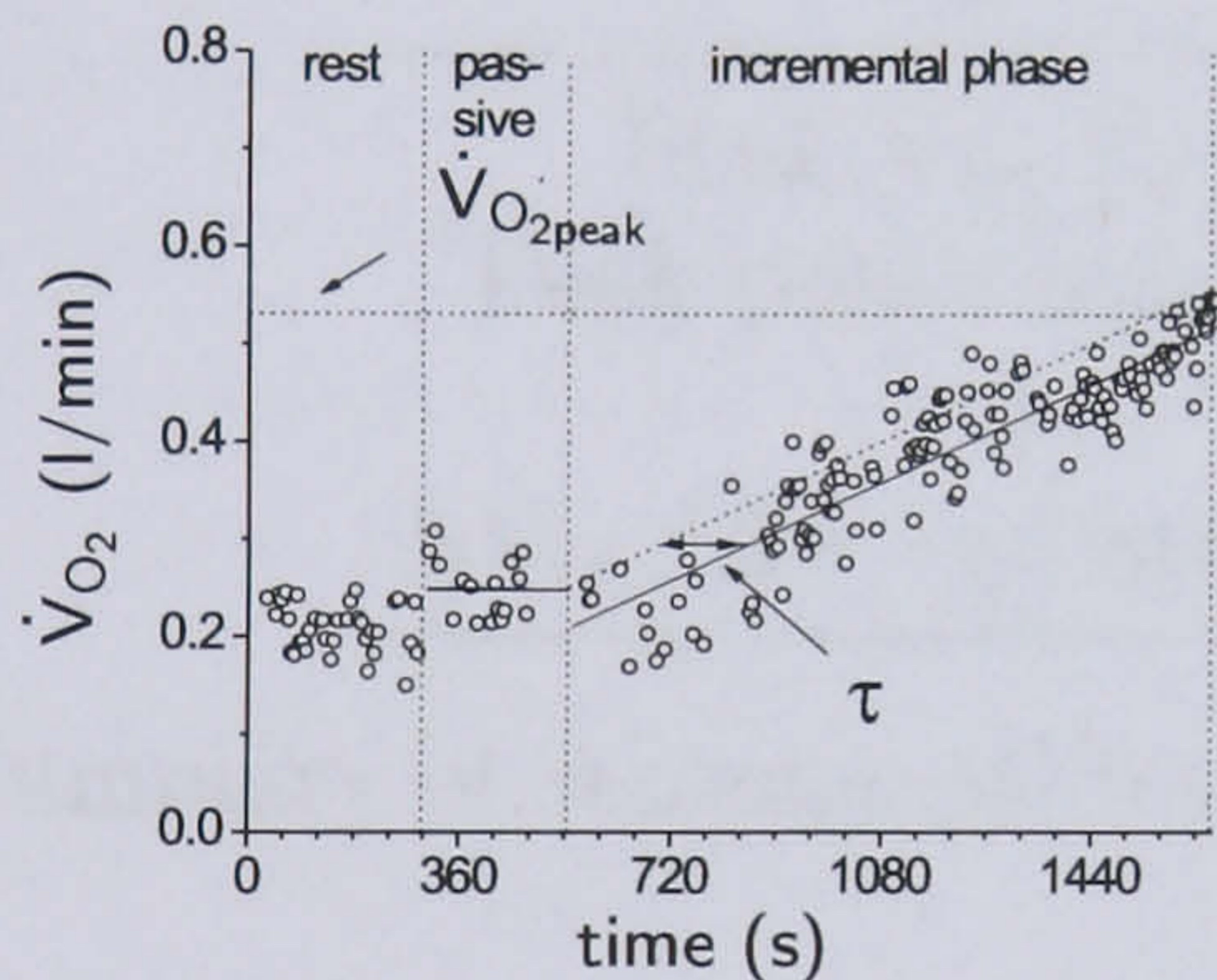
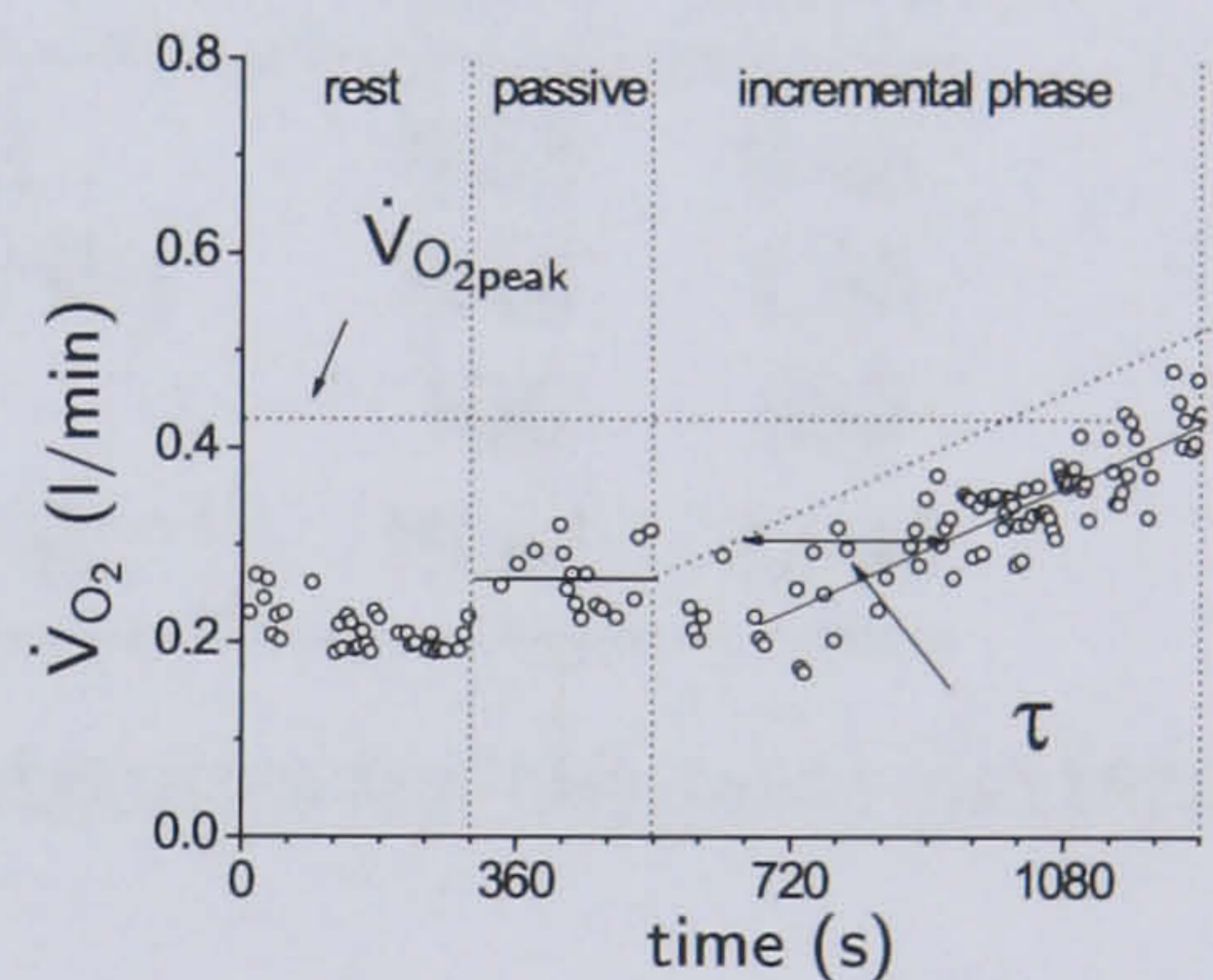
(e) \dot{V}_{O_2} time course, IET1(f) \dot{V}_{O_2} time course, IET2

Figure 4.5: Incremental exercise tests (subject S2): power output, stimulation pulsewidth and oxygen uptake. P_{peak} indicates the peak power output reached by the subject. $\dot{V}_{O_{2\text{peak}}}$ is the corresponding peak oxygen uptake. τ is the time constant of the response of \dot{V}_{O_2} to the increase in power output.

fitted to the \dot{V}_{O_2} data to try to approximate the expected linear behaviour. However, as can be seen in figure 4.6(a), the relationship between \dot{V}_{O_2} and power output is not linear. Figure 4.6(b) shows that in IET2, when the power control was more accurate, the relationship is more linear. Actually, the standard deviation from linearity is 0.024 ml/min for IET1 and 0.016 ml/min for IET2.

The outcome measures obtained from the incremental tests are summarized in

table 4.5.

No SET data are available for subject S2.

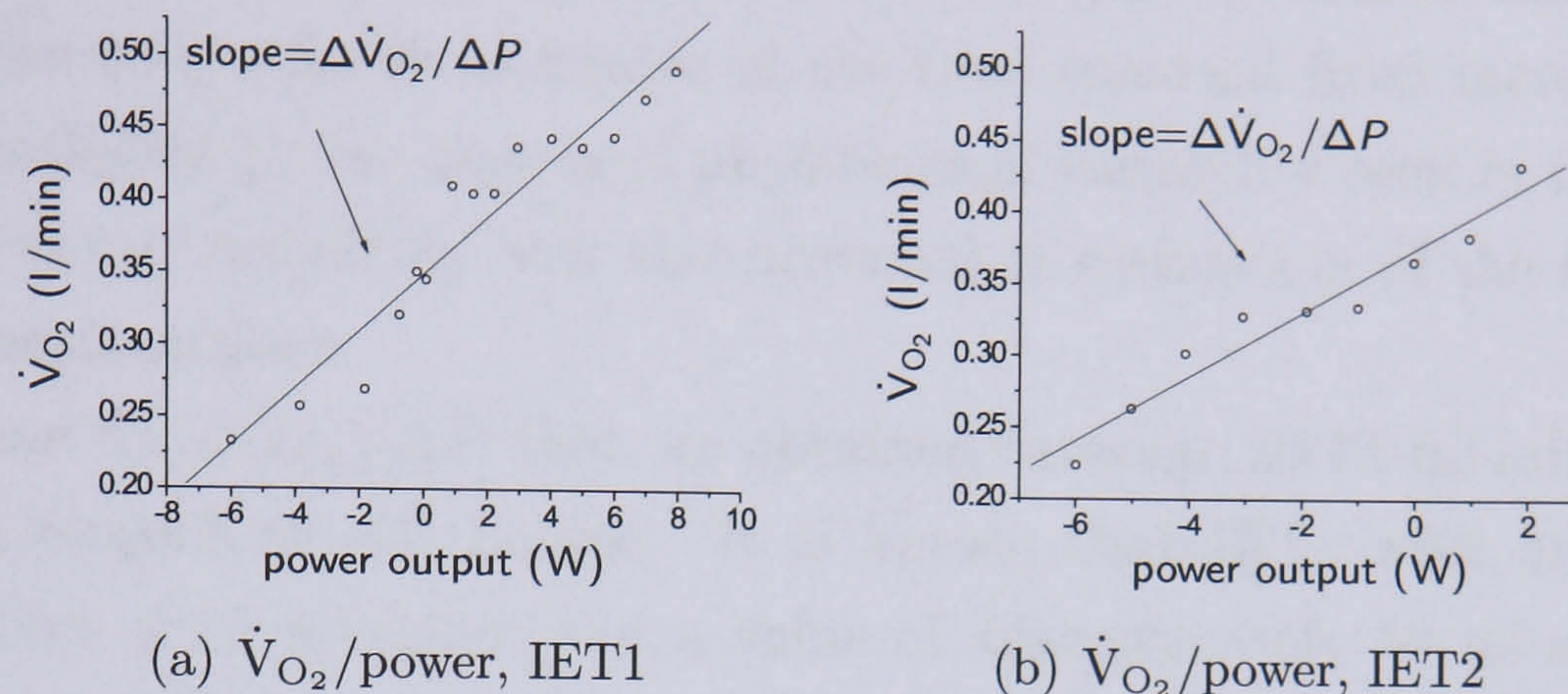


Figure 4.6: $\dot{V}_{O_2}/\text{power}$ output relationship during the incremental phase of the tests (subject S2). The slope of each linear regression gives the relationship between oxygen uptake and power output, $\Delta\dot{V}_{O_2}/\Delta P$.

Test	IET1	IET2
Peak \dot{V}_{O_2} (l/min)	0.53	0.43
Peak power output (W)	8.16	1.85
τ (s)	156	285
$\Delta\dot{V}_{O_2}/\Delta P$ (ml·min ⁻¹ ·W ⁻¹)	19.81	22.46

Table 4.5: Summary of incremental test outcomes for the tests performed by subject S2.

4.5 Discussion

4.5.1 Case Study S1

Incremental exercise test

In case study S1, the characteristics of the technical setup result in accurate determination of peak workrate, fairly repeatable determination of peak oxygen uptake and of the oxygen uptake-workrate relationship ($\Delta\dot{V}_{O_2}/\Delta P$): see table 4.1.

The estimates of oxygen uptake response kinetics, τ , obtained from the incremental exercise tests are seen to be highly variable. This finding corroborates results

seen previously in able-bodied subjects: Hughson and Inman [59] reported an intra-subject variability with a factor of more than two in the estimates of τ obtained from incremental tests. The results reported here may therefore reflect a fundamental difficulty in obtaining reliable estimates of the time constant from incremental tests. This is exacerbated by the increased physiological variability seen in the SCI population. Significant variability was also observed in estimation of the time constant from step response data.

The values for $\Delta\dot{V}_{O_2}/\Delta P$ that we obtained (average $20.13 \text{ ml}\cdot\text{min}^{-1}\cdot\text{W}^{-1}$) are higher with respect to AB people. It is known that IETs with an incremental phase duration of 10 minutes yield a value of approximately $10 \text{ ml}\cdot\text{min}^{-1}\cdot\text{W}^{-1}$ in AB subjects, while longer durations give higher $\Delta\dot{V}_{O_2}/\Delta P$ values [125]. However, the values obtained here are probably a reflection mainly of the low efficiency of FES-cycling with SCI subjects [45].

Step exercise tests

The accurate power/cadence control setup, together with accurate estimates of the ventilatory anaerobic threshold from the incremental tests (see chapter 5), allows imposition of step changes in workrate which result in operation either below or above the VT, for estimation of respiratory response kinetics in these regimes, and also for estimation of steady-state oxygen uptake. Steady-state oxygen uptake estimation shows good repeatability across the tests reported here. However, estimation of the response time constants τ for \dot{V}_{O_2} , \dot{V}_{CO_2} and \dot{V}_E again show high variability. This may be due to the relatively poor signal to noise ratio resulting from the very low absolute exercise workrates achievable during FES-cycling by SCI subjects. However, the \dot{V}_{CO_2} and \dot{V}_E kinetics are slower than the \dot{V}_{O_2} kinetics, as happens in AB subjects [17, 127].

The power output for the sub- and supra-threshold phases can be chosen as a set percentage of P_{peak} or in order to elicit \dot{V}_{O_2} values that are a set percentage of peak \dot{V}_{O_2} or of the ventilatory threshold. Therefore, the protocol can be personalized and it will be easier to compare endurance, \dot{V}_{O_2} level and kinetics within and between subjects.

The stimulation pulsewidth time-course confirms the hypothesis that 0 W is a level below the VT and 12 W is above. Indeed, during the 0 W phase the stimulation pulsewidth remains approximately constant at a level of about 100-150 μs . During the supra-threshold phase it increases until the subject fatigues, i.e. stimulation pulsewidth reaches saturation.

During the sub-threshold stage of the exercise, we estimated that 6 minutes would be sufficient for \dot{V}_{O_2} to reach a metabolic steady state. As expected, \dot{V}_{O_2} reaches a plateau within the 0 W stage in all the tests. R is lower than 1 for SET1 and slightly above 1 for SET3 and this confirms the hypothesis of aerobic steady state. In SET2 R is clearly above 1, thus indicating that the subject is in part exercising anaerobically. An explanation for this is that the subject could have been hyperventilating. However, if this had been the case, in correspondence with the increment in R there should have been a decrease in $P_{ET}CO_2$, which did not occur. Thus, the high R could be explained by the fact that the passive power output in SET2 was lower than in the other tests. Indeed, it was equal to -7.77 W, while in the other two tests it was approximately -5 W. Thus, we suggest that in the second test the gap between passive and 0 W was just above the VT, causing R to be higher than 1. Previous studies found that R during 0 W cycling was higher than 1 and this was explained as a characteristic of SCI people, since \dot{V}_{O_2} seemed to reach a plateau [2, 6, 29, 57, 89]. \dot{V}_{O_2} can reach a plateau when exercising above the ventilatory threshold, up to the critical power, but R values are above 1 [127]. Thus, we suggest that the subjects performing constant load tests in previous studies were exercising at a level above the ventilatory threshold. The fact that R was slightly above 1 in IET3 suggests the hypothesis that 0 W is a power output level too close to the VT. It is possible that 25-35% of P_{peak} is still too high a level for SCI people to exercise completely aerobically. The high R could also be explained by the inverse or by the non-selective fibre recruitment pattern due to FES (see section 2.3). This could be one of the causes of the higher contribution of the anaerobic metabolism at power output percentages that can be considered very low for AB subjects.

During the 12 W phase \dot{V}_{O_2} initially rises exponentially, followed after some minutes by a slow component in SET1 and SET3. In SET2 the exponential rise cannot be seen. A possible explanation is that during the 0 W phase the subject was already exercising anaerobically, thus the typical \dot{V}_{O_2} time-course for a step increment in power output cannot be seen. In all cases \dot{V}_{O_2} then continues to rise without reaching a steady state, until exercise has to be stopped because the power output required cannot be sustained any longer.

Interestingly, the average \dot{V}_{O_2} values estimated from the final minute of the constant load tests (mean of 0.72 l/min across the three SETs) are higher than the peak \dot{V}_{O_2} values estimated from the incremental tests (mean of 0.66 l/min across the three IETs). Thus, the IET as proposed here may underestimate the true $\dot{V}_{O_{2peak}}$, and may require further tailoring for the SCI population. One of the options

available is aiming to prolong the duration of the IET ramp phase by reducing the amplitude of the steps. However, the fact that the IET as proposed here does appear to provide a useful means of estimating the VT (this will be discussed more widely in chapter 5) supports the concept that the initial part of the IET testing protocol should be retained. Thus, the final part of the incremental phase can possibly be prolonged beyond the point where the maximum allowable stimulation level is reached. In other words, the test could proceed beyond the time when maximum stimulation is reached and be extended until the power output developed by the subject drops under a pre-specified level, or for a pre-specified duration.

4.5.2 Case Study S2

Incremental exercise test

The power control in the two IETs for subject S2 appears not to be adequately accurate. A possible explanation is that the warm-up for the subject was not carried out properly. The power output level was set arbitrarily at 4W. We suggest that for each subject the warm-up has to be personalized. Not only the power output level but also the duration has to be tailored to the capacities of the subject. The power output level has to be chosen low enough to avoid the subject fatiguing. On the other hand it has to be high enough to actually warm the muscles. The other factor is the duration of the warm-up interval. If it is too short the muscles remain cold even if the power level is relatively high. If the duration of the warm-up is too long, it is likely that subject will fatigue before starting the actual exercise session. Moreover, the length of the rest interval following the warm-up has to be defined so that the gas exchange variables return to resting values. However, it cannot be too extended otherwise the muscles cool down again and the whole aim of the warm-up itself is lost. If the warm-up is not properly done the muscles are more subjected to spasms. It is possible that in these tests the subject's muscles were not warm enough. After some minutes of cycling, the subject warmed up and then the control became smooth again.

Contrary to what has been seen for subject S1, the two IETs for subject S2 do not give similar results. The duration of the incremental phase is 18 minutes in the first test, which is much longer than expected. Due to the poor power control in the first test, we decided not to change the step amplitude in the second test and to repeat it in the same way to verify the obtained results. The outcome of the second test did not confirm what found from the first one. The duration of the

incremental phase is 12 minutes, which is the aim of the protocol we used. However, durations that are too long are known to give values of P_{peak} that underestimate the real ones. From our tests we can see that the P_{peak} for IET1 is higher than for IET2. This finding suggests that IET2 had been interrupted for a reason other than the limit reached of the subject. Moreover, the fact that the longer test gives higher P_{peak} values leads us to question the validity of the 12 minutes rule for SCI people. The fact that the $\dot{V}_{\text{O}_{2\text{peak}}}$ found in the IETs with subject S1 is lower than the \dot{V}_{O_2} measured at the end of the SETs also supports this hypothesis. Prolonging the duration of the incremental phase may be useful in finding the real $\dot{V}_{\text{O}_{2\text{peak}}}$. This can be achieved by reducing the amplitude of the steps or allowing the subject to continue exercise after stimulation pulsewidth has reached saturation.

The oxygen uptake at rest and during passive cycling is similar in the two tests. However, the peak oxygen uptake is different: 0.53 l/min compared to 0.43 l/min. For AB people a difference of 0.1 l/min is not significant, but for SCI people it is a significant amount considering the low level of \dot{V}_{O_2} they can reach. The difference in $\dot{V}_{\text{O}_{2\text{peak}}}$ could be due to the different duration of the incremental phase, and consequently of the power output, in the two cases: 18 and 12 minutes. It is known that for AB people prolonged IETs result in lower values for $\dot{V}_{\text{O}_{2\text{peak}}}$ [125]. In this case the longer IET gave a higher $\dot{V}_{\text{O}_{2\text{peak}}}$, which could be expected considering that P_{peak} was also higher in IET1. The differences between the two tests may be due to day-to-day variability in the subject's physiological status. This is supported by the fact that the \dot{V}_{O_2} time course is similar for the two tests up to the point where the second test stops. This highlights that day-to-day intra-subject variability is significantly higher in SCI than in AB subjects.

The time constant for the two tests is quite different. This result confirms the conclusions reached for the results from subject S1.

4.6 Conclusions

We have proposed new protocols for incremental and constant-load exercise testing, for estimation of the key markers of cardiopulmonary status.

The incremental exercise test provided fairly repeatable estimation of peak exercise workrate and oxygen uptake-workrate relationship in one subject. The IET, as implemented here, provides an apparently low peak oxygen uptake value and may require further modification for SCI subjects performing FES-cycling exercise. In particular, the higher \dot{V}_{O_2} values observed during constant-load cycling suggest that

the IET duration should be extended beyond the onset of the maximum allowable stimulation level.

Highly variable results were observed in estimation of the oxygen uptake response kinetics in both the IET and SET protocols. This probably reflects: (i) a fundamental difficulty in obtaining reliable time-constant estimates from a ramp test [59], in part due to violation of the assumption of 1st-order linear and time-invariant dynamics; and (ii) the low magnitude of workrate steps in the SET giving poor signal-to-noise properties for estimation.

The SET protocol provides a measure of steady-state oxygen cost and metabolic efficiency measures for constant-load cycling, with good repeatability.

The ventilatory threshold and efficiency outcomes from the IET and SET are discussed separately, in chapters 5 and 7, respectively.

Chapter 5

Ventilatory Threshold

5.1 Summary

In this chapter we demonstrate, for the first time, detection of a ventilatory anaerobic threshold in SCI subjects during FES-cycle ergometry. Results are reported from IETs performed by two subjects. The repeatability of the VT and the power output (PO) at which it occurs are shown in one subject over three tests. Moreover, the detection of the VT at negative power output levels is shown in the second subject. The data relating to the first subject can be found also in the paper [33].

5.2 Introduction

The data analyzed in this chapter have been obtained from the incremental exercise tests described in chapter 4.

5.3 Methods

We followed the method described by Wasserman *et al.* [124, 125] to detect the presence of the ventilatory threshold (see also section 1.4.1). For each test we analysed the following gas exchange variables: \dot{V}_{O_2} , \dot{V}_{CO_2} , \dot{V}_E , end tidal pressure for O_2 ($P_{ET}O_2$) and CO_2 ($P_{ET}CO_2$). Moreover, we analysed also the ventilatory equivalent for oxygen uptake (\dot{V}_E/\dot{V}_{O_2}) and for carbon dioxide output (\dot{V}_E/\dot{V}_{CO_2}).

We studied the plot of \dot{V}_E against \dot{V}_{CO_2} during the incremental phase of the test to verify if the respiratory compensation point (RCP) was present. The RCP is the point where \dot{V}_{CO_2} starts to increase more rapidly than \dot{V}_E , thus causing an increase

in the \dot{V}_E/\dot{V}_{CO_2} slope (see also section 1.5.1). Thus, if a deflection from linearity was present in the plot, all the data points after the shift from linearity were excluded from the analysis. Moreover, we studied the kinetics of \dot{V}_{CO_2} in the incremental phase. \dot{V}_{CO_2} shows a delay following the power output increase. The data points belonging to the interval in which \dot{V}_{CO_2} was still constant were excluded from the analysis for the detection of the ventilatory threshold.

The remaining data were analysed with the V-slope method and with the ventilatory equivalent method. The $\dot{V}_{CO_2}/\dot{V}_{O_2}$ plot was analysed in order to find the deflection from linearity that indicates the presence of the ventilatory threshold (see also section 1.4.1). Two lines were drawn over the first and the second half of the $\dot{V}_{CO_2}/\dot{V}_{O_2}$ data. The point where the two lines crossed was assumed to be the VT. To corroborate the V-slope method finding we used also the ventilatory equivalent method (see also section 1.4.1). End tidal oxygen and carbon dioxide pressures were analysed. The point where $P_{ET}O_2$ started to decrease and $P_{ET}CO_2$ remained constant was considered to be the VT. To further confirm the results the ventilatory equivalent for oxygen uptake and for carbon dioxide output were also studied. The point where \dot{V}_E/\dot{V}_{O_2} increased and \dot{V}_E/\dot{V}_{CO_2} remained constant was considered to be the VT.

When the VT obtained with the different methods did not occur at the same \dot{V}_{O_2} value, we assumed that the V-slope finding was the correct one [85].

5.4 Results

5.4.1 Case Study S1

Figures 5.1, 5.2 and 5.3 show the graphs for the gas exchange variables used to detect the VT. The outcome is similar in the three tests. In figures 5.1(a), 5.2(a) and 5.3(a) \dot{V}_E is plotted against \dot{V}_{CO_2} to detect the presence of the respiratory compensation point. In all three tests it is not possible to detect a deflection in the slope of the plot.

In figures 5.1(b), 5.2(b) and 5.3(b) \dot{V}_{CO_2} is plotted against \dot{V}_{O_2} . The V-slope method to detect VT clearly indicates that the change in slope occurs at a value of \dot{V}_{O_2} in the range 0.33-0.37 l/min. The VT point is found by prolonging the two regression lines fitted on the first and the second half of the \dot{V}_{CO_2} vs \dot{V}_{O_2} plot; the point at which the two lines intersect is indicated by the vertical dotted line.

Figures 5.1(c), 5.2(c) and 5.3(c) and figures 5.1(e), 5.2(e) and 5.3(e) show \dot{V}_{O_2}

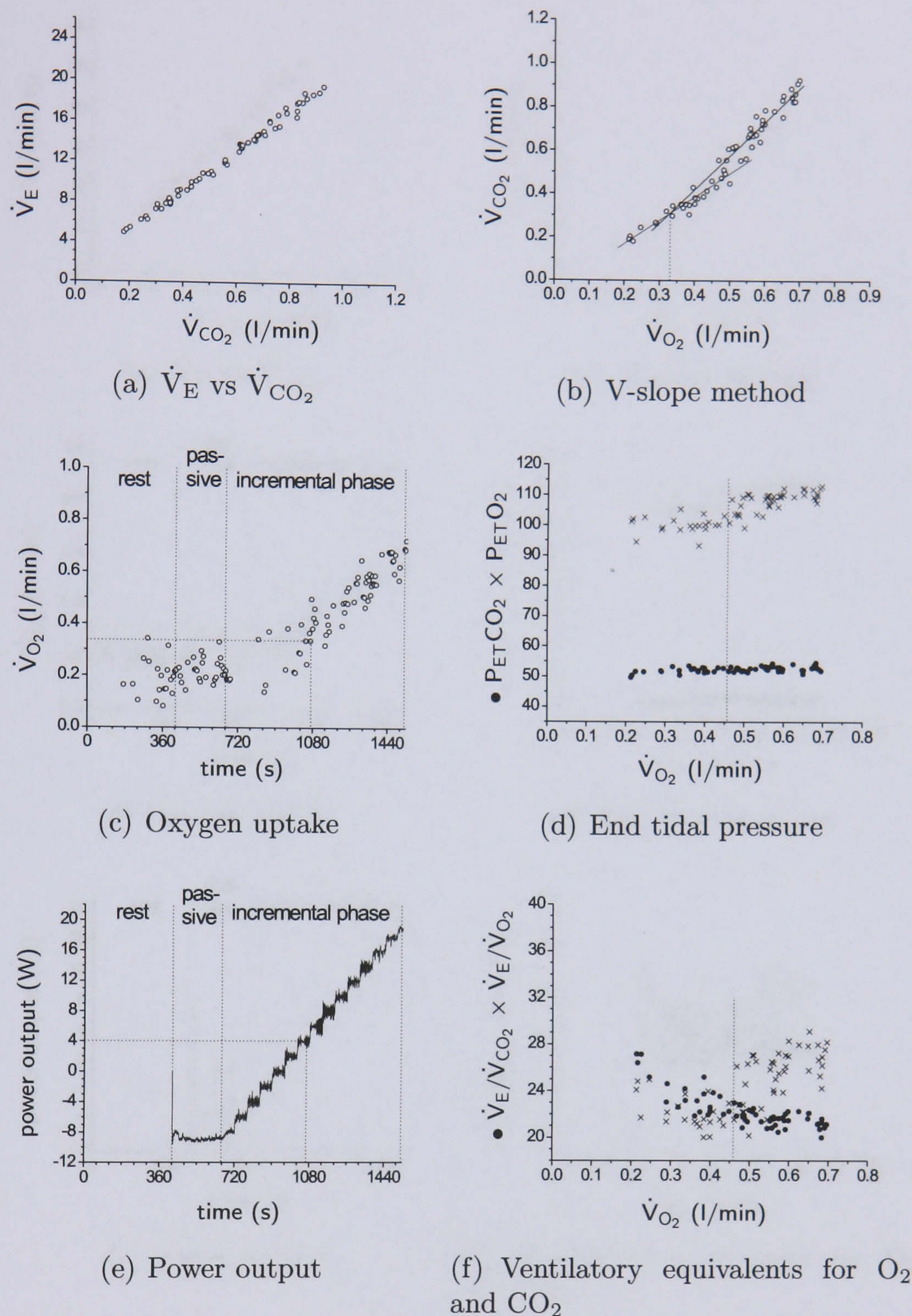


Figure 5.1: Ventilatory threshold detection in IET1 (subject S1). In figure (b) the two lines cross at the VT, that is indicated by the vertical dotted line. The dotted lines in figures (c) and (e) show where the VT occurs in terms of \dot{V}_{O_2} and power output. In figures (d) and (f) the vertical dotted lines show where the VT could occur according to the end tidal pressure and the ventilatory equivalents method.

and power output time-course, respectively. On both graphs, for each test, the dotted lines indicate where the VT occurs in terms of \dot{V}_{O_2} and power output. The results for the three tests are similar. Table 5.1 summarizes the ventilatory threshold values and the corresponding power output for the three tests.

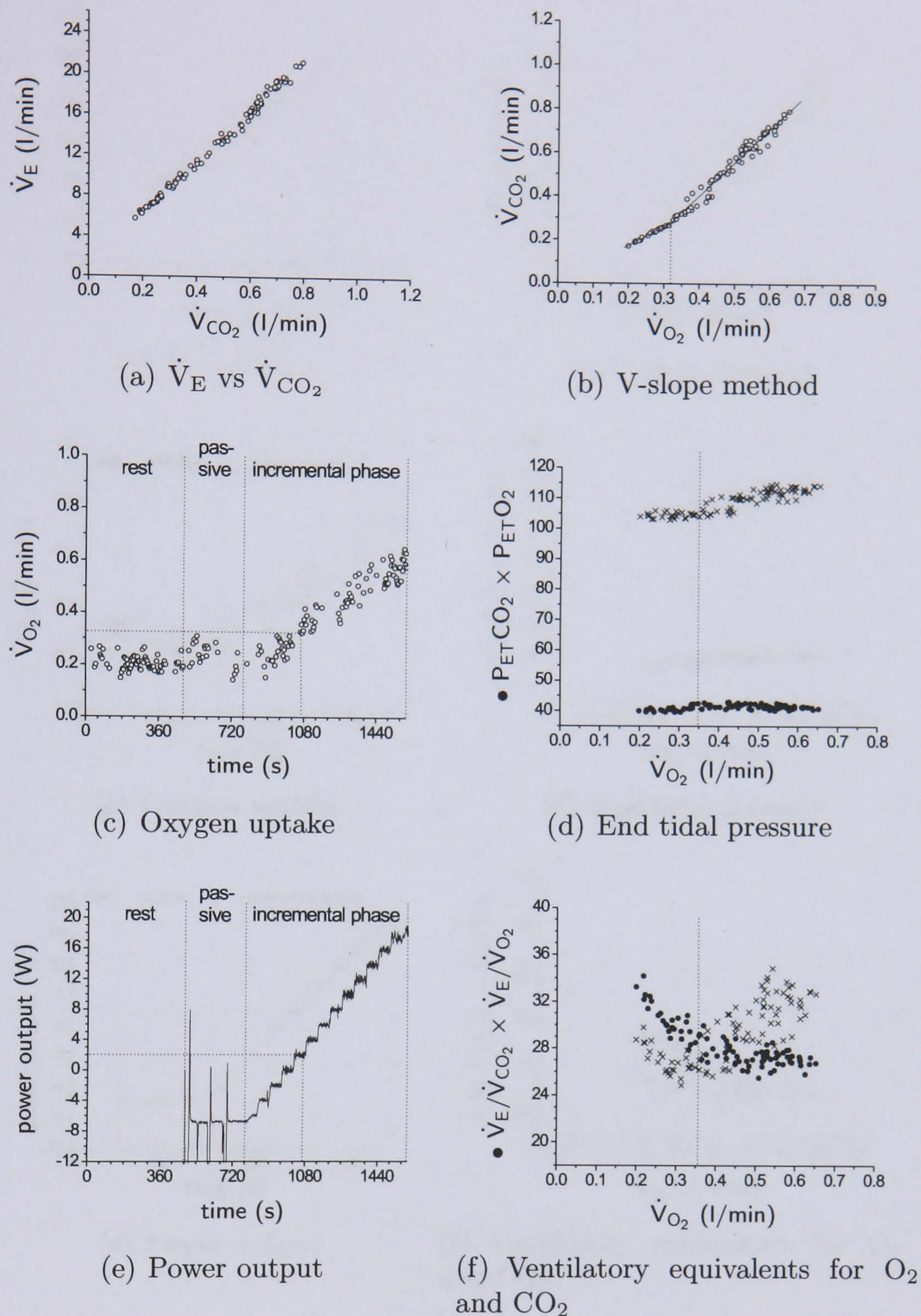


Figure 5.2: Ventilatory threshold detection in IET2 (subject S1). In figure (b) the two lines cross at the VT, that is indicated by the vertical dotted line. The dotted lines in figures (c) and (e) show where the VT occurs in terms of \dot{V}_{O_2} and power output. In figures (d) and (f) the vertical dotted lines show where the VT could occur according to the end tidal pressure and the ventilatory equivalents method.

Figures 5.1(d), 5.2(d) and 5.3(d) show both P_{ETO_2} and P_{ETCO_2} plotted against \dot{V}_{O_2} . P_{ETO_2} starts to rise when the rate of rise of \dot{V}_{O_2} increases linearly and \dot{V}_E accelerates, while at the same time P_{ETCO_2} remains constant. All this occurs at \dot{V}_{O_2} values slightly higher with respect to those found with the V-slope method in

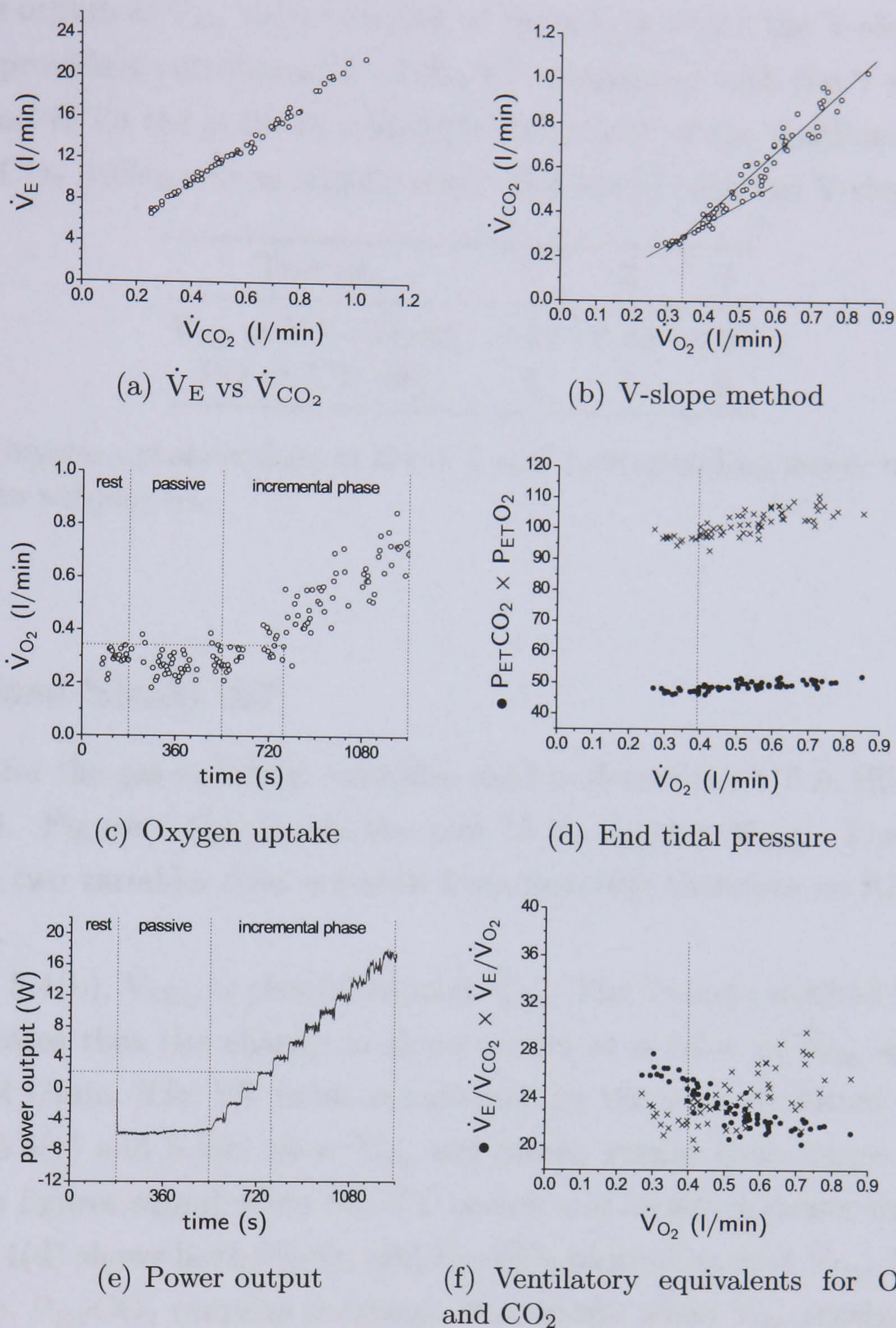


Figure 5.3: Ventilatory threshold detection in IET3 (subject S1). In figure (b) the two lines cross at the VT, that is indicated by the vertical dotted line. The dotted lines in figures (c) and (e) show where the VT occurs in terms of \dot{V}_{O_2} and power output. In figures (d) and (f) the vertical dotted lines show where the VT could occur according to the end tidal pressure and the ventilatory equivalents method.

the three tests.

In addition, the ventilation responses have been analyzed. Figures 5.1(f), 5.2(f) and 5.3(f) show in the same graph \dot{V}_E/\dot{V}_{O_2} and \dot{V}_E/\dot{V}_{CO_2} plotted against \dot{V}_{O_2} . \dot{V}_E/\dot{V}_{CO_2} decreases or becomes constant during the test, indicating that \dot{V}_{CO_2} accelerates with \dot{V}_E after the VT, whereas \dot{V}_E increases disproportionately to \dot{V}_{O_2} above

VT. All this occurs at \dot{V}_{O_2} values similar to those found with the V-slope method in IET2, thus providing corroboration of the VT established with the V-slope method. For IET1 and IET3 the point at which the behaviour of the ventilatory equivalent for O_2 and CO_2 differs occurs slightly after that found with the V-slope method.

Test nr.	1	2	3
\dot{V}_{O_2} at VT (l/min)	0.34	0.33	0.35
PO at VT (W)	4	2	2

Table 5.1: Oxygen uptake values at the VT and corresponding power output for the three IETs in subject S1.

5.4.2 Case Study S2

The graphs for the gas exchange variables used to detect the VT in IET1 are shown in figure 5.4. Figure 5.4(a) shows the plot of \dot{V}_E against \dot{V}_{CO_2} . The relationship between the two variables does not shift from linearity, therefore no RCP occurs for this subject.

In figure 5.4(b), \dot{V}_{CO_2} is plotted against \dot{V}_{O_2} . The V-slope method to detect VT clearly indicates that the change in slope occurs at a value of \dot{V}_{O_2} approximately equal to 0.34 l/min. The VT point is indicated by the vertical dotted line.

Figures 5.4(c) and 5.4(e) show \dot{V}_{O_2} and power output time-course. The dotted lines in both figures signal when the VT occurs and at which power output.

Figure 5.4(d) shows both $P_{ET}O_2$ and $P_{ET}CO_2$ plotted against \dot{V}_{O_2} . When $P_{ET}O_2$ starts to rise, $P_{ET}CO_2$ remains constant: this occurs when \dot{V}_{O_2} reaches an approximate value of 0.36 l/min, i.e. a value slightly higher than the one found with the V-slope method. The ventilation responses show results similar to those found with the end tidal pressure analysis. Figure 5.4(f) shows in the same graph \dot{V}_E/\dot{V}_{O_2} and \dot{V}_E/\dot{V}_{CO_2} plotted against \dot{V}_{O_2} . \dot{V}_E/\dot{V}_{CO_2} decreases along the whole test. \dot{V}_E/\dot{V}_{O_2} instead starts to increase when \dot{V}_{O_2} reaches a value of 0.38 l/min.

In IET2 (figure 5.5), the relationship between \dot{V}_E and \dot{V}_{CO_2} is linear, but the data points are noisier than in IET1 (figure 5.5(a)). Figures 5.5(c) and 5.5(e) show the time-course of \dot{V}_{O_2} and power output.

The presence of the VT is not clear, and it could be argued that VT does not occur at all (figure 5.5(b)). Studying the $P_{ET}O_2$ and $P_{ET}CO_2$ graphs (see figure 5.5(f)), it can be seen that there is no rise in $P_{ET}O_2$. The analysis of the

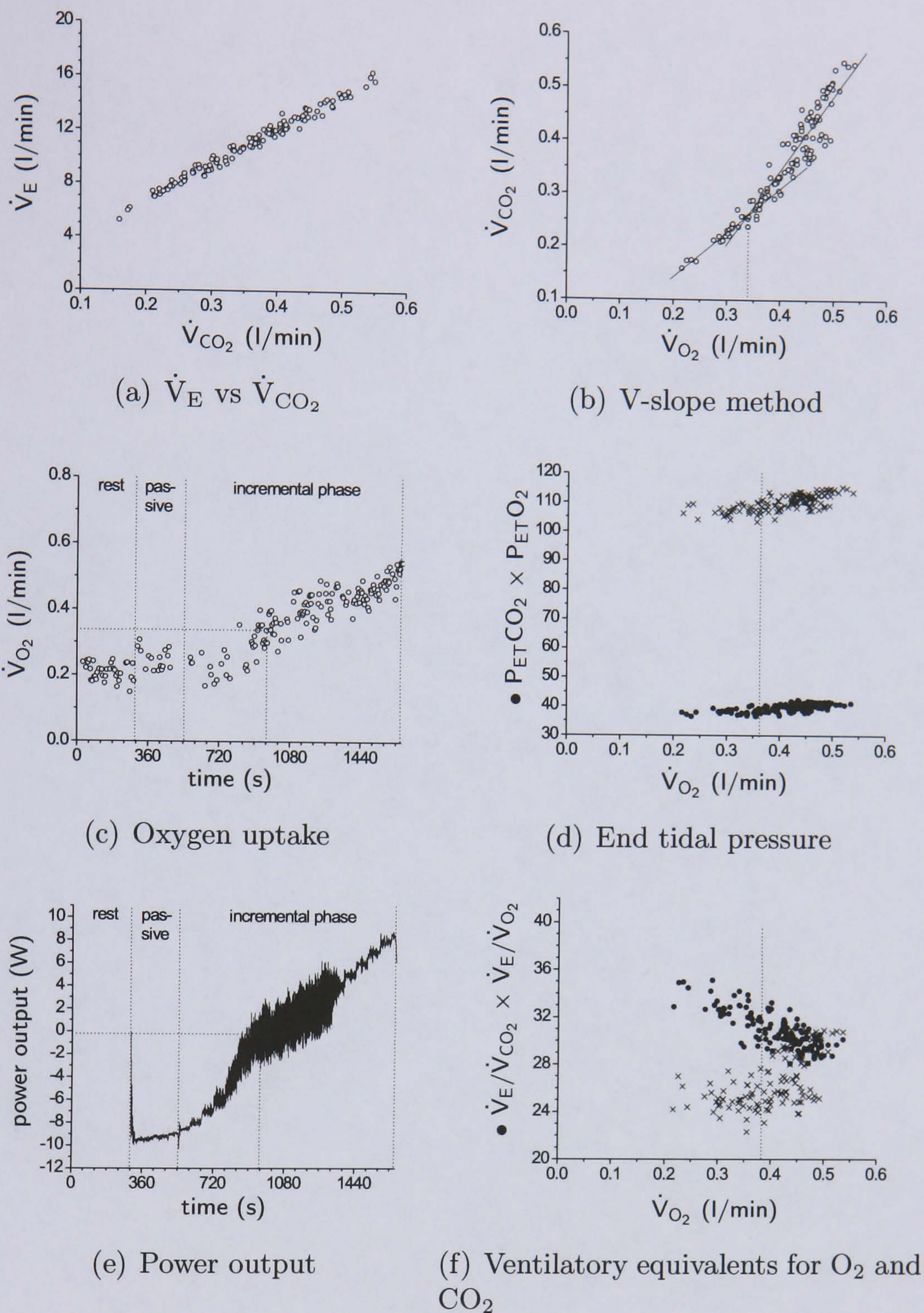


Figure 5.4: Ventilatory threshold detection in IET1 (subject S2). In figure (b) the two lines cross at the VT, that is indicated by the vertical dotted line. The dotted lines in figures (c) and (e) show where the VT occurs in terms of \dot{V}_{O_2} and power output. In figures (d) and (f) the vertical dotted lines show where the VT could occur according to the end tidal pressure and the ventilatory equivalents method.

ventilatory equivalents for O_2 and CO_2 (figure 5.5(f)) does not give any clue as to where the VT could be located, or if it exists at all. $\dot{V}_E / \dot{V}_{CO_2}$ has a behaviour similar to the typical one, as it decreases along the test. However, $\dot{V}_E / \dot{V}_{O_2}$ is quite noisy and it does not increase at any point.

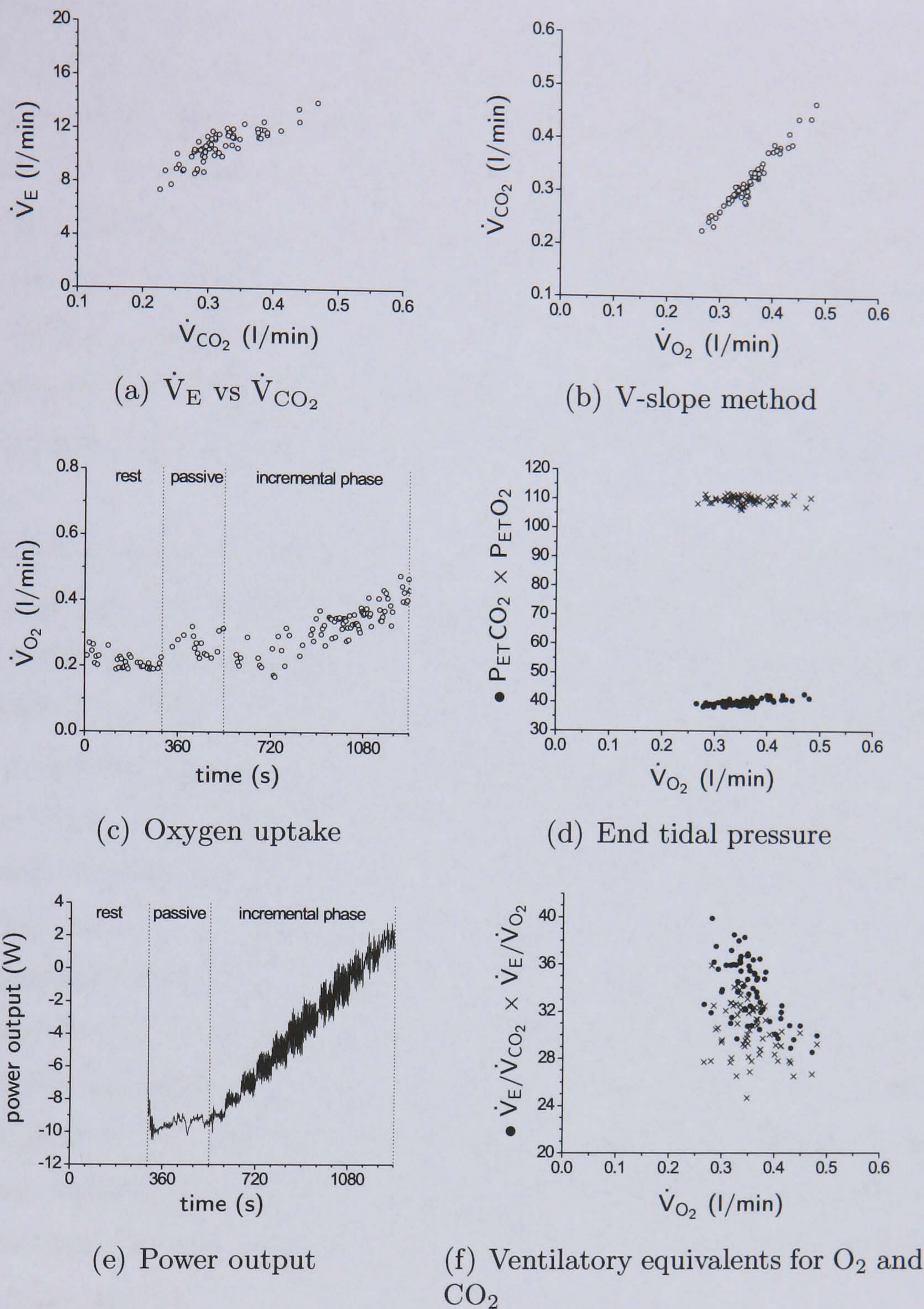


Figure 5.5: Graphs used for the detection of the ventilatory threshold for IET2 (subject S2). No dotted lines have been added because no VT can be detected.

5.5 Discussion

5.5.1 Case Study S1

The linear relationship between \dot{V}_E and \dot{V}_{CO_2} in the three IETs suggests that the respiratory compensation point has not been reached. RCP is the level above which no metabolic steady state can be reached and above which exercise is termed severe [127]. Meyer *et al.* [85] suggest that the point of inflexion in the \dot{V}_E vs \dot{V}_{CO_2} plot

cannot be seen in patients with low endurance, because subjective exhaustion occurs earlier. In SCI subjects it is not possible to strictly speak of subjective exhaustion, as exercise is stopped when the pulsewidth reaches saturation. However, since SCI subjects have a very reduced endurance and are more subject to fatigue than AB subjects, it is possible that the ventilatory compensation for CO_2 does not occur. In other words, the intensity of exercise necessary to reach the RCP could be too high for the SCI population.

The estimated VT outcomes (i.e. the oxygen uptake and exercise workrate at the threshold) are seen to be fairly repeatable across the three incremental tests (see table 5.1).

The analysis of $P_{\text{ET}}\text{O}_2$ and $P_{\text{ET}}\text{CO}_2$ can usually help to confirm the findings of the V-slope method. In the three IETs $P_{\text{ET}}\text{O}_2$ starts rising at \dot{V}_{O_2} values higher than those found with the V-slope method. The analysis of the ventilatory equivalents for O_2 and CO_2 is another means of confirming the V-slope method findings. In the past it was a method preferred to the V-slope, because of the lack of appropriate gas analysers [109, 124]. However, if the subjects have problems in ventilation or have abnormal breathing patterns, it is not possible to use this method. Thus, it is possible that the discrepancy in results obtained with the different methods may be due to problems in ventilation related to the SCI pathology. The higher breath-to-breath noise found in SCI with respect to AB gas exchange data appears also to suggest that the breathing pattern is more irregular in SCI than in AB subjects. Thus, the higher VT found with the ventilatory equivalent method may be due to the uneven breathing pattern. Meyers *et al.* [85] suggest that the ventilatory equivalent method should be used only when the detection of the VT is not clear with the V-slope method.

Further discussion on the meaning of the concept of VT in SCI subjects is given below.

5.5.2 Case Study S2

Subject S2 is an example of VT occurring at a negative power output. This result is not surprising, as SCI subjects are very deconditioned. However, to be able to actually detect it is quite remarkable. In the past it would have not been possible to obtain this result, because of the limitations in the apparatus used. In this case, the possibility of working in the negative range of power outputs increases the flexibility and the adaptability of the incremental exercise test protocol to populations that

have very limited mobility.

The relationship between \dot{V}_E and \dot{V}_{CO_2} is linear in both IETs for subject S2, thus confirming the hypothesis that it is not possible to detect the presence of the RCP in SCI subjects.

In IET1 the power output control was not accurate. The reference power output level corresponding to the VT is -3 W, but the actual mean power output was approximately -0.2 W. Thus, we can affirm that VT occurred at a negative power output level. The V-slope analysis clearly indicates the presence of the VT at a \dot{V}_{O_2} level of 0.34 l/min. The analysis of $P_{ET}O_2$ and $P_{ET}CO_2$ delivers again a value of \dot{V}_{O_2} that is slightly higher than the one found with the V-slope method. The same result was obtained with the analysis of $\dot{V}_E / \dot{V}_{O_2}$ and $\dot{V}_E / \dot{V}_{CO_2}$.

In IET2 the power output is better controlled. However, the test stopped at a power output of 2 W, which is just above the one corresponding to the VT, according to IET1. Thus, it is possible that the VT has been reached by the subject but it is very difficult to be seen as the test stopped immediately after. Another hypothesis is that the subject did not reach the VT at all, as it is not possible to detect it with the V-slope method. The $P_{ET}O_2$ and $P_{ET}CO_2$ analysis confirms this hypothesis, as there is no detectable rise in $P_{ET}O_2$. $\dot{V}_E / \dot{V}_{CO_2}$ and $\dot{V}_E / \dot{V}_{O_2}$ data are very noisy and do not present any particular trend. An hypothesis for the justification of the results obtained with IET2 is that the subject's characteristics may have differed due to day-to-day variability in the subject's physiological status resulting in early fatigue. Thus, he had to stop the test before reaching his VT. A wide range in physiological status is a feature of SCI subjects and may be due to disruption of neurological function.

5.5.3 Concept of Ventilatory Threshold in SCI Subjects

If the theory of the non-selective, spatially fixed and temporally synchronous muscle fibre recruitment with FES is true, then the concept of VT in SCI subjects has to be revised. In FES when stimulation intensity increases, the force developed by the subject increases as a consequence because more fibres are recruited. Indeed, the higher charge delivered reaches deeper in the muscle bulk and also activates the fibres that are positioned further from the surface. If the different fibre types are recruited together, then anaerobic metabolism is active from the beginning of exercise. Stimulation is applied with a frequency of 30 Hz in our tests. This frequency corresponds to the optimal voluntary firing frequency of fast fibres, and it is higher

than the one for slow fibres (i.e. 10 Hz) [49]. Thus, it could be that slow fibres fatigue first and eventually drop out and only fast fibres are left, since SCI subjects' muscles are composed primarily of type II fibres [50, 111]. Therefore, \dot{V}_{CO_2} would increase with time and be higher when the slow fibres that were contributing to the force production fatigue. Therefore, it could still be possible to detect a "Ventilatory Threshold". The VT in SCI subjects would then represent the passage from mixed energy metabolism to anaerobic energy metabolism only, as opposed to AB subjects, for whom VT occurs at the point where anaerobic metabolism starts to overtake the aerobic one. However, having seen that VT appears to be reproducible within subjects, it could still be used to compare fitness in different subjects. It could be argued that different people have different percentages of type II muscle fibres that contribute to the overall energy expenditure to a different extent. As a consequence it may not be possible to compare different subjects' VT, because it is not possible to determine how much of the energy expenditure is due to aerobic and how much to anaerobic metabolism. However, reports of shift in fibre type distribution due to training have been published [21, 40, 67, 80]. A higher percentage of type I muscle fibres implies a greater contribution of these to the production of force. Thus, \dot{V}_{O_2} will be lower for the same power output and the VT will possibly occur later, as a result of a period of training. Therefore, it could still be possible to use the VT as a measure of fitness for SCI subjects. However, it is also possible that, since the concept of VT seems to be different in SCI subject with respect to AB subjects, the method for detecting the ventilatory threshold may have to be refined.

It appears that a VT can be detected in SCI subjects but further work using blood lactate samples is needed to verify that in SCI subjects the VT found is really reflective of the "lactate threshold". Therefore, further investigations of the underlying mechanisms of the VT is also warranted, since both slow and fast fibres can produce lactate.

5.6 Conclusions

For the first time, we have shown the possibility of detecting the presence of the ventilatory anaerobic threshold in SCI patients performing FES-cycle ergometry. Detection of the VT has been made possible by the novel testbed used for our tests. Indeed, cadence was accurately controlled throughout the tests. Moreover, the power output could be set in small increments, as required from Wasserman *et al.* [125]. In particular, workrate control allows approximation of a true ramp thereby achieving

a sensitivity of testing not previously attained in FES-cycle ergometry.

Results for subject S1 show good repeatability, thus suggesting that the VT could be characteristic of the subject and thus could represent a reliable index of fitness.

Results for Subject S2 show that VT can occur at negative power output levels. Thus, it is fundamental to be able to use also the negative power output range in exercise testing with SCI subjects.

The concept of VT in SCI subject has been discussed and it seems that the ventilatory threshold could be the transition from mixed metabolism to anaerobic metabolism only.

Chapter 6

Study for Angle-Range Variation

6.1 Summary

This chapter reports the results of an investigation on the influence of stimulation parameters on the metabolic and stimulation cost of FES-cycling exercise. These results have been published in a journal paper [60] and in a conference paper [34]. We empirically studied the selection of muscle activation angles using the following variables: real-time, breath-by-breath measurement of pulmonary oxygen uptake rate, and a new real-time measure of total stimulation charge rate, which can be viewed as the *stimulation cost*. In particular, the aim of this work was to determine whether oxygen-cost and stimulation-cost measurements are sensitive enough to allow discrimination between the efficacy of different activation ranges for stimulation of each muscle group during constant-power cycling.

6.2 Introduction

One of the aims of FES is to try and temporarily replace part of the function of the central nervous system. Thus, it is important that the muscles are activated at the right time and with the appropriate sequence, so that the appropriate movements are performed [47]. In most of the previous studies timing of muscle activation during cycling has mostly been based on electromyographic (EMG) measurements of muscle activation in healthy subjects [41, 95, 97, 102].

Phillips *et al.* [99] evaluated the effect of FES on muscular, respiratory and cardiovascular parameters in SCI subjects. In their study, they found that minute ventilation and respiratory rate had improved with training. However, the vari-

ance of the measurements was too high to establish statistical significance. They maintain that optimisation of the pattern of FES exercise could have improved the significance.

Several adjustable parameters are associated with the control and coordination of muscle stimulation during cycling. The stimulation parameters include: the stimulation frequency, or, if the frequency is not constant, the variable inter-pulse interval; the choice of pulsewidth and/or pulse-amplitude modulation; and the timing of muscle-group stimulation, i.e. the choice of crank-angle ranges over which each muscle group is activated. Each of these parameters have some effect on the resulting efficiency [28, 42, 62, 66, 93, 95, 97, 102, 106]. Efficiency will be described and discussed in more detail in chapter 7.

Generally, the frequency used is the lowest that still allows smooth contractions, typically 20 to 35 Hz [19, 26, 28, 53, 98, 107]. However, Eser *et al.* [28] found that the power output developed during FES-cycling was higher if the frequency was 50 Hz or 60 Hz. They also found that PO during the 30th minute of the session was almost always higher than the average during the same session. Moreover, Matsunaga *et al.* [81] report that fatigue occurs earlier when using lower stimulation frequencies. This is true when intermittent stimulation is applied, but not with continuous stimulation.

Many previous studies have analysed the electromyographic data obtained from AB subjects during volitional cycling [66, 93, 95, 97, 102]. The aim was to identify the most appropriate timing and the ranges of activation, that subsequently would have been used to design a useful stimulation pattern for FES-cycling. Two of these studies [66, 102] found that the activation patterns obtained during normal, volitional cycling had to be manually adjusted in order to achieve smooth cycling motion with paraplegic subjects. Petrofsky [93, 95, 97] reports in various studies the measurement of EMG activation patterns from normal subjects as the guideline for the stimulation pattern in FES. Apparently, the use of these to set the timing and stimulation intensity variables for paraplegic cycling is successful. The power outputs achieved by his subjects are very much higher than those reported elsewhere (e.g. approximately 100 W power output is reported in [93]), but these have not been replicated by any other group.

Another possibility for choosing the best stimulation pattern is to numerically optimise the activation angles by maximising an analytical cost function which captures mechanical output forces. Gföhler *et al.* [42] used a model of electrically stimulated muscle instead of physiologically recruited muscles. The cost function to be optimised depends on the power output developed. Moreover, they suggest to

use as the optimisation criterion a limit for muscle stress or a joint moment function. Rasmussen *et al.* [106] tried to eliminate the presence of dead points in the crank cycle through a model of a four-bar pedaling mechanism. Idsø *et al.* [62] developed a model of legs, muscles and energy consumption rate. The aim was to find the angle activation range that led to consuming the lowest amount of energy possible at a given power output and cadence. They concluded that the angle activation range should be controlled instead of the stimulation intensity. These approaches have not thus far been experimentally verified. Alternatively, Gföhler *et al.* [41] have empirically measured output forces in response to stimulation over large angle ranges, and have used these results to choose desirable activation ranges.

There is considerable scope for the development of measures and methods which can be used to evaluate the effect on cycling performance of changes in these parameters, and which might therefore be used to optimise them. In the present work we investigated outcome measures which might be used to characterize the efficacy of a given set of parameters, and which might be sensitive enough to reflect changes in the parameters.

6.3 Methods

6.3.1 Subjects and Apparatus

Subject S2 participated in this study. Details of this subject can be found in section 3.3. The apparatus used for the tests described in this chapter has been described in detail in section 3.3.

6.3.2 Stimulation Parameters

The cycling motion was achieved by stimulation of the quadriceps, hamstrings and gluteal muscles, through surface electrodes (see section 3.3). Two stimulation patterns were evaluated, denoted “P1” and “P2”, at a constant cadence of 50 rpm. The patterns are shown schematically in figure 6.1. The arcs show when the stimulation was on for each muscle over the crank cycle. In the zero position, the crank is horizontal and the right foot is at its shortest distance from the body. The start and stop angles with P1 and P2 for the muscle groups in the right leg are given in table 6.1. The angle ranges during which the quadriceps and hamstring muscles were activated in pattern P2 were each extended by 30 degrees with respect to pattern P1. Pattern P1 is the standard pattern used for all the experiments that are

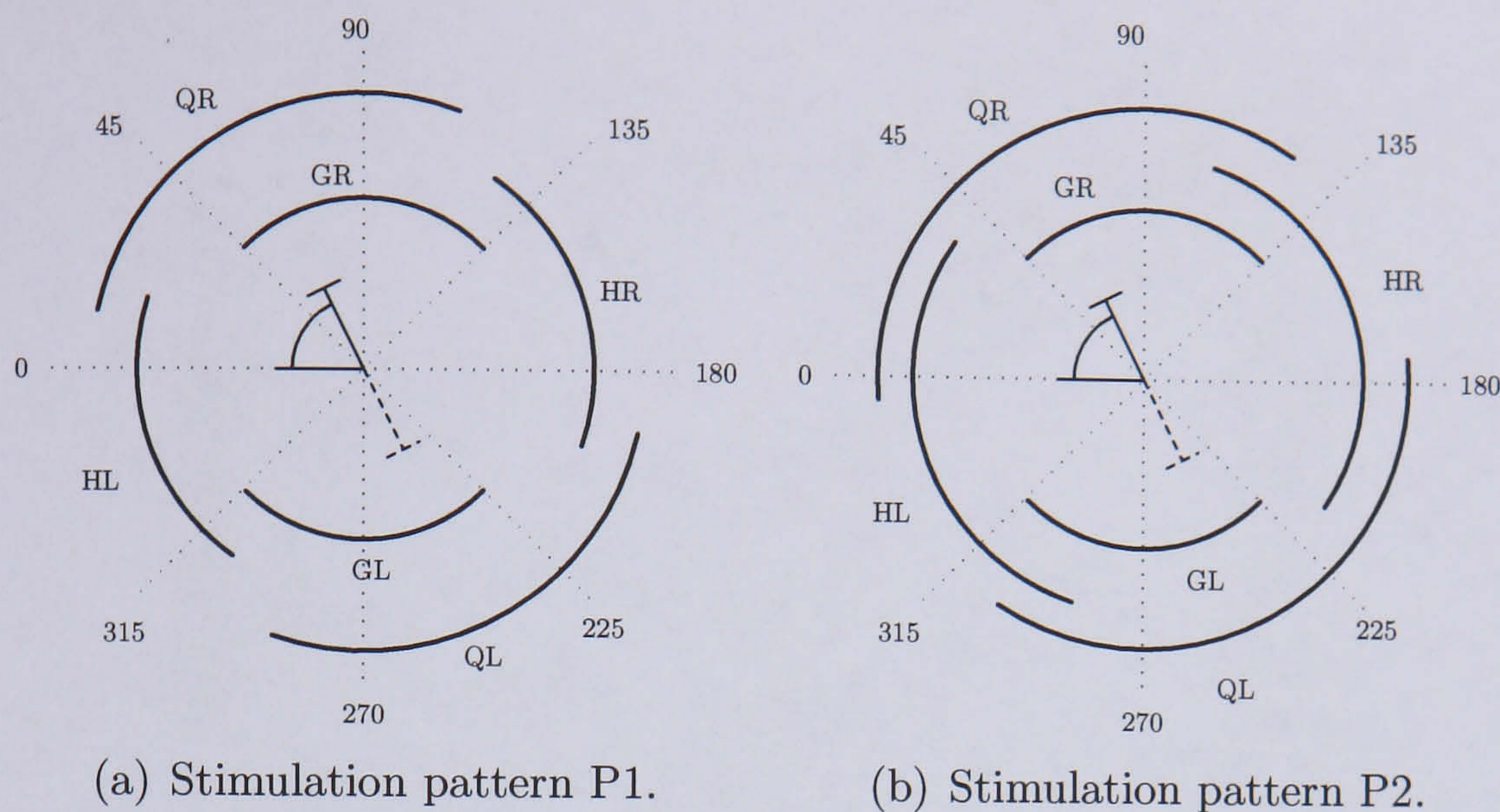


Figure 6.1: Diagram of the stimulation patterns. The arcs show when stimulation was on for each muscle group: QL -Quadriceps Left; QR - Quadriceps Right; HL - Hamstring Left; HR - Hamstring Right; GL - Gluteus Left; GR - Gluteus Right. Zero position has the crank horizontal with the right foot close to the body.

Pattern	Quadriceps	Hamstring	Gluteus
P1	10°-110°	123°-200°	45°-135°
P2	355°-125°	108°-215°	45°-135°

Table 6.1: Stimulation patterns for the three groups of muscles (right side).

included in this thesis (see also section 3.3.3). Pattern P2 represents an arbitrary perturbation from this nominal pattern.

We utilised a constant stimulation frequency of 20 Hz, and the following current amplitudes for each channel: quadriceps - 120 mA, hamstrings - 110 mA, and gluteus - 90 mA. The stimulation pulsewidth was varied in real time by feedback control (see section 3.3.2) within the range 0-700 μ s in order to achieve a pre-specified exercise workrate, and was the same for all muscles.

6.3.3 Evaluation Protocol

The test for the evaluation of patterns P1 and P2 (Two Pattern Test or TPT) followed the protocol illustrated in figure 6.2. The first stage of the test was a stimulated warm-up period of 6 minutes cycling at a constant low-level workrate (approximately +5 W), while the motor and its control loop maintained a cadence of 50 rpm. Warm-up was followed by a 9-minute rest period, and then a further 6 min. of recorded rest (i.e. the subject was connected to the cardiorespiratory

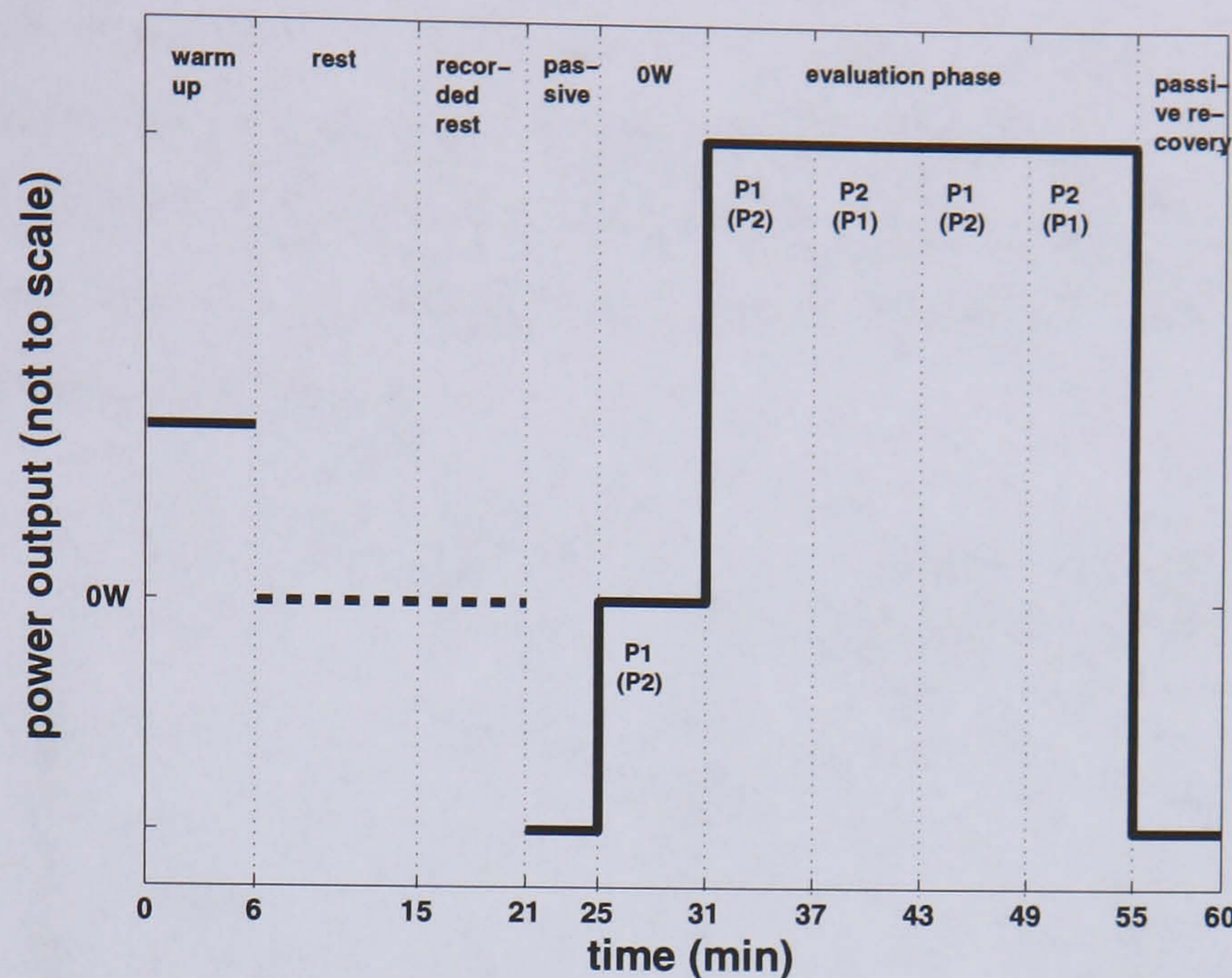


Figure 6.2: Schematic diagram of the Two Pattern Test protocol. The vertical lines delimit the various stages. The dotted line at the rest stage indicates that rest does not correspond to any definite power output level. The notation “P1” and “P2” indicates which pattern was used during the stage: it was either the sequence P1-P2-P1-P2 or P2-P1-P2-P1.

monitoring system).

Following rest, there was an initial passive cycling phase of 4 minutes in order to accommodate the leg muscles and their possible spastic reflexes to the cyclic motion, with only the motor driving the legs and no stimulation applied. A stimulated cycling phase followed for 6 minutes at a workrate of 0 W.

After the 0 W phase the subject cycled at a constant power output level corresponding to a total effective workrate of approximately 14 W with respect to passive, for 24 minutes (the “evaluation phase”). During each cycling phase the motor and its controller maintained a constant cadence of 50 rpm, independent of the level of stimulation. During the evaluation phase each stimulation pattern was applied for 6 minutes, in order to allow the gas exchange responses to reach a steady state, and then an instantaneous switch was made to the other pattern. During each 24-minute evaluation phase, the patterns were applied either in the order P1-P2-P1-P2 or P2-P1-P2-P1.

A total of four tests were carried out, with each of the above sequences applied twice, resulting in the availability of eight 6-minute stages with P1 and seven 6-minute stages with P2 (one P2 stage was not completed).

Two further tests (One Pattern Test or OPT) were carried out following the

protocol shown in figure 6.3. The protocol is similar to the previous one, but in this test the pattern was kept constant during the evaluation phase. One test was performed using pattern P1 and the other using pattern P2. These two tests were carried out with the aim of investigating the extent of the variation in oxygen uptake when the pattern was not changed.

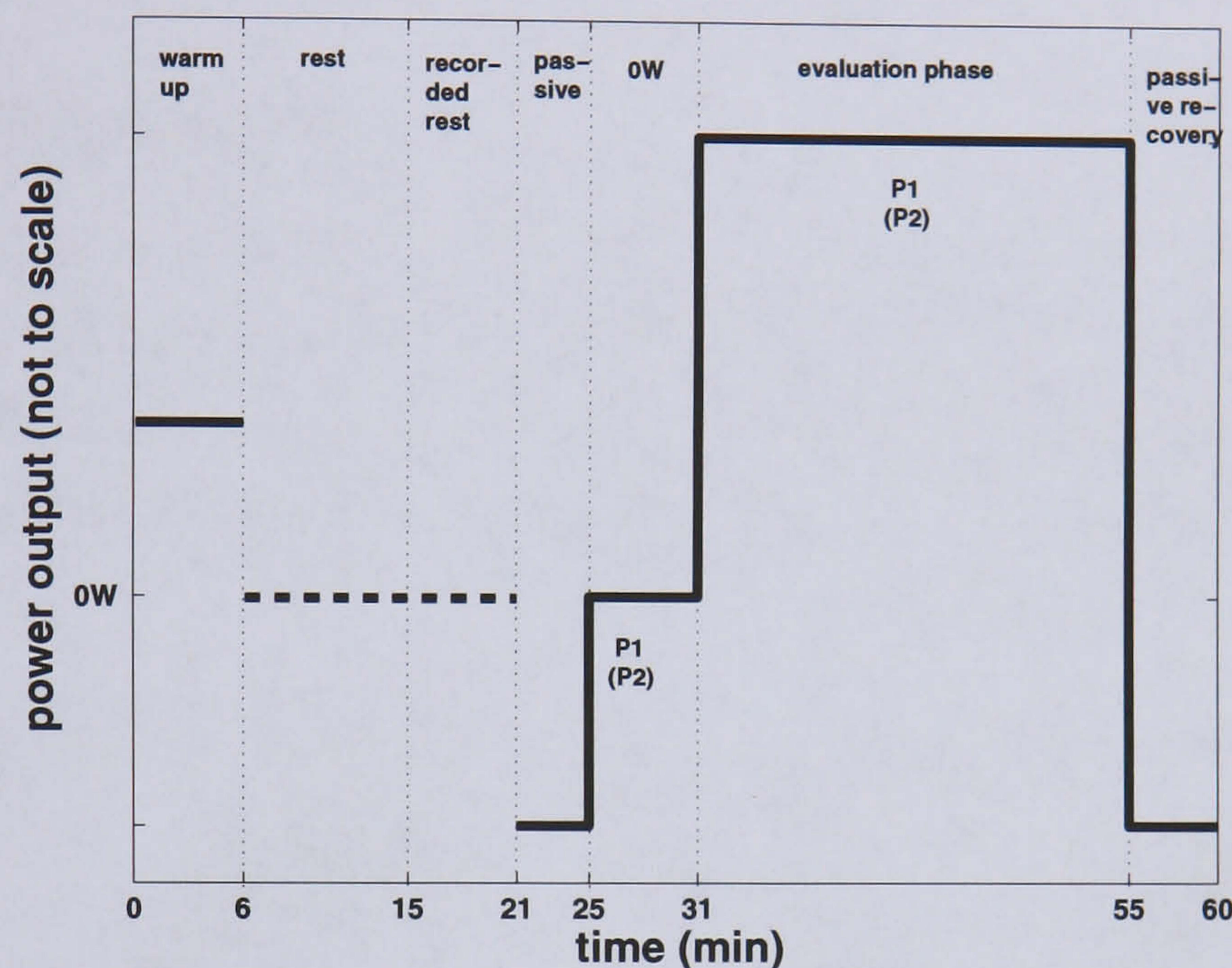


Figure 6.3: Schematic diagram of the One Pattern Test protocol, where the patterns are not changed. The vertical lines delimit the various stages. The dotted line at the rest stage indicates that rest does not correspond to any definite power output level. The notation “P1” and “P2” indicates which pattern was used during each stage.

6.3.4 Data Analysis and Outcome Measures

Editing of the raw gas exchange variables was carried out as described in chapter 4. The oxygen uptake responses for each test were averaged over the final minute of each stage.

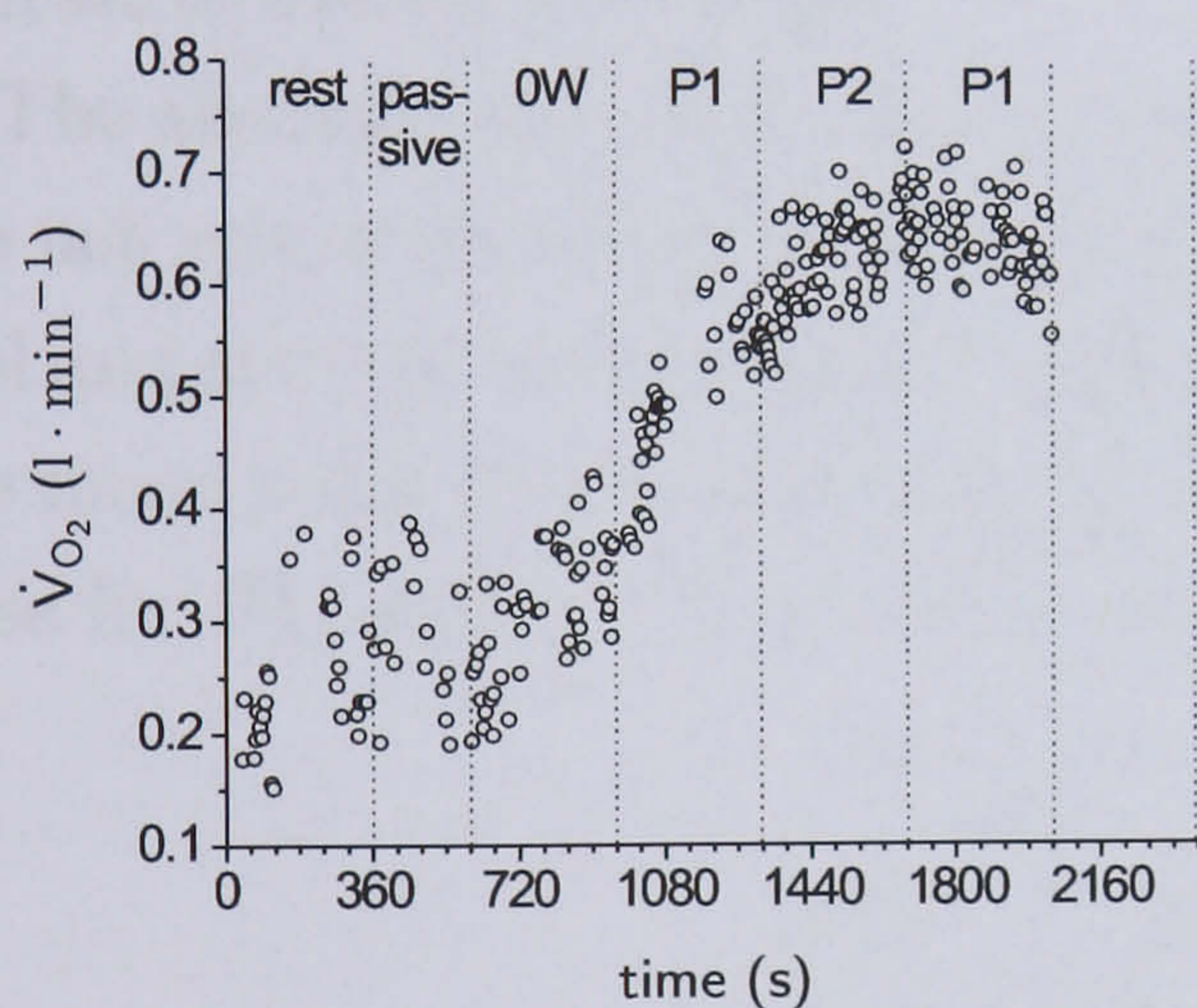
The total electrical charge delivery rate for the stimulated muscle groups during exercise was calculated as follows. The charge for each individual pulse is obtained from the product of instantaneous pulsewidth and current. These values were summed over the six muscle groups, and then due account taken of the on/off times of each group during each crank rotation. The *stimulation cost* of the exercise is defined as the average value of this total charge rate over a given time interval. Here, the stimulation cost was taken as the average over the final minute of each stage in the evaluation phase.

A Mann-Whitney test was used to compare the outcome measures for the two different patterns to determine whether any differences in sample means were statistically significant, with significance deemed to hold for $p < 0.05$.

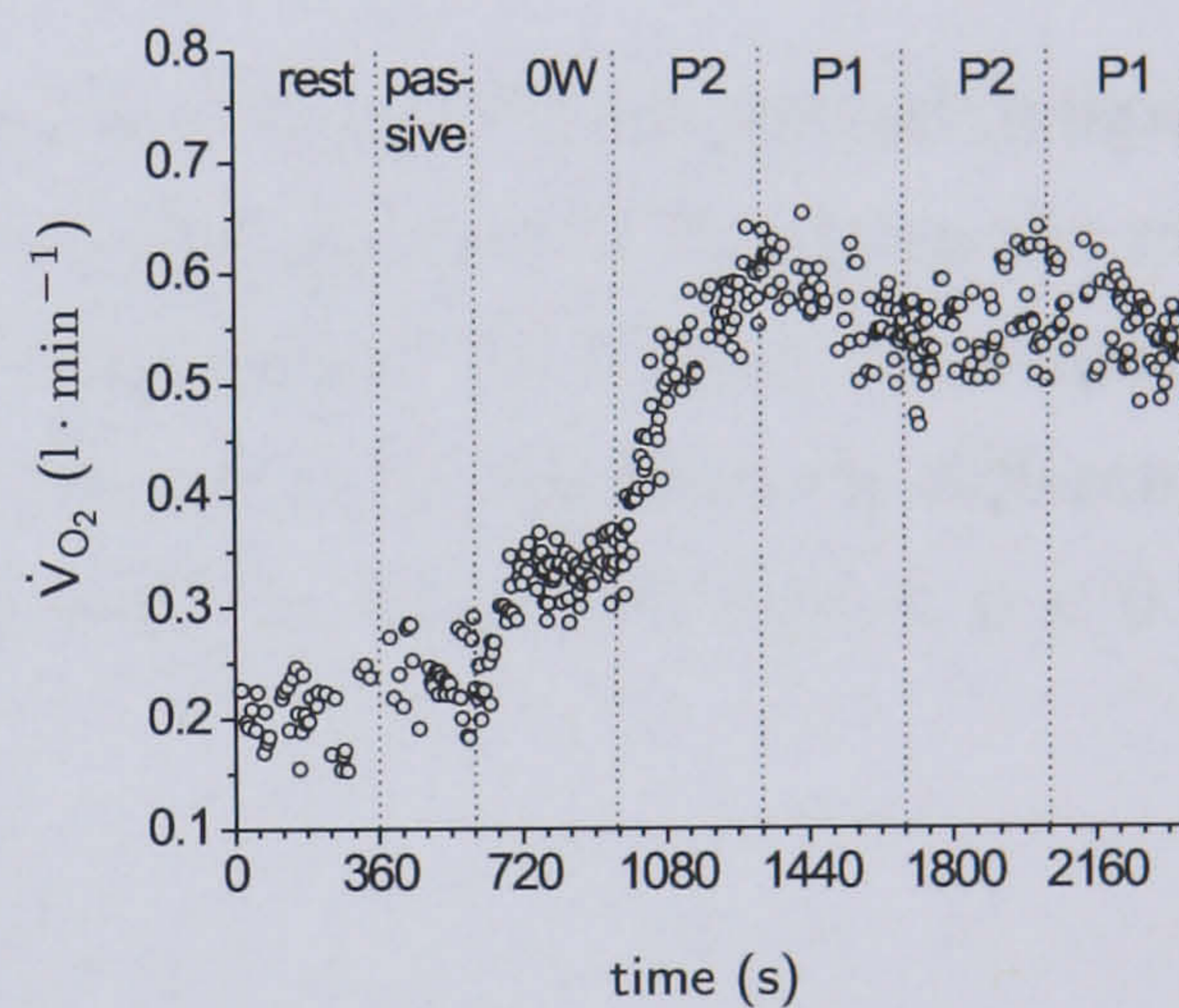
6.4 Results

6.4.1 Oxygen Uptake

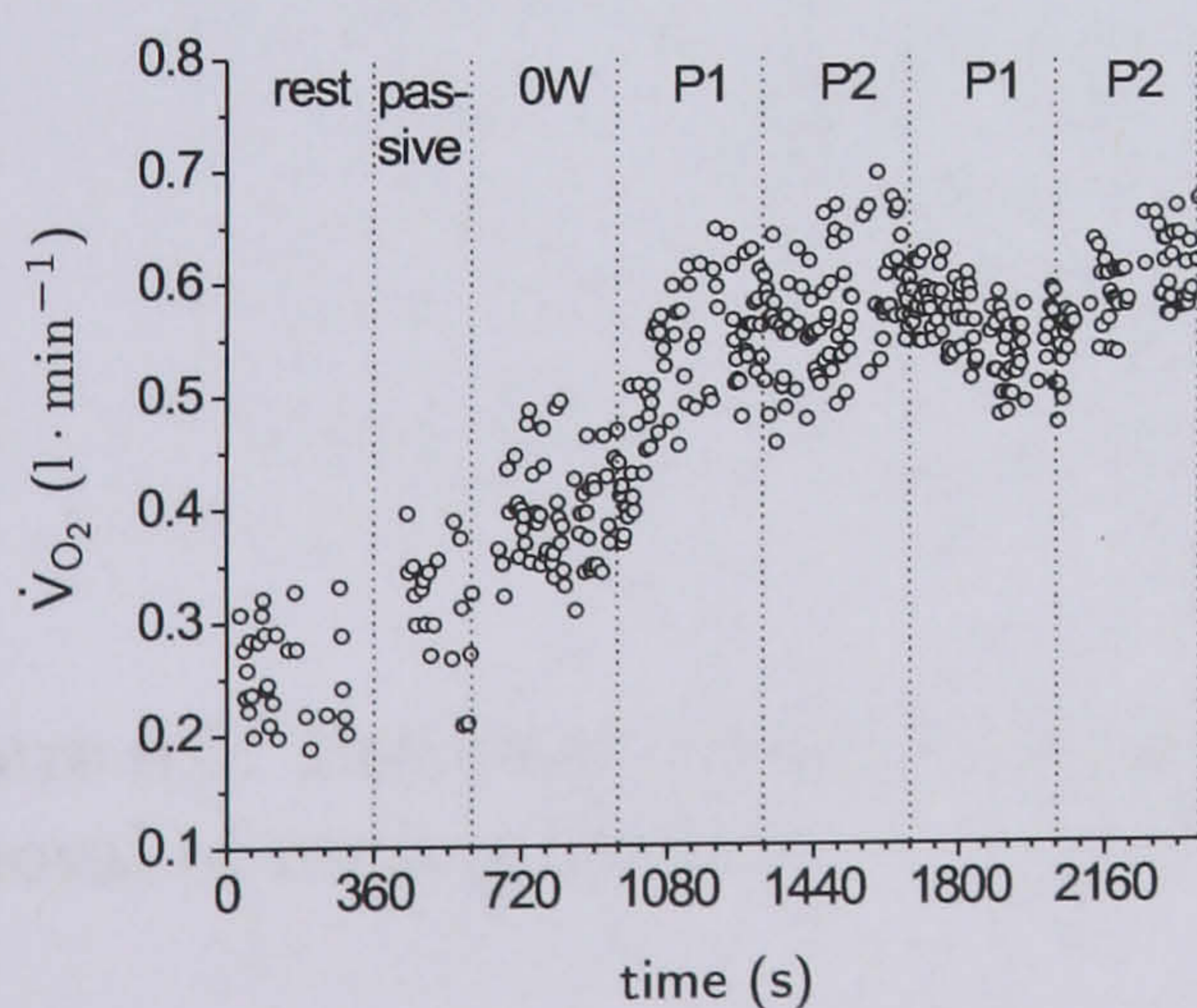
Figure 6.4 shows the time-course for oxygen uptake for the four Two Pattern Tests. The average \dot{V}_{O_2} for each pattern during the final minute of each stage of exercise is reported in table 6.2. The mean values for the eight presentations of P1 and seven presentations of P2 were 0.56 ± 0.03 and 0.61 ± 0.04 ($l \cdot \text{min}^{-1}$, mean \pm sd),



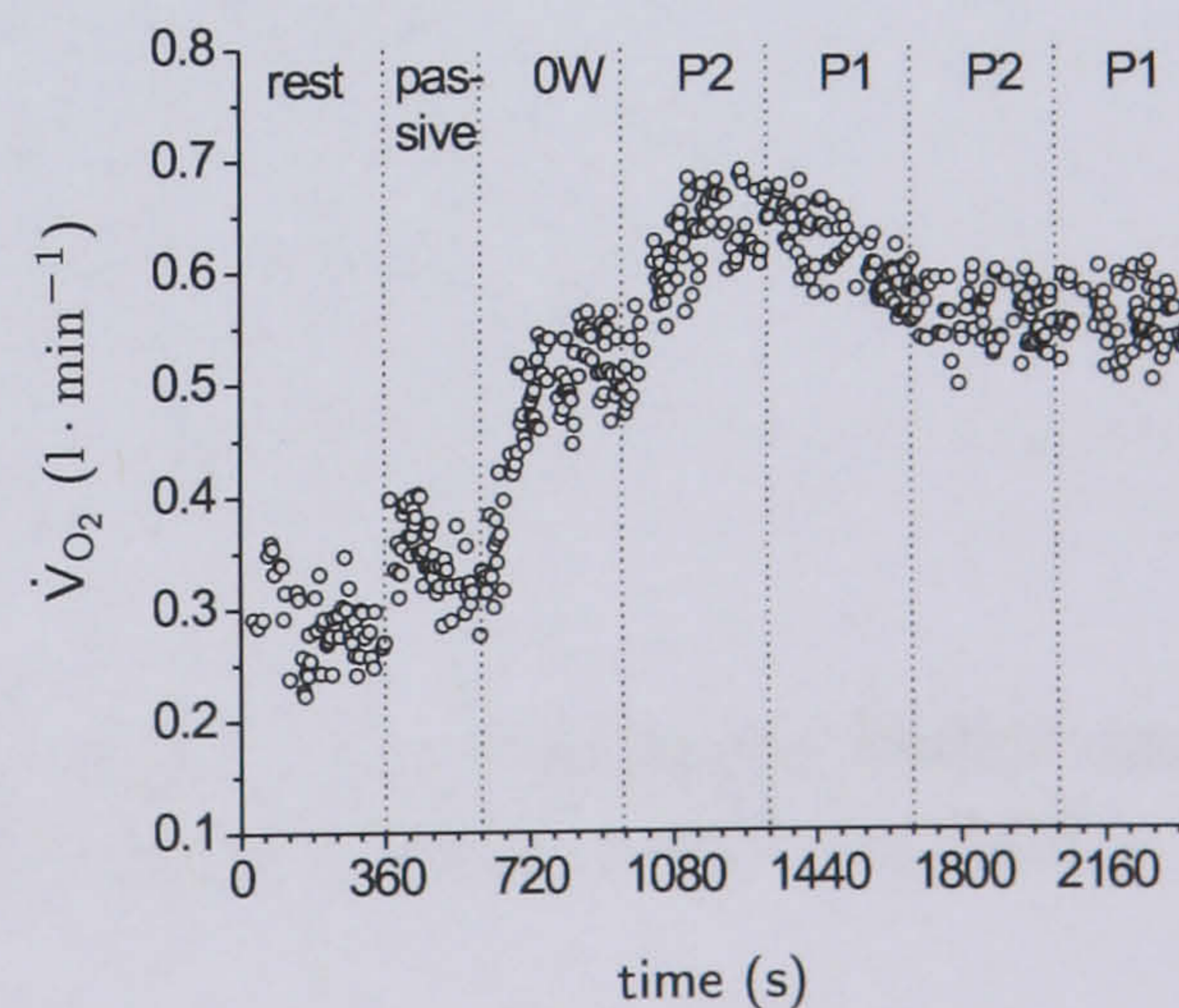
(a) Oxygen uptake for TPT1



(b) Oxygen uptake for TPT2



(c) Oxygen uptake for TPT3



(d) Oxygen uptake for TPT4

Figure 6.4: Time-course for the oxygen uptake during the four TPTs.

Test nr.	1	2	3	4
Order	1-2-1-2	1-2-1-2	2-1-2-1	2-1-2-1
Rest	0.27	0.25	0.24	0.28
Passive	0.26	0.29	0.24	0.32
0W	0.35 _(P1)	0.41 _(P1)	0.34 _(P2)	0.52 _(P2)
Stage 1	0.55 _(P1)	0.56 _(P1)	0.59 _(P2)	0.64 _(P2)
Stage 2	0.68 _(P2)	0.60 _(P2)	0.55 _(P1)	0.58 _(P1)
Stage 3	0.63 _(P1)	0.56 _(P1)	0.57 _(P2)	0.55 _(P2)
Stage 4		0.61 _(P2)	0.54 _(P1)	0.55 _(P1)

Table 6.2: \dot{V}_{O_2} values ($l \cdot \text{min}^{-1}$) for the TPTs averaged over the last minute of each stage.

respectively. Stage 4 for the first test is not available because the pulsewidth reached saturation during that stage.

The absolute and net oxygen uptake values for P1 and P2 are plotted in figure 6.5. The net values are obtained by subtracting the resting level of \dot{V}_{O_2} from the exercise level and are $0.31 \pm 0.02 l \cdot \text{min}^{-1}$ and $0.35 \pm 0.04 l \cdot \text{min}^{-1}$ for P1 and P2, respectively. The mean value of absolute \dot{V}_{O_2} for P2 was found to be significantly different from those for P1, with $p < 0.05$, while the mean net \dot{V}_{O_2} value had $0.05 < p < 0.1$.

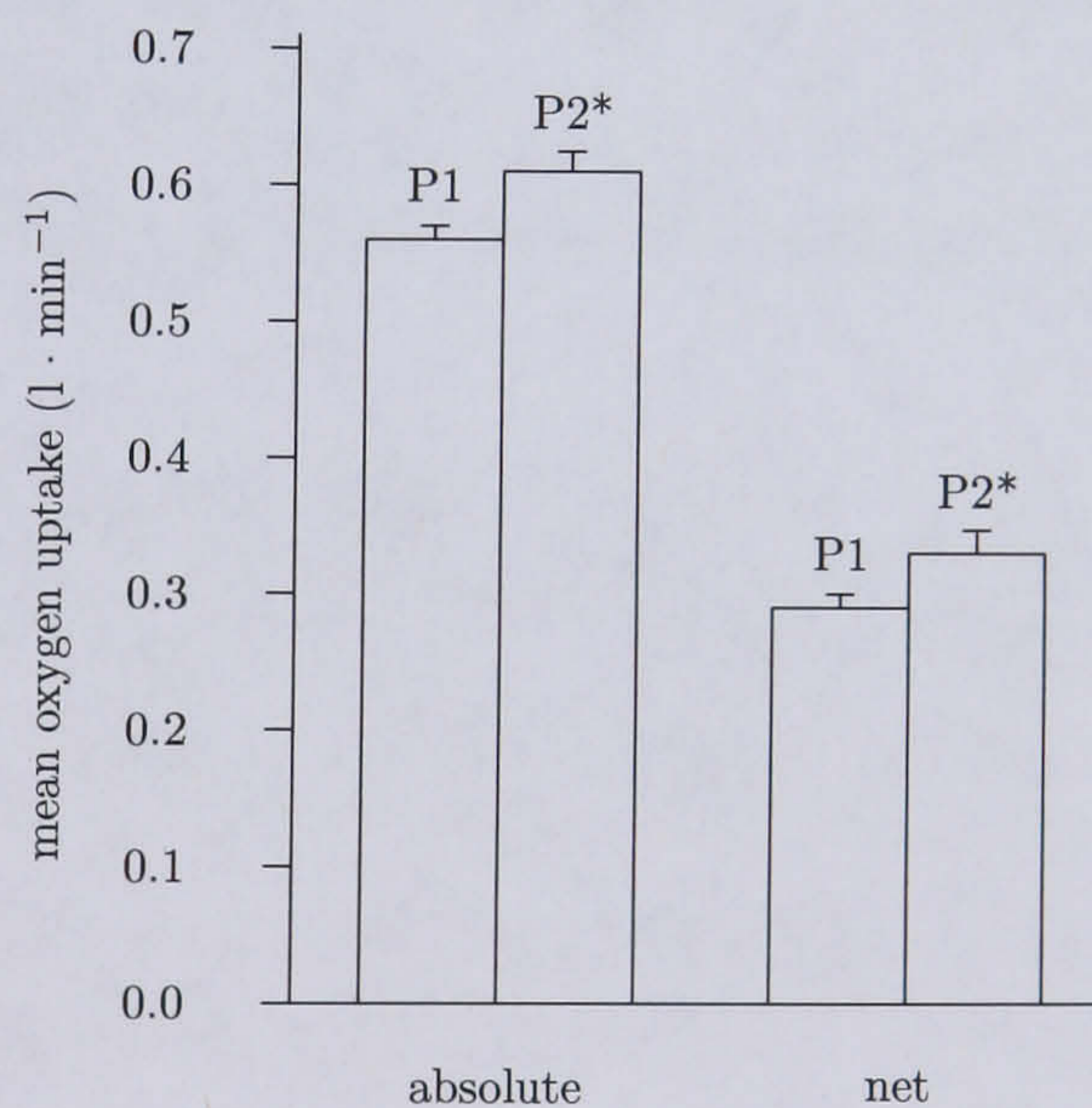


Figure 6.5: Bar chart showing mean \dot{V}_{O_2} (+ sd) for both patterns before and after removal of resting baseline. * denotes a significant difference with $p < 0.05$.

Figure 6.6 shows the oxygen uptake for the two One Pattern Tests. Figure 6.6(a) shows the test in which pattern P1 was used, and figure 6.6(b) shows the test in which pattern P2 was used. Mean (\pm sd) \dot{V}_{O_2} values averaged over the evaluation phase from the 6th minute onwards are $0.62 \pm 0.014 l \cdot \text{min}^{-1}$ for P1 and $0.61 \pm 0.013 l \cdot$

min^{-1} for P2. The difference between the two means was found not to be statistically significant ($0.1 < p < 0.2$). The last two minutes of the test in which pattern P2 was used have not been included in the calculations, because external factors influenced the gas exchange.

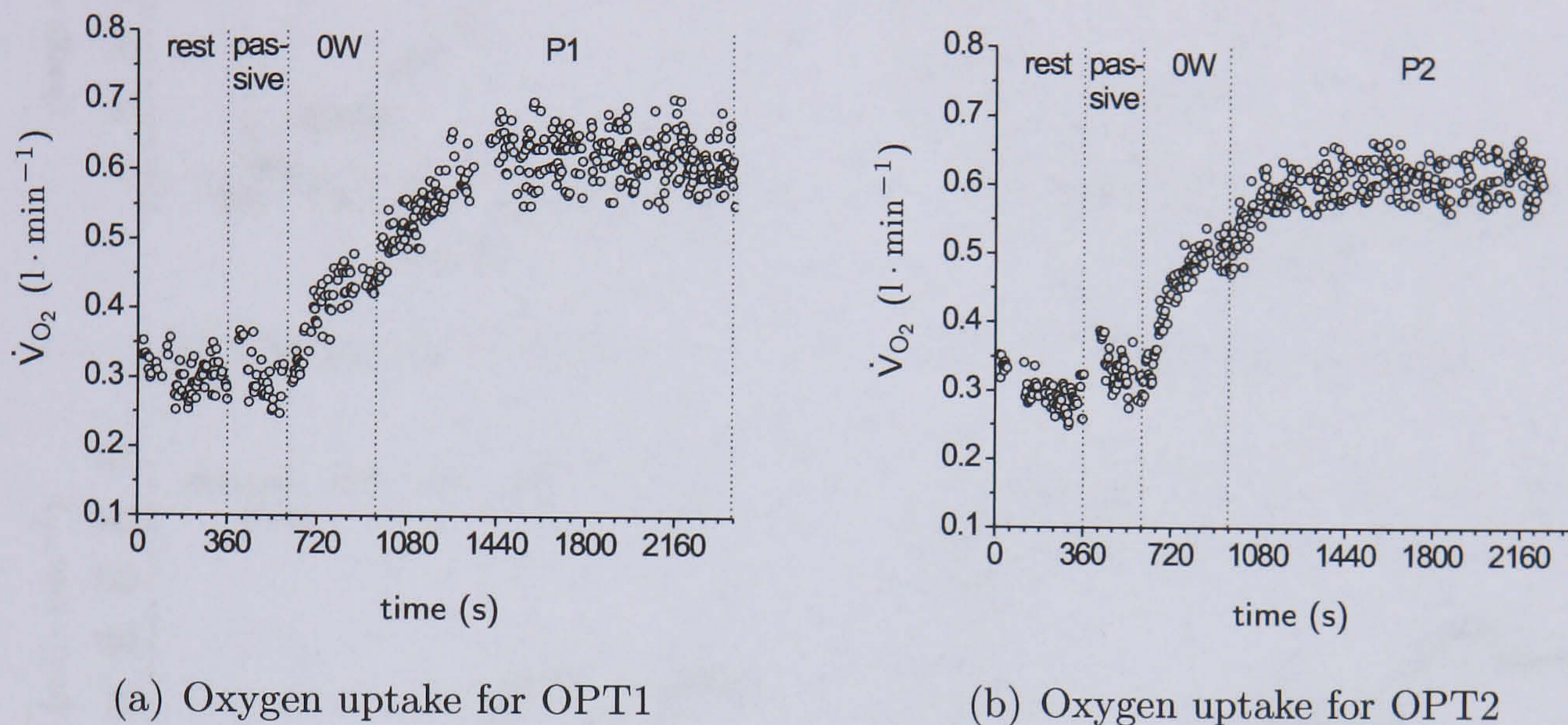


Figure 6.6: Time-course for the oxygen uptake during the two OPTs.

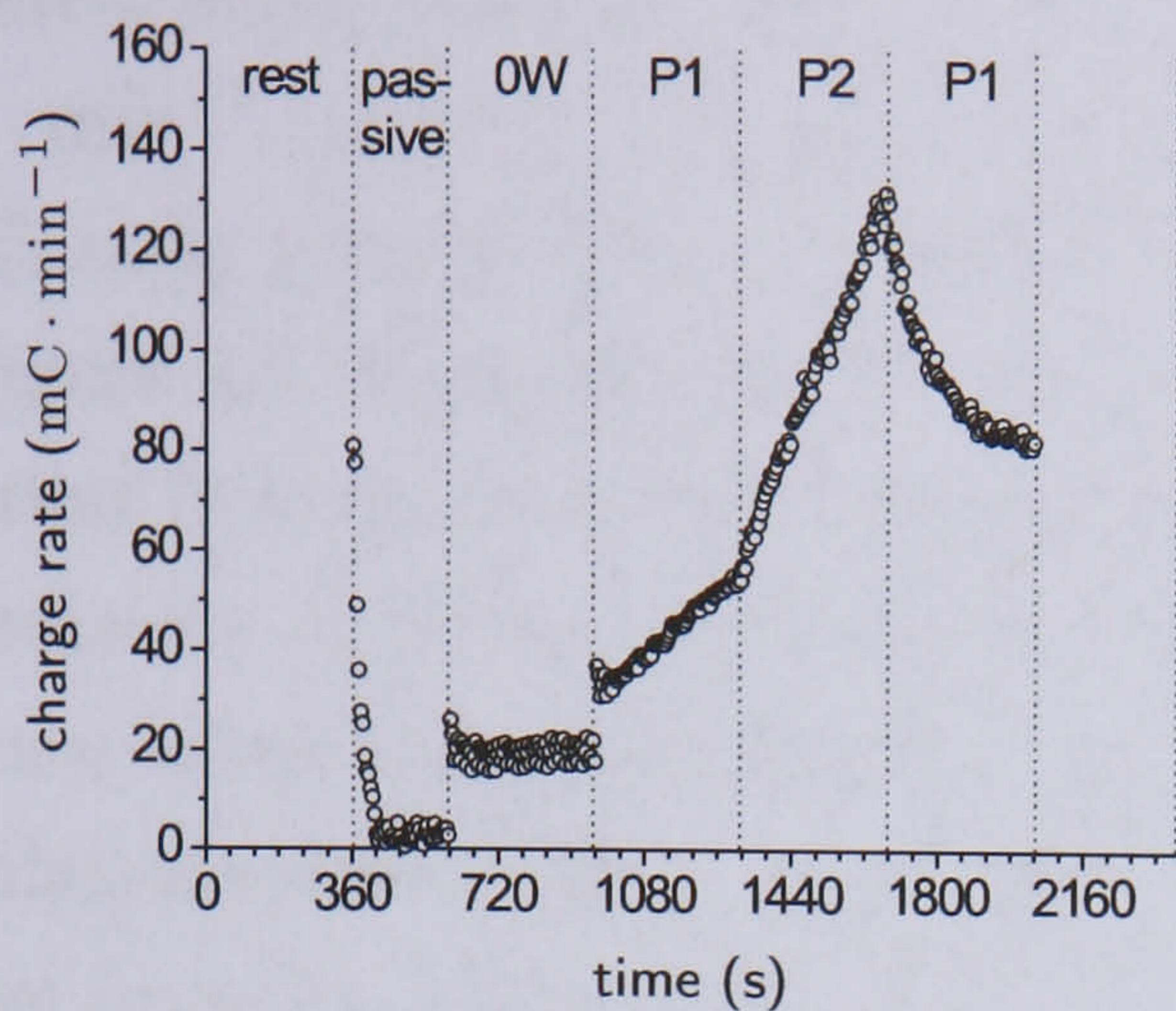
The mean and standard deviation values for \dot{V}_{O_2} in the evaluation phase of the tests where the activation range was changed and of the tests where the activation range was not changed are reported in table 6.3. \dot{V}_{O_2} data are averaged over the interval from the 6th minute of the evaluation phase to the end of the evaluation phase.

\dot{V}_{O_2} ($\text{l} \cdot \text{min}^{-1}$)	TPT1	TPT2	TPT3	TPT4	OPT1	OPT2
mean	0.62	0.57	0.56	0.58	0.62	0.61
sd	0.045	0.044	0.038	0.040	0.034	0.029

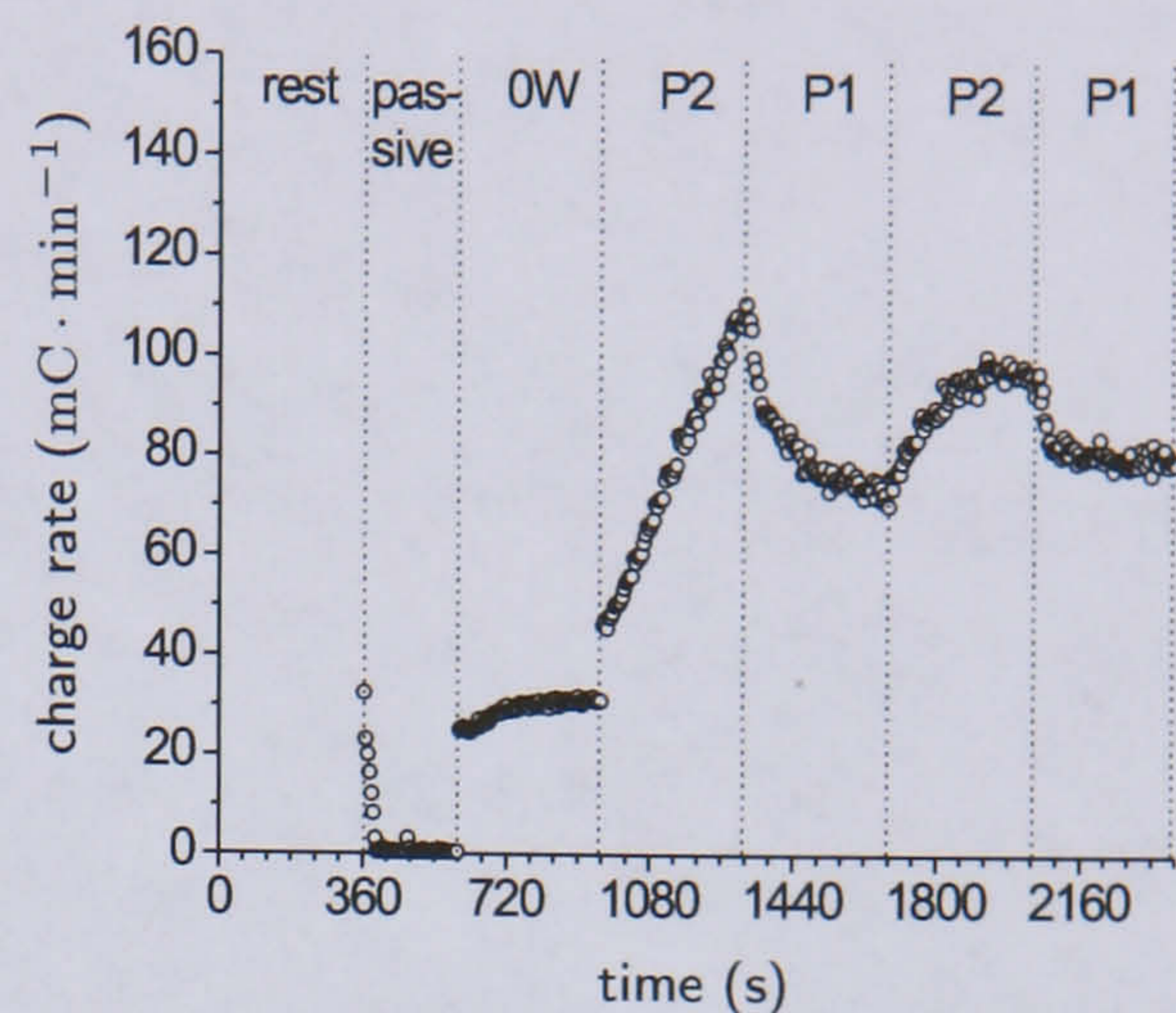
Table 6.3: Mean and standard deviation values for \dot{V}_{O_2} calculated over the evaluation phase of the four TPTs and the two OPTs, from the 6th minute to the end of exercise.

6.4.2 Stimulation Cost

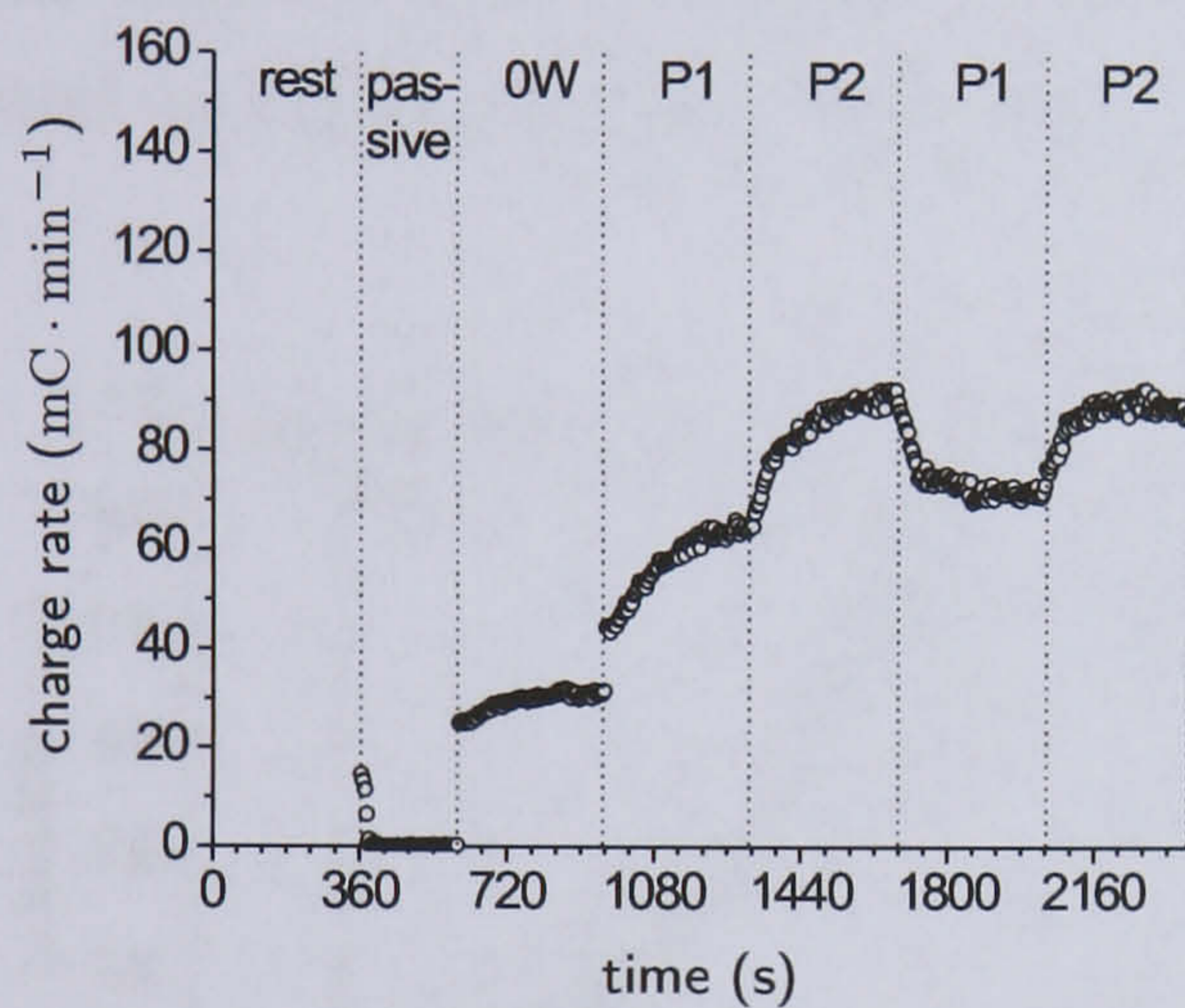
Figure 6.7 shows the time-course for the total charge rate during the four TPTs, computed as described in section 6.3. The change in the value of the total charge rate delivered to the muscles depending on the pattern used is clear: the charge rate increases when P2 is used and decreases when P1 is used.



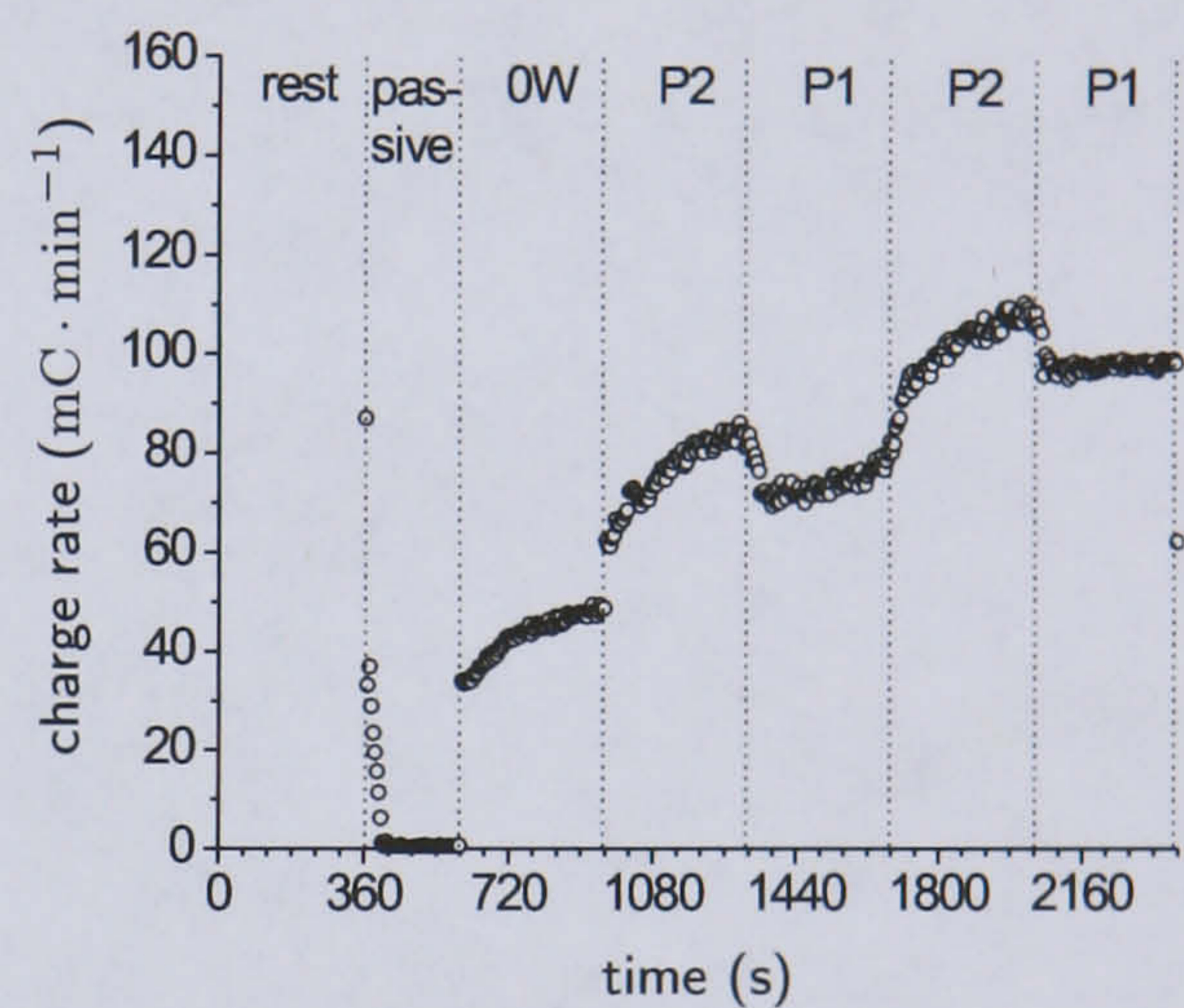
(a) Charge rate for TPT1



(b) Charge rate for TPT2



(c) Charge rate for TPT3



(d) Charge rate for TPT4

Figure 6.7: Time-course for the rate of total charge delivered to the muscles during the four TPTs.

The rate of delivery of total charge, averaged over the last minute of each stage (the stimulation cost), is reported in table 6.4. Mean values for the rate of charge

Test nr.	1	2	3	4
Order	1-2-1-2	1-2-1-2	2-1-2-1	2-1-2-1
0W	19.85 _(P1)	30.88 _(P1)	31.21 _(P2)	48.25 _(P2)
Stage 1	53.59 _(P1)	64.68 _(P1)	106.20 _(P2)	83.42 _(P2)
Stage 2	127.13 _(P2)	91.08 _(P2)	73.44 _(P1)	77.52 _(P1)
Stage 3	83.39 _(P1)	72.30 _(P1)	97.84 _(P2)	107.51 _(P2)
Stage 4		88.93 _(P2)	80.73 _(P1)	93.67 _(P1)

Table 6.4: Total charge rate for all muscles averaged over the last minute of each stage, measured in $\text{mC} \cdot \text{min}^{-1}$: stimulation cost.

delivered when using patterns P1 and P2 are 74.91 ± 12.15 and 100.30 ± 14.78 ($\text{mC} \cdot \text{min}^{-1}$, mean \pm sd), respectively. The mean values for P2 were found to be significantly greater than those for P1, with $p < 0.05$.

Figure 6.8 shows the time course of the pulsewidth for the four TPTs. It can be seen that in most cases when the pattern was switched from P1 to P2 the pulsewidth immediately decreased, only to rise again after about one minute. The converse is the case when changing from pattern P2 to P1. This is a reflection of the longer stimulation on-time (P2). Thus, P2 requires a lower instantaneous pulsewidth after a change from P1, while maintaining a constant power, before the confounding effects of differing efficiency and fatigue properties of the two patterns intervene.

The values for the average pulsewidth during the last minute of each stage are reported in table 6.5. Mean values for the pulsewidth when using pattern P1 and

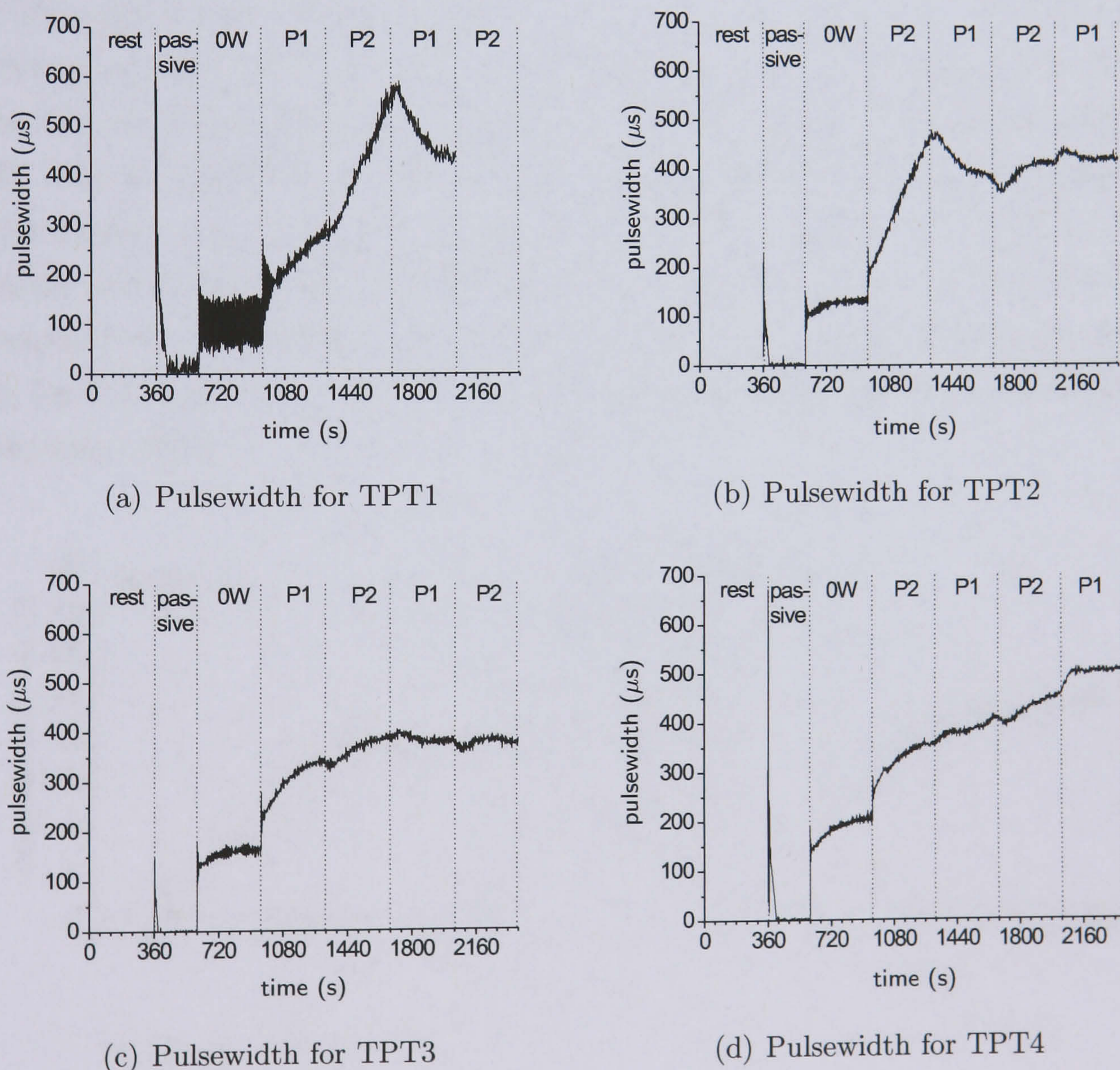


Figure 6.8: Time-course for the pulsewidth during the four TPTs.

Test nr.	1	2	3	4
Order	1-2-1-2	1-2-1-2	2-1-2-1	2-1-2-1
0W	104.98 _(P1)	162.13 _(P1)	132.24 _(P2)	204.89 _(P2)
Stage 1	281.43 _(P1)	339.25 _(P1)	443.67 _(P2)	354.20 _(P2)
Stage 2	539.71 _(P2)	386.63 _(P2)	385.66 _(P1)	404.49 _(P1)
Stage 3	439.41 _(P1)	380.51 _(P1)	411.83 _(P2)	451.32 _(P2)
Stage 4		375.78 _(P2)	420.45 _(P1)	489.25 _(P1)

Table 6.5: Average pulsewidth during the last minute of each stage in the four TPTs, measured in μs .

P2 are 392.56 ± 63.07 and 423.30 ± 62.26 (μs , mean \pm sd), respectively. Thus, the pulsewidth for pattern P1 is lower than for pattern P2, but the difference between these values is not statistically significant.

Figure 6.9 shows the total charge rate during the two OPTs. The time course for charge rate is similar in the two tests, but the value of the charge rate is higher in the test in which pattern P2 was used. Moreover, the charge rate stabilizes in OPT1 over the evaluation phase, while it keeps increasing in OPT2. Mean values for the charge rate, calculated during the evaluation phase from the 6th minute onwards, are 78.03 ± 3.05 and 90.76 ± 3.77 ($\text{mC} \cdot \text{min}^{-1}$, mean \pm sd), for P1 and P2 respectively. The mean values for P2 were found to be significantly greater than those for P1, with $p < 0.05$. Figure 6.10 shows the time course of the pulsewidth for the two OPTs.

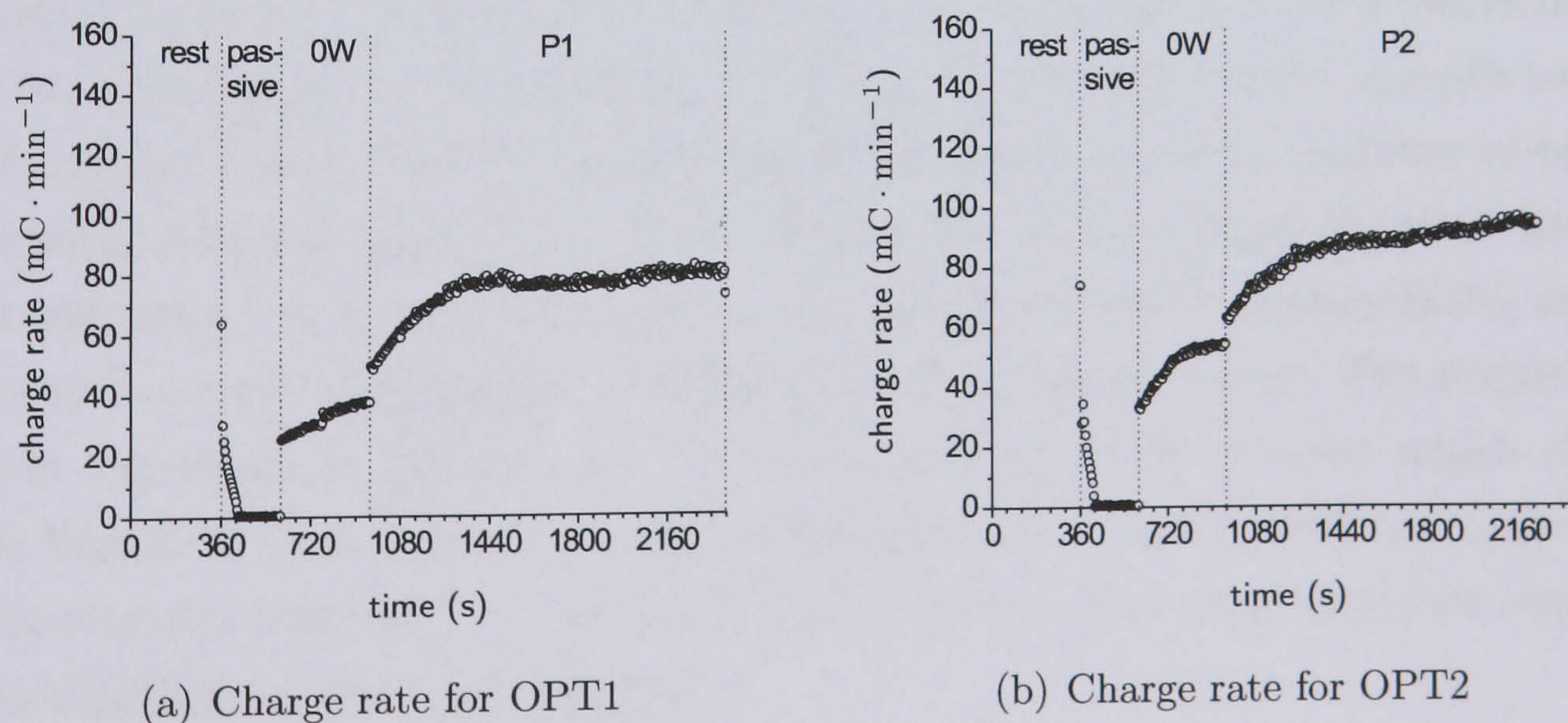
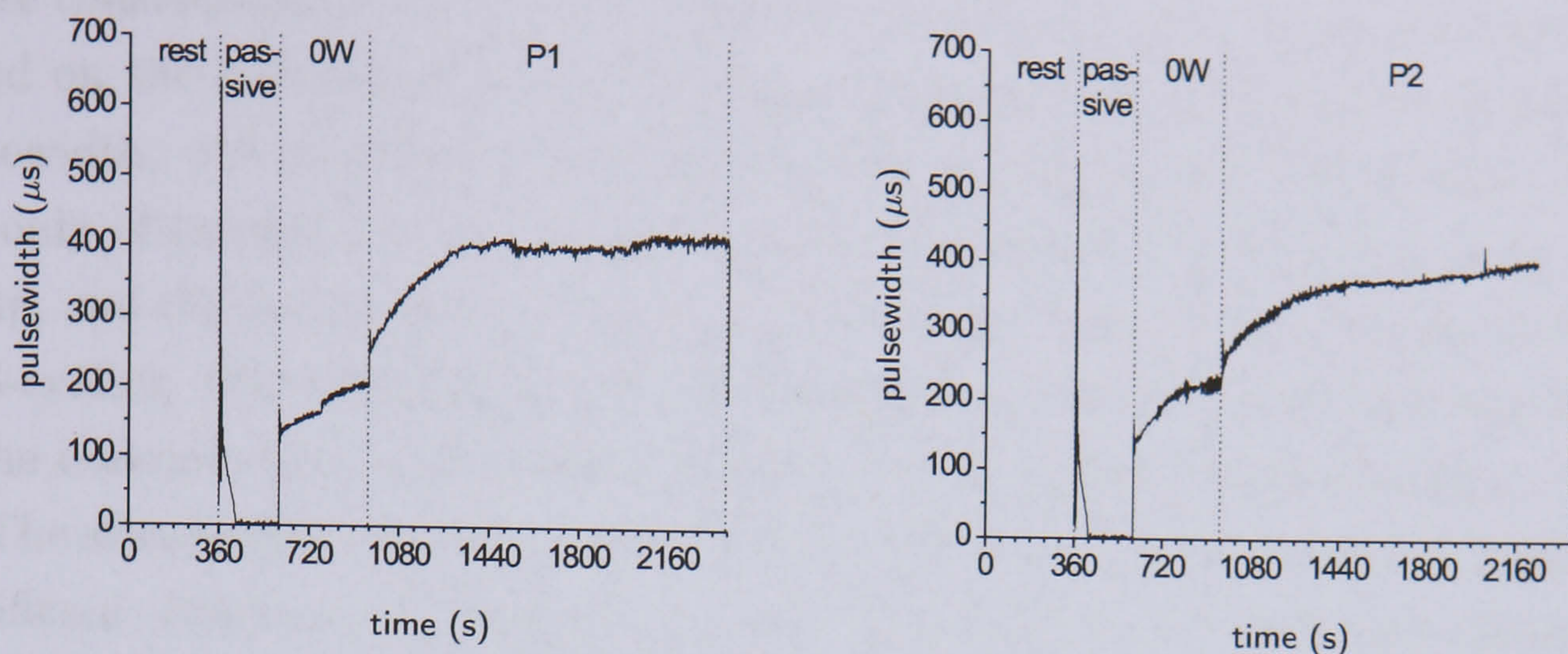


Figure 6.9: Time-course for the rate of total charge delivered to the muscles during the two OPTs.



(a) Pulsewidth for OPT1

(b) Pulsewidth for OPT2

Figure 6.10: Time-course for the pulsewidth during the two OPTs.

6.5 Discussion

The observations reported here suggest that both oxygen uptake and stimulation cost of constant-power FES cycling can be appreciably influenced by the muscle stimulation paradigm employed. Moreover, these cost measurements may provide sufficient discriminatory power to allow assessment of different muscle stimulation patterns during FES-cycling exercise.

We chose to switch each pattern every 6 minutes because we wished to ensure that each stage was of sufficient duration that a metabolic steady state was attained. We estimated that 6 minutes was the minimum time necessary for the respiratory responses to reach a steady state, based on the knowledge that SCI subjects typically have prolonged \dot{V}_{O_2} kinetics [2, 7]. On the other hand, it was desirable to make the duration of each stage as short as possible to allow a greater number of pattern repetitions within a given test period. The choice of a 6-minute duration for each stage was therefore a compromise between the need to reach a steady state, and the desire to maximize the number of repetitions in each test period. The requirement for test repetition is dictated by the relatively high levels of noise which characterize breath-by-breath gas exchange measurements. Repeat tests are required to obtain response averages for improved signal-to-noise ratio and therefore improved discriminability of response differences.

The practicality of pulmonary gas exchange measurement means that testing can be time consuming, which is an important consideration as the subject must remain connected to the specialised measurement equipment throughout each test.

These considerations led us to investigate alternative indices of the cost of exercise, based on the stimulation intensity. Rather than simply analysing the stimulation pulsewidth, we developed a new measure of stimulation cost which takes account not only of pulsewidth, but also of the differing current amplitudes in each muscle group, and the on/off times of each channel during crank rotation. In the context of FES-cycling, this stimulation cost variable represents the total charge rate applied to the muscles and therefore gives a true measure of stimulation intensity.

The stimulation cost and oxygen uptake variables are in agreement in identifying significant differences between the two patterns overall. It would also appear that the stimulation cost variable responds more rapidly than \dot{V}_{O_2} to changes in the stimulation paradigm. It is clearly seen in several of the pattern transitions in figure 6.7 that the stimulation response dynamic takes approximately 1 minute. The response kinetics of \dot{V}_{O_2} , while not clearly discernible in these tests due to noise (figure 6.4), would, as discussed above, be expected to be considerably longer.

Stimulation cost has several advantages over \dot{V}_{O_2} , when viewed as a means of optimising stimulation parameters to improve exercise efficacy. Stimulation cost is easy to determine in real time: it does not require the subject to be connected to any pulmonary gas exchange recording apparatus. It appears to respond more rapidly and with greatly improved signal-to-noise characteristics, which would facilitate more accurate and rapid testing.

Overall, the responses reported here suggest that exercise with pattern P2 is less efficacious than with P1. This might be a result of P2 having much wider stimulation angles, and therefore larger areas of the crank cycle where muscle force is less effectively translated into work-producing torque (i.e. due to a reduced moment arm). In addition, P2 results in muscle activation over a wider range of muscle lengths (including areas of activation where muscle lengths are both longer and shorter than with P1, and where force transmission may be less effective). Moreover, longer stimulation arcs (see figure 6.1) result in muscle activation to be prolonged to the point where quadriceps and hamstrings are activated at the same time. This can hinder the movement.

Analysis of the pulsewidth data also points to the poor efficacy of P2. Since with P2 each stimulation channel is switched on over a larger part of the crank cycle, it would be expected that for constant-power cycling lower peak forces would require to be developed. Therefore, the pulsewidth with P2 would be less than that for P1. The pulsewidth plots in figure 6.8 show that this is indeed the case in the brief periods following pattern changes: in all transitions from P1 to P2 there is

a small but rapid decrease in pulsewidth. However, the combined effects of lower efficiency and more rapid fatigue then cause the pulsewidth with P2 to progressively rise, to the extent that the average pulsewidth in the final minute of each stage in the evaluation phase is actually greater with P2 than with P1.

The One Pattern Tests were carried out with the main aim of establishing if the variations in \dot{V}_{O_2} in the Two Pattern Tests were due to the different patterns used or to the high noise level that is characteristic of breath-by-breath gas exchange measurements in SCI subjects. Figures 6.6(a) and 6.6(b) show that \dot{V}_{O_2} is stable after the 6th minute during the evaluation phase in both tests. The analysis of the standard deviation values for \dot{V}_{O_2} data from the 6th minute to the end of exercise in both TPTs and OPTs confirms that the use of different patterns affects oxygen uptake. Indeed, standard deviation values are higher in TPTs than in OPTs (see table 6.3).

The \dot{V}_{O_2} for OPT1 is higher than for OPT2, but the difference is not statistically significant. Since only one OPT for each pattern has been performed, this result could be due to the high day-to-day variability of the subject's physiological status. As previously mentioned, it is necessary to have repetitions of the same test in order to be able to draw statistically significant conclusions.

Interestingly, the stimulation cost is higher for pattern P2 than for pattern P1, indicating a lower overall efficacy of stimulation. This finding apparently contradicts the \dot{V}_{O_2} results for the OPTs, however it is in accordance with the results obtained from the TPTs. The higher level of noise characterizing breath-by-breath measurements with respect to stimulation cost might be the cause of the discordant results. Stimulation cost might be considered a more reliable index of efficacy of exercise than \dot{V}_{O_2} measurements also because it is not subject to external disturbances, such as the presence of people in the testing room. Thus, stimulation cost might be used to assess efficacy of exercise instead or in addition to \dot{V}_{O_2} . However, it is necessary to perform a wider study on the correlation between \dot{V}_{O_2} and stimulation cost to verify the hypothesis here suggested.

6.6 Conclusions

These results raise the possibility that oxygen uptake and stimulation cost measurements may allow discrimination between the efficacy of different muscle activation patterns. Moreover, it appears that the discriminatory power of the \dot{V}_{O_2} is reflected by a more easily determined index of cycling efficacy, i.e. the cost in terms of the

applied rate of stimulation charge (and therefore the overall intensity of muscle activation). This stimulation cost variable is preferable as it is easy to determine in real time, it does not require the subject to be connected to physiological measurement sensors, and it appears to respond more rapidly and with greatly improved signal-to-noise properties than ventilatory oxygen uptake measurements. Further work is required with a larger group of subjects to determine if these findings are typical for the spinal cord injured population.

Chapter 7

Efficiency in SCI Subjects

7.1 Summary

In this chapter the concept of efficiency of exercise is introduced. The definition of traditional efficiency measures is given and efficiency in AB and SCI subjects is discussed. A new definition of efficiency is introduced, where the negative workrate range is taken into account. Values for efficiency calculated with the new definition in SCI subjects are reported and the concept of efficiency in paraplegic subjects is discussed. The new definition of efficiency and part of the results reported here can also be found in [60].

7.2 Introduction

7.2.1 Traditional Definition of Efficiency

Exercise efficiency has been defined by Gaesser *et al.* [38] as “the ratio of work accomplished to energy expended” within a given time interval. The work accomplished is easily measured on a cycle ergometer and the energy expended during exercise can be calculated as explained in section 1.3.3. However, it is necessary to make a fundamental assumption in order to be able to compute efficiency: respiration has to be a reliable index of the energy requirements. This is true only in a metabolic steady state [130].

The definition of efficiency depends on the power output range used (P^{out}), on the metabolic power (P^{in}) and on the correction employed for the losses in the system (P^0 for unloaded exercise and P^r for rest). The following are widely accepted

definitions of efficiency [38] (see also figure 7.1):

$$\text{Gross Efficiency: } \epsilon_g = \frac{P^{out}}{P^{in}} \times 100\% \quad (7.1)$$

$$\text{Net Efficiency: } \epsilon_n = \frac{P^{out}}{P^{in} - P^r} \times 100\% \quad (7.2)$$

$$\text{Work Efficiency: } \epsilon_w = \frac{P^{out}}{P^{in} - P^0} \times 100\% \quad (7.3)$$

$$\text{Delta Efficiency: } \epsilon_\Delta = \frac{\Delta P^{out}}{\Delta P^{in}} \times 100\% \quad (7.4)$$

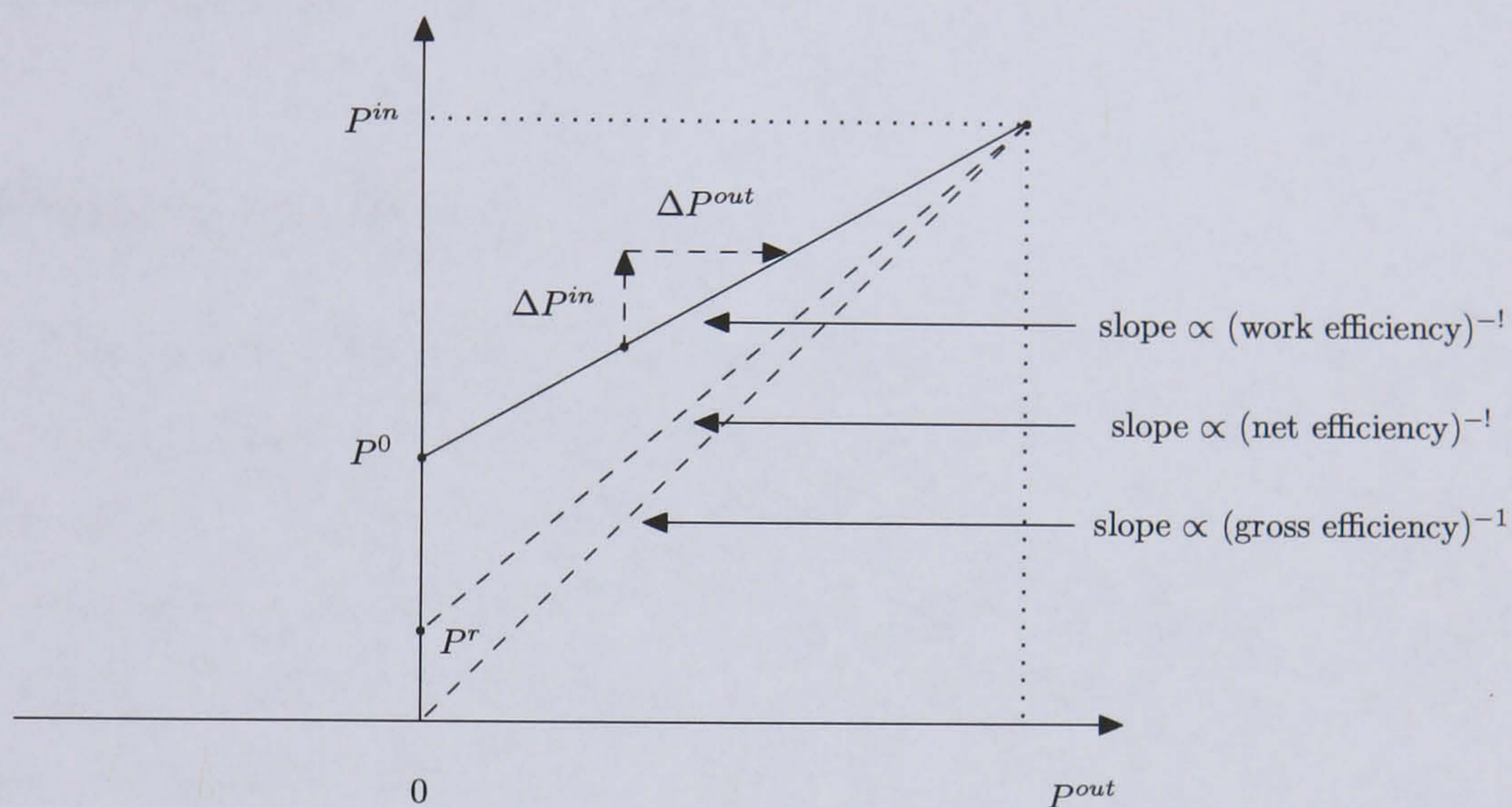


Figure 7.1: Graphical representation of the traditional measures of efficiency.

The efficiencies defined with equations (7.1)-(7.4) are characterised by different energy baselines. ϵ_g takes into account the entire energy consumed by the subject to sustain a given workrate. ϵ_n separates the energy required for muscle contraction and the energy required for the resting body activity. The resting energy expenditure is subtracted from the exercise energy expenditure. ϵ_w takes into account the energy required to move the legs during unloaded cycling, i.e. when no external resistance is applied. The energy required to overcome the inertia of the legs is subtracted from the total energy expenditure. The work done is supposed to be 0 W for unloaded exercise. ϵ_Δ is the ratio between an increment in workrate and the corresponding increment in the rate of energy expenditure due to the increase in \dot{V}_{O_2} .

Typical values found in the literature for the four traditional efficiency measures in AB subjects during cycle ergometry are reported in table 7.1.

author	ϵ_g	ϵ_n	ϵ_w	ϵ_Δ
Coyle ^s <i>et al.</i> [20]	18.3-22.6%	-	-	18.3-25.6%
Moseley ^g <i>et al.</i> [88]	19.8	-	-	25.8%
Nicleberry ^g <i>et al.</i> [90]	12.8-22.3%	-	-	20.6-29.5%
Mallory ^s <i>et al.</i> [79]	-	-	-	29.7%
Whipp ^s <i>et al.</i> [130]	-	29.8	-	-
Hintzy ^s <i>et al.</i> [55]	-	-	32.4-46.2%	-
Gaesser ^s <i>et al.</i> [38]	7.6-20.4%	9.8-24.1%	24.8-29.5%	14.6-30.5%
Bijker ^g <i>et al.</i> [13]	-	-	-	21-33%
Bijker ^s <i>et al.</i> [13]	-	-	-	18-34%

Table 7.1: Efficiency measurement values found in the literature. ^g: graded exercise test; ^s: step exercise test.

7.2.2 Efficiency Baselines

The debate about what baseline, and consequently which efficiency index, describes better the actual efficacy of exercise is still open.

Stainbsy *et al.* [117] maintain that a baseline can be considered valid if the amount of energy consumed relative to the baseline remains unchanged through changes in work rates or exercise conditions. However, it is quite obvious that these requirements are seldom verified.

Whipp *et al.* [130] argue that the workrate level can affect the accuracy of the efficiency calculations. If the workrate is too high it is possible that a steady state is not reached, thus efficiency would be overestimated. In addition, if the exercise phase is too long, the O₂ cost of breathing could become a large percentage of the overall O₂ consumption. Thus, efficiency would be underestimated.

ϵ_g does not use any baseline. Figure 7.2 shows how ϵ_g changes when power output (PO) changes. The slope decreases when PO increases, i.e. from P₂ to P₁, thus efficiency increases. It is also quite obvious that at high power output levels the difference in ϵ_g decreases. A study from Moseley *et al.* [88] confirms this finding, since they found that ϵ_g increases with power output. However, they explained this with the higher energy needed to stabilize the body at lower workrates. Some authors [38, 88] maintain that since ϵ_g increases with workrate, the relationship between energy expenditure and workrate cannot be linear, otherwise ϵ_g would be constant. However, in figure 7.2 it is clearly shown that the increment in ϵ_g does not depend on the non-linearity of the relationship between energy expenditure and power output, but it is intrinsic in the definition of efficiency. On the other hand

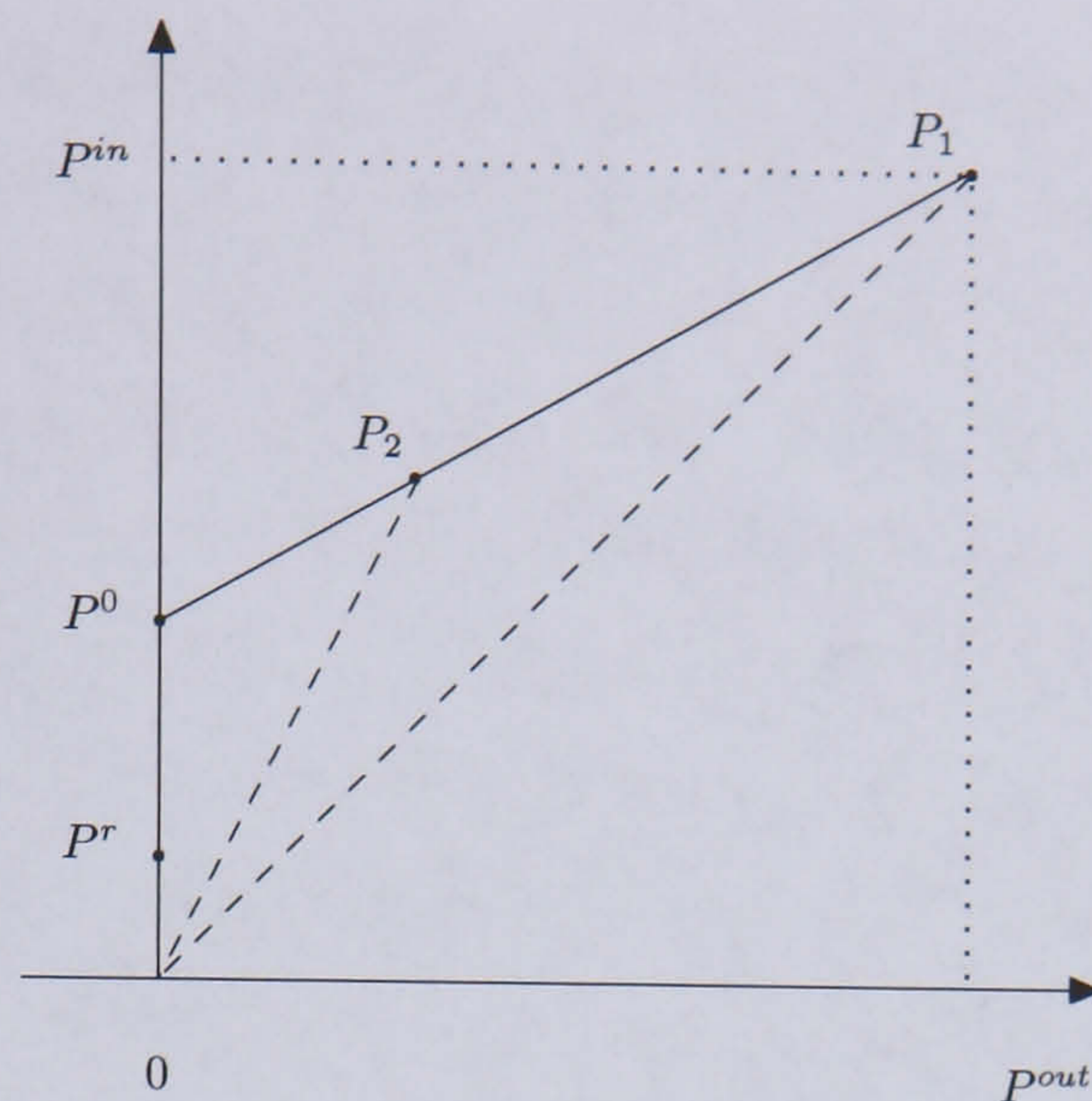


Figure 7.2: Graphical representation of the slopes proportional to the inverse of gross efficiency at two different power output levels.

Coyle *et al.* [20] report that ϵ_g was similar across a range of workrates that elicited 50 to 70% of $\dot{V}_{O_{2max}}$. An explanation for the different findings could be that the power output levels corresponding to the range from 50 to 70% of $\dot{V}_{O_{2max}}$ in Coyle *et al.* [20] were close, thus the efficiency values did not differ significantly.

ϵ_n can be considered the “classical” efficiency measurement. Gaesser *et al.* [38] state that ϵ_n does not consider the work of moving the legs, which leads to an underestimation of the real muscular efficiency. They argue that the calculation of ϵ_n involves the use of a constant (i.e. \dot{V}_{O_2} at rest) which lies much below the line that describes the relationship between energy expenditure and workrate.

ϵ_w is difficult to obtain, since generally the protocol and/or the cycle ergometer used do not permit measurement of the true zero muscular workload, i.e. passive power output. In most investigations [6, 55] the unloaded power output level (i.e. 0 W) is used. It corresponds to a workrate level without any additional external resistance.

ϵ_Δ uses a floating baseline, thus representing all the changes in energy expenditure. Gaesser *et al.* [38] say that if every increment in energy expenditure represents only the additional work done by the muscles, then ϵ_Δ is the most accurate measure of muscular efficiency. However, they do not demonstrate that this is the case in their paper. On the other hand, Stainsby *et al.* [117] argue that the factors that define a baseline are subject to change between workrates. Thus, they conclude that ϵ_Δ is not better than the other measures of efficiency. Moseley *et al.* [88] report that ϵ_Δ , although having been chosen as the most valid estimate of muscular efficiency, is not the most reliable.

Stainsby *et al.* [117] say that energy expenditure during exercise is constituted by two terms: a first term that quantifies the energy expended by the muscles and a second term that quantifies the energy necessary for the basic body functions. Among these functions they include: accelerating and decelerating limbs, breathing, transporting ions against electrochemical gradients, stabilization of body parts, synthesis of substrates, mobilization of substrates and circulation of blood. Moreover, at different workrate levels the amount of elastic energy that is stored by tendons and muscles changes. This affects the efficiency calculations. Thus, they conclude that none of the defined efficiencies is a proper index of muscular efficiency. They argue that the problem lies in the interpretation of such efficiencies.

In summary, it is possible to say that as long as there is awareness of the limitations in the efficiency measurements, it is possible to use them to compare the fitness or the efficacy of exercise of different subjects.

7.2.3 Parameters That Influence Efficiency

Mechanical parameters

The main mechanical parameters that affect \dot{V}_{O_2} and consequently the various efficiency measures are power output, cadence and resistance.

Croissant *et al.* [22] found that \dot{V}_{O_2} increases linearly with cadence, when the torque is kept constant. The same is true for the torque, when the cadence does not vary. Since the power output is given by the product of torque measured at the crank and the angular velocity of the crank, \dot{V}_{O_2} increases linearly with PO when either cadence or torque are kept constant. Moreover, for each set power output there is a number of combinations of cadence and torque. It has been proven that each combination can deliver a different value for oxygen uptake. Croissant *et al.* [22] found that both cadence and torque increase, in the particular combination that gives the minimum energy expenditure, with increasing power output. They pointed out that experimenters using an electrically braked bicycle, in which the power output is kept constant by adjusting the brake resistance as a response to variations in cadence, should note that the change in the condition of exercise affects \dot{V}_{O_2} . The energy cost necessary for accelerating and decelerating the legs during exercise can be a significant part of the overall energy cost in some situations (i.e. in SCI subjects). Thus, it is important to keep velocity constant [13].

MacIntosh *et al.* [77] maintain that the need to utilize more fast-twitch fibres when the power output increases is the cause of the shift in the optimal cadence.

Their study shows that, for each power output, there is a cadence at which the muscle activation is minimal and this cadence increases with power output. Londeree *et al.* [76] state that \dot{V}_{O_2} is nonlinearly related to work rate and pedalling cadence. They too suggest as an explanation the fibre type recruitment order. Slow-twitch fibres work at low intensities, while at high intensities the more inefficient fast-twitch fibres are recruited, causing the nonlinear rise in \dot{V}_{O_2} . Another reason for the non-linearity is that, at equal power outputs, with a low cadence the force needed is higher and it is applied longer in each pedal cycle than with high cadences. Thus, they hypothesize that the combination of high cadence and low force application requires a higher use of fast-twitch fibres.

Lepers *et al.* [75] tested the effect of three different pedalling cadences (in the range 69-103 rpm) at the same power output on metabolic expenditure during cycling. No significant difference was found in \dot{V}_{O_2} and heart rate at different cadences. However, they found significant differences for \dot{V}_E and R during the initial part of exercise. This finding could be due to the limited number of cadences that were tested. Moreover, the tested cadences were all in the upper part of the range of pedalling rates used for cycling. This could have contributed to the lack of significance in the difference.

Barstow *et al.* [3] report that the amplitude of $\Delta\dot{V}_{O_2}$ decreases with an increase in pedal frequency and they explain this with the different contribution of the stored elastic energy at different cadences. The time constant was not affected by cadence in their study.

Foss *et al.* [37] state that $\dot{V}_{O_{2max}}$ does not change with cadence. They also report that with increasing power outputs, the cadence that gives the lower steady state \dot{V}_{O_2} increases. They also maintain that unloaded \dot{V}_{O_2} increases with cadence and hypothesize that difficulties in coordinating movements at high cadences could be the reason for the high \dot{V}_{O_2} . They showed that the accelerations and decelerations of the flywheel at high cadences caused an increment in the oxygen uptake during unloaded cycling. Thus, they warn that if the unloaded cycling is to be used as a baseline, it is necessary to be able to control cadence precisely.

Zoladz *et al.* [136] showed that both $\dot{V}_{O_{2max}}$ and P_{max} do not change with cadences between 60-100 rpm. However, the maximum power output was significantly reduced at very low or high pedalling cadences (i.e. 40 rpm or 120 rpm).

Ferguson *et al.* [32], in a study of knee extension, found that \dot{V}_{O_2} levels are higher for a contraction frequency of 60 rpm than for 100 rpm, at similar power outputs. Thus, at higher contraction frequencies the mechanical efficiency appears

to be lower.

Muscle fibre type percentage

A physiological parameter that affects \dot{V}_{O_2} and consequently efficiency is the fibre type composition of the muscle.

Barstow *et al.* [3] found that the fibre type composition in the muscle was not correlated with the total increase in \dot{V}_{O_2} (i.e. the sum of the fast and the slow component), but it was strongly correlated with the amplitude of the fast component only. The latter was also correlated with $\dot{V}_{O_{2peak}}$. Moreover, they reported that $\dot{V}_{O_{2peak}}$ was correlated with the percentage of type I muscle fibres.

Mallory *et al.* [79] tested twenty-two subjects and found that there were less differences in efficiency and \dot{V}_{O_2} increase within a subject than between subjects. Thus, they suggested that physiological differences could be detected through efficiency. They did not find any relationship between efficiency and percentage of fibres present in the muscles. This was explained by the fact that the exercise intensity was low and therefore predominantly type I fibres would have been recruited. Indeed, the higher percentage of type II fibres present in some subjects does not imply that those fibres are always used. They also suggested that at the chosen cadence the difference in efficiencies for the two fibre types could be minimal.

Barstow *et al.* [4] maintain that the increase in \dot{V}_{O_2} reflects the increase in energy expenditure due to muscle contraction and also to activation heat. They argue that it is still not completely clear if the energy due to the heat remains constant during exercise or if it varies depending on the frequency of contraction and fatigue. They also add that both fibre type and level of fitness are correlated with the \dot{V}_{O_2} response, but it is not possible to distinguish between the effect of fibre type or fitness on the performance.

Coyle *et al.* [20] found that subjects with a higher percentage of type I muscle fibres had a higher efficiency. This probably was because the experiments were done at a cadence closer to the one that elicited the peak efficiency in this type of fibre.

Jones *et al.* [68] found that the $\Delta\dot{V}_{O_2}/\Delta PO$ slope was correlated with the percentage of type II muscle fibres present in the muscles. The slope of the second half of the data in the V-slope graph (i.e. the graph of \dot{V}_{CO_2} plotted against \dot{V}_{O_2}) was steeper in subjects with a higher percentage of type II muscle fibres. They also suggested that at high pedal rates, type II muscle fibres could be recruited at low workrates. They concluded that the higher or lower efficiency of type II muscle fibres with respect to type I depends on exercise intensity and contraction velocity.

7.2.4 Efficiency in FES-Cycling

The efficiency of SCI subjects performing FES-cycling is lower than that of AB subjects cycling under volitional control. Glaser *et al.* [45] compared the efficiency in SCI and AB subjects cycling on a cycle ergometer. Net efficiency was much lower for SCI subjects, 5%, compared to AB subjects, 10-18%, in the same power output range. Moreover, they suggested that the real efficiency could possibly have been lower than that calculated. Indeed, they found that the capillary blood lactate concentration in SCI subjects was higher than in AB subjects. Therefore, the SCI subjects were in part exercising anaerobically. The amount of energy produced anaerobically was not quantifiable, thus efficiency could have been overestimated.

Raymond *et al.* [108] obtained similar results in one of their studies. A group of SCI subjects cycled by means of FES and a group of AB subjects voluntarily cycled on the same ergometer. The maximum power output sustained was 9.2 W for SCI subjects and 42.8 W for AB subjects. The \dot{V}_{O_2} values elicited by these workrates were 0.75 l/min and 0.74 l/min for SCI and AB subjects, respectively. Thus, the metabolic expenditure was quite similar. The estimated net efficiency is approximately 5% for SCI and 22% for AB subjects.

Care must be exercised in the interpretation of the approximate efficiency values quoted above. Theisen *et al.* [119] have shown that efficiency can vary significantly during prolonged, constant-stimulation FES-cycling exercise. Five subjects were involved in their study. In a session lasting approximately 40 minutes, the efficiency increased from 5.8% after 6 minutes to 8.6% at the end of the session. However, the absolute values for efficiency are still much lower than the values obtainable from AB subjects. Moreover, Glaser *et al.* [45] caution that these figures may overestimate the efficiency of cycling, since the calculations are based upon an assumption of steady-state aerobic metabolism. In the SCI population, however, blood-lactate levels are known to be elevated early in FES-cycling exercise [43], indicating an energy contribution from anaerobic metabolism which is neglected in the efficiency calculations. They also suggest that the mechanisms that waste energy during FES-cycling include FES-induced spasms. Moreover, other factors can increase energy consumption, such as higher rates of pulmonary ventilation or higher body temperature.

Kjaer *et al.* [72] investigated the performance of eight healthy young males in both volitional and FES-induced cycling. The group performed volitional cycling at a workrate which elicited an average oxygen uptake of 1.9 l/min. Complete epidural anaesthesia was then administered, to eliminate any volitional control of the legs.

Cycling was subsequently achieved by means of FES at a workrate which elicited the same oxygen uptake rate of 1.9 l/min. The average workrate for this oxygen cost was found to be approximately 120 W during volitional cycling, but less than 40 W for FES-cycling. The estimated net efficiencies for FES-cycling and for volitional cycling in this group are 7% and 22%, respectively [72]. This establishes that even in subjects where the underlying muscle condition is normal, FES-induced cycling is less efficient by a factor of approximately 3 than cycling achieved by volitional muscle control. These results suggest that the low efficiency of FES-cycling is primarily due to the recruitment properties of electrically-stimulated muscle, together with the unfavourable biomechanics of the FES-cycling arrangement.

Schutte *et al.* [113] have shown that optimising the mechanical configuration of the exercise apparatus can increase the number of subjects who are able to use FES. They analysed the seat configuration to optimise efficiency. They took into account the inclination of the seat back, the orientation of the ergometer and the distance of the hip from the crank. The distance of the hip from the crank influences the performance of the quadriceps and hamstring muscles. If the seat back is close to the horizontal or vertical positions, the cycling motion becomes more difficult. They also studied how loading affects performance during FES-cycling. At high pedalling cadences (i.e. 60 rpm) the percentage of people that can cycle becomes lower with respect to cadences equal to 40 or 50 rpm. The ability to sustain a given power output at a set cadence depends on the capacity of the subject to overcome internal energy losses, such as inertia. At high cadences these energy losses are higher, thus the total power output required increases. Therefore, the number of SCI subjects able to develop a given PO decreases when cadence increases. They conclude that using a lower cadence allows a greater number of subjects to use FES-cycling exercise.

7.3 Methods

7.3.1 A New Efficiency Measurement

The definition of efficiency depends upon the effective output work range used, and any correction employed for losses in the system, as stated above. In impaired subjects, the work done in moving the legs can be a large proportion of the overall workrate range. Thus, it becomes fundamental to take this work into consideration in the efficiency calculations. A distinguishing feature of our technical setup is

the ability to perform passive, non-stimulated cycling, and therefore to directly measure the workrate required to move the mass of the legs. Within our setup for FES-cycling the total workrate ranges from the negative value of workrate measured during passive, non-stimulated cycling to the positive workrate value reached during maximal stimulated exercise. This is illustrated in figure 7.3. We define the total workrate range as $P^t = P^{out} - P^-$, where P^- is the negative, passive power output. Further, we define the rate of metabolic energy expenditure during passive, non-stimulated cycling as P^p .

We then redefine the traditional efficiency measures by taking into account the total workrate range as follows:

$$\text{Total Gross Efficiency: } \epsilon_g^t = \frac{P^t}{P^{in}} \times 100\% \quad (7.5)$$

$$\text{Total Net Efficiency: } \epsilon_n^t = \frac{P^t}{P^{in} - P^p} \times 100\% \quad (7.6)$$

where these definitions are valid under conditions of steady-state aerobic exercise. The total gross efficiency measure is useful for characterising the overall efficacy of the exercise, but makes no adjustment for losses associated with the passive (or resting) metabolism, which varies between subjects. The Total Net Efficiency is a preferred measure for the evaluation of the muscular and biomechanical efficacy, and can be used for comparison both within and between subjects.

The newly defined efficiency measures should be contrasted with those employed in previous studies, where cycling began in an “unloaded” condition, corresponding

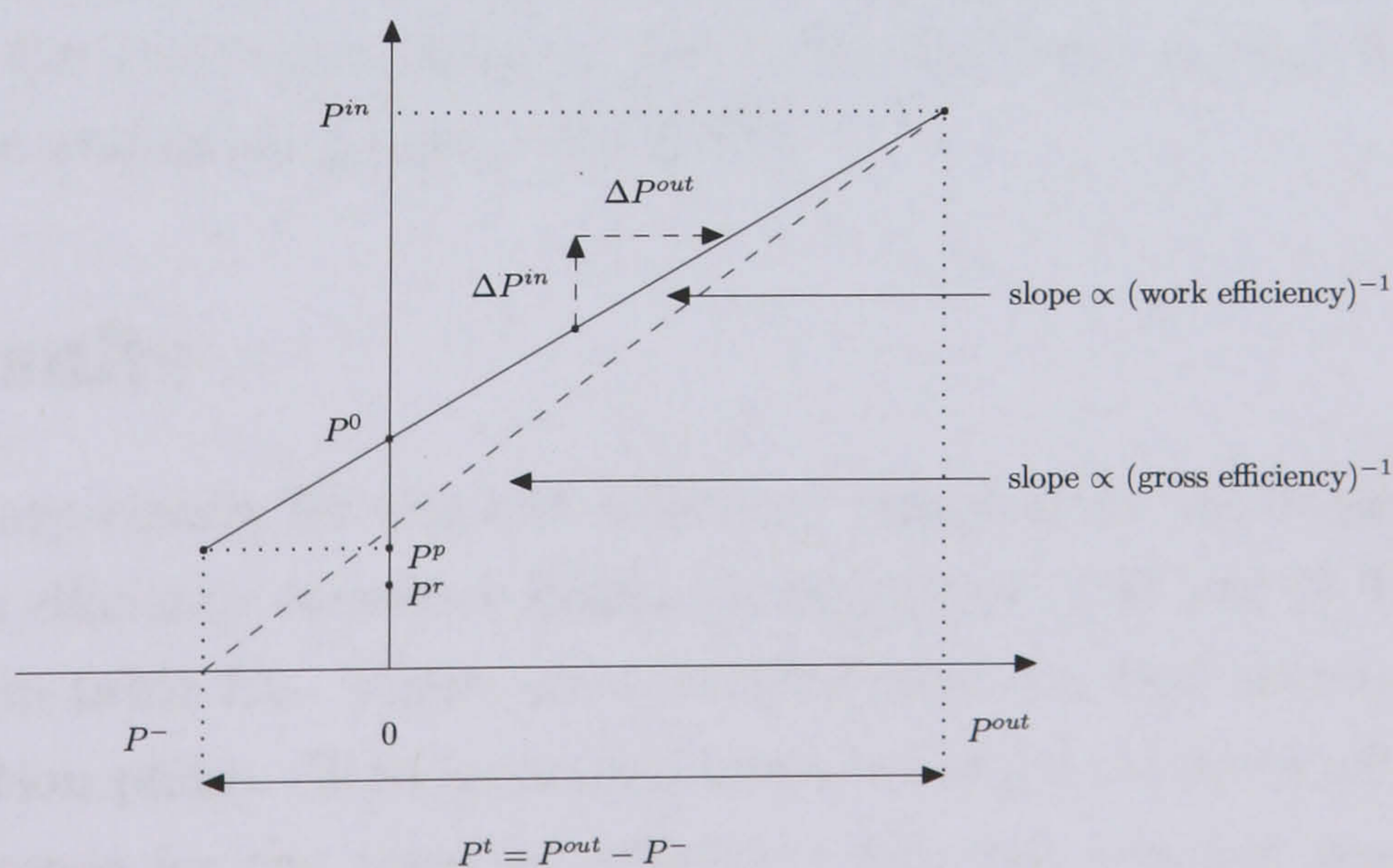


Figure 7.3: Graphical representation of the extended measures of efficiency.

to a workrate of 0 W. In this condition stimulation has to be applied, just sufficient to turn the mass of the legs at the required cadence. The corresponding efficiency measures can therefore only include the “positive” work done above 0 W. On the other hand our experimental setup allows measurements of power output levels in the negative range. Moreover, impaired populations may well have their P_{peak} or ventilatory threshold at a negative level. For example in chapter 5 we have shown that for one of our subjects the VT occurs below 0 W. Thus, the new efficiency measurements can be used with a wider population. Another disadvantage of the traditional measures of net and gross efficiency is that they are biased by the metabolic energy cost of moving the legs, which limits their applicability for comparing efficiency between subjects of different masses.

7.3.2 Experimental Setup

The preliminary results reported in this chapter are based on the tests described in chapter 6: four Two Pattern Tests (TPT) and two One Pattern Tests (OPT). The subject cycled by means of FES on a motorized trike. The experimental setup has been described in detail in chapter 3. The cycling exercise consisted of a resting period, followed by passive cycling and by a stage of unloaded cycling, i.e. 0 W. The evaluation phase followed. It consisted of constant cycling at a power output higher than 0 W. The protocols for the TPT and OPT have been described in more detail in chapter 6.

The new efficiency measurements have been used to calculate efficiency in the six tests. Efficiency measurements have been computed over the last minute of each stage during the evaluation phase in the TPTs and every minute from the 6th to the end of the evaluation phase in the OPTs.

7.4 Results

Our preliminary results for the new efficiency calculations are reported here. The values for the efficiency measures defined in equations (7.5) and (7.6) for the TPTs are reported in table 7.2. These are calculated over the final minute of each stage in the evaluation phase. Both measures indicate that P1 is more efficient than P2, but the difference for the total net efficiency measure was not determined to be statistically significant ($p > 0.05$).

The mean values (\pm sd) for the two efficiency indices during the two OPTs are

reported in table 7.3. The difference between the efficiency values of both measures is statistically significant.

Pattern	Total Net Efficiency	Total Gross Efficiency
P1	13.81%± 0.02	7.21%± 0.004
P2	12.08%± 0.02	6.64*%± 0.004

Table 7.2: Mean \pm sd values for the Total Net and Total Gross Efficiency measurements for the four TPTs. * denotes a significant difference with $p < 0.05$.

	Total Net Efficiency	Total Gross Efficiency
P1	10.49%± 0.004	5.87%± 0.001
P2	11.75*%± 0.004	6.08*%± 0.001

Table 7.3: Mean \pm sd values for the Total Net and Total Gross Efficiency measurements in the two OPTs. * denotes a significant difference with $p < 0.05$.

7.5 Discussion

As previously reported (see chapter 2), there are two main theories regarding the fibre type recruitment order during FES: the theory of the inverse recruitment pattern and the theory of non-selective, spatially fixed and temporally synchronous recruitment.

If the theory of the inverse recruitment pattern for muscle fibres in SCI subjects during FES-cycling is true, then it is possible that even during sub-threshold exercise the amount of work done by the anaerobic metabolism is significant. Thus, even during light exercise the efficiency calculations probably do not deliver a true estimate of the real efficiency. If the anaerobic metabolism is active even at very low power outputs, then efficiency is overestimated. However, using only gas exchange measurements it is not possible to quantify exactly how much lower the true efficiency is with respect to the computed value. Thus, the question is whether this approximated efficiency can be used to compare different subjects or not. If the amount of anaerobic energy produced is the same across the subjects, then it would be possible to compare different subjects. However, it is not likely that the anaerobic metabolism would be similar in different subject, as it depends on

physiological parameters (such as relative percentage of fibre types present) that differ from subject to subject. Moreover, without invasive techniques such as lactate measurements, it does not seem possible to be able to quantify the contribution of anaerobic metabolism. It would be interesting to test a higher number of subjects and to see how efficiency varies during the tests and also to correlate the findings with measures of blood lactate concentration.

On the other hand, recent studies suggest that the muscle fibre type recruitment with FES is non-selective, spatially fixed and temporally synchronous [49, 73, 120]. If this theory is true, type II fibres are activated over the whole duration of exercise. This means that anaerobic metabolism occurs from the very beginning of exercise. Thus, efficiency would be overestimated also in this case.

Thus, with both theories, the result of efficiency calculations is a value that can be reasonably considered as an upper limit for the real efficiency. It is not possible to know the exact efficiency value, but it is certain that it cannot be higher than that calculated. Thus, a higher efficiency implies a higher efficacy of exercise or a higher fitness level, even if it is not possible to quantify it precisely. Therefore, efficiency measurements can be used to study changes in fitness in the training history of a single subject. Moreover, it is still possible to qualitatively assess higher or lower efficacy between SCI and AB subjects.

Our new efficiency definitions allow the calculation of efficiency for SCI subjects who cannot develop a power output level higher than 0 W. Thus, Total Net and Total Gross Efficiency can be very useful in assessing the fitness of very deconditioned subjects or subjects that are at the beginning of a training period. It would not have been possible to use these novel efficiency definitions in the past, since different experimental setups that did not allow measurement of negative power output were used [2, 6, 56, 57]. Moreover, in the SCI population the work done to move the legs largely affects the overall performance. Thus, it is important to be able to take that work into account in the calculation of efficiency. As expected, our results from the OPTs show that efficiency calculated with the new definitions is higher than previously found [45, 119], thus confirming the importance of adding the negative power output to efficiency calculations.

In principle, the new measures of Total Efficiency introduced here, which exploit the full workrate range of the exercising muscles (starting from the negative, passive workrate), should give improved signal to noise characteristics for these computations and therefore a more accurate representation of muscular and biomechanical efficacy. However, these are preliminary results obtained from data from only one

subject. Thus, it is necessary to perform a higher number of tests on different subjects to study the numerical properties of the newly defined efficiency measures.

Our results show that there is a difference in efficiency depending on the pattern used for stimulation. In the TPTs, pattern P1 seems to be more efficient than pattern P2 (see also table 7.2). In the OPTs, pattern P2 seems more efficient than pattern P1 (see also table 7.3). These apparently contradictory results might suggest that the exercise protocol affects the efficiency results. However, since only one OPT has been done with pattern P1 and one with pattern P2, it could be possible that the discrepancy is due to the high day-to-day variability in physiological status that characterizes SCI subjects. Thus, efficiency could still be considered a sensitive index of the efficacy of exercise, even if it is only the upper limit of the range in which the real efficiency value could be. However, as mentioned above, it is necessary to perform a higher number of tests, possibly with analysis of blood lactate concentration, to quantify the relationship between the real efficiency values and the upper limit of efficiency that can be calculated with gas exchange data. This would help in determining if the efficiency values here calculated are a reliable measure of exercise efficacy.

7.6 Conclusions

The new definitions of efficiency take into account the negative part of the power output range. This allows measurement of exercise efficiency also for those subjects that have a limited or negative workrate range, such as SCI subjects. The Total Efficiency measurements are expected to deliver efficiency values with better numerical properties. However, it is necessary to perform a higher number of tests to verify this hypothesis.

Chapter 8

Future Work

8.1 Summary

In the previous chapters suggestions have been given about possible future research fields. In this chapter those suggestions are developed.

8.2 Identification of Open Investigation Areas

The exercise test protocols that have been developed in this work were determined using the knowledge of AB exercise testing and scaling the power output for SCI subjects, thanks to the novel testbed used. The results obtained show that it is possible that the traditional methods used with AB subjects are not optimal for testing SCI subjects. Indeed the $\dot{V}_{O_{2peak}}$ obtained with the IET is not the maximum the subject can achieve, as the \dot{V}_{O_2} delivered by the SET is higher. Thus, it is important to develop a new protocol whose aim would be to deliver the true $\dot{V}_{O_{2peak}}$. A possible solution could be to prolong the test beyond the point where the stimulation intensity reaches saturation. In other words, once saturation is reached it is possible to let the subject cycle for a set duration, until the \dot{V}_{O_2} reaches the peak. The end of the session could also be set at the moment in which the power output developed by the subject drops below a predefined level. It will be necessary to study the meaning of such a peak, since it obviously will not correspond to the maximum power output developed by the subject, and its implications.

Our results show that it is possible to detect a deflection from linearity in the V-slope graph obtained with an IET in SCI subjects. The meaning of the ventilatory

threshold found in SCI subjects has been discussed and it has been hypothesized that anaerobic metabolism is present from the beginning of exercise. However, in this study blood samples during the tests were not taken. Thus, we suggest to use blood lactate concentration analysis to investigate the correlation between the ventilatory threshold and the lactate threshold in the SCI population.

Both IET and SET deliver variable values for the time constant. Even with AB people the time constant varies across tests [59]. With SCI people the gas exchange data are noisier, thus it seems advisable to carry out more tests. A possible finding is that the gas exchange response in SCI subjects cannot be compared to the response obtained with a linear system, while in AB subjects this is possible with good approximation. However, to ascertain if it is possible to use the time constant obtained from tests with SCI subjects to draw conclusions about fitness, it would be better to perform a higher number of tests with the same and also with different subjects.

The stimulation cost has been defined in this work as a possible parameter to quantify the energy cost of exercise. It is a promising measure, but more tests need to be done in order to gain a higher statistical significance for the results. It seems that the time constant for stimulation cost is lower than for oxygen uptake. To quantify the difference between the time constants it is necessary to perform new sets of tests. A suggestion would be to prolong each stage to at least 8 minutes, since for some subjects 6 minutes are not enough to reach a steady state. It would also be necessary to find the correlation between oxygen uptake and stimulation cost.

Once found that there is a correlation, it would also be interesting to study the variability of the time constant of the stimulation cost. From our preliminary results apparently the time constant does not vary greatly. With a higher number of tests it will be possible to determine if this finding is true. If the time constant for the stimulation cost does not vary across the tests in the same subject, it will be possible to utilize it to characterize the fitness of the subjects. A SET is the suggested test for this kind of investigation, with the subject performing a step in power output from unloaded cycling to the desired level. In this investigation it will be interesting to repeat tests at the same and at different workrate levels to study the variability depending on the test itself and on the power output required. Possibly a lower number of tests will be necessary to characterize the fitness level of a subject using the stimulation cost, since this variable is less noisy than oxygen uptake.

New efficiency definitions have been introduced in this thesis. However, the number of tests performed is not high enough to draw statistically significant conclusions on their numeric properties. Therefore, a suggestion is to perform a higher number of SET at different power output levels and on different subjects in order to study Total Gross and Total Net Efficiency measures. Moreover, the concept of efficiency in SCI subjects has been discussed and it has been concluded that the real efficiency value is overestimated in this population when calculated with gas exchange measurements. Thus, it is important to perform blood lactate concentration analysis to quantify the amount of anaerobic metabolism during FES exercise.

8.3 Conclusions

In conclusion, we have identified some open questions that have arisen from this work. New developments for the IET protocol have been proposed. Moreover, problems with the response of the control system to spasms have been addressed. A wider utilization of the stimulation cost has been hypothesized and new testing procedures to verify its usefulness have been suggested. A deeper investigation about VT and efficiency measurements have also been suggested. Therefore, there is considerable scope for future research in this field.

Chapter 9

Conclusions

We developed new protocols for exercise testing. The new experimental setup used allowed the determination of all the key cardiopulmonary variables necessary to assess a subject's fitness.

We had the possibility of using small increments in power output in both IET and SET. This allowed us to define a IET protocol similar to that used for AB subjects. Thus, we could compare the outcomes obtained with a test on SCI subjects with those obtained from tests with AB subjects, since the conditions were the same.

We have been able to detect the presence of the ventilatory threshold with the IET. We have also been able to point out that in very deconditioned subjects the VT can occur at negative power outputs. Thus, the experimental setup used in this work is vital for a complete and accurate evaluation of the subject's fitness. The question whether the ventilatory threshold can be considered the same as in AB subjects is still open. The different muscle fibre recruitment order with FES with respect to voluntary contractions raises the possibility that no absolute aerobic metabolism is present in FES-exercise. On the contrary we suggest that both aerobic and anaerobic metabolism are present since the onset of exercise and successively the anaerobic metabolism takes over completely. However, we suggest that as long as the VT is used to compare SCI subjects it remains a valid fitness index.

The possibility of imposing arbitrarily small increments in power output allows more precise testing of SCI subjects. Indeed, it is possible to exercise at well defined percentages of the peak power output, $\dot{V}_{O_{2peak}}$ or VT.

The protocols proposed here, and the associated technical measurement and control setup, are currently being used in a multi-centre study of FES-cycling in a large group of subjects. This will allow us to determine whether the results are representative for a larger cross section of the SCI population.

Going further into exercise analysis, we determined that it is possible to detect changes in oxygen uptake depending on the stimulation pattern used. We found that one of the two examined patterns demanded a lower \dot{V}_{O_2} level and was thus more efficacious for performing FES-cycling exercise.

We have also defined a new index of cycling efficacy, the stimulation cost. It takes into account the total charge delivered to muscles during exercise, thus it reflects the amount of energy necessary to move the legs during cycling. It has been demonstrated that it reflects the discriminatory power of the oxygen uptake. Moreover, it is easier to be measured in real time and it is less subjected to noise. It also shows quicker kinetics, thus suggesting that it could be useful in terms of the overall length of the exercise session.

We also defined new efficiency measures that take into account the additional negative range of power output that is used in our tests: Total Gross and Total Net Efficiency. However, the question about the real meaning of efficiency when working with SCI subjects is still open. We have addressed the possibility of calculating efficiency when anaerobic metabolism is contributing to the production of the energy necessary to exercise. We have concluded that efficiency measurement can still be used to assess a subject's fitness. Moreover, comparison of efficiency values can still be valid among SCI subjects and between SCI and AB subjects.

In conclusion, we have identified the need to redefine exercise testing protocols using a more sophisticated experimental setup than those used in the past. Through the new protocols we have been able to identify with precision the key outcomes of traditional exercise testing. We have discovered the presence of the ventilatory threshold in SCI subjects and we have defined a novel outcome: the stimulation cost. Having the possibility of utilizing also the negative power output range, we deemed it necessary to redefine the efficiency measures used in the literature.

List of References

- [1] P.B. Arnold, P.P. McVey, W.J. Farrell, T.M. Deurloo, and A.R. Grasso. Functional electrical stimulation: its efficacy and safety in improving pulmonary function and musculoskeletal fitness. *Arch Phys Med Rehabil*, 73:665–668, July 1992.
- [2] T. Barstow, E. Scremin, D. Mutton, C. Kunkel, T. Cagle, and B. Whipp. Changes in gas exchange kinetics with training in patients with spinal cord injury. *Med Sci Sports Exerc*, 28(10):1221–1228, 1996.
- [3] T.J. Barstow, A.M. Jones, P.H. Nguyen, and R. Casaburi. Influence of muscle fiber type and pedal frequency on oxygen uptake kinetics of heavy exercise. *J Appl Physiol*, 81(4):1642–1650, 1996.
- [4] T.J. Barstow, A.M. Jones, P.H. Nguyen, and R. Casaburi. Influence of muscle fibre type and fitness on the oxygen uptake/power output slope during incremental exercise in humans. *Experimental Physiology*, 85(1):109–116, 2000.
- [5] T.J. Barstow and P.A. Molé. Linear and nonlinear characteristics of oxygen uptake kinetics during heavy exercise. *J Appl Physiol*, 71(6):2099–2106, 1991.
- [6] T.J. Barstow, A.M.E. Scremin, D.L. Mutton, C.F. Kunkel, T.G. Cagle, and B.J. Whipp. Gas exchange kinetics during functional electrical stimulation in subjects with spinal cord injury. *Med Sci Sports Exerc*, 27(9):1284–1291, 1995.
- [7] T.J. Barstow, A.M.E. Scremin, D.L. Mutton, C.F. Kunkel, T.G. Cagle, and B.J. Whipp. Peak and kinetic cardiorespiratory responses during arm and leg exercise in patients with spinal cord injury. *Spinal Cord*, 38:340–345, 2000.
- [8] S.E. Bearden, P.C. Henning, T.A. Bearden, and R.J. Moffatt. The slow component of $\dot{V}O_2$ kinetics in very heavy and fatiguing square-wave exercise. *Eur J Appl Physiol*, 91:586–594, 2004.

- [9] W.L. Beaver, K. Wasserman, and B.J. Whipp. Bicarbonate buffering of lactic acid generated during exercise. *J Appl Physiol*, 60(2):472–478, 1986.
- [10] W.L. Beaver, K. Wasserman, and B.J. Whipp. A new method for detecting anaerobic threshold by gas exchange. *J Appl Physiol*, 60(6):2020–2027, 1986.
- [11] K.K. BeDell, A.M.E. Scremin, K.L. Perell, and C.F. Kunkel. Effects of functional electrical stimulation-induced lower extremity cycling on bone density of spinal cord-injured patients. *Am J Phys Med Rehabil*, 75:29–34, 1996.
- [12] L.A. Benton, L.L. Baker, B.R. Bowman, and R.L. Waters. *Functional electrical stimulation — A Practical Clinical Guide*. Rancho Rehabilitation Engineering Program, Rancho Los Amigos Medical Center, 7601 East Imperial Highway, Downey, California, 2nd edition, 1981.
- [13] K.E. Bijker, G. De Groot, and A.P. Hollander. Delta efficiencies of running and cycling. *Med Sci Sports Exerc*, 33(9):1546–1551, 2001.
- [14] C.J. Brittain, H.B. Rossier, J.M. Kowalchuck, and B.J. Whipp. Effect of prior metabolic rate on the kinetics of oxygen uptake during moderate-intensity exercise. *Eur J Appl Physiol*, 86:125–134, 2001.
- [15] R. Burnham, T. Martin, R. Stein, G. Bell, I. MacLean, and R. Steadward. Skeletal muscle fibre type transformation following spinal cord injury. *Spinal Cord*, 35(2):86–91, 1997.
- [16] H. Carter, A. Jones, T. Barstow, M. Burnley, C. Williams, and J. Doust. Oxygen uptake kinetics in treadmill running and cycle ergometry: a comparison. *J Appl Physiol*, 89:899–907, 2000.
- [17] R. Casaburi, T.J. Barstow, T. Robinson, and K. Wasserman. Influence of work rate on ventilatory gas exchange kinetics. *J Appl Physiol*, 67(2):547–555, 1989.
- [18] S.C. Chen, C.H. Lai, W.P. Chan, M.H. Huang, H.W. Tsai, and J.J.J. Chen. Increases in bone mineral density after functional electrical stimulation cycling exercises in spinal cord injured patients. *Dis and Rehab*, 27(22):1337–1341, 2005.
- [19] P.D. Chilibeck, G. Bell, J. Jeon, C.B. Weiss, G. Murdoch, I. MacLean, E. Ryan, and R. Burnham. Functional electrical stimulation exercise increases

- GLUT-1 and GLUT-4 in paralyzed skeletal muscles. *Metabolism*, 48(11):1409–1413, November 1999.
- [20] E.F. Coyle, L.S. Sidossis, J.F. Horowitz, and J.D. Beltz. Cycling efficiency is related to the percentage of type I muscle fibers. *Med Sci Sports Exerc*, 24(7):782–788, 1992.
- [21] R.M. Crameri, A. Weston, M. Climstein, G.M. Davis, and J.R. Sutton. Effects of electrical stimulation-induced leg training on skeletal muscle adaptability in spinal cord injury. *Scand J Med Sci Sports*, 12:316–322, 2002.
- [22] P.T. Croisant and R.A. Boileau. Effect of pedal rate, brake load and power on metabolic responses to bicycle ergometer work. *Ergonomics*, 27(6):691–700, 1984.
- [23] csm.jmu.edu/biology/danie2jc/respiration.htm.
- [24] G.M. Davis. Exercise capacity of individuals with paraplegia. *Med Sci Sports Exerc*, 25(4):423–432, 1993.
- [25] G.M. Davis, F.J. Servedio R.M. Glaser, S.C. Gupta, and A.G. Suryaprasad. Cardiovascular responses to arm-cranking and FNS-induced leg exercise in paraplegics. *J Appl Physiol*, 69(2):671–677, 1990.
- [26] N. Donaldson, T.A. Perkins, R. Fitzwater, D.E. Wood, and F. Middleton. FES cycling may promote recovery of leg function after incomplete spinal cord injury. *Spinal Cord*, 38:680–682, 2000.
- [27] S.B. Draper, D.M. Wood, and J.L. Fallowfield. The $\dot{V}O_2$ response to exhaustive square wave exercise: influence of exercise intensity and mode. *Eur J Appl Physiol*, 90:92–99, 2003.
- [28] P.C. Eser, N.deN. Donaldson, H. Knecht, and E. Stüssi. Influence of different stimulation frequencies on power output and fatigue during FES-cycling in recently injured sci people. *IEEE Trans Neural Syst Rehabil Eng*, 11(3):236–240, 2003.
- [29] D. Faghri, R.M. Glaser, and S.F. Figoni. Functional electrical stimulation leg cycle ergometer exercise: training effects on cardiorespiratory responses of spinal cord injured subjects at rest and during submaximal exercise. *Arch Phys Med Rehabil*, 73:1085–93, 1992.

- [30] Z.P. Fang and J.T. Mortimer. A method to effect physiological recruitment order in electrically activated muscle. *IEEE Trans Biomed Eng*, 38(2):175–179, 1991.
- [31] P. Feiereisen, J. Duchateau, and K. Hainaut. Motor unit recruitment order during voluntary and electrically induced contractions in the tibialis anterior. *Exp Brain Res*, 114:117–123, 1997.
- [32] R.A. Ferguson, P. Aagaard, D. Ball, A.J. Sargeant, and J. Bangsbo. Total power output generated during dynamic knee extensor exercise at different contraction frequencies. *J Appl Physiol*, 89:1912–1918, 2000.
- [33] C. Ferrario, K.J. Hunt, S. Grant, A.N. McLean, M.H. Fraser, and D.B. Allan. Novel protocol for high sensitivity cardio-pulmonary exercise testing during Functional Electrical Stimulation cycle ergometry in spinal cord injured subjects. Submitted, 2005.
- [34] C. Ferrario, B. Stone, K.J. Hunt, S.A. Wardand, A.N. McLean, and M.H. Fraser. Oxygen cost of different stimulation patterns for FES cycling. In *Proceedings of the 9th Annual International Functional Electrical Stimulation Society Conference*, pages 171–173, Bournemouth, UK, September 2004.
- [35] S.F. Figoni, R.M. Glaser, D.M. Hendershot, S.C. Gupta, A.G. Suryaprasad, M.M. Rodgers, and B.N. Ezenwa. Hemodynamic responses of quadriplegics to maximal arm-cranking and FNS leg cycling exercise. In *Proceedings of the 10th annual international conference of the IEEE engineering in medicine and biology society*, pages 1636–1637, 1988.
- [36] S.F. Figoni, M.M. Rodgers, R.M. Glaser, S.P. Hooker, P.D. Feghri, B.N. Ezenwa, T. Mathews, A.G. Suryaprasad, and S.C. Gupta. Physiologic responses of paraplegics and quadriplegics to passive and active leg cycle ergometry. *J Am Paraplegia Soc*, 13(3):33–39, July 1990.
- [37] Ø. Foss and J. Hallén. The most economical cadence increases with increasing workload. *Eur J Appl Physiol*, 92:443–451, 2004.
- [38] G.A. Gaesser and G.A. Brooks. Muscular efficiency during steady-state exercise: effects of speed and work rate. *J Appl Physiol*, 38(6):1132–1139. June 1975.

- [39] S.W. Garland, D.J. Newham, and D.L. Turner. The amplitude of the slow component of oxygen uptake is related to muscle contractile properties. *Eur J Appl Physiol*, 91:192–198, 2004.
- [40] H.L. Gerrits, A. de Haan, A.J. Sargeant, A. Dallmeijer, and M.T.E. Hopman. Altered contractile properties of the quadriceps muscle in people with spinal cord injury following functional electrical stimulated cycle training. *Spinal Cord*, 38:214–223, 2000.
- [41] M. Gföhler, T. Angeli, T. Eberharter, P. Lugner, W. Mayr, and C. Hofer. Test bed with force-measuring crank for static and dynamic investigations on cycling by means of functional electrical stimulation. *IEEE Trans Neural Syst Rehabil Eng*, 9(2):169–180, June 2001.
- [42] M. Gföhler and P. Lugner. Cycling by means of functional electrical stimulation. *IEEE Trans Rehab Eng*, 8(2):233–243, June 2000.
- [43] R.M. Glaser. Physiology of functional electrical stimulation-induced exercise: basic science perspective. *J Neuro Rehab*, 5:49–61, 1991.
- [44] R.M. Glaser, S.F. Figoni, S.R. Collins, M.M. Rodgers, A.G. Suryaprasad, S.C. Gupta, and T. Mathews. Physiological responses of SCI subjects to electrically induced leg cycle ergometry. In *Proceedings of the 10th annual international conference of the IEEE Engineering in medicine and biology society*, pages 1638–1640, 1988.
- [45] R.M. Glaser, S.F. Figoni, S.P. Hooker, M.M. Rodgers, B.N. Ezenwa, A.G. Suryaprasad, S.C. Gupta, and T. Mathews. Efficiency of FNS leg cycle ergometry. In *Proceedings of the 11th annual international conference of the IEEE engineering in medicine and biology society*, pages 961–963, 1989.
- [46] H. Gollee, K.J. Hunt, S. Coupaud, A.N. McLean, and M.H. Fraser. An apparatus for FES-assisted arm-cranking exercise in tetraplegia. In *Proceedings of the 7th Annual Conference of the International Functional Electrical Stimulation Society*, pages 298–300, Ljubljana, Slovenia, June 2002.
- [47] T. Gordon and J. Mao. Muscle atrophy and procedures for training after spinal cord injury. *Physical Therapy*, 74(1):50–61, 1994.

- [48] F.G. Goss, A. McDermott, and R.J. Robertson. Changes in peak oxygen uptake following computerized functional electrical stimulation in the spinal cord injured. *Res Q Exerc Sport*, 63(1):76–79, 1992.
- [49] C.M. Gregory and C.S. Bickel. Recruitment patterns in human skeletal muscle during electrical stimulation. *Phys Ther*, 85(4):358–364, April 2005.
- [50] G. Grimby, C. Broberg, I. Krotkiewska, and M. Krotkiewski. Muscle fiber composition in patients with traumatic cord lesion. *Scand J Rehab Med*, 8:37–42, 1976.
- [51] L. Guttman. *Spinal Cord Injuries - comprehensive management and research*. Blackwell Scientific Publications, Oxford, 2nd edition, 1976.
- [52] T. Hamada, T. Kimura, and T. Moritani. Selective fatigue of fast motor units after electrically elicited muscle contractions. *J Electromyogr Kinesiol*, 14:531–538, 2004.
- [53] T.N. Hangartner, M.M. Rodgers, R.M. Glaser, and P.S. Barre. Tibial bone density loss in spinal cord injured patients: Effects of FES exercise. *J Rehab Res Develop*, 31:50–61, 1994.
- [54] B.W. Heller. *The production and control of FES swing-through gait*. PhD thesis, University of Strathclyde, Glasgow, Scotland, 1992.
- [55] F. Hintzy-Cloutier, K. Zameziati, and A. Belli. Influence of the base-line determination on work efficiency during submaximal cycling. *J Sports Med Phys Fitness*, 43:51–56, 2003.
- [56] S.P. Hooker, S.F. Figoni, M.M. Rodgers, R.M. Glaser, T. Mathews, A.G. Suryaprasad, and S.C. Gupta. Physiologic effects of electrical stimulation leg cycle exercise training in spinal cord injured persons. *Arch Phys Med Rehabil*, 73:470–476, 1992.
- [57] S.P. Hooker, A.M.E. Scremin, D.L. Mutton, C.H. Kunkel, and G. Cagle. Peak and submaximal physiologic responses following electrical stimulation leg cycle ergometer training. *J Rehabil Res Dev*, 32(4):361–366, November 1995.
- [58] <http://www.spinal.co.uk/publications>.
- [59] R.L. Hughson and M.D. Inman. Oxygen uptake kinetics from ramp work tests: variability of single test values. *J Appl Physiol*, 61(1):373–376, 1986.

- [60] K.J. Hunt, C. Ferrario, S. Grant, B. Stone, A.N. McLean, M.H. Fraser, and D.B. Allan. Comparison of stimulation patterns for FES-cycling using measures of oxygen cost and stimulation cost. To be published in *Med Eng Phys*, 2005.
- [61] K.J. Hunt, B. Stone, N. Negård, T. Schauer, M.H. Fraser, A.J. Cathcart, C. Ferrario, S. Grant, and S.A. Ward. Control strategies for integration of electric motor assist and functional electrical stimulation in paraplegic cycling: utility for exercise testing and mobile cycling. *IEEE Trans Neural Syst Rehabil Eng*, 12(1):89–101, March 2004.
- [62] E.S. Idsø, T.A. Johansen, and K.J. Hunt. Finding the metabolically optimal stimulation pattern for FES-cycling. In *Proceedings of the 9th Annual Conference of the International Functional Stimulation Society*, Bournemouth, UK, September 2004.
- [63] P. Jacobs, E. Mahoney, A. Robbins, and M. Nash. Hypokinetic circulation in persons with paraplegia. *Med Sci Sports Exerc*, 34(9):1401–1407, 2002.
- [64] P.L. Jacobs and M.S. Nash. Exercise recommendations for individuals with spinal cord injury. *Sports Med*, 34(11):727–751, 2004.
- [65] R.J. Jaeger. Principles underlying functional electrical stimulation techniques. *J Spinal Cord Med*, 19(2):93–96, April 1996.
- [66] G.C. Jang, J.J.J. Chen, C.T. Shih, and T.C. Huseh. Design of FES-cycling system and its stimulation patterns. *Chinese J Med Biol Eng*, 13(4):305–315, December 1993.
- [67] T.W.J. Janssen, R.M. Glaser, and D.B. Shuster. Clinical efficacy of electrical stimulation exercise training: effects on health, fitness and function. *Topics in Spinal Cord Injury Rehabilitation*, 3(3):33–49, 1998.
- [68] A.M. Jones, I.T. Campbell, and J.S.M. Pringle. Influence of muscle fibre type and pedal rate on the \dot{V}_{O_2} -work rate slope during ramp exercise. *Eur J Appl Physiol*, 91:238–245, 2004.
- [69] D.A. Jones and J.M. Round. *Skeletal muscle in health and disease - A textbook of muscle physiology*. Manchester University Press, Manchester, 1990.

- [70] B.A. Kakulas. The applied neuropathology of human spinal cord injury. *Spinal Cord*, 37:79–88, 1999.
- [71] B.A. Kakulas. Neuropathology: the foundation for new treatments in spinal cord injury. *Spinal Cord*, 42:549–563, 2004.
- [72] M. Kjaer, G. Perko, N.H. Secher, R. Boushel, N. Beyer, S. Pollack, A. Horn, A. Fernandes, T. Mohr, S.F. Lewis, and H. Galbo. Cardiovascular and ventilatory responses to electrically induced cycling with complete epidural anaesthesia in humans. *Acta Physiol Scand*, 151:199–207, 1994.
- [73] M. Knafitz, R. Merletti, and C.J. De Luca. Inference of motor unit recruitment order in voluntary and electrically elicited contractions. *J Appl Physiol*, 68(4):1657–1667, 1990.
- [74] S. Koga, D.C. Poole, T. Shiojiri, N. Kondo, Y. Fukuba, A. Miura, and T.J. Barstow. Comparison of oxygen uptake kinetics during knee extension and cycle exercise. *Am J Physiol Regul Integr Comp Physiol*, 288:R212–R220, 2005.
- [75] R. Lepers, G.Y. Millet, N.A. Maffiuletti, C. Hausswirth, and J. Brisswalter. Effect of pedalling rates on physiological response during endurance cycling. *Eur J Appl Physiol*, 85:392–395, 2001.
- [76] B.R. Londeree, J. Moffitt-Gerstenberger, J.A. Padfield, and D. Lottmann. Oxygen consumption of cycle ergometry is non linearly related to work rate and pedal rate. *Med Sci Sports Exerc*, 29(6):775–780, 1997.
- [77] B.R. MacIntosh, R.R. Neptune, and J.F. Horton. Cadence, power and muscle activation in cycle ergometry. *Med Sci Sports Exerc*, 32(7):1281–1287, 2000.
- [78] M.S. Malagodi, M.W. Ferguson-Pell, and R.D. Masiello. A functional electrical stimulation exercise system designed to increase bone density in spinal cord injured individuals. *IEEE Trans Rehab Eng*, 1(4):213–219, December 1993.
- [79] L.A. Mallory, B.W. Scheuermann, B.D. Hoelting, M.L. Weiss, R.M. McAllister, and T.J. Barstow. Influence of peak \dot{V}_{O_2} and muscle fiber type on the efficiency of moderate exercise. *Med Sci Sports Exerc*, 34(8):1279–1287, 2002.

- [80] T.P. Martin, R.B. Stein, P.H. Hoepfner, and D.C. Reid. Influence of electrical stimulation on the morphological and metabolic properties of paralyzed muscles. *J Appl Physiol*, 72(4):1401–1406, 1992.
- [81] T. Matsunaga, Y. Shimada, and K. Sato. Muscle fatigue from intermittent stimulation with low and high frequency electrical pulses. *Arch Phys Med Rehabil*, 80:48–53, January 1999.
- [82] F.M. Maynard, M.B. Bracken, G. Creasey, J.F. Ditunno, W.H. Donovan, T.B. Ducker, S.L. Garber, R.J. Marino, S.L. Stover, C.H. Tator, R.L. Waters, J.E. Wilberger, and W. Young. International standards for neurological and functional classification of spinal cord injury. *Spinal Cord*, 35:266–274, 1997.
- [83] A.J. McComas. *Skeletal muscle: form and function*. Human kinetics, 1996.
- [84] J.W. McDonald and C. Sadowsky. Spinal-cord injury. *The Lancet*, 359:417–425, February 2002.
- [85] T. Meyer, A. Lucía, C.P. Earnest, and W. Kindermann. A conceptual framework for performance diagnosis and training prescription from submaximal gas exchange parameters - Theory and application. *Int J Sports Med*, 26(Suppl 1):S38–S48, 2005.
- [86] T. Mohr, J.L. Andersen, F. Biering-Sørensen, H. Galbo, G. Bangsbo, A. Wagner, and M. Kjær. Long term adaptation to electrically induced cycle training in severe spinal cord injured individuals. *Spinal Cord*, 35:1–16, 1997.
- [87] T. Mohr, J. Pødenphant, F. Biering-Sørensen, H. Galbo, G. Thamsborg, and M. Kjær. Increased bone mineral density after prolonged electrically induced cycle training of paralyzed limbs in spinal cord injured man. *Calcif Tissue Int*, 61:22–25, 1997.
- [88] L. Moseley and A.E. Jeukendrup. The reliability of cycling efficiency. *Med Sci Sports Exerc*, 33(4):621–627, 2001.
- [89] D.L. Mutton, A.M.E. Scremin, T.J. Barstow, M.D. Scott, C.F. Kunkel, and T.G. Cagle. Physiologic responses during functional electrical stimulation leg cycling and hybrid exercise in spinal cord injured subjects. *Arch Phys Med Rehabil*, 78:712–718, July 1997.

- [90] B.L. Nickleberry and G.A. Brooks. No effect of cycling experience on leg cycle ergometer efficiency. *Med Sci Sports Exerc*, 28(11):1396–1401, November 1996.
- [91] P.J. Pacy, R. Hesp, D.A. Halliday, D. Katz, G. Cameron, and J. Reeve. Muscle and bone in paraplegic patients, and the effect of functional electrical stimulation. *Clinical Science*, 75:481–487, 1988.
- [92] J.S. Petrofsky. Functional electrical stimulation: a two-year study. *J Rehabil*, 58:29–34, 1992.
- [93] J.S. Petrofsky. New algorithm to control a cycle ergometer using electrical stimulation. *Med Biol Eng Comput*, 41:18–27, 2003.
- [94] J.S. Petrofsky, H. Heaton III, and C.A. Phillips. Outdoor bicycle for exercise in paraplegics and quadriplegics. *J Biomed Eng*, 5:292–296, October 1983.
- [95] J.S. Petrofsky, C.A. Phillips, J. Almeida, R. Briggs, W. Couch, and W. Colby. Aerobic trainer with physiological monitoring for exercise in paraplegic and quadriplegic patients. *Journal of Clinical Engineering*, 10(4):307–315, October–December 1985.
- [96] J.S. Petrofsky, C.A. Phillips, H.H. Heaton, and R.M. Glaser. Bicycle ergometer for paralyzed muscle. *Journal of Clinical Engineering*, 9(1):13–18, January–March 1984.
- [97] J.S. Petrofsky and J. Smith. Three-wheel cycle ergometer for use by men and women with paralysis. *Med & Biol Eng & Comput*, 30:364–369, 1992.
- [98] J.S. Petrofsky and R. Stacy. The effect of training on endurance and the cardiovascular responses of individuals with paraplegia during dynamic exercise induced by functional electrical stimulation. *Eur J Appl Physiol*, 64:487–492, 1992.
- [99] C.A. Phillips, D. Danopoulos, P. Kezdi, and D. Hendershot. Muscular, respiratory and cardiovascular responses of quadriplegic persons to a FES bicycle ergometer conditioning program. *Int J Rehab Research*, 12(2):147–157, 1989.
- [100] W.T. Phillips, B.J. Kirtali, M. Sarkarati, and G. Weraarchakul. Effect of spinal cord injury on the heart and cardiovascular fitness. *Current Problems in Cardiology*, 23(11):649–717, November 1998.

- [101] S.F. Pollack, K. Axen, N. Spielholz, N. Levin, F. Haas, and K.T. Ragnarsson. Aerobic training effects of electrically induced lower extremity exercises in spinal cord injured people. *Arch Phys Med Rehabil*, 70:214–219, 1989.
- [102] D.J. Pons, C.L. Vaughan, and G.G. Jaros. Cycling device powered by the electrically stimulated muscles of paraplegics. *Med & Biol Eng & Comput*, 27:1–7, 1989.
- [103] D.B. Popović and T. Sinkjær. *Control of Movement for the Physically Disabled*. Springer, 2000.
- [104] S.K. Powers and E.T. Howley. *Exercise Physiology*. Mc Grow Hill, 1995.
- [105] K.T. Ragnarsson, S. Pollack, W. O’Daniel, R. Edgar, J. Petrofsky, and M.S. Nash. Clinical evaluation of computerized functional electrical stimulation after spinal cord injury: a multicenter pilot study. *Arch Phys Med Rehabil*, 69:672–677, 1988.
- [106] J. Rasmussen, S.T. Christensen, M. Gföhler, M. Damsgaard, and T. Angeli. Design optimization of a pedaling mechanism for paraplegics. *Struct Multidisc Optim*, 26:132–138, 2004.
- [107] J. Raymond, G.M. Davis, M. Climstein, and J.R. Sutton. Cardiorespiratory responses to arm cranking and electrical stimulation leg cycling in people with paraplegia. *Med Sci Sports Exerc*, 31:822–828, 1999.
- [108] J. Raymond, G.M. Davis, and M. van der Plas. Cardiovascular responses during submaximal electrical stimulation-induced leg cycling in individuals with paraplegia. *Clin Physiol Funct Imaging*, 22(2):92–98, 2002.
- [109] J. Roca, B.J. Whipp, A.G.N. Agustí, S.D. Anderson, R. Casaburi, J.E. Cotes, C.F. Donner, M. Estenne, H. Folgering, T.W. Higenbottam, K.J. Killian, P. Palange, A. Patessio, C. Prefaut, R. Sergysels, P.D. Wagner, and I. Weisman. Clinical exercise testing with reference to lung disease: indications, standardization and interpretation strategies. *Eur Respir J*, 10:2662–2689, 1997.
- [110] M.M. Rodgers and R.M. Glaser. Musculoskeletal responses of spinal cord injured individuals to functional neuromuscular stimulation-induced knee extension exercise training. *J Rehabil Res Dev*, 28(4):19–26. 1991.

- [111] J.M. Round, F.M.D. Barr, B. Moffat, and D.A. Jones. Fibre areas and histochemical fibre types in the quadriceps muscle of paraplegic subjects. *J Neurol Sci*, 116:207–211, 1993.
- [112] C. Sadowsky, O. Volshteyn, L. Schultz, and J.W. McDonald. Spinal cord injury. *Disabil Rehabil*, 24(13):680–687, 2002.
- [113] L.M. Schutte, M.M. Rodgers, F.E. Zajac, and R.M. Glaser. Improving the efficacy of electrical stimulation-induced leg cycle ergometry: an analysis based on a dynamic musculoskeletal model. *IEEE Trans Rehab Eng*, 1(2):109–125, June 1993.
- [114] L. Sherwood. *Human physiology: from cells to systems*. Pacific Grove, California: Brooks/Cole, 4th edition, 2001.
- [115] M.L. Sipski, J.A. Delisa, and S. Schweer. Functional electrical stimulation bicycle ergometry: Patient perceptions. *Am J Phys Med Rehabil*, 68(3):147–149, June 1989.
- [116] K.E. Sloan, L.A. Bremner, J. Byrne, R.E. Day, and E.R. Scull. Musculoskeletal effects of an electrical stimulation induced cycling programme in the spinal injured. *Paraplegia*, 32:407–415, 1994.
- [117] W.N. Stainbsy, L.B. Gladden, J.K. Barclay, and B.A. Wilson. Exercise efficiency: validity of base-line subtractions. *J Appl Physiol: Respirat Environ Exercise Physiol*, 48(3):518–522, 1980.
- [118] K. Svedahl and B.R. MacIntosh. Anaerobic threshold: the concept and methods of measurement. *Can J Appl Physiol*, 28(2):299–323, April 2003.
- [119] D. Theisen, C. Fornusek, J. Raymond, and G.M. Davis. External power output changes during prolonged cycling with electrical stimulation. *J Rehabil Med*, 34(4):171–175, July 2002.
- [120] C.K. Thomas, G. Nelson, L. Than, and I. Zijdewind. Motor unit activation order during electrically evoked contractions of paralyzed or partially paralyzed muscles. *Muscle Nerve*, 25:797–804, 2002.
- [121] R.B. Trieschmann. *Spinal Cord Injuries: Psychological, Social and Vocational Adjustment*. Pergamon General Psychology Series, 1980.

- [122] M.H. Trimble and R.M. Enoka. Mechanisms underlying the training effects associated with neuromuscular electrical stimulation. *Phys Ther*, 71(4):273–282, 1991.
- [123] J.M. Vallier, A.X. Bigard, F. Carré, J.P. Eclache, and J. Mercier. Détermination des seuils lactiques et ventilatoires. Position de la Société française de médecine du sport. *Science and Sports*, 15:133–140, 2000.
- [124] K. Wasserman, W.L. Beaver, and B.J. Whipp. Gas exchange theory and the lactic acidosis (anaerobic) threshold. *Circulation*, 81(supp II):II–14–II–30, 1990.
- [125] K. Wasserman, J.E. Hansen, D.Y. Sue, R. Casaburi, and B.J. Whipp. *Principles of Exercise Testing and Interpretation*. Lippincott Williams & Wilkins, 1999.
- [126] K. Wasserman, B.J. Whipp, S.N. Koyal, and W.L. Beaver. Anaerobic threshold and respiratory gas exchange during exercise. *J Appl Physiol*, 35(2):236–243, August 1973.
- [127] B.J. Whipp. The bioenergetic and gas exchange basis of exercise testing. *Clin Chest Med*, 15(2):173–192, June 1994.
- [128] B.J. Whipp, J.A. Davis, F. Torres, and K. Wasserman. A test to determine parameters of aerobic function during exercise. *J Appl Physiol*, 50(1):217–221, 1981.
- [129] B.J. Whipp, S.A. Ward, N. Lamarra, J.A. Davis, and K. Wasserman. Parameters of ventilatory and gas exchange dynamics during exercise. *J Appl Physiol*, 52(6):1506–1513, 1982.
- [130] B.J. Whipp and K. Wasserman. Efficiency of muscular work. *J Appl Physiol*, 26(5):644–648, 1969.
- [131] B.J. Whipp and K. Wasserman. Oxygen uptake kinetics for various intensities of constant-load work. *J Appl Physiol*, 33(3):351–356, 1972.
- [132] R.P. Wilder, E.V. Jones, T.C. Wind, and R.F. Edlich. Functional electrical stimulation cycle ergometer exercise for spinal cord injured patients. *Journal of Long-Term Effects of Medical Implants*, 12(3):161–174. 2002.

- [133] D.P. Wilkerson, K. Koppo, T.J. Barstow, and A.M. Jones. Effect of work rate on the functional 'gain' of phase II pulmonary O₂ uptake response to exercise. *Respir Physiol Neurobiol*, 142:211–223, 2004.
- [134] www.cornwallis.kent.sch.uk/.../1organs1.htm.
- [135] www.enchantedlearning.com.
- [136] J.A. Zoladz, A.C.H.J. Rademaker, and A.J. Sargeant. Human muscle power generating capability during cycling at different pedalling rates. *Exp Physiol*, 85(1):117–124, 2000.

